

TECHNISCHE UNIVERSITÄT MÜNCHEN

Lehrstuhl für Bodenkunde

Evolution of mineral-associated organic matter in paddy soils – a chronosequence study

Livia Wissing

Vollständiger Abdruck der von der Fakultät Wissenschaftszentrum Weihenstephan für Ernährung, Landnutzung und Umwelt der Technischen Universität München zur Erlangung des akademischen Grades eines

Doktors der Naturwissenschaften

genehmigten Dissertation.

Vorsitzender: Univ.-Prof. Dr. J.P. Geist

Prüfer der Dissertation:

1. Univ.-Prof. Dr. I. Kögel-Knabner
2. Univ.-Prof. Dr. W. Amelung
(Rheinische Friedrich-Wilhelms-Universität Bonn)

Die Dissertation wurde am 03.12.2012 bei der Technischen Universität München eingereicht und durch die Fakultät Wissenschaftszentrum Weihenstephan für Ernährung, Landnutzung und Umwelt am 03.02.2013 angenommen.

MARIANNE by Steamy Raimon



To

LENI WISSING

SUMMARY

In the Chinese Zhejiang Province, new farmland has been created through consecutive land reclamation by protective dikes over the past 2000 years. The construction of the dikes is historically well-dated and provides chronosequences of soil formation under agricultural use. Parts of the land were used for rice cultivation under flooded conditions (paddy soils), other parts for a variety of non-inundated croplands (non-paddy soils). These soil chronosequences, derived from calcareous marine/estuarine sediments, provide the opportunity to evaluate the effect of the soil management over long time periods on the evolution and distribution of soil organic matter (SOM) during pedogenesis.

The **Publication I** examined the organic carbon (OC) accumulation in a 2000-years-old chronosequence of paddy soil evolution, focusing on those soil fractions, which are involved in the OC accumulation. Objectives of the study were to: (1) allocate the OC distribution within particle size fractions, (2) identify the soil fractions, which are involved in OC accumulation depending on the duration of paddy soil evolution and (3) investigate the OC saturation in the $<20\ \mu\text{m}$ fraction. In this context, a physical fractionation according to particle size was applied to the paddy soil material. The results showed that the OC accumulation was driven by the strong OC accretion in the silt-sized fractions and the large capacity for OC accumulation in coarse clay, whereas the OC amount in the 2000-63 μm fraction remained constant. The coarse clay as well as the fine silt fractions are characterized by the largest capacity for OC accumulation. Coarse and medium silt was identified to be an important long-term OC sink during paddy soil evolution, which is replenished in a continuous process. The calculated actual OC saturation of the $<20\ \mu\text{m}$ fraction increased with soil age, except for the fine clay fraction, which already seems to be OC saturated after 50 years of soil evolution. The findings underline the importance of $<20\ \mu\text{m}$ fraction for increasing OC storage, although the process of OC accumulation in this fractions seems not to be complete even after 2000 years of paddy soil evolution.

Further, soil samples obtained from horizontal sampling were analyzed for bulk density, OC as well as inorganic carbon (IC) concentrations and OC stocks of bulk soils. Paddy soils are characterized by typical low bulk densities in the puddled topsoil horizons and high values in the plow pan, indicating the compacting of this horizon due to periodic puddling. The development and depth distribution of bulk densities were finalized within the first 50 years of paddy soil evolution and showed no further differentiation between the soil ages. Decalcification of marine-derived paddy soils is a two phase process: fast substantial loss of carbonate during topsoil formation, as the upper-most A horizon of the topsoil were free of carbonate in 100-years-old paddy soils and slow decalcification of subsoils over 700 years of rice cultivation due to the plow pan, decoupling of soil formation in topsoil from subsoil. Topsoil OC stocks increased with slight variations within the 2000 years of soil formation, whereas the subsoil is dominated by an overall loss of OC inherited from the marine sediment.

My contribution to these findings was the adaption of the physical fractionation scheme and the identification of the soil fractions silt and coarse clay as the most relevant fractions for OC accumulation in paddy soils. A physical fractionation according to particle size has not been applied previously to paddy soils. I identified the contribution of the different soil fractions to the topsoil OC accumulation in paddy soils because the chronosequence approach clearly showed different OC accretions for silt- and clay-sized fractions. Further, I was responsible for the calculation and the estimation of the actual and potential OC saturation, the graphical presentation and statistical analysis of the data. The findings of **Publication I** allow me to differentiate time intervals for the pedogenesis of paddy soils, which constitute the foundation for an integrative manuscript (Kölbl et al., submitted). (1) The formation of the plow pan as indicated by the bulk density profile is a short-term process, developing over few decades of puddling and is already finalized within the first 50 years of paddy soil evolution. This leads to a decoupling between topsoil and subsoil of the subsequent processes of soil IC loss and OC accumulation. (2) Decalcification of paddy soils is identified as an intermediate soil forming process. Fast decalcification of the upper-most A horizon needed 100 years of soil evolution, whereas the complete carbonate removal from the entire soil profile requires few centuries and is finished after 700 years of paddy soil management. (3) The accumulation of OC is a long-term process as it develops differently in top- and subsoil over several centuries of paddy soil evolution. The paddy soil management favours the accumulation of OC in the topsoil, but interrupts it in the subsoils due to low permeability of the plow pan.

In addition to the investigation on the OC accumulation in the paddy soil fractions (**Publication I**), the research topic of **Publication II** focused on the role of organo-mineral associations in OC accumulation. Iron (Fe) oxides interact with OM in soils and play an important role in the stabilization of OM in organo-mineral associations. These processes are often influenced by soil cultivation, crop rotation and irrigation. The study assessed the effect of Fe oxides on topsoil OC accumulation during soil development. The objectives were to: (1) investigate the influence of both soil management systems on the proportion of oxalate-extractable Fe (Fe_{ox}), (2) elucidate if presumably increasing Fe_{ox} proportions within the paddy soil chronosequence will lead to higher proportions of accumulated SOM than in non-paddy soils and (3) determine the SOM decomposition in paddy and non-paddy soils and if lignin-derived phenols will accumulate during paddy soil development.

In addition to the OC concentration, bulk soil samples and soil fractions were analyzed for their soil mineralogy and SOM composition to reveal differentiation of OC accumulation processes between paddy and non-paddy soils. Results from solid-state ^{13}C nuclear magnetic resonance (NMR) spectroscopy showed in both in bulk soils and clay fractions no differences in SOM composition. Further, no change in SOM composition was observed in paddy and non-paddy soils and during pedogenesis. Selective enrichment of lignin-derived compounds, caused by long-term paddy rice management, could not be confirmed by the present study. Paddy management resulted in higher OM

quantities but did not affect the SOM composition during soil development. The management of paddy soils creates an environment of Fe oxide formation which is different to those in non-paddy soils. Paddy topsoils are dominated by Fe_{ox} and significantly lower proportions of dithionite-extractable Fe (Fe_d)- Fe_{ox} . This was in contrast to non-paddy soils, which are characterized by high proportions of Fe_d - Fe_{ox} . The paddy-specific Fe formation was effective after only 50 years of soil development and the Fe proportion did not change during further pedogenesis. The higher proportions of Fe_{ox} in paddy soils are associated with larger OC concentrations within the fine silt fraction and both clay fractions compared to non-paddy soils. The literature described already good correlations of OC with Fe_{ox} . Thus, the OC accumulation due to organo-mineral associations, especially by association with Fe_{ox} , is more pronounced during paddy soil evolution. Paddy soils are characterized by markedly higher potential for OC accumulation since the earliest stages of pedogenesis due to higher proportions of Fe_{ox} than in non-paddy soils.

My contribution to this new finding was the solid-state ^{13}C NMR spectroscopically analyses of bulk soil and physical fractionation SOM of the paddy and non-paddy topsoils. The general assumption for paddy soils that lignin-derived phenols will accumulate under anaerobic conditions due to the inhibited decomposition could thus be refuted. Further, I was responsible for the evaluation of OC and Fe contributions at the level of the individual fractions and their interpretation during soil evolution. The findings of **Publication II** allowed me to differentiate the OC accumulation process in paddy soils from those in non-paddy soils which enabled me to conclude that OC accumulation due to Fe_{ox} -OM associations was favoured in paddy soils. Therefore, the potential for OC accumulation seems to be higher in paddy soils. The results of have major implications for the assessment of new management techniques for paddy soils such as alternating wetting and drying, as these will affect redox conditions and thus most probably also formation of Fe and OC storage potential.

The concept of **Publication II** was extended by the idea that OC accumulation due to organo-mineral associations is more effective in paddy soils because of the accelerated decalcification during soil development. On the first soil forming processes on calcareous parent material is decalcification which has to be completed before secondary minerals start to form, providing additional mineral surfaces for OM accumulation. **Publication III** focused on the accessibility of soil mineral surfaces for OC covering. The objectives included to: (1) investigate if decalcification controls the OC accumulation and if the formation of clay minerals and Fe oxides accelerated in decalcified (paddy) soils, (2) estimate the OC covering of the clay mineral and Fe oxide surfaces during paddy and non-paddy soils development and (3) elucidate if clay minerals and Fe (hydr) oxides contribute in equal amounts to the OC accumulation.

In this context, the specific surface area (SSA) of the isolated silt- and clay-sized fractions was measured by Brunauer-Emmett-Teller (BET- N_2) method under four conditions: untreated, after OM removal, after Fe_d removal and after removal of both. Using selective removal of OM and Fe_d by

combining hydrogen peroxide (H_2O_2) and dithionite-citrate-bicarbonate (DCB) treatments, it was possible to assign the accessibility for OC covering to the respective silicate or oxide surface. The higher OM content in paddy soils results in smaller untreated mineral surfaces than in non-paddy soils. The removal of OM especially in paddy soils causes large OC losses for the clay-sized fractions and leads to markedly higher mineral surfaces than in non-paddy soils.

Based on the results, the understanding of mineral surfaces, their coverage with OM and the effect of the four different treatments was illustrated in a schematic overview in **Publication III**. Mineral surfaces, which are covered by OM does not contribute significantly to the nitrogen area. The H_2O_2 treatment most likely had no effect on pure Fe oxides and pure clay minerals without OM and also no effect on OM, which was protected by soil minerals. The clay-sized fraction had Fe_d concentrations of 1%–3%. The removal of Fe_d led to declining SSA values in the clay fraction. Losses of surface area were induced if Fe oxides occurred without being protected by OM or if the surface area of clay minerals covered by Fe oxides was smaller than the entire outer surface area of the Fe oxides. The subsequent removal of Fe_d by DCB treatment after OM removal caused an increase in SSA and presented the largest mineral surface for almost all silt-sized fractions of both soil groups and for paddy fine clay and non-paddy coarse clay. The literature explained that removal of oxyhydroxides may break up the aggregation with the clay-sized particles and cause a markedly increase in SSA. In the SOM-rich paddy soils of the study, the described break-up of soil aggregates was only achieved after the removal of protective SOM. There are three indications why silicate minerals play the dominate role in OC stabilization: (1) the clay-sized fractions are characterized by low Fe_d concentrations. (2) There was no correlation between the constant Fe values and the increasing OC concentrations in the clay-sized fraction. (3) The combined treatment (H_2O_2 + DCB) showed a higher effect on SSA than each treatment alone although the surface of Fe oxides has been removed by the DCB treatment. Unexpectedly, there was no evidence of formation of secondary minerals during initial soil formation, which could provide new surfaces for OC accumulation. Paddy soils are characterized by an accelerated decalcification, higher OC contents and a pronounced accumulation of recent OC in addition to the inherited carbon. However, the study revealed higher coverings of mineral surfaces by OC only after decalcification in paddy soils. In contrast, the surface area of minerals in non-paddy soils, in which decalcification was much lower, seemed to be partly inaccessible due to strong microaggregation by carbonate cementation and Ca^{2+} -bridging. The accelerated decalcification of paddy soils led to enhanced accessibility of mineral surfaces for OC covering, which intensified OC accumulation from the early stages of soil formation onward.

The selective removal of OC and Fe_d had not been applied to paddy soils previously. These findings allowed me to identify different OC accumulation processes in paddy and non-paddy soils which enabled me to conclude higher OC coverings in paddy than in non-paddy topsoils. My contributions to these findings are the identification of paddy-specific soil-forming processes (**Publication III**) which were markedly different from those of non-paddy soils:

- (1) Larger proportions of modern carbon are added to the inherited carbon in paddy soils (also confirmed by higher OC accumulation) than in non-paddy soils. This markedly proportion of OC is in paddy soils associated with the silicate mineral surfaces.
- (2) The decalcification of the upper-most topsoil horizon was already finished within 100 years of paddy soil development, whereas the decalcification of non-paddy soils required almost 700 years. The assumption is that potentially strong aggregation by calcium carbonate and Ca²⁺-bridges most likely reduces the OM accumulation in non-paddy soils.
- (3) The periodical changes in redox conditions and the higher amounts of OM in paddy soils allowed the persistence of Fe_{ox}.

ZUSAMMENFASSUNG

Durch die sukzessive Eindeichung der Küstengebiete kam es in der chinesischen Zhejiang Provinz während der vergangenen 2000 Jahre zur Landgewinnung. Die Errichtung der Deiche ist historisch gut dokumentiert und liefert somit eine Zeitabfolge (Chronosequenz) der Entwicklung der landwirtschaftlich genutzten Böden. Teile dieses neu gewonnenen Ackerlandes werden für den Nassreisbau unter periodisch gefluteten Bedingungen genutzt, so genannte *paddy soils*. Andere Teile des Landes werden mit einer Vielzahl von Ackerpflanzen ohne periodische Überflutung bewirtschaftet, hier *non-paddy soils* genannt. Die *paddy* und *non-paddy soils* entwickelten sich aus kalkhaltigen, marinen Sedimenten bzw. Flussmündungssedimenten und bieten die Möglichkeit, den Einfluss der unterschiedlichen Bewirtschaftung auf die Entwicklung und Verteilung der organischen Bodensubstanz (OBS) über einen langen Zeitraum der Pedogenese zu beurteilen. Das Thema von **Publikation I** ist die Akkumulation des organischen Kohlenstoffes (C_{org}) während einer 2000-jährigen Nassreisbodengenese. Dabei liegt der Fokus auf denjenigen Bodenfraktionen, welche an der C_{org} -Akkumulation in den *paddy soils* beteiligt sind. Die Studie beinhaltet folgende Ziele: (1) die Bestimmung der Verteilung der C_{org} -Konzentrationen in den Bodenfraktionen. (2) Die Identifizierung der Bodenfraktionen, welche im Laufe der Pedogenese an der C_{org} -Akkumulation in den *paddy soils* beteiligt sind. (3) Die Untersuchung der C_{org} -Sättigung in der $<20 \mu\text{m}$ Fraktion. Dazu wurde eine physikalische Fraktionierung nach Korngrößen an den *paddy soils* durchgeführt.

Die Ergebnisse zeigen, dass die C_{org} -Akkumulation in den *paddy soils* weitgehend durch den starken C_{org} -Zuwachs in den Schlufffraktionen, aber auch durch die hohe Kapazität der Grobtonfraktion zur C_{org} -Akkumulation zu Stande kommt. Der C_{org} -Gehalt der $2000\text{-}63 \mu\text{m}$ Fraktion bleibt hingegen konstant. Die höchsten Kapazitäten zur C_{org} -Akkumulation bieten die Feinschluff- und Grobtonfraktion. Mittel- und Grobschluff sind als langfristige C_{org} -Senken während der *paddy soil* Entwicklung identifiziert worden, was vor allem in späteren Stadien der Pedogenese zum Tragen kommt. Die aktuelle C_{org} -Sättigung in der $<20 \mu\text{m}$ Fraktion zeigt, mit Ausnahme der Feintonfraktion, eine chronologische Zunahme. Das führt zu der Annahme, dass die Feintonfraktion bereits innerhalb der ersten 50 Jahre der Pedogenese mit C_{org} gesättigt ist. Die Ergebnisse heben die Bedeutung der $<20 \mu\text{m}$ Fraktion für die C_{org} -Speicherung hervor, wobei die C_{org} -Akkumulation in dieser Fraktion selbst nach über 2000 Jahren Pedogenese noch nicht abgeschlossen scheint.

Des Weiteren wurden die Gesamtböden aller Profile hinsichtlich ihrer Lagerungsdichten, C_{org} - und anorganischen Kohlenstoff (C_{anorg})-Konzentrationen sowie der C_{org} -Vorräte analysiert. Während der durch *puddling* (Bodenbearbeitung unter wassergesättigten Bedingungen) bearbeitete Oberboden durch niedrige Lagerungsdichten charakterisiert ist, führt das *puddling* in der Pflugsohle zu einer Bodenverdichtung. Die Entwicklung der Pflugsohle sowie die Verteilung der Lagerungsdichten im Profil sind bereits nach nur 50 Jahren Pedogenese abgeschlossen. Die Entkalkung, der aus marinen Sedimenten entstandenen *paddy soils*, läuft in zwei Phasen ab: eine schnelle Entkalkung des obersten

A Horizontes innerhalb von 100 Jahren und eine langsame Entkalkung des Unterbodens (über 700 Jahre), da die dazwischenliegende Pflugsohle die Pedogenese des Oberbodens von der des Unterbodens trennt. Die C_{org} -Vorräte des Oberbodens nehmen trotz leichter Schwankungen innerhalb von 2000 Jahren der Bodenentwicklung deutlich zu. Der Unterboden wird hingegen durch einen Verlust des ererbten „alten“ Kohlenstoffes aus den marinen Sedimenten dominiert.

Mein Beitrag zu diesen Befunden war die Anpassung des Fraktionierungsschemas, da eine physikalische Fraktionierung nach Korngrößen in der Vergangenheit bei *paddy soils* bislang noch nicht praktiziert wurde. Durch die Fraktionierung der *paddy soils* gelang mir die Identifizierung derjenigen Bodenfraktionen (Schlufffraktionen und Grobton), welche zur C_{org} -Akkumulation in den *paddy soils* beitragen. In diesem Zusammenhang konnte ich eindeutig unterschiedliche C_{org} -Zuwächse für die Schluff- und für die Tonfraktionen zeigen. Des Weiteren war ich für die Kalkulationen von aktueller und potentieller C_{org} -Sättigung, der graphischen Darstellung sowie der statistischen Auswertung des Datensatzes verantwortlich. Die Ergebnisse aus **Publikation I** ermöglichen mir die Differenzierung der *paddy soil* Entwicklung in drei Zeitintervalle, welche zusätzlich die Grundlage für ein integratives Manuskript darstellen (Kölbl et al., eingereicht). (1) Die Entwicklung der Tiefenverteilung der Lagerungsdichten im *paddy soil* Profil ist ein kurzfristiger Prozess von wenigen Jahrzehnten und bereits frühzeitig nach 50 Jahren der Pedogenese abgeschlossen. Das wiederum führt zu einer Entkoppelung von den im Ober- und Unterboden nachfolgenden Prozessen der Entkalkung und C_{org} -Akkumulation. (2) Die Entkalkung der *paddy soils* ist ein mittelschneller Prozess der Pedogenese. Der oberste A Horizont entkalkt innerhalb von 100 Jahren; die Entkalkung des kompletten Bodenprofils benötigt hingegen weitere Jahrhunderte und ist erst nach 700 Jahre abgeschlossen. (3) Die C_{org} -Akkumulation wird als langfristiger Prozess der Pedogenese eingestuft, da dieser über mehrere Jahrhunderte hinweg recht unterschiedlich in Ober- und Unterboden abläuft. Das Management der *paddy soils* begünstigt die C_{org} -Akkumulation im Oberboden, verzögert diese jedoch im Unterboden aufgrund der geringen Permeabilität der Pflugsohle.

Zusätzlich zur C_{org} -Akkumulation in den Bodenfraktionen der *paddy soils* (**Publikation I**), geht es in **Publikation II** um die Rolle der organo-mineralischen Assoziationen bei der C_{org} -Akkumulation. Eisen-(Fe)oxide interagieren mit der OBS und übernehmen somit eine bedeutende Rolle bei der Stabilisierung der OBS in organo-mineralischen Assoziationen. Beeinflusst werden diese Prozesse oftmals durch Bodenmanagement, Fruchtfolge und Bewässerung. Die Studie untersucht den Einfluss der Eisenoxide auf die C_{org} -Akkumulation im Oberboden während der Pedogenese. Zu den Zielen gehörten: (1) die Einschätzung, welchen Effekt beide Managementsysteme auf den Anteil des oxalatlöslichen Eisens (Fe_{ox}) haben. (2) Die Aufklärung, ob die vermutete Zunahme des Anteiles an Fe_{ox} in der *paddy soil* Chronosequenz zu einem höheren Anteil an stabilisierter OBS führt als in den *non-paddy soils*. (3) Die Bestimmung der Zusammensetzung der OBS in den *paddy* und *non-paddy*

soils und ob es während der *paddy soil* Entwicklung zu einer Akkumulation von Phenolen, welche aus Lignin hervorgehen, kommt.

Zusätzlich zur Bestimmung der C_{org} -Konzentration wurden die Gesamtböden sowie die Bodenfraktionen auf ihre Mineralogie und die Zusammensetzung der OBS untersucht. Die Festkörper ^{13}C Kernspinresonanzspektroskopie (NMR-Spektroskopie von englisch nuclear magnetic resonance) zeigt sowohl im Gesamtboden als auch in der Tonfraktion keine Unterschiede in der OBS-Zusammensetzung. Des Weiteren gab es weder in den *paddy* und *non-paddy soils* noch während der Pedogenese Unterschiede in der OBS-Zusammensetzung. Das *paddy soil* Management begünstigt keine selektive Anreicherung von Phenolen im Oberboden, sondern resultiert stattdessen in einer hohen C_{org} -Akkumulation während der Pedogenese. Weiterhin entsteht durch das Management eine *paddy soil* spezifische Formation an Eisenoxiden, welche weitestgehend verschieden zu der in den *non-paddy soils* ist. Dominiert werden die Oberböden der *paddy soils* durch oxalatlösliches Eisen und einem bedeutend geringeren Anteil an dithionitlöslichem Eisen (Fe_d)- Fe_{ox} . Die *non-paddy soils* hingegen sind durch einen hohen Anteil an Fe_d - Fe_{ox} charakterisiert. Bereits nach 50 Jahren Pedogenese war die *paddy*-spezifische Zusammensetzung an Eisenoxiden etabliert und der Anteil der Eisenoxide hat sich mit fortlaufender Entwicklung der *paddy soils* nicht verändert. Der hohe Anteil an Fe_{ox} in den *paddy soils* geht mit hohen C_{org} -Konzentration in der Feinschluff- und beiden Tonfraktionen einher. Aus der Literatur ist bereits eine gute Korrelation von OC und Fe_{ox} bekannt. Somit scheint die C_{org} -Akkumulation durch organo-mineralische Assoziationen, insbesondere durch die Assoziation mit Fe_{ox} , während der hier untersuchten Periode an *paddy soil* Entwicklung begünstigt. Die *paddy soils* besitzen bereits seit den frühesten Stadien der Pedogenese auch aufgrund der höheren Fe_{ox} -Anteile ein wesentlich höheres Potential zur C_{org} -Akkumulation als die *non-paddy soils*.

Mein Beitrag zu diesen neuen Befunden beinhaltet die Analyse der Oberboden OBS mittels Kernspinresonanzspektroskopie sowohl für die Gesamtböden als auch für die physikalischen Fraktionen der *paddy* und *non-paddy soils*. Somit kann die generelle Annahme für *paddy soils*, dass es zu einer Anreicherung von Phenole unter anaeroben Bedingungen aufgrund des gehemmten Abbaus kommt, widerlegt werden. Die C_{org} - und Eisenanteile auf der Ebene einzelner Fraktionen und deren zeitliche Entwicklung in den *paddy*- und *non-paddy* Oberböden wurden von mir bestimmt. Die Ergebnisse erlauben mir den C_{org} -Akkumulationsprozess der *paddy soils* von dem der *non-paddy soils* zu differenzieren. Dies ermöglicht die Schlussfolgerung, dass die C_{org} -Akkumulation durch Fe_{ox} -OBS Assoziationen in den *paddy soils* bereits in den frühesten Stadien der Pedogenese begünstigt wird und dass diese Böden demzufolge ein höheres Potential zur C_{org} -Akkumulation besitzen. Diese Ergebnisse liefern bedeutende Implikationen im Bezug auf die Beurteilung neuer Managementtechniken für *paddy soils*, wie alternierende Bewässerung bzw. Drainage (eine Technologie zur Wassereinsparung bei der Reisproduktion), da diese das Redoxsystem und somit auch wahrscheinlich die Eisenoxidzusammensetzung und damit das C_{org} -Speicherpotential von den *paddy soils* beeinflussen.

Das Konzept aus **Publikation II** wurde durch die Idee erweitert, dass die C_{org} -Akkumulation durch organo-mineralische Assoziationen aufgrund der beschleunigten Entkalkung während der Pedogenese in den *paddy soils* effektiver ist. Bestimmte bodenbildende Prozesse wie zum Beispiel die C_{org} -Akkumulation werden durch kalkhaltiges Ausgangsmaterial beeinflusst. Die Entkalkung eines Bodens gehört zu den Initialprozessen der Pedogenese. Erst nach Abschluss dieses Prozesses können Sekundärminerale gebildet werden, welche wiederum zusätzlich Oberflächen für die C_{org} -Belegung bereitstellen und somit zur C_{org} -Akkumulation beitragen. **Publikation III** befasst sich mit der C_{org} -Akkumulation durch organo-mineralische Assoziationen und fokussiert dabei auf die Zugänglichkeit der Mineraloberflächen für die C_{org} -Belegung. Zu den Untersuchungszielen gehörten: (1) die Beurteilung, ob die unterschiedliche Entkalkung von den *paddy* und *non-paddy soils* die C_{org} -Akkumulation kontrolliert und ob die Bildung von Tonmineralen und Eisenoxiden in entkalkten (*paddy*) Böden beschleunigt ist. (2) Die Bestimmung der C_{org} -Bedeckung von Tonmineralen und Eisenoxiden während der Pedogenese von *paddy* und *non-paddy soils*. (3) Die Klärung, ob Tonminerale und Eisenoxide zu gleichen Teilen zur C_{org} -Akkumulation beitragen.

Vor diesem Hintergrund wurden die spezifische Mineraloberfläche der gewonnenen Schluff- und Tonfraktionen mit Hilfe der Brunauer-Emmett-Teller (BET- N_2) Methode unter vier Bedingungen gemessen: unbehandelt, nach Entfernung der OBS, nach Entfernung der Eisenoxide und nach Entfernung von OBS und Eisenoxiden. Durch die selektive Entfernung von OBS sowie Eisenoxiden durch die Kombination der Behandlung mit Wasserstoffperoxid (H_2O_2) und Dithionit-Citrat-Bicarbonat (DCB) gelang es, die Zugänglichkeit der Silikat- bzw. Eisenoxidoberflächen für die C_{org} -Bedeckung zu bestimmen. Aufgrund des höheren C_{org} -Gehaltes in den *paddy soils* sind die unbehandelten Mineraloberflächen bedeutend kleiner als in den *non-paddy soils*. Die OBS Entfernung führt besonders in den *paddy soils* zu einem hohen C_{org} -Verlust in der Tonfraktion und zu deutlich größeren Mineraloberflächen als in den *non-paddy soils*.

Basierend auf diesen Ergebnissen und um das Verständnis von Mineraloberflächen und deren Belegung mit OBS zu illustrieren, ist der Effekt von H_2O_2 - und DCB Behandlung auf die spezifische Mineraloberfläche in einer schematischen Abbildung in **Publikation III** veranschaulicht. Mineraloberflächen, welche mit OBS belegt sind, werden durch die BET- N_2 Methode nicht erfasst. Auf reine Eisenoxide und Tonminerale, die frei von OBS vorliegen, scheint eine Behandlung mit H_2O_2 keinen Effekt zu haben. Ebenso bleibt die OBS, welche durch Aggregation mit Eisenoxiden oder Tonmineralen geschützt ist, von einer H_2O_2 Behandlung unbeeinflusst. Die Konzentration an Fe_d in der Tonfraktion ist niedrig und beträgt zwischen 1%–3%. Die Entfernung der Eisenoxide resultiert in einer Abnahme der spezifischen Mineraloberfläche in der Tonfraktion. Der Verlust an spezifischer Mineraloberfläche wird durch eine DCB Behandlung induziert, wenn Eisenoxide ohne den schützenden Effekt durch die OBS auftreten oder wenn die spezifische Mineraloberfläche der Tonminerale, welche mit Eisenoxide belegt ist, kleiner ist als die gesamte äußere Oberfläche der Eisenoxide. Die Entfernung der Eisenoxide im Anschluss an die H_2O_2 Behandlung resultiert jedoch in

einer Zunahme der spezifischen Mineraloberfläche und zeigt die größte Oberfläche für nahezu alle Schlufffraktionen sowie für *paddy* Feinton und *non-paddy* Grobton. Die Literatur beschreibt eine Disaggregation von Tonpartikel und Oxyhydroxiden durch die Entfernung der Eisenoxiden, welches wiederum zu einer bedeutenden Zunahme der spezifischen Mineraloberfläche führt. In den OBS-reichen *paddy soils* dieser Studie ist die beschriebene Disaggregation der Bodenaggregate erst nach Entfernung der schützenden OBS mit anschließender Entfernung der Eisenoxide erreicht worden.

Es gibt drei Hinweise dafür, dass hauptsächlich die spezifische Mineraloberfläche der Silikate an der C_{org} -Stabilisierung beteiligt ist: (1) die Fe_d Konzentration in der Tonfraktion ist sehr gering. (2) Es bestand keine Korrelation zwischen den konstanten Werten der Eisenoxide und der ansteigenden C_{org} -Konzentrationen. (3) Beide Behandlungen (H_2O_2 + DCB) zeigten zusammen einen höheren Effekt auf die spezifische Mineraloberfläche als einzeln angewendet, obwohl durch die DCB Behandlung die Oberfläche der Eisenoxide entfernt wurde. Entgegen der Erwartungen gab es keinen Hinweis auf eine zusätzliche Bildung von Sekundärmineralen während der Bodenentwicklung, welche somit zusätzlich Oberfläche zur C_{org} -Akkumulation zur Verfügung stellen würde. Die *paddy soils* sind durch eine beschleunigte Entkalkung, höhere C_{org} -Gehalte und einer deutlichen Akkumulation an jungem Kohlenstoff zusätzlich zum „alten“, ererbten Kohlenstoff charakterisiert. Nichtsdestotrotz dokumentiert die Studie erst nach Entkalkung der *paddy soils* eine höhere Belegung der Mineraloberflächen mit C_{org} . Im Gegensatz dazu scheinen die Mineraloberflächen der *non-paddy soils*, welche bedeutend langsamer entkalken, teilweise durch starke Mikroaggregation durch Zementierung mit Karbonat und Brückenbildung mit Ca^{2+} unzugänglich zu sein. Die beschleunigte Entkalkung der *paddy soils* führt zur verbesserten Zugänglichkeit der Mineraloberflächen für die C_{org} -Belegung, wodurch die C_{org} -Akkumulation wiederum seit den frühesten Entwicklungsstadien der *paddy soils* intensiviert ablaufen konnte.

Die selektive Entfernung von OBS und Eisenoxiden wurde in der Vergangenheit bei *paddy soils* noch nicht angewendet. Die Ergebnisse erlauben es mir den Prozess der C_{org} -Akkumulation in *paddy soils* von dem der *non-paddy soils* zu unterscheiden. Dies ermöglichte die Schlussfolgerung, dass die C_{org} -Belegung in den Oberböden der *paddy soils* höher ist, als in den *non-paddy soils*. Mein Leistungsbeitrag zu diesen Befunden ist die Identifikation von *paddy soil* spezifischen Bodenbildungsprozessen (**Publikation III**), welche äußerst verschieden zu den in den *non-paddy soils* sind:

- (1) Ein größerer Anteil an „jungem“ Kohlenstoff wird zum ererbten Kohlenstoff in den *paddy soil* hinzugefügt als in den *non-paddy soils*. Dieser bedeutende Anteil des C_{org} liegt in den *paddy soils* an silikatischen Mineraloberflächen gebunden vor.
- (2) Die Entkalkung des obersten A Horizontes war bereits nach 100 Jahren *paddy soil* Entwicklung beendet, während erst nach 700 Jahren das komplette *non-paddy soil* Profil entkalkt ist. Hieraus lässt sich vermuten, dass die C_{org} -Akkumulation aufgrund der starken

Aggregation mit Ca^{2+} -Brücken und durch Zementierung mit Karbonat reduziert wird, da hierdurch die spezifische Mineraloberfläche weniger zugänglich ist.

- (3) Die sich periodisch verändernden Redoxbedingungen und die höheren C_{org} -Gehalte in den *paddy soils* verursachen einen höheren Anteil von Fe_{ox} an Fe_{d} , was wiederum zu einer höheren C_{org} -Akkumulation beiträgt (vgl. **Publikation II**).

CONTENTS

SUMMARY	I
ZUSAMMENFASSUNG	VI
CONTENTS	XII
LIST OF FIGURES	XIV
LIST OF TABLES	XV
LIST OF PUBLICATIONS AND CONTRIBUTIONS	XVI
1 STATE OF THE ART AND OBJECTIVES.....	1
1.1 Soil formation and soil-forming factors.....	1
1.2 Soil chronosequences – a tool for studying soil formation.....	2
1.3 Paddy management influences soil formation.....	5
1.3.1 Rice cultivation.....	5
1.3.2 Land management for paddy rice cultivation.....	5
1.3.3 Paddy soils – man-made soils with special characteristics.....	7
1.3.4 Biogeochemistry of paddy soils.....	8
1.4 Objectives.....	11
2 MATERIAL & METHODS.....	13
2.1 Investigation area.....	13
2.1.1 Location and climate.....	13
2.1.2 Characterization of the soil chronosequences.....	13
2.1.3 Land management.....	14
2.2 Soils and sampling.....	14
2.2.1 Soil sampling	14
2.2.2 Soil description and horizons.....	15
2.3 Work schedule and methods.....	18
3 DISCUSSION.....	23
3.1 SOM accumulation in paddy soils is due to the strong OC accretion and high OC storage capacity in the <20 µm fraction.....	23
3.2 Paddy soil management favours high OC accumulation due to management-induced Fe oxide formation.....	24
3.3 Soil mineral surfaces of paddy soils are accessible for OC accumulation after decalcification.....	27

4 CONCLUSIONS & OUTLOOK.....	30
5 REFERENCES.....	31
6 ACKNOWLEDGMENT.....	39
APPENDIX.....	41
Publication I	
Publication II	
Publication III	
Curriculum vitae	
List of oral and poster presentations	

LIST OF FIGURES

Figure 1:	Soil formation is influenced by five factors: climate, parent material, organisms, topography, and time.	1
Figure 2:	Model of a post-incisive chronosequence. The bars represent time intervals of soil development (from Vreeken, 1975).	3
Figure 3:	Model of a pre-incisive chronosequence (from Vreeken, 1975).	3
Figure 4:	Model of a fully time-transgressive chronosequence with historical overlap of development of soil members (from Vreeken, 1975).	4
Figure 5:	Model of a fully time-transgressive chronosequence without historical overlap of development of soil members (from Vreeken, 1975).	4
Figure 6:	Flooded paddy rice field in the Cixi region (left) of the PR China and the traditional way of puddling by animals (right).	6
Figure 7:	The compacted plow pan is responsible for the standing irrigation water.	6
Figure 8:	Water outlet to control the height of standing irrigation water.	6
Figure 9:	Horizon sequence of a paddy soil according to FAO (2006) (Kögel-Knabner et al., 2010).	7
Figure 10:	Geographic position of the study area around the city Cixi in Eastern China, Zhejiang Province. Close-up view of sampling sites showing the paddy and non-paddy soil chronosequences; consisting of P 50, P 100, P 300, P 700; P 1000; P 2000 and NP 50, NP 100, NP 300, NP 700, respectively.	14
Figure 11:	Chronosequence of soil formation with soils used for growing lowland rice (paddy soils; 50, 100, 300, 700, 1000, 2000 years) in comparison to soils not used for rice (non-paddy soil; 50, 100, 300, 700 years). Soils were classified according to IUSS Working Group WRB 2006 (from Kölbl et al., submitted).	15

LIST OF TABLES

Table 1:	Overview of the applied methods and the determined soil parameters of Publication I.	19
Table 2:	Overview of the applied methods and the determined soil parameters of Publication II.	21
Table 3:	Overview of the applied methods and the determined soil parameters of Publication III.	22

LIST OF PUBLICATIONS & CONTRIBUTIONS

Research paper as first author

- I. **Wissing, L.**, Kölbl, A., Vogelsang, V., Fu, J., Cao, Z-H., Kögel-Knabner, I., 2011. Organic carbon accumulation in a 2000-year chronosequence of paddy soil evolution. *Catena* 87, 376–385.
- II. **Wissing, L.**, Kölbl, A., Häusler, W., Schad, P., Cao, Z-H., Kögel-Knabner, I., 2013. Management-induced organic carbon accumulation in paddy soils: The role of organo-mineral associations. *Soil Tillage Research* 126, 60–71.
- III. **Wissing, L.**, Kölbl, A., Schad, P., Bräuer, T., Cao, Z-H., Kögel-Knabner, I. (submitted for publication in *Geoderma*). Decalcification increases the accessibility of soil mineral surfaces for organic carbon accumulation in paddy soils.

The dissertation is based on the above named publications.

Research paper as co-author

- IV. Roth, P. J., Lehdorff, E., Cao, Z-H., Zhuang, S., Bannert, A., **Wissing, L.**, Schloter, M., Kögel-Knabner, I., Amelung, W., 2011. Accumulation of nitrogen and microbial residues during 2000 years of rice paddy and non-paddy soil development in the Yangtze River Delta, China. *Global Change Biology* 17 (11), 3405–3417.
- V. Bannert, A., Kleinedam, K., **Wissing, L.**, Müller-Niggemann, C., Vogelsang, V., Cao, Z-H., Schloter, M., 2011. Changes in diversity and functional gene abundances of microbial communities involved in nitrogen fixation, nitrification and denitrification comparing a tidal wetland to paddy soils cultivated for different time periods. *Applied and Environmental Microbiology* 77, 6109–6116.
- VI. Bannert, A., Müller-Niggemann, C., Kleinedam, K., **Wissing, L.**, Cao, Z-H., Schwark, L., Schloter, M., 2011. Comparison of lipid biomarker and gene abundance characterizing the archaeal ammonia-oxidizing community in flooded soils. *Biology and Fertility of Soils* 47, 839–843

- VII. Kalbitz, K., Kaiser, K., Fiedler, S., Kölbl, A., Amelung, W., Bräuer, T., Cao, Z-H., Don, A., Grootes, P., Jahn, R., Schwark, L., Vogelsang, V., **Wissing, L.**, Kögel-Knabner I., 2012 (Global Change Biology, doi: 10.1111/gcb.12080). The carbon count of 2000 years of rice cultivation.
- VIII. Kölbl, A., Schad, P., Jahn, R., Amelung, W., Bannert, A., Cao, Z.H., Fiedler, S., Kalbitz, K., Lehdorff, E., Müller-Niggemann, C., Schloter, M., Schwark, L., Vogelsang, V., **Wissing, L.**, Kögel-Knabner, I., (submitted for publication in *Geoderma*). Accelerated soil formation due to paddy management on marshlands (Zhejiang Province, China).

My contributions to the publications were the following:

- I. – III. I was involved in the sampling campaign in China and the sample preparation. Basic soil parameters were mainly determined and measured on my contribution. Further I was responsible for preparations of the data set, all calculations, graphical representations of the data and the statistical analysis. The preparation of the manuscripts is mainly based on my contribution.
- IV. – VIII. The measurements of total organic carbon data are based on my contribution. I was responsible for the calculation of the organic carbon data which was then provided by me for the publications.
- VII. Presented data of organic carbon for the depth distribution were calculated and provided by me for publication. The calculation of organic carbon stocks, including bulk density values, based on my contribution.
- VIII. The preparation of the manuscript chapter “Land management for paddy rice cultivation” is mainly based on my contribution.

1 STATE OF THE ART AND OBJECTIVES

1.1 Soil formation and soil-forming factors

Soils, soil properties and soil formation are affected by independent variables, commonly called “soil-forming factors”: climate, parent material, organisms, topography and time (Jenny, 1941; Veldkamp, 2005). The nature and importance of each of these soil-forming factors vary, and most soils are still in the process of change as shown in pedogenic profile differentiations and weathering (Veldkamp, 2005).

A sequence of soil-forming factors, processes and soil properties is underlying the soil formation (<http://www.soils.wisc.edu/courses/SS325/formation.gif>):

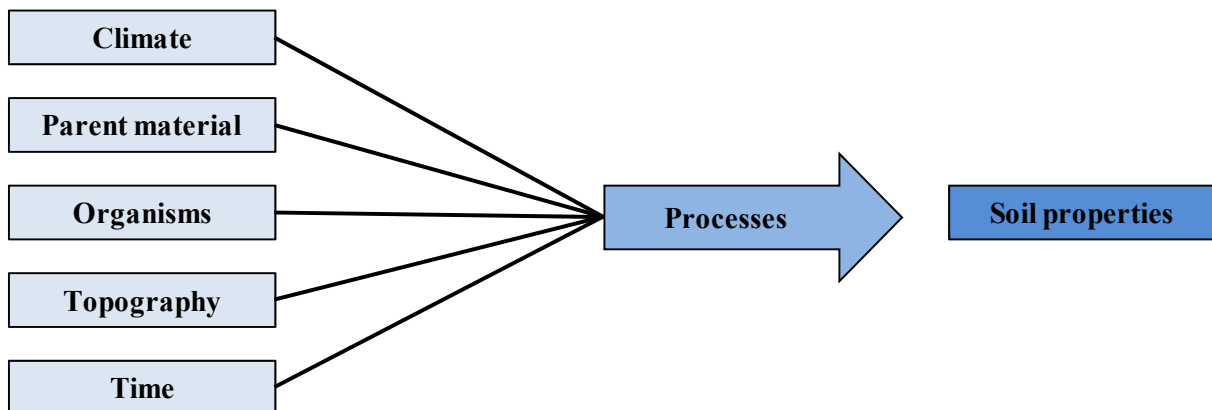
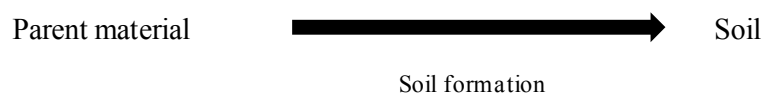


Figure 1: Soil formation is influenced by five factors: climate, parent material, organisms, topography, and time.

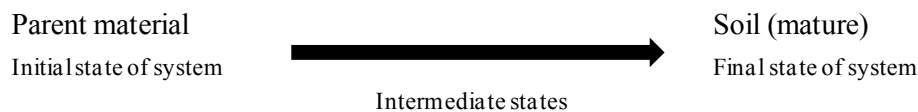
Jenny (1941) defined soil formation as the transformation of rock into soil. The relationship between soil formation, parent material and soil is expressed as (from Jenny, 1941):



The states of the soil system vary with time, and Jenny (1941) described the following time phases of soil formation: “Suppose we consider a piece of granite that is brought to the surface of the earth. In the interior of the earth, the granite may have been in equilibrium with its immediate surroundings; but

now, on the surface of the earth, granite is in an entirely new environment, and the rock system is highly unstable. It is continuously changing its properties in a definite direction, namely toward a new equilibrium state. When the final equilibrium state has been completed, the rock has become a mature soil. It is customary to designate the intermediate, unstable states as immature soil.”

In the following formulation, soil is treated as a dynamic system (from Jenny, 1941):



Soil properties and soil-forming processes strongly affect land use options. Not all forms of land use are possible on all soils, and certain uses require specific management strategies (Veldkamp, 2005).

The best opportunity for studying the effects of soil-forming factors is to investigate soil chronosequences, wherein four out of five soil-forming factors are constant or vary ineffectively (Stevens and Walker, 1970).

1.2 Soil chronosequences – a tool for studying soil formation

Soil chronosequences are defined as a genetically related set of sites formed from the same parent material (Harden, 1982; Walker et al., 2010) under similar conditions of climate, vegetation and topography (Harden, 1982). Vreeken (1975) described four types of soil chronosequences that differ in age: post-incisive sequences (Fig. 2), pre-incisive sequences (Fig. 3), fully time-transgressive sequences with partial historical overlap (Fig. 4) and fully time-transgressive sequences with no historical overlap (Fig. 5). The term incisive was first used by Meyer (1960) and indicates the geomorphic or anthropogenic incisions in the landscape that bury older surfaces, or create new surfaces, or both (Huggett, 1998).

The post-incisive chronosequence (Fig. 2): units of soils with different starting times of soil formation, but in all soils the development continues to present. In the pre-incisive chronosequence (Fig. 3), formation of all soils starts at the same time, but pedogenesis was interrupted at different moments by pre-incisive events like burying (Vreeken, 1975; Huggett, 1998).

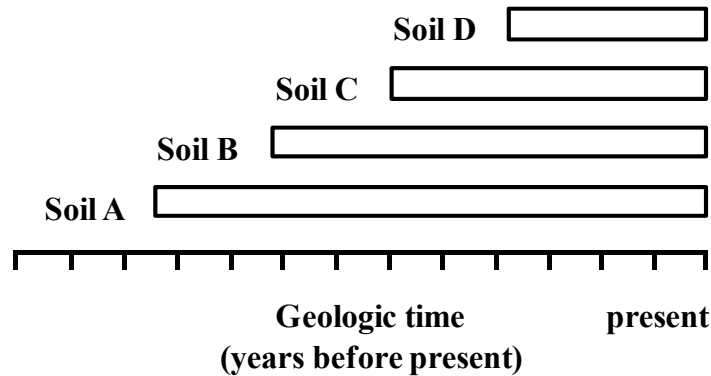


Figure 2: Model of a post-incisive chronosequence. The bars represent time intervals of soil development (from Vreeken, 1975).

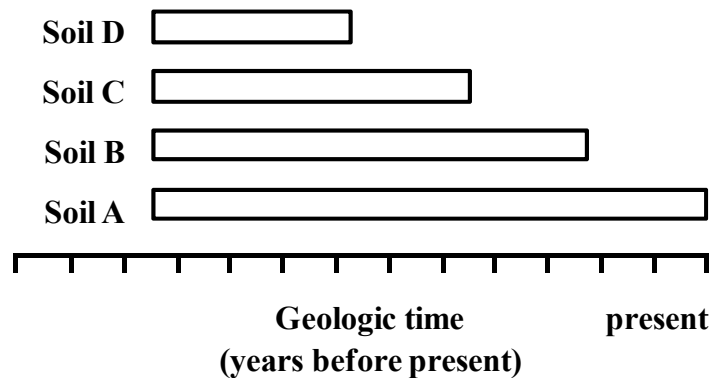


Figure 3: Model of a pre-incisive chronosequence (from Vreeken, 1975).

The fully time-transgressive chronosequence with partial historical overlap (Fig. 4) is characterized by different start times of pedogenesis, followed by some coeval evolution and ending with different stop times of pedogenesis.

In contrast, soils from a fully time-transgressive chronosequence with no historical overlap (Fig. 5) were never coeval (Vreeken, 1975; Huggett, 1998). Post-incisive chronosequences like sand dunes, glacial moraines, floodplains, river and marine terraces are the most common type of chronosequence (Huggett, 1998).

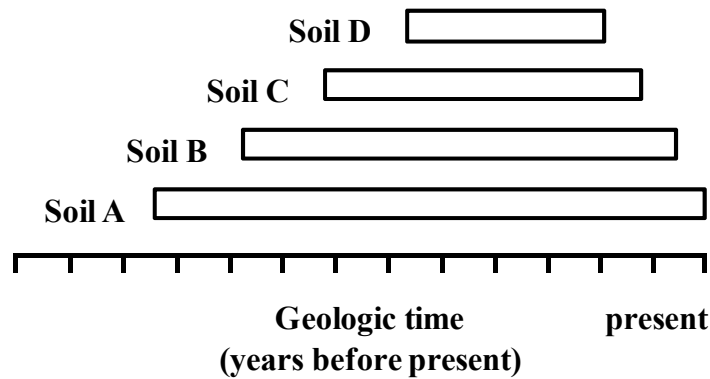


Figure 4: Model of a fully time-transgressive chronosequence with historical overlap of development of soil members (from Vreeken, 1975).

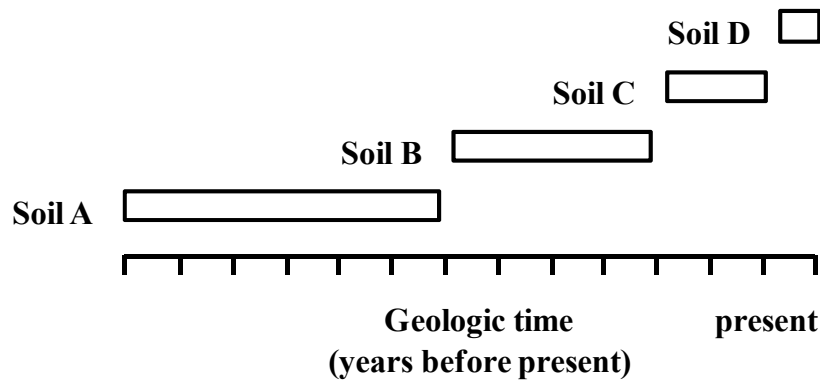


Figure 5: Model of a fully time-transgressive chronosequence without historical overlap of development of soil members (from Vreeken, 1975).

Soil chronosequences are perfect indicators for rate and direction of pedogenic changes and provide an important opportunity for studying temporal dynamics, ecological processes and soil evolution across multiple time scales (Walker et al., 2010). Chronosequences imply the presence of ecological succession (Walker et al., 2010).

Despite the variety of different chronosequences, Stevens and Walker (1970) mentioned that many sequences are similar. Similarities among several chronosequences are often more frequent than

differences, and many chronosequences which extend over sufficient periods of time show broadly similar trends (some examples selected from Stevens and Walker, 1970):

(i) Rapid initial changes are characterized mainly by accretion of organic matter (OM) in and above mineral topsoils. Depth gradients of a number of soil parameters were set up, such as pH, cation exchange capacity, contents of calcium carbonate and nitrogen (N). (ii) Eluviation-illuviation processes come to dominate pedogenesis and (iii) changes in the mechanical composition of soils play an important role. (iv) Nearly all chronosequence studies report that very early in the vegetation succession, plants with symbiotic bacteria capable of fixing atmospheric N are present.

1.3 Paddy management influences soil formation

1.3.1 Rice cultivation

Rice is one of the world's major crops and has fed a larger number of people for longer period of time than other crops (MacLean et al., 2002). World rice production in 2009 was approximately 700 million tons, with more than 90% produced in Asia (640 million tons) (http://www.irri.org/index.php?option=com_k2&view=item&id=9151&Itemid=100480&lang=en).

China is the world's largest rice producer, accounting for 30% of total world production, followed by India (22%), Indonesia (9%), and Bangladesh (7%) (<http://beta.irri.org/statistics>). Cultivated rice (*Oryza sativa*) is an annual grass that evolved from a semi-aquatic ancestor and because of its semi-aquatic ancestry; rice is extremely sensitive to water shortage (Kögel-Knabner et al., 2010). Therefore, rice is mostly grown on flooded lowland conditions. A large proportion of the total rice-growing area is flooded and banded (paddies) (Gaunt et al., 1995; Liesack et al., 2000; Kögel-Knabner et al., 2010) and worldwide, about 80 million ha of irrigated lowland rice provides 75% of the world's rice production

(http://www.irri.org/index.php?option=com_k2&view=item&id=9151&Itemid=100480&lang=en).

1.3.2 Land management for paddy rice cultivation

A specific feature of the paddy soil management is puddling, i. e., tilling the soil when waterlogged (Kögel-Knabner et al., 2010) before transplanting or seeding. The purpose of puddling rice soils is to break down aggregates, to intermix soils with fertilizer (Yoshida and Adachi, 2002), to reduce the water percolation by producing a nearly impermeable plow pan and so to retain standing water in the field (Painuli et al., 1988). Janssen and Lennartz (2006) showed that puddling reduces the percolation rate about 35-fold after 20 years and 175-fold after 100 years of paddy rice cultivation.

The need to minimize the percolation is especially important for rice systems that are either rainfed or only partially irrigated (Painuli et al., 1988). Generally, the puddling practice leads to a large-pored and less dense topsoil layer which overlies the plow pan and is able to store a high amount of irrigation water (Yoshida and Adachi, 2002; Mousavi et al., 2009). The irrigation water controls weeds, promotes oxidation-reduction cycles and creates a soft medium for transplanting rice-seedlings (Sanchez, 1973; de Datta and Kerim, 1974). The compacted plow pan is also the result of periodic puddling, which increases in strength and compaction during drying (IRRI, 1986).

The puddling is followed by transplanting the rice plants and growing them in a flooded environment from crop establishment until close to harvest (Gong, 1983; Sahrawat, 2005). The fields are usually discharged 10–15 days before the expected harvest date (Janssen and Lennartz, 2006).



Figure 6: Flooded paddy rice field in the Cixi region (left) of the PR China and the traditional way of puddling by animals (right).

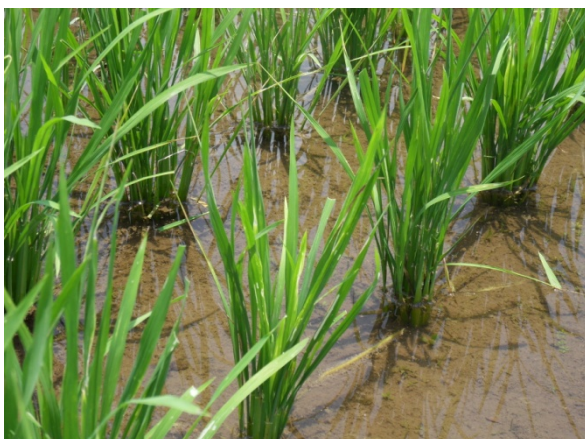


Figure 7: The compacted plow pan is responsible for the standing irrigation water.



Figure 8: Water outlet to control the height of standing irrigation water.

Paddy soils receive fertilization by organic matter (animal manure, rice straw and other crop residues, often fermented with sediments taken from the river or channel, but also charred residues) and liming (Cao et al., 2006; Gong, 1983; Kögel-Knabner et al., 2010). In the main rice-growing regions of China, the amount of organic manure applied has doubled since 1952, and it is assumed that organic manure and chemical fertilizers complement each other in intensive agriculture (Wen, 1984).

1.3.3 Paddy soils – man-made soils with special characteristics

Paddy soils are hydromorphic soils formed under intense land use (Gong, 1983), which causes the formation of specific soil properties. Long-term paddy management leads to Hydragric Anthrosols according to the World Reference Base for Soil Resources (IUSS Working Group, WRB 2007). The diagnostic horizons are an anthraquic horizon overlying a hydragric horizon, with a total minimum thickness of 50 cm. The anthraquic horizon develops rapidly whereas the formation of hydragric horizon takes longer time (Kölbl et al., submitted). The anthraquic horizon is at least 20 cm thick and consists of a puddled layer overlying a plow pan. The paddy-specific sequence of horizons is shown by Figure 9 (from Kögel-Knabner et al., 2010, modified):

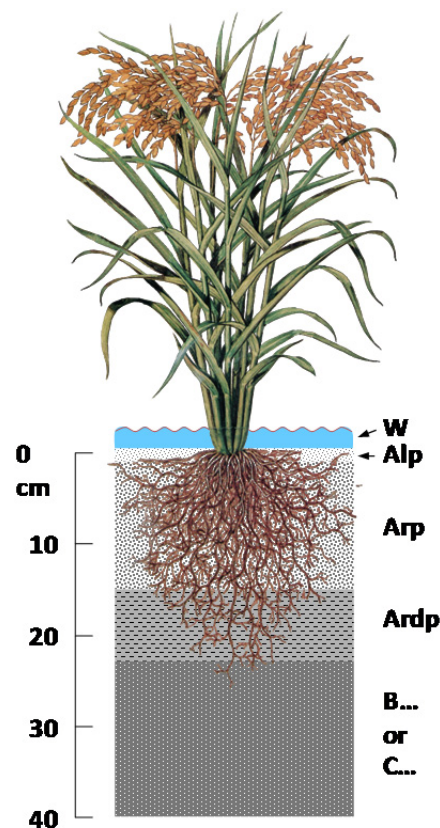


Figure 9: Horizon sequence of a paddy soil according to FAO (2006) (Kögel-Knabner et al., 2010).

The nomenclature of horizons is given according to FAO, 2006:

W: mainly oxic zone. Thin water layer caused by artificial submerging or irrigation water from rainfall. **Alp:** oxic and partly oxic zone. The thickness of this horizon ranges from several mm after irrigation to several cm when rice plants start to release oxygen from their roots (Frenzel et al., 1992). **Arp:** the major part of the upper anthraquic horizon; reduced puddled layer. The puddled layer shows sorted soil aggregates, vesicular pores, and a reduced matrix. **Ardp:** the lower part of the anthraquic horizon; plow pan. The plow pan has a laminar structure, a bulk density that is at least 20% higher than that of the puddled layer and, yellowish-brown, brown or reddish-brown iron (Fe)–manganese (Mn) mottles or coatings (IUSS Working Group, WRB 2007). **Bg:** reducing and oxidizing conditions, the latter especially inside the aggregates. The hydric horizon is characterized by the accumulation of Fe and Mn mobilized by the surface water that slowly penetrates the plow pan; in the Bg horizon, Fe–Mn eventually move to the interiors of the aggregates (Kölbl et al., submitted). The hydric horizon, Fe and Mn is at least 10 cm thick and shows Fe-Mn mottles or coatings or higher dithionite-citrate-bicarbonate (DCB) -extractable Fe or Mn or redox-depleted zones along macrospores (IUSS Working Group, WRB 2007).

1.3.4 Biogeochemistry of paddy soils

The redox conditions of paddy soils vary during cultivation, with anoxic conditions prevailing during the rice growing season. Between rice crops, artificial drainage leads to oxic conditions, and the soils are cultivated with upland crops or kept dry and fallow (Gaunt et al., 1995). The properties of paddy soils are influenced by the redox cycles of the water regime; it changes between submerged, puddled condition and drainage (Eickhorst and Tippkötter, 2009; Kögel-Knabner et al., 2010). The redox cycles induced by specific paddy soil management strategies have strong effects on long-term biogeochemical processes e.g., mineral weathering, mineral transformation in the presence of OM and accumulation and stabilization of soil organic matter (SOM) (Kögel-Knabner et al., 2010) and can result in permanent and temporary changes in soil properties (Bahmanyar, 2007). For example, Thompson et al. (2006b) observed an increasing crystallinity of Fe oxides during soil redox alternation (200–700 mV) in short-term batch experiments (56 days). The authors' findings fit very well with the observation that (1) pedogenic Fe (DCB-extractable iron (Fe_d)) and its ratio with total Fe (Fe_t) (i.e. Fe_d/Fe_t) increase with the length of paddy cultivation (Zhang and Gong, 2003). Thus, the physical, chemical and biological properties are different from those of upland soils (Li et al., 2005) used for cultivation of non-inundated crops.

The paddy management with rice cropping under flooded, anaerobic conditions is considered to favours the accumulation of SOM (Zhang and He, 2004; Sahrawat, 2004). The organic carbon (OC) accumulation in paddy ecosystems was studied by Wu (2011), showing that the ability to accumulate

OC is faster and more pronounced in paddy soils than in other arable ecosystems. Furthermore, in a study on surveying storage and sequestration potential of OC in China's paddy soils, Pan et al. (2003a) found higher topsoil OC contents than in corresponding soils in dry cropland. In a report on OC storage of soils in SE China, Zhao et al. (1997) identified paddy soils as an important SOM accumulator, with the second highest SOM stocks beside natural forest soils. However, the mechanisms of OC accumulation under paddy management are not well understood. The following is assumed in the literature for the higher OC accumulation in paddy soils than in non-inundated croplands:

(i) Paddy soils receive large carbon inputs via organic fertilizers and plant residues (Gong and Xu, 1990; Tanji et al., 2003).

(ii) Rice cropping under waterlogged conditions enhances the SOM accumulation (Neue et al., 1997; Lal, 2002). The decomposition rates of SOM are considered to be smaller under anaerobic conditions than under aerobic conditions (Sahrawat, 2004), resulting in SOM accumulation. Changes in SOM composition under rice cropping have been studied only in humic acid extracts (Olk et al., 1996, 1998, 2002; Mahieu et al., 2002), but physical fractions of paddy soils has not been investigated yet. Olk et al. (1996) and Smernik et al. (2004) showed an accumulation of lignin residues in paddy soil humic acids using solid-state ^{13}C NMR spectroscopic analysis. Lignin accumulation is considered to be caused by the resistance of the aromatic lignin structures to degradation under anaerobic conditions (Colberg, 1988; Olk et al., 2002). As a consequence of oxygen deficiency, phenolic functional groups are incorporated into young SOM fractions (Olk et al., 1996). Bierke et al. (2008) explained that adding crop residue under intensified rice cropping increases lignin-derived phenols, which may accumulate because of anaerobic conditions and incomplete decomposition.

(iii) Organo-mineral associations are considered to be the major mechanism of SOM stabilization (Balabane and Plante, 2004; Eusterhues et al., 2005) because organo-mineral associations are more resistant to biodegradation (Chenu and Plante, 2006).

A positive correlation between SOM and clay contents is described by several studies (Jenkinson and Rayner, 1977; Jenkinson et al., 1987; Bosatta and Agren, 1997). This is accredited to a slow turnover time of the clay-bound OM (Balesdent et al., 1987). Clay minerals, such as smectites and vermiculites, provide a high surface area up to $800 \text{ m}^2 \text{ g}^{-1}$ (Carter et al., 1986; Robert and Chenu, 1992) and in general stabilize more SOM than the sand fraction (Balabane and Plante, 2004). In a study on the relationship between mineral surfaces and OC concentrations, Mayer (1994) showed that the availability of the surface area controls its concentration of OM. Thus, the sorption to

mineral surfaces seems to be an important process in stabilization of SOM (Kaiser and Guggenberger, 2003).

Furthermore, a strong interaction between Fe oxides and SOM is established (Shang and Tiessen, 1998; Kaiser and Guggenberger, 2000; Kiem and Kögel-Knabner, 2002) and the following mechanisms for OC stabilization by Fe oxides are known: (1) OM stabilization due to protection of OM via soil aggregation induced by Fe oxides (Shang and Tiessen, 1998; Wagai and Mayer, 2007). (2) OM is stabilized by adsorption to the mineral surface of Fe oxides (Tipping, 1981; Wagai and Mayer, 2007). Especially, oxalate extractable Fe (Fe_{ox}) oxides are known to have a highly reactive mineral surface (Parfitt, 1989; Torn et al., 1997; Eusterhues et al., 2005), with values between 200 and $1200 \text{ m}^2 \text{ g}^{-1}$ (Bracewell et al., 1970; Borggaard, 1982; Parfitt, 1989) and are known to stabilize OC. (3) OM is stabilized by co-precipitation with Fe oxides (Eusterhues et al., 2011). It has been shown that OM bound to ferrihydrite (an oxalate extractable Fe oxide) is stabilized. In natural environments, ferrihydrite often forms in the presence of dissolved OM, which leads to co-precipitation of OM with ferrihydrite (Eusterhues et al., 2011). Co-precipitation is defined as the carrying down of a normally soluble substance as the consequence of another substance's precipitation by inclusion, occlusion, or adsorption (Eusterhues et al., 2011). Schwertmann et al. (2005) found that co-precipitation of ferrihydrite with dissolved OM lowered its crystallinity and may retard or inhibit the transformation of ferrihydrite into more crystalline forms.

The stabilization of SOM by association with Fe_{ox} has already been identified as a relevant feature in paddy soils (Pan et al., 2003a, 2003b). The literature provides little information about the crystallinity of Fe oxides in different soil fractions during pedogenesis. Only a few authors have investigated the distribution of Fe oxides between particle size fractions and found mainly increasing Fe_{d} and Fe_{ox} contents with decreasing size of soil fractions in oxic soils (Eusterhues et al., 2005; Pronk et al., 2011). The effect of long-term paddy rice management on Fe oxide formation and the accumulation of OC have not yet been investigated.

1.4 Objectives

The Research Unit “Biogeochemistry of paddy soil evolution” was granted by the German Research Foundation (DFG) in 2008 in order to gain a better understanding of the biogeochemistry of paddy rice soils. The interdisciplinary Research Unit 995 is comprised of different research teams and concentrated on the identification of the main processes involved in the formation of paddy soils.

Management-induced redox cycling is the specific and overall feature of paddy soils, which is considered to have strong effects on long-term biogeochemical processes e.g., mineral weathering and accumulation and stabilization of SOM. Paddy soils are characterized by preservation of OC predominately derived from rice plants itself, from manure or straw combustion residues, and from associated microbial consortia under at least periodically anaerobic conditions due to soil flooding. A major focus was to investigate the intensified weathering, (trans)formation and redistribution of soil minerals with increasing duration of paddy soil management and the associated OM composition and the OM depth gradients.

For this approach, the Hangzhou Bay (PR China), characterized by continuous land reclamation of coastal marine sediments derived from the Yangtze River, provides a unique setting with soil chronosequences of 50 to 2000 years of paddy soil management and of 50 to 700 years of non-inundated croplands. Based on the overall aims of the Research Unit, the focus of the investigation of the dissertation defined three major research topics with following objectives included:

Publication I: Organic carbon accumulation in a 2000-year chronosequence of paddy soil evolution

Considerable amounts of OC are stabilized in paddy soils, and thus a large proportion of terrestrial carbon is conserved in wetland rice soils. Based on a chronosequence of soil formation, the objective was to investigate the OC accumulation during paddy soil evolution. The question was: which role plays the fine mineral-associated fraction (<20 μm) for OC accumulation during aging of paddy soils? A particle size fractionation was used to identify the soil fractions, which are involved in OC accumulation. The objectives were to:

- (i) ... allocate the OC distribution within particle size fractions.
- (ii) ... identify those soil fractions, which are involved in OC accumulation depending on the duration of paddy soil evolution.
- (iii) ... investigate the OC saturation in the fine mineral-associated fraction.

Publication II: Management-induced organic carbon accumulation in paddy soils: The role of organo-mineral associations

Iron oxides strongly interact with OM in soils and play an important role in SOM stabilization due to organo-mineral associations. The SOM accumulation due to organo-mineral associations is often influenced by soil cultivation, crop rotation and irrigation. The study focused on the OC accumulation in association with Fe_{ox} , developed under paddy and non-paddy management. Therefore, the objectives were to:

- (i) ... assess the influence of both soil management systems on the proportion of Fe_{ox} .
- (ii) ... elucidate if presumably increasing Fe_{ox} proportions within the paddy soil chronosequence will lead to higher proportions of accumulated SOM than in non-paddy soils.
- (iii) ... investigate the SOM decomposition in paddy and non-paddy soils and if lignin-derived phenols will accumulate during paddy soil development.

Publication III: Decalcification increases the accessibility of soil mineral surfaces for organic carbon accumulation in paddy soils

Initial soil formation on calcareous marine sediments includes soil decalcification and OC accumulation. Decalcification of soils has to be completed before secondary minerals start to form (Talibudeen and Arambarri, 1964), providing additional mineral surfaces for SOM accumulation. The study focused on the accessibility of soil mineral surfaces for OC covering after decalcification. The objectives included to:

- (iv) ... investigate if decalcification controls the OC accumulation and if the formation of clay minerals and Fe oxides is accelerated in decalcified (paddy) soils.
- (v) ... estimate the OC covering of the clay mineral and Fe oxide surfaces during paddy and non-paddy soils development.
- (vi) ... elucidate if clay minerals and Fe (hydr) oxides contribute in equal amounts to the OC accumulation.

2 MATERIALS & METHODS

2.1 Investigation area

2.1.1 Location and climate

The study area is located in the eastern part of the PR China, near the city Cixi (30° 10' N, 121° 14' E), Zhejiang Province, approximately 180 km south of Shanghai and 150 km east of Hangzhou (**Publication I**: Fig. 1). The overall area covers 433 km² (in 1988), with a variation of altitude from 2.6 to 5.7 m above sea level (Zhang et al., 2004). The investigation region is influenced by river runoff and tide and the parent material consists of estuarine sediment, which originated from the Yangtze (Changjiang) River.

The climate is subtropical with periodical monsoon rain. Mean annual temperature is 16.3° C with an average range from 9.3° C to 38.5° C, and the mean annual precipitation is 1325 mm with highest values from April to October (Cheng et al., 2009). Due to a total evaporation of 1000 mm in this region, irrigation is needed to maintain standing water in certain periods of rice growing. More detailed information regarding ground water table, geography and geochemistry of the study area was described by Cheng et al. (2009).

2.1.2 Characterization of the soil chronosequences

The paddy (50 to 1000 years) and non-paddy (50 to 700 years) soil sequence was determined according to the record in the county annals of the Zhejiang Province. The county annals contain detailed information about the exact position and construction of dikes (Cheng et al., 2009). Information in Chinese is obtainable at <http://www.cixi.gov.cn/> (Cheng et al., 2009). The description of the 2000-years-old paddy site can be found in Zou et al. (2011).

The paddy chronosequence consists of 6 different stages: 50, 100, 300, 700, 1000 and 2000 years, which were named P 50, P 100, etc (**Publication I**: Fig. 1). The non-paddy soil sequence consists of 4 different age stages of soil development: 50, 100, 300 and 700 years, which are abbreviated NP 50, NP 100, etc (Fig. 10).

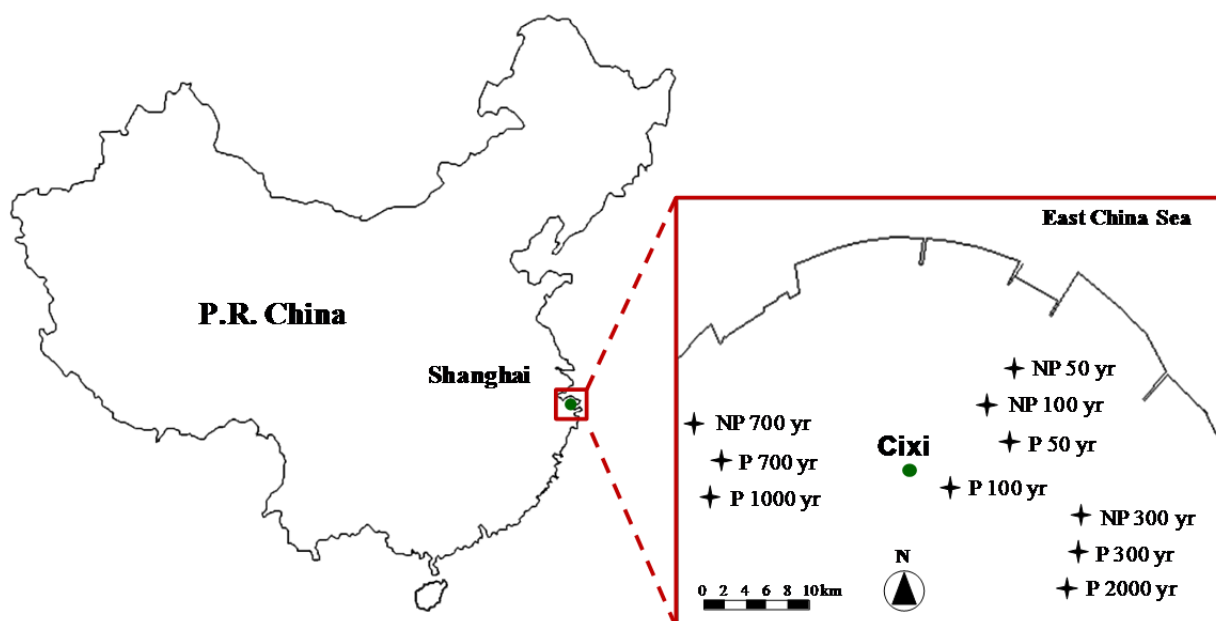


Figure 10: Geographic position of the study area around the city Cixi in Eastern China, Zhejiang Province. Close-up view of sampling sites showing the paddy and non-paddy soil chronosequences; consisting of P 50, P 100, P 300, P 700; P 1000; P 2000 and NP 50, NP 100, NP 300, NP 700, respectively.

2.1.3 Land management

During the past 2000 years, several dikes were built for land reclamation, which has resulted in a chronosequence of soils under agricultural use. Parts of the land were used more than 5 months per year (Zou et al., 2011) for irrigated paddy rice cultivation, followed by an upland crop (paddy soils). Other parts were used year-round for a variety of non-inundated upland crops e. g. cotton, wheat, barley, oil rape, broad bean and vegetables (non-paddy soils). From June until October, paddy soils are flooded, and thus the soils are under anoxic conditions. After drainage, soils are oxic and can be planted with non-inundated crops like oilseed rape, wheat and watermelons (Cheng et al., 2009).

2.2 Soils and sampling

2.2.1 Soil sampling

During a sampling campaign in June 2008, soil profiles of the chronosequences described above were sampled in triplicate from three adjacent independent fields (main site, subsite 1 and subsite 2). The fields had a distance of at least 50 m from each other and were sampled in comparable depth increments but guided by the diagnostic horizon (Kölbl et al., submitted). Soil profiles were excavated and the complete soils horizontally described according to the FAO Guidelines for Soil Description (FAO, 2006). All soils have been sampled under similar soil moisture and weather conditions in the field. From each horizon, bulk soil samples and additionally three undisturbed core samples were taken (core volume: 100 cm³).

2.2.2 Soil description and horizons

The soils were classified according to IUSS Working Group (WRB, 2007). The determination of the texture classes was done according to FAO (2006), ranging in paddy soils from Silt loam to Silty clay loam to Silty clay without trend throughout the chronosequence (**Publication I**: Table 1). The texture classes in non-paddy soils were Silt loam and Silty clay loam without trend throughout the chronosequence

The following soil types were identified (**Publication I**: revised from Wissing et al. (2011)): Endogleyic Anthraquic Cambisols (P 50, 100, 300) and Endogleyic Hydragric Anthrosols (P 700, 1000, 2000). Non-paddy soils are classified as Endogleyic Cambisols (NP 50, 100) and Haplic Cambisols (NP 300, 700). Figure 11 shows a photo series of all investigated soils:

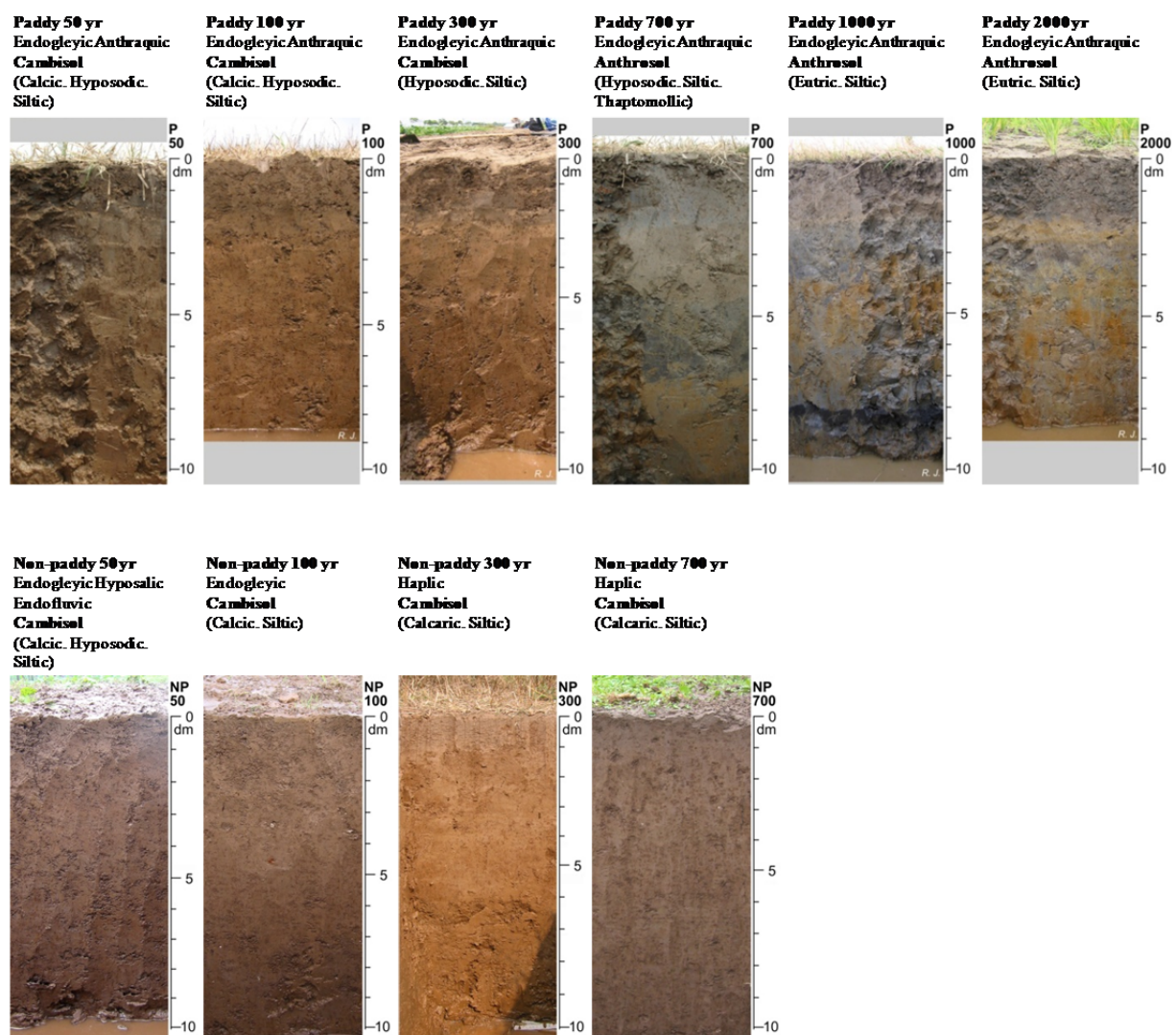


Figure 11: Chronosequence of soil formation with soils used for growing lowland rice (paddy soils; 50, 100, 300, 700, 1000, 2000 years) in comparison to soils not used for rice (non-paddy soil; 50, 100, 300, 700 years). Soils were classified according to WRB (2006) (from Kölbl et al., submitted).

The A horizon of all soils is darker than the underlying parts of the soil. In the paddy soils, these A horizons are subdivided into a loose puddled layer overlying a denser plough pan (section 1.3.3) which are both characterized by reduced matrix colours and intensively red oxide mottles in the root channels (Kölbl et al., submitted).

This less pronounced colour pattern is also found in the deeper subsoils of all paddy and the younger non-paddy profiles (NP 50, NP 100) (Kölbl et al., submitted). The subsoil is characterized by oxide concentrations in the interiors of the aggregates and reduced colours at the aggregate surfaces, especially in the older paddy soils (P 700, P 1000 and P 2000) (Kölbl et al., submitted). Buried A horizons appear in the older paddy soils (P 700, P 1000, P 2000), some of them being very dark (Kölbl, et al., submitted).

The investigated paddy soils consist of the following horizon sequence: The puddled horizon(s) and the plough pan (A horizons) represent the topsoil, with the following subordinate characteristics (FAO, 2006): d = dense layer; l = capillary fringe mottling; p = ploughing or other human influence; r = strong reduction. In the subsoil, down to 130 cm, several B horizons were identified (B horizons: b = buried genetic horizon; g = stagnic conditions; h = accumulation of OM; l = capillary fringe mottling; w = development of colour or structure). The non-paddy soils consist of the following horizon sequence: The puddled horizon(s) (A horizons) represent the topsoil, with the following subordinate characteristics (FAO, 2006): p = ploughing or other human influence; h = accumulation of OM. NP 50 has a transition horizon (AB). In the subsoil, down to 100 cm, several B horizons were identified (B horizons: b = buried genetic horizon; g = stagnic conditions; l = capillary fringe mottling; w = development of colour or structure).

The study discusses the basic soil parameters of the paddy bulk soil samples (mean of main site, subsite 1 and subsite 2) throughout the entire soil profile (**Publication I**: Table 1). To focus on the mechanisms of OC accumulation in paddy and non-paddy topsoils, selected parameters of the physical soil fractions were analyzed on the uppermost A horizon of the main site (**Publication II** and **III**). Where the upper part of the Alp horizon in paddy soils had more pronounced redox features, a differentiation was made into Alp1 and Alp2, and only the Alp1 was analyzed (**Publication II** and **III**). Similarly, thick Ap horizons in non-paddy soils were subdivided into Ap1 and Ap2, analyzing here only the Ap1 (**Publication II** and **III**).

The redox potential (Eh) of paddy soils was measured of the Institute for Agricultural and Nutritional Sciences at the Martin-Luther University of Halle-Wittenberg. Eh dynamics were monitored during one entire paddy–winter crop cycle (March 2009 to March 2010). Redox measurements were done manually (daily after flooding and biweekly after drainage of the fields), using a portable pH/Eh-meter (Kölbl et al., submitted). The Eh values in the uppermost 10 cm of the paddy soils ranged between 570

mV and -12 mV during the upland crop phase and -170 mV to -200 mV during the paddy soil phase invariably in young (P 100), medium (P 700) and old paddy soils (P 2000) (personal communication Vanessa Vogelsang, Sabine Fiedler).

2.3 Work schedule and methods

The study investigated the evolution of mineral-associated OM in a chronosequence of paddy soil use during the duration of management-induced paddy soil formation compared to soil formation under upland crops. The approach consists of laboratory assessment of SOM and mineralogy composition in paddy and non-paddy soils and to establish a concept on the OC accumulation in paddy soils. Focused on the objectives of the study (section 1.4), a work schedule consisting of the following major components, was conceived:

- Adaptation of established fractionation procedures to the paddy and non-paddy soil materials.
- Characterization of bulk SOM and SOM in fractions from soil profiles at the chronosequence sites.
- Characterisation of the soil mineral phase with respect to its OM-binding specifications.

Based on the work schedule, the methods listed below, were applied to determine different soil parameters.

In **Publication I**, the study combined the OC accumulation in the paddy soil profile, developed within 2000 years of soil management, with data on inorganic carbon (IC) and OC stock (**Publication I**: Table 1). Further, a fractionation scheme according to particle-size was adapted to the paddy soils to isolate specific mineral soil fractions which were obtained after dispersion by sonication and by sedimentation in Atterberg cylinders. Only the topsoils (A horizons) were fractionated, because they were characterized by the highest bulk soil OC concentrations. The following six soil fractions were isolated: sand and particulate organic matter (2000 μm –63 μm), coarse silt (63 μm –20 μm), medium silt (20 μm –6.3 μm), fine silt (6.3 μm –2.0 μm), coarse clay (2.0 μm –0.2 μm) and fine clay (<0.2 μm). Afterwards, the mass proportion and OC contribution of the fractions to the bulk soil were determined (**Publication I**: Fig. 3a; b; c and d; Fig. 4a; b). Actual OC saturation was calculated to assess the OC accrual of the fine mineral fractions (<20 μm) during paddy soil evolution. The calculated values were compared with the potential OC saturation according to the empirical equation of Hassink (1997) (**Publication I**: Fig. 4a; b) in order to evaluate the maximum possible OC storage capacity in paddy soils.

The applied methods and the determined soil parameters of **Publication I** are summarized in table 1.

Table 1: Overview of the applied methods and the determined soil parameters of Publication I.

Publication I: Organic carbon accumulation in a 2000-year chronosequence of paddy soil evolution	
Objectives were to	<p>(i) ... allocate the OC distribution within particle size fractions.</p> <p>(ii) ... identify soil fractions which are involved in OC accumulation depending on the duration of paddy soil evolution.</p> <p>(iii) ... investigate the OC saturation in the fine mineral-associated fraction.</p>
Methods + parameters	<p>Profile parameters (main site, subsite I and subsite II)</p> <ul style="list-style-type: none"> • Texture class according to FAO (2006) • Bulk density by dividing oven-dried soil mass by the core volume • Total carbon (C_{tot}) concentration by dry combustion with a Vario EL elemental analyzer (Elementar Analysensysteme, Hanau, Germany) • IC concentration by dissolution of carbonates with 42% phosphoric acid and subsequent infrared detection of the evolving CO_2 (C-MAT 550 Ströhlein GmbH, Viersen, Germany) • OC concentration by subtracting the content of IC from C_{tot} • OC stocks by multiplying the OC content with bulk density and the horizon thickness • Statistical analyses by using SPSS Statistics 19 (IBM SPSS Company) • Physical fractionation according to particle size of the A horizons and carbonate removal with hydrochloric acid (HCL) (main site) <p>Soil fraction parameters (A horizons) (main site)</p> <ul style="list-style-type: none"> • OC concentration by dry combustion with elemental analyzer (EuroEA Elemental Analyzer 3000, HEKAtech, Wegberg, Germany) • Mass distribution to the bulk soil • OC contribution to the bulk soil by multiplying the mass of the individual fraction with the OC concentration • Actual OC saturation by adding up the OC contributions of the <20 μm fraction • Potential OC saturation according to the empirical equation of Hassink (1996)

Paddy and corresponding non-inundated non-paddy soils are characterized by markedly different managements (section 1.3.2) which cause special soil properties (section 1.3.3). Therefore, **Publication II** focused on the comparison of the chemical SOM composition and the soil mineralogy of paddy and non-paddy soils to assess the effect of Fe oxides on topsoil OC accumulation during soil development. The bulk soil samples and the isolated clay fractions of the uppermost A horizon have been analyzed for their SOM composition by solid-state ^{13}C NMR spectroscopy (**Publication II**: Fig. 1 and 2). Clay minerals were characterized by X-ray diffraction (XRD) (**Publication II**: Fig. 4a; b). Fe_d of the isolated soil fractions were determined by using the DCB method according to Mehra and Jackson (1960) and the proportion Fe_{ox} were extracted using the oxalate method of Schwertmann (1964) (**Publication II**: Table 3; Fig. 3a; b). Further, to evaluate the effect of the presence of Fe oxides on OM accumulation, the study investigated the relationship between the content of Fe_{ox} and the OC concentration (**Publication II**: Fig. 5).

The applied methods and the determined soil parameters of **Publication II** are summarized in table 2.

Table 2: Overview of the applied methods and the determined soil parameters of Publication II.

Publication II: Management-induced organic carbon accumulation in paddy soils: The role of organo-mineral associations	
Objectives were to	<p>(i) ... assess the influence of both soil management systems on the Fe_{ox} proportion.</p> <p>(ii) ... elucidate if presumably increasing Fe_{ox} proportions within the paddy soil chronosequence will lead to higher proportions of accumulated SOM than in non-paddy soils.</p> <p>(iii) ... determine the SOM decomposition in paddy and non-paddy soils and if lignin-derived phenols will accumulate during paddy soil development.</p>
Methods + parameters	<p>Bulk soil parameters (uppermost A horizon) (main site)</p> <ul style="list-style-type: none"> • pH values • Soil mineralogy Fe_d and Fe_{ox} concentration: oxide extraction by DCB method according to Mehra and Jackson (1960) and oxalate treatment according to Schwertmann (1964) • Soil texture after dissolution of carbonates with HCL and OM oxidation by hydrogen peroxide (H₂O₂) treatment • SOM composition by solid-state CPMAS ¹³C NMR spectroscopy (Bruker Biospin DSX 200 NMR spectrometer, Rheinstetten, Germany) after destruction of the mineral phase by treatment with hydrofluoric acid (HF) • Statistical analyses by using SPSS Statistics 19 (IBM SPSS Company) <p>Soil fraction parameters (A horizons) (main site)</p> <ul style="list-style-type: none"> • Soil mineralogy Fe_d and Fe_{ox} concentration: (see above) of the <20 µm fraction Clay minerals by XRD (Philips PW 1070 diffractometer) after OM oxidation by H₂O₂ treatment of the <2 µm fraction • SOM composition (see above) of the <6.3 µm fraction • Statistical analyses by using SPSS Statistics 19 (IBM SPSS Company)

One of the first soil forming processes on calcareous parent material is decalcification which has to be completed before secondary minerals start to form (Talibudeen and Arambarri, 1964), providing additional mineral surfaces for OM accumulation. Therefore, **Publication III** focused on OC covering of the specific surfaces area (SSA) of soil minerals during soil development on calcareous parent material. The SSA of clay minerals and Fe oxides were measured by Brunauer-Emmett-Teller (BET-N₂) method (Brunauer et al., 1938) (**Publication III**: Fig. 1). To investigate the accessibility of those mineral surfaces for OC covering during pedogenesis, we used selective removal of OM and Fe oxides by combining H₂O₂ and DCB treatments (**Publication III**: Table 4). The applied methods and the determined soil parameters of **Publication III** are summarized in table 3.

Table 3: Overview of the applied methods and the determined soil parameters of Publication III.

Publication III: Decalcification increases the accessibility of soil mineral surfaces for organic carbon accumulation in paddy soils	
Objectives were to	(i) ... investigate if the rates of decalcification control the OC accumulation and if the formation of clay minerals and Fe oxides accelerated in decalcified (paddy) soils. (ii) ... estimate the OC covering of the clay mineral and Fe oxide surfaces during paddy and non-paddy soils development. (iii) ... elucidate if clay minerals and iron (hydr) oxides contribute in equal amounts to the OC accumulation.
Methods + parameters	Bulk soil parameters (uppermost A horizon) (main site) <ul style="list-style-type: none"> ● Base saturation ● Radiocarbon (¹⁴C) concentration was determined with a 3 Million Volt HVE Tandatron accelerator mass spectrometry system Soil fraction parameters (A horizons) (main site) <ul style="list-style-type: none"> ● ¹⁴C concentration (see above) of the <0.2 μm fraction ● Specific surface area (SSA) by N₂-BET method of the <20 μm fraction (Brunauer et al., 1938) <ul style="list-style-type: none"> SSA on untreated samples SSA after H₂O₂ treatment SSA after DCB treatment SSA after H₂O₂ and DCB treatment ● Statistical analyses by using SPSS Statistics 19 (IBM SPSS Company)

3 DISCUSSION

3.1 SOM accumulation in paddy soils is due to the strong OC accretion and high OC storage capacity in the <20 µm fraction

The paddy topsoils are characterized by increasing OC concentrations and –stocks (**Publication I**: Table 1 and Fig. 2), but the OC amount in the 2000–63 µm fraction remained constant during pedogenesis. The literature provides two options why paddy management favours the accumulation of OC: (1) paddy soils obtain high inputs of OC (Gong and Xu, 1990; Tanji et al., 2003) and (2) the management of the soils seems to retard the OC decomposition (Neue et al., 1997; Sahrawat, 2004), both leading to an enhanced OC accumulation. Therefore, **Publication I** focused on the mechanisms of OC accumulation and on the identification of those soil fractions, which are responsible for OC accumulation during paddy soil evolution.

The topsoil OC accumulation during 2000 years of paddy soil formation is due to strong OC accretion in the coarse and medium silt fraction (**Publication I**: Fig. 3c; d) and the large OC storage capacity in the coarse clay fraction (**Publication I**: Fig. 4a; b). The chronosequence approach in combination with the physical fractionation confirms different OC accretions for silt- and clay-sized fractions. Coarse and medium silt were identified as an important long-term OC sink during paddy soil evolution. These fractions showed the largest OC accretions, starting with low initial OC contributions in the “young” paddy soils, which increased to a high OC contribution in the 2000-years-old paddy site (**Publication I**: Fig. 3c; d). However, coarse and medium silt are characterized by still lower absolute OC amounts after 2000 years of soil evolution than coarse clay. Coarse clay presented the highest OC storage capacity and absolute OC amounts of all fractions (**Publication I**: Fig. 4a; b) and is the most important fraction for OC accumulation during soil evolution. This is in line with findings of Chivenge et al. (2007), who described the clay-sized fraction as the most stable soil fraction for OC accumulation.

The strong OC accretion in coarse and medium silt is explained by the formation of silt-sized microaggregates, which are known to have more OC per unit material because additional OC binds the primary organo-mineral complexes into silt-sized aggregates (Tisdall and Oades, 1982; Six et al., 2002). Huang et al. (2010) mentioned that OC in the silt-sized fraction is physically protected by microaggregates and chemically by silt particles. It is further assumed that the retarded OC decomposition under waterlogged conditions during several months of the year is responsible for OC accumulation (Kögel-Knabner et al., 2010), also in coarser particle size fractions.

In contrast, fine clay seems to be already saturated after 50 years of soil evolution because the OC contributions are very low and changed only slightly during 2000 years of paddy soil evolution (**Publication I**: Fig. 3c; d and Fig. 4a; b). Von Lützow et al. (2007) already observed that fine clay does not always follow the usual distribution of higher OC contributions with declining particle sizes and the authors further mentioned that the dispersion procedures during physical fractionation could

lead to an incomplete disaggregation of the particles. Therefore, coarse clay fractions could consist of aggregated fine clay particles which protected SOM, which may contribute to the observed higher OC concentrations in the coarse clay fraction. A second possible explanation relates to the different OC storage capacities in clay subfractions due to a shift in the mineral composition and a resulting selective adsorption of SOM with different functional groups on specific clay minerals (Laird et al., 2001).

The potential OC saturation of the soil fractions $<20\ \mu\text{m}$ remained constant over the years of paddy soil evolution when calculated with the empirical equation of Hassink (1997) (**Publication I**: small graphs in Fig. 4a; b). This is due to the fact that the mineral composition and texture do not change during the evolution of the paddy soils in the chronosequence studied here (see **Publication II** and **Publication III**). The calculated actual OC saturation values were much lower than the potential OC saturation. The correlation between the years of paddy soil evolution and actual OC saturation did not reach the calculated maximum (potential OC saturation), indicating a deceleration of OC accumulation over time (**Publication I**: Fig. 4a; b). Silt and clay fractions are important OC accumulators, and Hassink (1997) explained the more effective OC association of the soil fractions $<20\ \mu\text{m}$ by the greater physical protection of SOM against decomposition. Hassink (1997) determined the potential OC saturation using grassland soils but other studies do not reach the calculated maxima (Steffens et al., 2009); therefore a re-evaluation and an adjustment of the potential OC saturation is necessary for paddy soils.

To summarize, OC accumulation in the paddy topsoils occurs in two different soil pools. Large amounts of OC accumulate in the coarse and medium silt fraction due to their high OC accretion during paddy soil evolution. The highest absolute OC amounts of all soil fractions accumulate in the coarse clay fraction, because this fraction has the largest capacity for OC accumulation.

3.2 Paddy soil management favours high OC accumulation due to management-induced Fe oxide formation

In addition to the investigation on the chronological OC accumulation in the paddy soil fractions and based on the results from (**Publication I**), **Publication II** focused on the role of organo-mineral associations in OC accumulation. Before discussing the OC associated with the clay fractions, it is important to elucidate in detail the mineralogy of the clay-sized fraction in the paddy and non-paddy soils.

XRD analyses (**Publication II**: Fig. 4a; b) emphasize that the clay mineralogy in paddy- and non-paddy soils is similar. Both management systems did not induce further changes in clay mineralogy during soil development as the clay mineralogy did not change from tidal flat (0 years) over marshland (30 years) (Kölbl et al., submitted) to paddy/non-paddy soil development over 2000/700 years.

Secondary clay minerals, e.g., mixed layer minerals and secondary chlorites were already present in the 50-years-old paddy site (**Publication III**: Table 3). The parent material consists of estuarine sediment, which originated from the Yangtze (Changjiang) River and is deposited along the Zhejiang region. With a sediment load of ca. 480 million tons per year, (Milliman and Meade, 1983; Milliman and Syvitski, 1992) the Yangtze is the dominant source of sediment delivered to the East China Sea (Wang et al. 2008). After passing the Yangtze delta, the sediments are re-deposited into the Hangzhou Bay under the influence of the Taiwan Warm Current and the Zhejiang–Fujian Coastal Current (Jilan and Kangshan, 1989; Guo et al., 2000; Xie et al., 2009).

In contrast to non-paddy soils, the paddy soil chronosequence is dominated by Fe_{ox} (**Publication II**: Fig. 3a), indicating that the management of the paddy soils creates an environment of Fe oxide formation which is different to those in non-paddy soils (**Publication II**: Fig. 3b). Few studies were carried out on the mineralogy of Fe oxides in soils subjected to alternating oxic and anoxic conditions. Sah et al. (1989) inferred that repeated periods of flooding and drainage increased the precipitation of Fe as Fe_{ox} oxides. Zhang and Lin (2002) and Zhang et al. (2003) reported in incubation experiments the transformation to higher Fe_{ox} proportions after soil flooding, resulting in a gradual reduction of the ratio of Fe_{ox} to Fe_{d} with time. The authors point out that the Fe_{ox} formation under flooded conditions is not understood yet. It was assumed that crystalline Fe oxides might partially be transformed to lower crystalline phase (Zhang et al., 2003). However, selective chemical extractions of Fe in the above studies are not mineral specific. An interpretation of Fe_{ox} data is not possible as long as the oxidation state of Fe_{ox} is unknown (Hearn et al., 1983) and therefore, their significance is limited. More recent studies determined the oxidation state of Fe with Mössbauer spectroscopy and nanocrystalline goethite was found rather than the assumed ferrihydrite in lacustrine and marine sediments (van der Zee et al., 2003). Wang et al. (1992) investigated Fe oxide minerals with Mössbauer spectroscopy and described that hematite in the parent material is dissolved by reduction and complexation, and then parts of them were oxidized and crystallized into goethite. So the authors could show the transformation of hematite to goethite during paddy soil formation. Thompson et al. (2006b) showed by Mössbauer spectroscopy the transformation of short-range ordered Fe minerals (e.g., nano-goethite) to micro-crystalline goethite and micro-crystalline hematite and the authors demonstrated that Fe oxide crystallinity increases during redox oscillations. Results from Mössbauer spectroscopy of Mansfeldt et al. (2011) indicated that under flooded, anaerobic conditions goethite rather than ferrihydrite is the predominate Fe oxide in the subsoil of an Fe-rich lowland Gleysol (Petrogleyic). The authors further mentioned that goethite occurs mainly as small particles, e. g., as nano-goethite. Van der Zee et al. (2003) investigated Fe oxide mineralogy by Mössbauer spectroscopy and postulated that diagenetic Fe cycling near the oxic–anoxic boundaries of lake and marine sediments occurs under conditions that directly lead to goethite precipitation, with growth poisoning from co-precipitation to produce nanoscale crystallites. The authors found a mean sediment nano-goethite size of only 5 nm and mentioned that these sizes are comparable to the values 1–3 nm for natural and synthetic two line ferrihydrites. Chemical extraction

methods are not mineral selective. For example, acid-ammonium oxalate dissolves not only ferrihydrite but also for the most part, if not completely, goethite with very small particle size, e.g., nano-goethite (see Cornell and Schwertmann 2003; Thompson et al. 2006b; 2011). Mansfeldt et al. (2011) had repeatedly pointed out that the extraction with oxalate is not specifically selective for ferrihydrite. Iron associated with OM will also be extracted by oxalate. This might be of major importance in the uppermost OM-rich soil horizons in paddy soils of the present study. Overall, oxalate extractable Fe in paddy soils may consist of ferrihydrite as well as nano-goethite.

Paddy management did not induce differences in the clay fraction, except for the Fe oxides. Paddy management leads to higher proportions of Fe_{ox} in clay-sized fractions than in those of non-paddy soils, which have a predominantly aerobic regime of Fe oxide formation, characterized by higher proportions of Fe_d-Fe_{ox} in the fine mineral fractions.

This higher Fe_{ox} proportion in paddy soils is associated with higher OC concentrations in the fine silt- and both clay fractions compared to the non-paddy soils (**Publication II**: Fig. 5). In contrast, the non-paddy soil fractions have lower proportions of Fe_{ox}, resulting in smaller OC concentrations in all soil fractions (**Publication II**: Fig. 5). Correlations of OC with Fe_{ox} have already been identified as a relevant feature in paddy soils (Pan et al., 2003b). Zhang and Lin (2002) also found a higher ratio of Fe_{ox}/Fe_d with ongoing paddy soil management and higher OC contents with longer paddy rice cultivation. Soils with high OC content contain more organic acids, which may have an inhibitory effect on crystallization and lead to retardation of Fe oxide crystallization (Schwertmann, 1966; Schwertmann et al., 1982). The paddy management induces the preferred formation of Fe_{ox} in early stages of soil development, leading to a higher ratio of Fe_{ox}/Fe_d. This favours the formation of Fe_{ox}-OM associations during the entire period of paddy soil evolution investigated in this study. Oxalate extractable Fe oxides (e.g., ferrihydrite and the above mentioned nano-goethite) are known to have a large mineral surface (Borggaard, 1982; Adams and Kassim, 1984; Kiem and Kögel-Knabner, 2002; Wagai and Mayer, 2007). Because of the higher Fe_{ox} content, the potential to accumulate OC is more pronounced in paddy clay fractions than in non-paddy soils.

Different management and thus different conditions of Fe oxide formation may affect the SOM composition in paddy soils compared to non-paddy soils. However, SOM composition does not significantly differ either between paddy and non-paddy soils or during soil development (**Publication II**: Fig. 1 and 2). The long-term rice cropping management results in higher OC content but does not affect the SOM composition with ongoing pedogenesis. Changes in SOM composition under rice cropping have been studied only in humic acid extracts (Olk et al., 1996, 1998; Mahieu et al., 2002), but physical fractions of paddy soils have not been investigated yet. Results of the present study are in contrast to results from Olk et al. (1996; 1998), who measured with solid-state ¹³C NMR an accumulation of phenolic compounds in humic acid extracts. The authors ascribed the clear change in

the chemical nature of SOM to the intensive rice cropping with more than once rice per year. Also, Bierke et al. (2008) demonstrated that multiple annual rice cropping systems (two or three times rice per year) shorten the fallow period, which reduces the time for aerobic degradation of lignin-derived phenols and crop residues. In contrast to these studies, a selective enrichment of lignin-derived phenols has not been found by solid-state ^{13}C NMR in the paddy soil fractions, even for long-term paddy soil management. The crop rotation in the investigated area was rice cropping only once per year for about five months and thus a relatively longer periods of aeration compared to multiple annual rice cropping systems may prevent the selective enrichment of lignin-derived phenols in paddy soils. The aryl-C chemical-shift region is remarkably similar for paddy and non-paddy mineral fractions $<2\ \mu\text{m}$ and does not show a specific accumulation of condensed aromatic structures in the paddy soils (**Publication II**: Fig. 2). Overall, the paddy management system investigated here induces higher OM quantity in all soil fractions, but it does not affect the chemical nature of SOM during paddy soil development.

In conclusion, OC accumulates preferentially in the fine mineral fraction, with highest capacities for OC accumulation in clay-sized fractions. These fine mineral fractions are characterized by a paddy-specific Fe oxide formation emerging already within 50 years of paddy management. In contrast to non-paddy soils, the large proportions of Fe_{ox} contributed to the higher OC accumulation in paddy topsoils.

3.3 Soil mineral surfaces of paddy soils are accessible for OC accumulation after decalcification

Results of **Publication II** did not show changes in clay mineralogy, but different Fe_d concentrations between paddy and non-paddy soils. As the content of Fe_d in these soils is generally low (0.1–3.3%), **Publication III** focused on the role of the clay minerals in the accumulation of OC. The concept is that different decalcification between paddy and non-paddy soils might be responsible for the different accessibility of mineral surfaces for OC covering, which causes markedly higher OC accumulation in paddy soils (**Publication II**: Table 1). Paddy soils showed a faster topsoil decalcification than non-paddy soils (**Publication I**: Table 1; **Publication III**: Table 1). However, both chronosequences do not show a further development of the clay minerals after deposition of the estuarine sediment. That is indicated by unchanged soil mineralogy during 2000/700 years of soil development and only slightly acidic pH values (**Publication II**). The unchanged soil mineralogy is confirmed by the measurement of the SSAs, which showed no increase after OM removal (**Publication III**: Fig. 1). Also after the combined removal of OM and Fe_d (**Publication III**: Fig. 2a; b), no additional formation of mineral surfaces during pedogenesis was observed. This study did not find a pronounced formation of soil silicate minerals and oxides in decalcified (paddy) soils. This is in line with Dümig et al. (2012) who

investigated a relatively young chronosequence (15–120 years) that developed after glacier retreat, and they could likewise not confirm increasing SSA values over time. The authors explained the OC accumulation may be faster than the supply of mineral surfaces by weathering during initial soil development, which appears to be opposite at later stages of pedogenesis. White et al. (1996) and Hodson et al. (1998) found increasing SSA values with ongoing soil development in much older soil chronosequences (0.2–3000 ky; 80–13,000 years), indicating decreasing particle sizes due to progressive weathering (Hodson et al., 1998).

Despite no additional formation of mineral surfaces during pedogenesis, the OC covering of the mineral surfaces increases with time of soil formation, especially in the clay-sized fractions (**Publication III**: Fig. 1). The OC covering was strongest in the $<0.2 \mu\text{m}$ fraction (having the highest mineral surface area). This is in contradiction to **Publication I**, showing that the $<0.2 \mu\text{m}$ fraction seems to be already saturated after 50 years of soil evolution (section 3.1). Results from ^{14}C measurements indicated that a marked proportion of modern carbon has replaced the inherited carbon in paddy soils (**Publication III**: Table 2). Thus, the OC amount is not increasing in the $<0.2 \mu\text{m}$ fraction, but probably the OC covering of these mineral surfaces seems to be more effective. For example, the proportion of SSA, which is covered by OC, rose from 31% (P 50) to 75% (P 2000) in the $<0.2 \mu\text{m}$ fraction (**Publication III**: Table 4). In contrast, the increase in non-paddy soils was much less, from about 30% (NP 50) to 41% in NP 700 (**Publication III**: Table 4). The OC content of both clay fractions increased with soil age, resulting in a decline of the mineral surface areas due to increasing OC coverage. This was reflected by a strong linear relationship of the $\text{SSA}_{\text{untreated}}$ values and the OC contents of both paddy and non-paddy clay-sized fractions (**Publication III**: Fig. 3a). The results suggested higher OM coverings of the mineral surfaces in decalcified paddy soils. Lower OC coverings in non-paddy soils may have been caused by a reduced accessibility of the mineral surfaces. Compared to the respective soil age of the paddy soils, non-paddy soils showed higher pH and higher BS values (**Publication III**: Table 1), suggesting a relatively high concentration of (bivalent) cations, which promotes aggregation of the clay minerals. Therefore, lower OM coverings and the smaller OM accumulation in non-paddy soils is attribute to a reduced accessibility of SSA due to strong microaggregation by Ca^{2+} ion bridging. Especially in the calcareous non-paddy soils (NP 50, NP 100, NP 300), cementation by calcium carbonate has additionally contributed to the aggregation of clay minerals (**Publication III**: Fig. 5). Thus, large parts of the mineral surface area might be not available for OC covering, leading to hampered OC accumulation in the non-decalcified soils.

The results clearly demonstrated that silicate minerals play a role in OC stabilization during early paddy soil formation after decalcification of the soils. This is supported by: (1) relatively low Fe_a concentrations in both soil groups. (2) The treatment with H_2O_2 and the subsequent removal of Fe_a revealed the largest mineral surface area, especially for the $<0.2 \mu\text{m}$ fractions in paddy 1000 and paddy 2000. (3) As pointed out earlier, this is attributed to the continuous disaggregation of clay

minerals due to the loss of carbonate cementation and Ca^{2+} ions bridges in paddy soils. The accessibility of silicate mineral surfaces for OC covering increased in paddy soils by decalcification and is responsible for the higher OC accumulation than in non-paddy soils.

4 CONCLUSIONS & OUTLOOK

Focusing on the evolution of mineral-associated OM in paddy soils, the development of paddy rice soils was studied on differently aged soils from a 2000-years-old chronosequence. The results were compared with a chronosequence of non-paddy soils which were managed without rice cultivation and without inundation. In order to elucidate the role of the organo-mineral associations for OC accumulation during paddy soil development, the soils were characterized by OC –and mass contributions to the bulk soil, SOM composition, oxide extraction, clay mineral and specific surface area determination.

The paddy and non-paddy soil evolution differs and is characterized by chronological changes of dominant soil-forming processes. Enhanced decalcification of paddy soils due to frequent flooding and discharge is accompanied by a high OC accumulation with time, leading to a replacement of the inherited carbon by more recent one. Management-induced redox cycles stabilize a paddy-specific Fe_{ox} to Fe_d proportion which remained constant over time. The paddy management leads to a higher proportion of Fe_{ox} which is associated with a larger accumulation of OC. The large mineral surface area of Fe_{ox} added to the surface area of clay minerals provided additional options for OC covering. Carbonate and Ca^{2+} ions seemed to interconnect clay minerals, making parts of their surface inaccessible to OC accumulation. Thus faster dissolution of carbonate and leaching of Ca^{2+} ions in paddy soils made additional clay mineral surfaces available to OC. The OC covering of the mineral surfaces increases in paddy soils with increasing OC accumulation although no additional formation of secondary mineral surfaces was observed. The higher OC accumulation in paddy soils is further confirmed by a marked proportion of modern carbon which was added to the inherited carbon mainly during the first 100 years of paddy soil development. The smaller accumulation of mineral-associated SOM in non-paddy soils was additionally confirmed by the retarded replacement of the inherited carbon. The enhanced accessibility of mineral surfaces for OC covering was obviously due to the accelerated decalcification of the paddy soils. In non-paddy soils, showing a low decalcification, the mineral surfaces are inaccessible due to cementation by carbonate and/or Ca^{2+} bridging.

The findings of the study are important contributions to a better understanding of the biogeochemical processes in paddy soils. The results revealed that paddy soils have a higher potential for OC accumulation since the earliest stages of pedogenesis than non-paddy soils. This is supported by the reduced SOM decomposition due to the periodically soil flooding, the paddy-specific composition of Fe oxides and the accessibility of the soil mineral surfaces for OC covering due to the enhanced decalcification. These processes lead to a higher accumulation of OC in paddy soils. The results have major implications on the understanding of man-made soils and the assessment of new management techniques for paddy soils such as alternating wetting and drying, as these will affect the redox conditions and thus most probably also Fe oxide composition and OC storage potential.

6 REFERENCES

- Adams, W.A., Kassim, J.K., 1984. Iron oxyhydroxides in soils developed from Lower Palaeozoic sedimentary rocks in mid-Wales and implications for some pedogenetic processes. *J. Soil Sci.* **35**, 117–126.
- Bahmanyar, M.A., 2007. The influence of continuous rice cultivation and different waterlogging periods on morphology, clay mineralogy, Eh, pH and K in paddy soils. *Pak. J. Biol. Sci.* **10** (17), 2844–2849.
- Balabane, M., Plante, A.F., 2004. Aggregation and carbon storage in silty soil using physical fractionation techniques. *Eur. J. Soil Sci.* **55**, 415–427.
- Balesdent, J., Mariotti, A., Guillet, B., 1987. Natural ¹³C abundance as a tracer for studies of soil organic matter dynamics. *Soil Biol. Biochem.* **19**, 25–30.
- Bierke, A., Kaiser, K., Guggenberger, G., 2008. Crop residue management effects on organic matter in paddy soils-The lignin component. *Geoderma* **146**, 48–57.
- Borggaard, O.K., 1982. The influence of iron oxides on the surface area of soil. *J. Soil Sci.* **33**, 443–449.
- Bosatta, E., Agren, G.I., 1997. Theoretical analyses of soil texture effects on organic matter dynamics. *Soil Biol. Biochem.* **29**, 1633–1638.
- Bracewell, J.M., Campbell, A.S., Mitchell B.D., 1970. An assessment of some thermal and chemical techniques used in the study of the poorly-ordered aluminosilicates in soil clays. *Clay Mineral.* **8**, 325–335.
- Brunauer, S., Emmett, P.H., Teller, E., (1938). Adsorption of gases in multimolecular layers. *Journal of American Chemical Society* **60** (2), 309–319.
- Cao, Z.H., Ding, J.L., Hu, Z.Y., Knicker, H., Kögel-Knabner, I., Yang, L.Z., Yin, R., Lin, X.G., Dong, Y.H., 2006. Ancient paddy soils from the Neolithic age in China's Yangtze River Delta. *Naturwissenschaften* **93**, 232–236.
- Carter, D.L., Mortland, M.M., Kemper, W.D., 1986. In *Methods of soil analysis, Part 1. Physical and mineralogical methods*. American Society of Agronomy— Soil Sci. Soc. Am., Madison, USA. Agronomy Monograph no. 9, second ed.
- Cheng, Y., Yang, L.-Z., Cao, Z.-H., Ci, E., Yin, S., 2009. Chronosequential changes of selected pedogenic properties in paddy soils as compared with non-paddy soils. *Geoderma* **151**, 31–41.
- Chenu, C., Plante, A.F., 2006. Clay-sized organo-mineral complexes in a cultivation chronosequence: revisiting the concept of the 'primary organo-mineral complex'. *Eur. J. Soil Sci.* **57** (4), 596–607.

- Chivenge, P.P., Muwira, H.K., Giller, K.E., Mapfumo, P., Six, J., 2007. Long-term impact of reduced tillage and residue management on soil carbon stabilization: Implications for conservation agriculture on contrasting soils. *Soil Tillage Res.* **94**, 328–337.
- Colberg, P.J., 1988. Anaerobic microbial degradation of cellulose, lignin, oligolignols, and monoaromatic lignin derivatives. In: *Biology of Anaerobic Microorganisms* (ed. A.J.B. Zehnder), pp. 333-372. Wiley, New York (cited from Olk et al., 1996).
- Cornell, R.M., Schwertmann, U., 2003. *The iron oxides. Structure, properties, reactions, occurrences and uses*, 2nd edn. Wiley-VHC, Weinheim.
- De Datta, S.K. and Kerim, M.S.A.A.A., 1974. Water and nitrogen economy of rainfed rice as affected by soil puddling. *Soil Sci. Soc. Proc.* **38**, 515–518.
- Dümig, A., Häusler, W., Steffens, M., Kögel-Knabner, I., 2012. Clay fractions from a soil chronosequence after glacier retreat reveal the initial evolution of organo-mineral associations. *Geochim. Cosmochim. Acta* **85**, 1–18.
- Eickhorst, T., Tippköter, R., 2009. Management-induced structural dynamics in paddy soils of south east China simulated in microcosms. *Soil Tillage Res.* **102**, 168–178.
- Eusterhues, K., Rennert, T., Knicker, H., Kögel-Knabner, I., Totsche, K.U., Schwertmann, U., 2011. Fractionation of organic matter due to reaction with ferrihydrite: Coprecipitation versus adsorption. *Environ. Sci. Technol.* **45**, 527–533.
- Eusterhues, K., Rumpel, C., Kögel-Knabner, I., 2005. Organo-mineral associations in sandy acid forest soils: importance of specific surface area, iron oxides and micropores. *Eur. J. Soil Sci.* **56**, 753–763.
- FAO, 2006. *Guidelines for soil description*. FAO, Rome, 97 pp.
- Frenzel, P., Rothfuss, F., Conrad, R., 1992. Oxygen profiles and methane turnover in a flooded rice microcosm. *Biol. Fertil. Soils* **14**, 84–89.
- Gaunt, J.L., Neue, H.-U., Cassman, K.G., Olk, D.C., Arah, J.R.M., Witt, C., Ottow, J.C.G., Grant, J.F., 1995. Microbial biomass and organic matter turnover in wetland rice soils. *Biol Fertil Soils* **19**, 333–342.
- Gong, Z., Xu, Q., 1990. Paddy soils. In: *Soils of China*, Science Press, Beijing, pp. 233-260.
- Gong, Z.-T., 1983. Pedogenesis of paddy soils and its significance in soil classification. *Soil Sci.* **135** (1), 5-10.
- Guo, Z.G., Yang, Z.S., Qu, Y.H., Fan, D.J., 2000. Study on comparison sedimentary geochemistry of mud area on East China Sea continental shelf. *Acta Sedimentol. Sin.* **18**, 284–289.
- Harden, J.W., 1982. A quantitative index of soil development from field description: Examples from a chronosequence in central California. *Geoderma* **28**, 1–28.
- Hassink, J., 1997. The capacity of soil to preserve organic C and N by their association with clay and silt particles. *Plant Soil* **191**, 77–87.

- Hearn, P.P., Parkhurst, D.L., Callender, E., 1983. Authigenic vivianite in Potomac River sediments: Control by ferric oxy-hydroxides. *J. Sedim. Petrol.* **53**, 165–177.
- Hodson, M.E., Langan, S.J., Kennedy, F.M., Bain, D.C., 1998. Variation in soil surface area in a chronosequence of soils from Glen Feshie, Scotland and its implications for mineral weathering rate calculations. *Geoderma* **85**, 1–18.
- Huang, S., Rui, W., Peng, X., Huang, Q., Zhang, W., 2010. Organic carbon fractions affected by long-term fertilization in a subtropical paddy soil. *Nutr. Cycl Agroecosyst* **86**, 153–160.
- Huggett, R.J., 1998. Conceptual models in pedogenesis – A discussion. *Geoderma* **16**, 261–262.
- International Union of Soil Sciences Working Group, 2007. World reference base for soil resources 2007. World Soil Resources Reports, vol. 103. FAO, Rome.
- International Rice Research Institute (IRRI), 1986. Annual Report for 1985, I.R.R.I., Los Bafios, Philippines, pp. 280–285.
- Janssen, M., Lennartz, B., 2006. Horizontal and vertical water fluxes in paddy rice fields of subtropical China. *Adv. Geo. Ecol.* **38**, 344–354.
- Jenkinson, D.S., Rayner, J.H., 1977. The turnover of soil organic matter in some of the Rothamsted classical experiments. *Soil Sci.* **123**, 298–305 (cited from Balabane and Plante, 2004).
- Jenkinson, D.S., Hart, P.B.S., Rayner, J.H., Parry, L.C., 1987. Modelling the turnover of organic matter in long-term experiments at Rothamsted. *INTECOL Bulletin* **15**, 1–8 (cited from Eusterhues et al., 2005).
- Jenny, H., 1941. Factors of soil formation. McGraw-Hill Co., New York, NY, 281 pp.
- Jilan, D., Kangshan, W., 1989. Changjiang river plume and suspended sediment transport in Hangzhou Bay, *Cont. Shelf Res.* **9**, 93–111.
- Kaiser, K., Guggenberger, G., 2000. The role of DOM sorption to mineral surfaces in the preservation of organic matter in soils. *Org. Geochem.* **31**, 711–725.
- Kaiser, K., Guggenberger, G., 2003. Mineral surfaces and soil organic matter. *Eur. J. Soil Sci.* **54** (2), 219–236.
- Kiem, R., Kögel-Knabner, I., 2002. Refractory organic carbon in particle-size fractions of arable soils II: organic carbon in relation to mineral surface area and iron oxides in fractions < 6 μm . *Org. Geochem.* **33**, 1699–1713.
- Kölbl, A., Schad, P., Jahn, R., Amelung, W., Bannert, A., Cao, Z.H., Fiedler, S., Kalbitz, K., Lehdorff, E., Müller-Niggemann, C., Schloter, M., Schwark, L., Vogelsang, V., Wissing, L., Kögel-Knabner, I., (submitted). Accelerated soil formation due to paddy management on marshlands (Zhejiang Province, China).
- Kögel-Knabner, I., Amelung, W., Cao, Z.-H., Fiedler, S., Frenzel, P., Jahn, R., Kalbitz, K., Kölbl, A., Schloter, M., 2010. Biogeochemistry of paddy soils. *Geoderma* **157**, 1–14.

- Laird, D.A., Martens, D.A., Kingery, W.L., 2001. Nature of clay-humic complexes in an agricultural soil. I. Chemical, biochemical, and spectroscopic analyses. *Soil Sci. Soc. Am. J.* **65**, 1413–1418.
- Lal, R., 2002. Soil carbon sequestration in China through agricultural intensification, and restoration of degraded and desertified ecosystems. *Land Degrad. Dev.* **13**, 469–478.
- Li, Z.-P., Zhang, T.-L., Li, D.-C., Velde, B., Han, F.-X., 2005. Changes in soil properties of paddy fields across a cultivation chronosequence in subtropical China. *Pedosphere* **15** (1), 110–119.
- Liesack, W., Schnell, S., Revsbech, N.P., 2000. Microbiology of flooded rice paddies. *FEMS Microbiol. Rev.* **24**, 625–645.
- Mahieu, N., Olk, D.C., Randall, E.W., 2002. Multinuclear magnetic resonance analysis of two humic acid fractions from lowland rice soils. *J. Environ. Qual.* **31**, 421–430.
- Mansfeldt, T., Schuth, S., Häusler, W., Wagner, F.E., Kaufhold, S., Overesch, M., 2011. Iron oxide mineralogy and stable iron isotope composition in a Gleysol with petrogleyic properties. *J Soils Sediments* **12** (1), 97–114.
- Mayer, L., 1994. Relationship between mineral surfaces and organic carbon concentrations in soils and sediments. *Chem. Geol.* **114**, 347–363.
- MacLean, J.L., Dawe, D.C., Hardy, B., Hettel, G.P., 2002. In *Rice Almanac: Source Book for the Most Important Economic Activity on Earth*, ed. by J.L. MacLean, D.C. Dawe, B. Hardy and G.P. Hettel, 3rd ed. (CABI Publishing, 2002), 270 pp.
- Mehra, O.P., Jackson, M.L., 1960. Iron oxide removal from soils and clays by a dithionite-citrate system buffered with sodium bicarbonate. *Clays and clay minerals, proceedings of the 7th national conference*: 317–327.
- Meyer, B., 1960. Zeitmarken in der Entwicklung mitteldeutscher Loss- und Kalksteinboden. *Proc. 7th Int. Congr. Soil Sci. Trans.*, pp. 177–183.
- Milliman, J.D., Syvitski, J.P.M., 1992. Geomorphic/tectonic control of sediment discharge to the ocean: the importance of small mountainous rivers. *Journal of Geology* **100**, 525–544.
- Milliman, J.D., Meade, R.H., 1983. World-wide delivery of river sediment to the oceans. *Journal of Geology* **91**, 1–21.
- Mousavi, S.F., Yousefi-Moghadam, Mostafazadeh-Fard, B., Hemmat, A., Yazdani, M.R., 2009. Effect of puddling intensity on physical properties of a silt clay soil under laboratory and field conditions. *Paddy Water Environ.* **7**, 45–54.
- Neue, H.U., Gaunt, J.L., Wang, Z.P., Becker-Heidmann, P., Quijano, C., 1997. Carbon in tropical wetlands. *Geoderma* **79**, 163–185.

- Olk, D.C., Cassman, K.G., Randall, E.W., Kinchesh, P., Sanger, L.J., Anderson, J.M., 1996. Changes in chemical properties of organic matter with intensified rice cropping in tropical lowland soil. *Eur. J. Soil Sci.* **47**, 293–303.
- Olk, D.C., Cassman, K.G., Mahieu, N., Randall, E.W., 1998. Conserved chemical properties of young humic acid fractions in tropical lowland soil under intensive irrigated rice cropping. *Eur. J. Soil Sci.* **49**, 337–349.
- Olk, D.C., Dancel, M.C., Moscoso, E., Jimenez, R.R., Dayrit, F.M., 2002. Accumulation of lignin residues in organic matter fractions of lowland rice soils: a pyrolysis-GC-MS study *Soil Sci.* **167**, 590–606.
- Painuli, D.K., Woodhead, T., Pagliai, M., 1988. Effective use of energy and water in rice-soil puddling. *Soil Tillage Res.* **12**, 149–161.
- Pan, G., Li, L., Wu, L., Zhang, X., 2003a. Storage and sequestration potential of topsoil organic carbon in China's paddy soils. *Glob. Chang. Biol.* **10**, 79–92.
- Pan, G.X., Li, L.Q., Zhang, X.H., Dai, J.Y., Zhou, Y.C., Zhang, P.J., 2003b. Soil organic carbon storage of China and the sequestration dynamics in agricultural lands. *Adv. Earth Sci.* **18**, 609–618 (in Chinese).
- Parfitt, R.L., 1989. Phosphate reactions with natural allophane, ferrihydrite and goethite. *J. Soil Sci.* **40**, 359–369.
- Pronk, G.J., Heister, K., Kögel-Knabner, I., 2011. Iron oxides as major available interfaces component in loamy arable topsoils. *Soil Sci. Soc. Am. J.* **75**, 1729–1732.
- Robert, M., Chenu, C., 1992. Interactions between soil minerals and microorganisms. In: G. Stotzky and J.M. Bollag (Editors), *Soil Biochemistry*, Vol. 7. Marcel Dekker, New York, pp. 307–404.
- Sah, R.N., Mikkelsen, D.S., Hafez, A.A., 1989. Phosphorus behaviour in flooded-drained soils. III. Phosphorus desorption and availability. *Soil Sci. Soc. Am. J.* **53**, 1729–1732.
- Sahrawat, K.L., 2005. Fertility and organic matter in submerged rice soil. *Curr. Sci.* **88**, 735–739.
- Sahrawat, K.L., 2004. Organic matter accumulation in submerged soils. *Adv. Agron.* **81**, 169–201.
- Sanchez, P.A., 1973. Puddling tropical rice soils: 2. Effects of water losses. *Soil Sci.* **115**, 303–308.
- Schwertmann, U., 1964. Differenzierung der Eisenoxide des Bodens durch Extraktion mit Ammoniumoxalat-Lösung. *Z. Pflanzenernähr. Düng. Bodenkd.* **105**, 194–202.
- Schwertmann, U., 1966. Inhibitory effect of soil organic matter on crystallization of amorphous ferric hydroxide. *Nature* **212**, 645–646.
- Schwertmann, U., Schulze, D.G., Murad, E., 1982. Identification of ferrihydrite in soils by dissolution kinetics, differential X-ray diffraction, and Mössbauer Spectroscopy. *Soil Sci. Soc. Am. J.* **46**, 869–875.
- Schwertmann, U., Wagner, F., Knicker, H., 2005. Ferrihydrite-humic associations: Magnetic hyperfine interactions. *Soil Sci. Soc. Am. J.* **69**, 1009–1015.

- Shang, C., Tiessen, H., 1998. Organic matter stabilization in two semiarid tropical soils: Size, density, and magnetic separations. *Soil Sci. Soc. Am. J.* **62**, 1247–1257.
- Six, J., Conant, R.T., Paul, E. A., Paustian, K., 2002. Stabilization mechanisms of soil organic matter: Implications for C-saturation of soils. *Plant Soil* **241**, 155–176.
- Smernik, R.J., Olk, D.C., Mahieu, N., 2004. Quantitative solid-state ¹³CNMR spectroscopy of organic matter fractions in lowland rice soils. *Eur. J. Soil Sci.* **55**, 367–379.
- Steffens, M., Kölbl, A., Kögel-Knabner, I., 2009. Alternation of soil organic matter pools and aggregation in semi-arid steppe topsoils as driven by organic matter input. *Eur. J. Soil Sci.* **60**, 198–212.
- Stevens, P.R., Walkers, T.W., 1970. The chronosequence concept and soil formation. *The Quarterly Review of Biology* **45** (4), 333–350.
- Talibudeen, O., Arambarri, P., 1964. The influence of the amount and the origin of calcium carbonates on the isotopically exchangeable phosphate in calcareous soils. *J. agric. Sci. Camb.* **62**, 93–7.
- Tanji, K.K., Gao S., Scardaci S.C., Chow A.T., 2003. Characterization redox status of paddy soils with incorporated rice straw. *Geoderma* **114**, 333–353.
- Thompson, A., Rancourt, D.G., Chadwick, O.A., Chorover, J., 2011. Iron solid-phase differentiation along a redox gradient in basaltic soils. *Geochim. Cosmochim. Acta* **75**, 119–133
- Thompson, A., Chadwick, O.A., Rancourt, D.G., Chorover, J., 2006b. Iron-oxide crystallinity increases during redox oscillations. *Geochim. Cosmochim. Acta* **70**, 1710–1727.
- Tipping, E., 1981. The adsorption of aquatic humic substances by iron oxides *Geochim. Cosmochim. Acta* **45** (2), 191–199.
- Tisdall, J.M., Oades, J.M., 1982. Organic matter and water-stable aggregates in soils. *J. Soil Sci.* **33**, 141–163.
- Torn, M.S., Trumbore, S.E., Chadwick, O.A., Vitousek, P.M., Hendricks, D.M., 1997. Mineral control of soil organic carbon storage and turnover. *Nature* **389**, 170–173.
- Veldkamp, A., 2005. Pedogenesis and soil forming factors, in *Land Use and Land Cover*, [Ed. Willy H. Verheye], in *Encyclopedia of Life Support Systems (EOLSS)*, Developed under the Auspices of the UNESCO, Eolss Publishers, Oxford ,UK, [<http://www.eolss.net>].
- van der Zee, C., Roberts, D.R., Rancourt, D.G., Slomp, C.P., 2003. Nanogoethite is the dominant reactive oxyhydroxide phase in lake and marine sediments. *Geology* **31**, 993–996.
- von Lützw, M., Kögel-Knabner, I., Ekschmitt, K., Flessa, H., Guggenberger, G., Matzner, E., Marschner, B., 2007. SOM fractionation methods: Relevance to functional pools and to stabilization mechanisms. *Soil Biol. Biochem.* **39**, 2183–2207.
- Vreeken, W.J., 1975. Principal kinds of chronosequences and their significance in soil history *J. Soil Sci.* **26** (4), 378–394.

- Wagai, R., Mayer, L.M., 2007. Sorptive stabilisation of organic matter in soils by hydrous iron oxides. *Geochim. Cosmochim. Acta* **71**, 25–35.
- Walker, L.R., Wardle, D.A., Bardgett, R.D., Clarkson, B.D., 2010. The use of chronosequences in studies of ecological succession and soil development. *J. Ecol.* **98**, 725–736.
- Wang, H., Zuosheng, Y., Saito, Y., Liu, J. P., 2008. Reconstruction of sediment flux from the Changjiang (Yangtze River) to the sea since the 1860s, *J. Hydrol.* **349**, 318–332.
- Wang, Y., Zhou, X., Wu, J., 1992. Mössbauer study on the iron oxide minerals of paddy soils derived from red soil in Fujian, China. *Hyperfine Interact.* **70**, 1037–1040.
- Wen, Q.-X., 1984. Utilization of organic materials in rice production in China. In: *Organic matter and rice*. Stephen Banta, Corazon V. Mendoza, International Rice Research Institute (cited from Kölbl et al., submitted).
- White, A.F., Blum, A.E., Schulz, M.S., Bullen, T.D., Harden, J.W., Peterson, M.L., 1996. Chemical weathering rates of a soil chronosequence on granitic alluvium: I. Quantification of mineralogical and surface area changes and calculation of primary silicate reaction rates. *Geochim. Cosmochim. Acta* **60**, (14) 2533–2550.
- Wissing, L., Kölbl, A., Vogelsang, V., Fu, J., Cao, Z.H., Kögel-Knabner, I., 2011. Organic carbon accumulation in a 2000-year chronosequence of paddy soil evolution. *Catena* **87**, 376–385.
- Wu, J., 2011. Carbon accumulation in paddy ecosystems in subtropical China: evidence from landscape studies. *Eur. J. Soil Sci.* **62**, 29–34.
- Xi, D., Wang, Z., Gao, S., De Vriend, H. J., 2009. Modeling the tidal channel morphodynamics in a macro-tidal embayment, Hangzhou Bay, China, *Cont. Shelf Res.* **29**, 1757–1767.
- Zhang, G.L., Gong, Z.T., 2003. Pedogenic evolution of paddy soils in different soil landscapes. *Geoderma* **115**, 15–29.
- Zhang, M., Lu, H., Zhao, X.J., Li, R.A., 2004. A comparative study of soil fertility change of upland soil in Cixi Country. *Chinese J. Soil Science* **35**, 91–93.
- Zhang, M., He, Z., 2004. Long-term changes in organic carbon and nutrients of an Ultisol under rice cropping in southeast China. *Geoderma* **118**, 167–179.
- Zhang, Y., Lin, X., Werner, W., 2003. The effect of soil flooding on the transformation of Fe oxides and the adsorption/desorption behaviour of phosphate. *J. Plant Nutr. Soil Sci.* **166**, 68–75.
- Zhang, Y., Lin, X., 2002. Relation between Fe-oxides transformation and phosphorus adsorption in the oxic and anoxic layers of two paddy soils as affected by flooding. *J. Zhejiang Univ.* **28** (5), 485–491.
- Zhao, Q., Zhong, L., Yingfei, X., 1997. Organic carbon storage in soils of southeast China. *Nutri. Cycl. Agroecosyst.* **49**, 229–234.
- Zou, P., Fu, J., Cao, Z., 2011. Chronosequence of paddy soils and phosphorus sorption–desorption properties. *Journal of Soil and Sediments* **11**, 249–259.

- Yoshida, S., Adachi, K., 2002. Influences of puddling intensity on the water retention characteristics of clayey paddy soil. In: IUSS (Ed.). Proceedings of the 17th World Congress of Soil Science, 14-21 August 2002, Vol. 5, Symposium no. 53, Bangkok, Thailand, pp. 2351–2359.

ACKNOWLEDGMENT (DANKSAGUNG)

Zum positiven Gelingen dieser Dissertation haben zahlreiche Menschen beigetragen, bei denen ich mich aufrichtig bedanken möchte.

Als erstes bedanke ich mich bei Prof. Dr. Ingrid Kögel-Knabner, dafür dass Sie mir als „Quereinsteigerin in die Bodenkunde“ die Möglichkeit gegeben haben, dieses spannende und komplexe Thema zu bearbeiten. Weiterhin vielen Dank für die Unterstützung bei der Interpretation umfangreicher Datensätze, die zahlreichen wissenschaftlichen Diskussionen sowie für die Hilfe beim Publizieren dieser Arbeit. Ich danke Prof. Dr. Jürgen Geist für den Vorsitz der Prüfungskommission und Prof. Dr. Wulf Amelung für die Begutachtung meiner Dissertation.

Der Deutsche Forschungsgemeinschaft (DFG) wird für die Finanzierung der internationalen Research Unit 995 „Biogeochemistry of paddy soil evolution“ gedankt. Die Finanzierung durch die DFG hat eine umfangreiche Probenahme und den Transport der Proben aus China ermöglicht, was die Grundlage für zahlreiche Analysen in Deutschland war.

Ich danke Prof. Dr. Reinhold Jahn, Dr. Sabine Fiedler und Vanessa Vogelsang vom Institut für Agra- und Ernährungswissenschaften der Martin-Luther Universität in Halle-Wittenberg für die Bereitstellung der anorganischen Kohlenstoffdaten, pH Werte sowie für die Redoxpotential- und Basensättigungsdaten. Ebenfalls gedankt sei Prof. Dr. Peter Grootes und Tino Bräuer vom Leibniz-Labor für Altersbestimmung und Isotopenforschung der Christian-Albrechts Universität zu Kiel für die Bereitstellung der ^{14}C Daten.

Mein größter und aufrichtigster Dank gilt Dr. Angelika Kölbl, meiner langjährigen Betreuerin. Liebe Angelika, Du hast im hohen Maß dazu beigetragen, dass ich diese Arbeit zu einem guten Ende gebracht habe. Danke für das Lesen und Korrigieren meiner Texte, für die unzähligen Diskussionen über „paddy soils“ und für Deine Engelsgeduld all meine Fragen zu beantworten. Ich bedanke mich für den mentalen Beistand auf Konferenzen sowie für das viele Lob zu meiner Arbeit, welches mich immer wieder von Neuem zum Weiterschreiben motiviert hat. Ich bin Dir unendlich dankbar für Deine aufbauenden Worte, in genau den Momenten, wo ich am „Durchhängen“ war. Danke auch für die lustigen Augenblicke, in denen wir in Deinem Büro herzlichst gelacht haben. Danke, danke und nochmals danke für alles!

Ich bedanke mich bei Dr. Peter Schad für die fachlichen Diskussionen sowie tatkräftige Unterstützung bei der Beprobungskampagne 2008 in China, bei der ich leider nicht dabei sein konnte. Jedoch hatten wir 2010 noch einmal die Möglichkeit für weitere Beprobungen zusammen nach China und

Indonesien zu reisen. Vielen Dank auch für die hilfreichen Kommentare zu meinen Manuskripten sowie beim Zusammenschreiben dieser Arbeit.

Besonders möchte ich mich bei Monika Heilmeier für Ihre schnelle, zuverlässige und extrem präzise Arbeit im Labor bedanken. Liebe Moni, ich hätte mir keine bessere Unterstützung im Labor vorstellen können. Des Weiteren sei Martina Bauer, Carolin Botond, Tahereh Javaheri, Juliane Teichmann, Maria Vonach, Christine Pfab und ganz besonders Robert U. Hagemann für die tatkräftige Unterstützung bei der Probenaufbereitung sowie den vielen Analysen im Labor gedankt.

Vielen Dank an Elfriede Schuhbauer, die mir immer wieder geduldig bei der graphischen Darstellung meiner Abbildungen sowie Fotos für Präsentation geholfen und mir somit viel Zeit gespart hat. Des Weiteren sei Dr. Markus Steffens für die Hilfestellung bei der statistischen Auswertung der Daten und Prof. Dr. Thilo Rennert für das Korrekturlesen dieser Arbeit und die zahlreichen Verbesserungen zum Thema „Eisenoxide“ gedankt. Zusätzlich danke ich Dr. Katja Heister für das Korrigieren der Zusammenfassung.

Ich danke meinen Doktoranden-Kollegen(Innen) Carolin Bimüller, Dominik Christophel, Cordula Vogel, Olivia Kreyling, Sven Bachmann, Susanne Drechsler für die gemeinsame Zeit. Des Weiteren möchte ich mich bei allen anderen Lehrstuhl-Kollegen für die angenehme Arbeitsatmosphäre sowie die fachlichen Diskussionen bedanken. Insbesondere danke ich meinem Bürokollegen Dr. Alexander Dümig (Alex) für den oftmals sehr lustigen Büroalltag und die vielen interessanten „Selbstgespräche“.

Ich bedanke mich bei meinen langjährigen Freundinnen Isabelle Natalia Ann Erdelji (Isa), Pascale Sarah Naumann (Pasi) und Juliane Teichmann (Jule) für Ihre Unterstützung in jeder Lebenslage und die vielen schönen Momente die wir zusammen erlebt haben. Danke Mädels, dass Ihr immer an mich geglaubt habt!

Meinem Verlobten Oliver Urbanski (Oli) möchte ich für seine Unterstützung und die Motivation in der Endphase meiner Promotion danken. Lieber Oli, Danke für Deinen mentalen Beistand und das Du genau so bist, wie Du bist.

Zu guter Letzt möchte ich mich vom ganzen Herzen bei meiner Familie, insbesondere bei meinen Eltern Jens und Kornelia Wissing, für Ihre jahrelange finanzielle und mentale Unterstützung bedanken. Liebe Mama, danke für Deine sensible Art, mit der Du mich immer wieder an die wichtigen Dinge im Leben erinnert hast. Lieber Papa, vielen Dank dass Du mir „ein Bett in Freising bestellt hast“ ohne das ich wahrscheinlich nicht zum Studium hier in Weihenstephan angetreten wäre.

APPENDIX**Publication I and permission****Publication II and permission****Publication III****Curriculum vitae****List of oral and poster presentations**

ELSEVIER LICENSE
TERMS AND CONDITIONS
Sep 18, 2012

This is a License Agreement between Livia Wissing ("You") and Elsevier ("Elsevier") provided by Copyright Clearance Center ("CCC"). The license consists of your order details, the terms and conditions provided by Elsevier, and the payment terms and conditions.

All payments must be made in full to CCC. For payment instructions, please see information listed at the bottom of this form.

Supplier	Elsevier Limited The Boulevard,Langford Lane Kidlington,Oxford,OX5 1GB,UK
Registered Company Number	1982084
Customer name	Livia Wissing
Customer address	Chair of Soil Science Freising, Bavaria 85354
License number	2991810587163
License date	Sep 18, 2012
Licensed content publisher	Elsevier
Licensed content publication	CATENA
Licensed content title	Organic carbon accumulation in a 2000-year chronosequence of paddy soil evolution
Licensed content author	Livia Wissing,Angelika Kölbl,Vanessa Vogelsang,Jian-Rong Fu,Zhi-Hong Cao,Ingrid Kögel-Knabner
Licensed content date	December 2011
Licensed content volume number	87
Licensed content issue number	3
Number of pages	10
Start Page	376
End Page	385
Type of Use	reuse in a thesis/dissertation
Portion	full article
Format	both print and electronic
Are you the author of this Elsevier article?	Yes
Will you be translating?	No
Order reference number	
Title of your thesis/dissertation	Evolution of mineral-associated organic matter in paddy soils - a chronosequence study
Expected completion date	Nov 2012
Estimated size (number of pages)	100
Elsevier VAT number	GB 494 6272 12
Permissions price	0.00 EUR
VAT/Local Sales Tax	0.0 USD / 0.0 GBP
Total	0.00 EUR
Terms and Conditions	

INTRODUCTION

1. The publisher for this copyrighted material is Elsevier. By clicking "accept" in connection with completing this licensing transaction, you agree that the following terms and conditions apply to this transaction (along with the Billing and Payment terms and conditions established by Copyright Clearance Center, Inc. ("CCC"), at the time that you opened your Rightslink account and that are available at any time at <http://myaccount.copyright.com>).

GENERAL TERMS

2. Elsevier hereby grants you permission to reproduce the aforementioned material subject to the terms and conditions indicated.

3. Acknowledgement: If any part of the material to be used (for example, figures) has appeared in our publication with credit or acknowledgement to another source, permission must also be sought from that source. If such permission is not obtained then that material may not be included in your publication/copies. Suitable acknowledgement to the source must be made, either as a footnote or in a reference list at the end of your publication, as follows:

“Reprinted from Publication title, Vol /edition number, Author(s), Title of article / title of chapter, Pages No., Copyright (Year), with permission from Elsevier [OR APPLICABLE SOCIETY COPYRIGHT OWNER].” Also Lancet special credit - “Reprinted from The Lancet, Vol. number, Author(s), Title of article, Pages No., Copyright (Year), with permission from Elsevier.”

4. Reproduction of this material is confined to the purpose and/or media for which permission is hereby given.

5. Altering/Modifying Material: Not Permitted. However figures and illustrations may be altered/adapted minimally to serve your work. Any other abbreviations, additions, deletions and/or any other alterations shall be made only with prior written authorization of Elsevier Ltd. (Please contact Elsevier at permissions@elsevier.com)

6. If the permission fee for the requested use of our material is waived in this instance, please be advised that your future requests for Elsevier materials may attract a fee.

7. Reservation of Rights: Publisher reserves all rights not specifically granted in the combination of (i) the license details provided by you and accepted in the course of this licensing transaction, (ii) these terms and conditions and (iii) CCC's Billing and Payment terms and conditions.

8. License Contingent Upon Payment: While you may exercise the rights licensed immediately upon issuance of the license at the end of the licensing process for the transaction, provided that you have disclosed complete and accurate details of your proposed use, no license is finally effective unless and until full payment is received from you (either by publisher or by CCC) as provided in CCC's Billing and Payment terms and conditions. If full payment is not received on a timely basis, then any license preliminarily granted shall be deemed automatically revoked and shall be void as if never granted. Further, in the event that you breach any of these terms and conditions or any of CCC's Billing and Payment terms and conditions, the license is automatically revoked and shall be void as if never granted. Use of materials as described in a revoked license, as well as any use of the materials beyond the scope of an unrevoked license, may constitute copyright infringement and publisher reserves the right to take any and all action to protect its copyright in the materials.

9. Warranties: Publisher makes no representations or warranties with respect to the licensed material.

10. Indemnity: You hereby indemnify and agree to hold harmless publisher and CCC, and their respective officers, directors, employees and agents, from and against any and all claims arising out of your use of the licensed material other than as specifically authorized pursuant to this license.

11. No Transfer of License: This license is personal to you and may not be sublicensed, assigned, or transferred by you to any other person without publisher's written permission.

12. No Amendment Except in Writing: This license may not be amended except in a writing signed by both parties (or, in the case of publisher, by CCC on publisher's behalf).

13. Objection to Contrary Terms: Publisher hereby objects to any terms contained in any purchase order, acknowledgment, check endorsement or other writing prepared by you, which terms are inconsistent with these terms and conditions or CCC's Billing and Payment terms and conditions.

These terms and conditions, together with CCC's Billing and Payment terms and conditions (which are incorporated herein), comprise the entire agreement between you and publisher (and CCC) concerning this licensing transaction. In the event of any conflict between your obligations established by these terms and conditions and those established by CCC's Billing and Payment terms and conditions, these terms and conditions shall control.

14. **Revocation:** Elsevier or Copyright Clearance Center may deny the permissions described in this License at their sole discretion, for any reason or no reason, with a full refund payable to you. Notice of such denial will be made using the contact information provided by you. Failure to receive such notice will not alter or invalidate the denial. In no event will Elsevier or Copyright Clearance Center be responsible or liable for any costs, expenses or damage incurred by you as a result of a denial of your permission request, other than a refund of the amount(s) paid by you to Elsevier and/or Copyright Clearance Center for denied permissions.

LIMITED LICENSE

The following terms and conditions apply only to specific license types:

15. **Translation:** This permission is granted for non-exclusive world **English** rights only unless your license was granted for translation rights. If you licensed translation rights you may only translate this content into the languages you requested. A professional translator must perform all translations and reproduce the content word for word preserving the integrity of the article. If this license is to re-use 1 or 2 figures then permission is granted for non-exclusive world rights in all languages.

16. **Website:** The following terms and conditions apply to electronic reserve and author websites:
Electronic reserve: If licensed material is to be posted to website, the web site is to be password-protected and made available only to bona fide students registered on a relevant course if: This license was made in connection with a course, This permission is granted for 1 year only. You may obtain a license for future website posting, All content posted to the web site must maintain the copyright information line on the bottom of each image,

A hyper-text must be included to the Homepage of the journal from which you are licensing at <http://www.sciencedirect.com/science/journal/xxxxx> or the Elsevier homepage for books at <http://www.elsevier.com> , and

Central Storage: This license does not include permission for a scanned version of the material to be stored in a central repository such as that provided by Heron/XanEdu.

17. **Author website** for journals with the following additional clauses:

All content posted to the web site must maintain the copyright information line on the bottom of each image, and the permission granted is limited to the personal version of your paper. You are not allowed to download and post the published electronic version of your article (whether PDF or HTML, proof or final version), nor may you scan the printed edition to create an electronic version. A hyper-text must be included to the Homepage of the journal from which you are licensing at <http://www.sciencedirect.com/science/journal/xxxxx> . As part of our normal production process, you will receive an e-mail notice when your article appears on Elsevier's online service ScienceDirect (www.sciencedirect.com). That e-mail will include the article's Digital Object Identifier (DOI). This number provides the electronic link to the published article and should be included in the posting of your personal version. We ask that you wait until you receive this e-mail and have the DOI to do any posting.

Central Storage: This license does not include permission for a scanned version of the material to be stored in a central repository such as that provided by Heron/XanEdu.

18. **Author website** for books with the following additional clauses: Authors are permitted to place a brief summary of their work online only. A hyper-text must be included to the Elsevier homepage at <http://www.elsevier.com> . All content posted to the web site must maintain the copyright information line on the bottom of each image. You are not allowed to download and post the published electronic version of your chapter, nor may you scan the printed edition to create an electronic version.

Central Storage: This license does not include permission for a scanned version of the material to be stored in a central repository such as that provided by Heron/XanEdu.

19. **Website** (regular and for author): A hyper-text must be included to the Homepage of the journal from which you are licensing at <http://www.sciencedirect.com/science/journal/xxxxx>. or for books to the Elsevier homepage at <http://www.elsevier.com>

20. **Thesis/Dissertation**: If your license is for use in a thesis/dissertation your thesis may be submitted to your institution in either print or electronic form. Should your thesis be published commercially, please reapply for permission. These requirements include permission for the Library and Archives of Canada to supply single copies, on demand, of the complete thesis and include permission for UMI to supply single copies, on demand, of the complete thesis. Should your thesis be published commercially, please reapply for permission.

21. **Other Conditions**:

v1.6

If you would like to pay for this license now, please remit this license along with your payment made payable to "COPYRIGHT CLEARANCE CENTER" otherwise you will be invoiced within 48 hours of the license date. Payment should be in the form of a check or money order referencing your account number and this invoice number RLNK500859367. Once you receive your invoice for this order, you may pay your invoice by credit card. Please follow instructions provided at that time.

Make Payment To:

Copyright Clearance Center

Dept 001

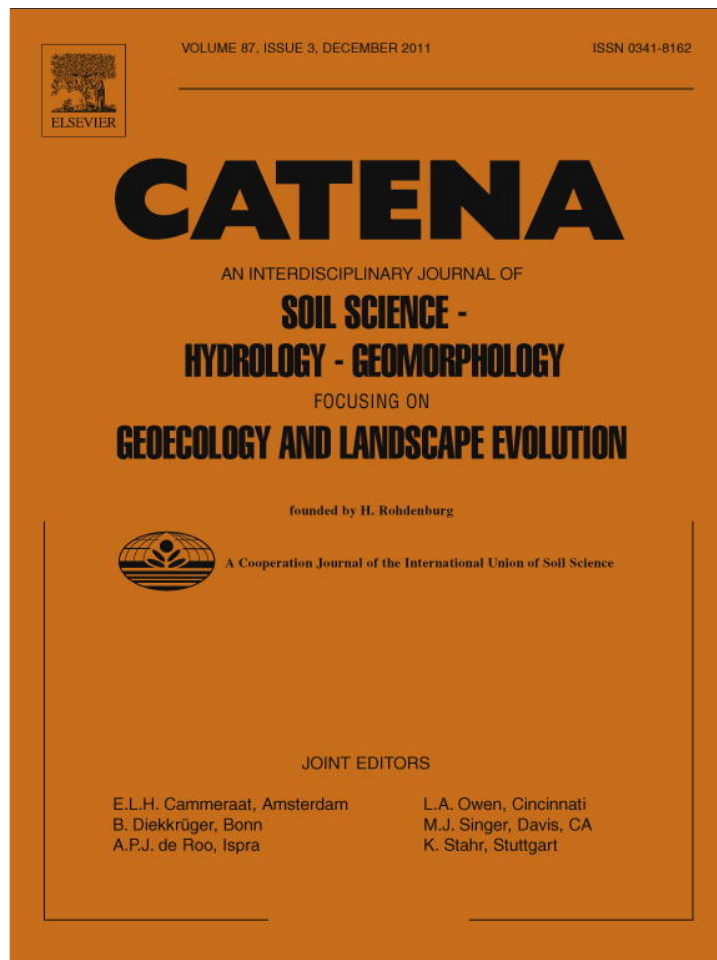
P.O. Box 843006

Boston, MA 02284-3006

For suggestions or comments regarding this order, contact RightsLink Customer Support: customercare@copyright.com or +1-877-622-5543 (toll free in the US) or +1-978-646-2777.

Gratis licenses (referencing \$0 in the Total field) are free. Please retain this printable license for your reference. No payment is required.

Provided for non-commercial research and education use.
Not for reproduction, distribution or commercial use.



This article appeared in a journal published by Elsevier. The attached copy is furnished to the author for internal non-commercial research and education use, including for instruction at the authors institution and sharing with colleagues.

Other uses, including reproduction and distribution, or selling or licensing copies, or posting to personal, institutional or third party websites are prohibited.

In most cases authors are permitted to post their version of the article (e.g. in Word or Tex form) to their personal website or institutional repository. Authors requiring further information regarding Elsevier's archiving and manuscript policies are encouraged to visit:

<http://www.elsevier.com/copyright>



Contents lists available at ScienceDirect

Catena

journal homepage: www.elsevier.com/locate/catena

Organic carbon accumulation in a 2000-year chronosequence of paddy soil evolution

Livia Wissing^{a,*}, Angelika Kölbl^a, Vanessa Vogelsang^b, Jian-Rong Fu^c,
Zhi-Hong Cao^d, Ingrid Kögel-Knabner^a

^a Lehrstuhl für Bodenkunde, Department Ecology and Ecosystem Sciences, Center of Life and Food Sciences Weihenstephan, Technische Universität München, D-85350 Freising-Weihenstephan, Germany

^b Soil Sciences, Martin-Luther-Universität Halle-Wittenberg, am-Seckendorff-Platz 3, D-06120 Halle/Saale, Germany

^c Institute of Environment and Soil Fertilizer Research, Zhejiang Academy of Agricultural Sciences, Hangzhou 310021, PR China

^d Institute of Soil Science, Chinese Academy of Sciences, Nanjing 210008, PR China

ARTICLE INFO

Article history:

Received 7 February 2011

Received in revised form 12 July 2011

Accepted 13 July 2011

Keywords:

Soil organic carbon (SOC)

Particle size fractionation

OC storage capacity

Pedogenesis

Fine mineral fraction

Cultivation history

ABSTRACT

Considerable amounts of soil organic matter (SOM) are stabilized in paddy soils, and thus a large proportion of the terrestrial carbon is conserved in wetland rice soils. Nonetheless, the mechanisms for stabilization of organic carbon (OC) in paddy soils are largely unknown. Based on a chronosequence derived from marine sediments, the objectives of this study are to investigate the accumulation of OC and the concurrent loss of inorganic carbon (IC) and to identify the role of the soil fractions for the stabilization of OC with increasing duration of paddy soil management. A chronosequence of six age groups of paddy soil formation was chosen in the Zhejiang Province (PR China), ranging from 50 to 2000 years (yrs) of paddy management. Soil samples obtained from horizontal sampling of three soil profiles within each age group were analyzed for bulk density (BD), OC as well as IC concentrations, OC stocks of bulk soil and the OC contributions to the bulk soil of the particle size fractions. Paddy soils are characterized by relatively low bulk densities in the puddled topsoil horizons (1.0 and 1.2 g cm^{-3}) and high values in the plow pan (1.6 g cm^{-3}). Our results demonstrate a substantial loss of carbonates during soil formation, as the upper 20 cm were free of carbonates in 100-year-old paddy soils, but carbonate removal from the entire soil profile required almost 700 yrs of rice cultivation. We observed an increase of topsoil OC stocks from 2.5 to 4.4 kg m^{-2} during 50 to 2000 yrs of paddy management. The OC accumulation in the bulk soil was dominated by the silt- and clay-sized fractions. The silt fraction showed a high accretion of OC and seems to be an important long-term OC sink during soil evolution. Fine clay in the puddled topsoil horizon was already saturated and the highest storage capacity for OC was calculated for coarse clay. With longer paddy management, the fractions $<20 \mu\text{m}$ showed an increasing actual OC saturation level, but did not reach the calculated potential storage capacity.

© 2011 Elsevier B.V. All rights reserved.

1. Introduction

Several studies underline the importance and specificity of wetland rice soils for world food production as well as for the contribution to terrestrial organic carbon (OC) storage (Neue et al., 1997; Scharpenseel et al., 1996; Zhang and Gong, 2003). A specific feature of paddy soil management is puddling, tilling the soil under waterlogged conditions (Kögel-Knabner et al., 2010). Puddling before transplanting or seeding is an elementary step of management and is necessary to break down the aggregates and reduce the water percolation as well as to intermix soils with fertilizer (Yoshida and Adachi, 2002). The periodic short-term redox cycles induced by this specific paddy management performed over long time periods have

strong effects on long-term biogeochemical processes. It is associated with a large accumulation of soil organic matter (SOM), which is observed in some, but not all paddy soils (Kögel-Knabner et al., 2010). In a study on evaluating the effect of paddy management on an Ultisol in China, Zhang and He (2004) reported the paddy soil management and irrigated anaerobic rice cropping are favorable for accumulation of SOM. This is attributed to the fact that paddy soils receive large carbon input via organic fertilizers and plant residues (Gong and Xu, 1990; Tanji et al., 2003). But it is also often stated that waterlogging associated with rice cropping enhances accumulation of soil organic carbon (SOC) (Lal, 2002; Neue et al., 1997). Rates of decomposition of added organic materials as well as of SOM are considered to be slower under anaerobic conditions than under aerobic conditions, leading to an accumulation of SOM. In a study on surveying storage and sequestration potential of OC in China's paddy soils, Pan et al. (2003) found higher topsoil OC content in comparison to corresponding soils in dry cropland. Furthermore, in a report on OC storage of soils in southeast China, Zhao et al. (1997) identified paddy soils as an important SOM accumulator,

* Corresponding author. Tel.: +49 8161 71 3734; fax: +49 8161 71 4466.

E-mail addresses: l.wissing@wzw.tum.de (L. Wissing), koelbl@wzw.tum.de (A. Kölbl), vanessa.vogelsang@landw.uni-halle.de (V. Vogelsang), fujr@mail.hz.zj.cn (J.-R. Fu), zhihongcaoli@126.com (Z.-H. Cao), koegel@wzw.tum.de (I. Kögel-Knabner).

with the second highest SOM stocks beside natural forest soils. The accumulation of OC in paddy ecosystems was studied by Wu (2011), showing that the ability to accumulate OC is faster and more pronounced in paddy soils than in other arable ecosystems. Cheng et al. (2009) reported higher OC contents in a paddy soil chronosequence under a rice/non-rice cropping system compared to an upland soil chronosequence in the same region as the present study. In an investigation on use of chronosequences and soil development define Walker et al. (2010) chronosequences as a set of sites formed from the same parent material and underlines the important opportunity for studying temporal dynamics and soil evolution. Thus, such a soil chronosequence is a unique tool for investigating SOM formation during paddy soil development. In the Chinese Zhejiang Province, new farmland has been created through consecutive land reclamation by protective dikes over the past 2000 years (yrs). The construction of the dikes is historically well-dated and provides a chronosequence of soil formation under agricultural use (Ci et al., 2008; Cheng et al., 2009; Li et al., 2007). Parts of the land were used for paddy rice, other parts for a variety of non-irrigated cropland (mostly wheat, but recently also other cash crops, such as watermelons). This soil chronosequence provides the opportunity to evaluate the effect of paddy soil management over long time periods on the evolution and distribution of SOM during pedogenesis. In the present investigation we used the soils from this unique chronosequence to elucidate SOM stabilization in paddy soils. With data on inorganic carbon (IC) and OC stock development during paddy soil evolution we are able to assign OC accumulation in the paddy soil profile developed within 2000 yrs of soil management. A particle size fractionation of differently aged paddy topsoils from 50 to 2000 yrs was used

- (i) to allocate OC distribution within particle size fractions;
- (ii) to identify soil fractions responsible for OC accumulation depending on the duration of paddy soil evolution, and
- (iii) to investigate OC saturation in the fine mineral-associated fraction.

This then made it possible to identify the role of different SOM fractions for OC accumulation during management-induced paddy soil formation.

2. Materials and methods

2.1. Study area

The study sites are located around Cixi (30° 10' N, 121° 14' E), Zhejiang Province, in the eastern part of the PR China, approximately 180 km south of Shanghai and 150 km east of Hangzhou (Fig. 1). The overall area covers 433 km² (in 1988), with a variation of altitude from 2.6 to 5.7 m above sea level (Zhang et al., 2004). The climate is subtropical with periodical monsoon rain. Mean annual temperature is 16.3 °C with an average range from 9.3 °C to 38.5 °C, and the mean annual precipitation is 1325 mm with highest values from April to October (Cheng et al., 2009). Due to a total evaporation of 1000 mm in this region, irrigation is needed to maintain standing water in certain periods of rice growing. More detailed information regarding ground water table, geography and geochemistry of the study area was described by Cheng et al. (2009). For the purpose of land reclamation, nine dikes were built over the past 2000 yrs, leading to a chronosequence of soil formation under agricultural use and therefore differently aged paddy fields. The investigated paddy soil chronosequence (50 to 1000 yrs) was determined according to the record in the Country Annals of the Zhejiang Province, as well as in Yuyao, Cixi and Shangyu Countries. Information in Chinese is obtainable at <http://www.cixi.gov.cn/> (Cheng et al., 2009). According to Cheng et al. (2009) those Country Annals were written during 1621–1627 and contain detailed information about the dikes, the exact position as well as the year of dike construction. The description of the 2000-year-old paddy site can be

found in Zou et al. (2011). The analyzed paddy soil chronosequence contains a succession of 50, 100, 300, 700, 1000 and 2000 yrs (further denominated as P 50, P 100, P 300, etc.) of cropping history (Fig. 1).

2.2. Soil sampling and description

During a sampling campaign in June 2008, soil profiles of the above described chronosequence were sampled in triplicate from three adjacent independent paddy fields. All soils have been sampled under similar soil moisture and weather conditions in the field. The soils were described according to FAO (2006) and classified according to IUSS Working Group WRB (2007). The following soil types were identified: P 50 = Stagnic Gleyic Cambisol (Calcaric Siltic); P 100 = Gleyic Cambisol (Eutric, Siltic); P 300 = Gleyic Cambisol (Eutric, Siltic); P 700 = Endogleyic Stagnosol (Albic, Eutric, Siltic, Thapptomollic); P 1000 = Endogleyic Stagnosol (Albic, Ruptic, Eutric, Siltic); and P 2000 = Endogleyic Stagnosol (Albic, Ruptic, Eutric, Siltic). The description of the texture classes was done according to FAO (2006), ranging from Silt loam to Silty clay loam to Silty clay without trend throughout the chronosequence (Table 1). From each horizon, bulk soil samples and additionally three undisturbed core samples were taken (core volume: 100 cm³). All samples were air-dried and the bulk soil was sieved to a size of <2 mm for further analyses. The investigated paddy soils consist of the following horizon sequence: The puddled layer(s) and the plow pan (A horizons) represent the topsoil, with the following subordinate characteristics: d = dense layer; l = capillary fringe mottling; p = plowing or other human influence; r = strong reduction. In the subsoil, down to 119 cm, several B horizons were identified (B horizons: b = buried genetic horizon; g = stagnic conditions; h = accumulation of OM; l = capillary fringe mottling; w = development of color or structure; Table 1).

2.3. Basic soil parameters

Total carbon concentration (C_{tot}) of each sample was determined in duplicate by dry combustion at 950 °C on a Vario EL elemental analyser (Elementar Analysensysteme, Hanau, Germany). The IC content was determined by dissolution of carbonates with 42% phosphoric acid and subsequent infrared detection of the evolving CO₂ (C-MAT 550, Ströhlein GmbH, Viersen, Germany). All of these measurements were done in duplicate. The OC concentration was calculated by subtracting the concentration of IC from C_{tot} :

$$OC(\text{mg g}^{-1}) = C_{tot}(\text{mg g}^{-1}) - IC(\text{mg g}^{-1}) \quad (1)$$

The bulk density (BD) was calculated by dividing the mass of oven-dried soil (105 °C) by the core volume. The OC stock was calculated for each horizon according to Eq. 2. For each soil, the OC stocks were added up with soil depth, in order to present the stocks as cumulative curves and compare the OC stocks of the upper 100 cm.

$$OC \text{ stock}(\text{kg m}^{-2}) = OC(\text{g kg}^{-1}) * \text{bulk density}(\text{kg dm}^{-3}) * \text{thickness}(\text{cm}) * 10^{-2} \quad (2)$$

2.4. Statistical analyses of basic soil parameters

All statistical analyses were done by using SPSS Statistics 19 (SPSS München, Germany) software. Data were analyzed for homogeneity of variances by Levene test and the analysis of normality was performed with Shapiro–Wilk test. We used the analysis of variance (ANOVA) to compare group means. By homogeneity of the variances, data were tested on differences between the groups by applying the post-hoc tests Bonferroni and Tukey–B test. Otherwise, the post-hoc tests Tamhane and Dunnett–T3 were used to test on differences between the groups. Significant differences ($p \leq 0.05$) between similar

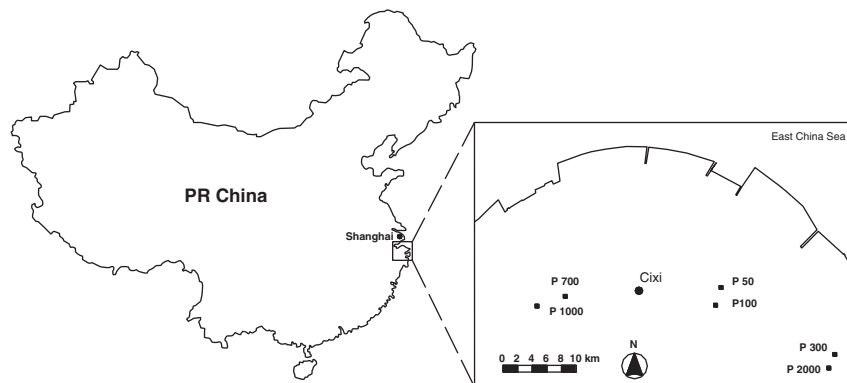


Fig. 1. Geographic position of the study area around Cixi in Eastern China, Zhejiang Province. Close-up view of sampling sites showing the paddy soil chronosequence; consisting of P 50, P 100, P 300, P 700, P 1000 and P 2000-year-old main profiles.

horizons of different soil age groups were indicated by different letters (Table 1).

2.5. Particle size fractionation of topsoil

Topsoil horizons of P 50 and P 100 were pre-treated with 0.1 M HCl (final pH value = 4.8) to remove CaCO_3 , HCl as well as the dissolved Ca^{2+} ions were removed by centrifugation (20 min, at 3423 g). Afterwards, 15 g of air-dried bulk soil (<2 mm) was suspended with demineralized water (1:5 ratio soil (g) to water (ml)). Macroaggregates (>200 μm) were destroyed by using a first ultrasonic treatment with an energy input of 60 J ml^{-1} (Sonoplus HD 2200, Bandelin, Berlin, Germany). After the first ultrasonic treatment, particles of >200 μm and particulate organic matter (POM) were separated by a wet sieving procedure. The dispersion of microaggregates (<200 μm) was achieved with an additional ultrasonic treatment (440 J ml^{-1}). The coarse silt fraction (20 μm –63 μm) was separated from the residue by wet sieving. The suspension less than 20 μm represents the fine mineral fraction (further denominated as fraction <20 μm) and was separated by sedimentation using Atterberg cylinders, dividing medium silt (6.3 μm –20 μm) from fine silt (2.0 μm –6.3 μm). The coarse clay fraction (0.2 μm –2.0 μm) was separated by centrifugation (18 min, at 3423 g). The fine clay fraction (<0.2 μm) was recovered from the suspension by pressure filtration (0.2 μm polymer filter). All fractions were freeze-dried and weighed to calculate the weight proportion of each fraction. The soil fractions were further denominated as sand and particulate organic matter (S + POM), coarse silt (cSi), medium silt (mSi), fine silt (fSi), coarse clay (cC) and fine clay (fC).

2.6. Actual and potential OC saturation of the fraction <20 μm

The C_{tot} concentrations of particle size fractions were measured in duplicate by dry combustion (EuroEA Elemental Analyzer 3000, HEKAtech, Wegberg, Germany). Due to the HCl treatment prior to the physical fractionation procedure, all mineral fractions are free of carbonates and the C_{tot} concentration equals the OC concentration. The mass proportion of all particle size fractions was multiplied by the respective OC concentration to obtain the contribution of the individual fractions to the bulk soil OC concentration.

The actual OC saturation level of the fraction <20 μm was calculated by adding up the OC contributions of the individual fractions using the following equation:

$$\begin{aligned} \text{OC}_{(\text{actual})} \text{ in fraction } < 20\mu\text{m} (\text{g kg}^{-1}) \\ = \text{mass proportion}_{6.3-20\mu\text{m}} (\text{g kg}^{-1}) * \text{OC}_{6.3-20\mu\text{m}} (\text{mg g}^{-1}) + \dots \\ + \text{mass proportion}_{<0.2\mu\text{m}} (\text{g kg}^{-1}) \text{OC}_{<0.2\mu\text{m}} (\text{mg g}^{-1}) \end{aligned} \quad (3)$$

The results were compared with the potential OC storage capacity which was calculated according to the empirical equation of Hassink (1997):

$$\text{OC}_{(\text{potential})} \text{ in fraction } < 20\mu\text{m} (\text{g kg}^{-1}) = 4.09 + 0.37 * \% \text{ particles } < 20\mu\text{m} \quad (4)$$

3. Results

Basic soil properties of the paddy soil chronosequence as well as statistical differences of the paddy characteristics (BD, OC, IC and OC stocks) between the same horizons of the different paddy age groups were shown in Table 1.

3.1. Depth distribution of bulk density, OC, IC and OC stocks

Bulk densities between 1.0 and 1.2 g cm^{-3} were found in all puddled topsoil horizons. The highest values were measured in the plow pan (1.6 g cm^{-3}). Below the plow pan, bulk densities were slightly decreasing in the subsoil but without chronological trend (Table 1). The OC concentration in the topsoils (sum of puddled horizon and plow pan) ranged from 19 mg g^{-1} (P 1000) to 51 mg g^{-1} (P 2000). We observed an increase of OC with soil evolution within the first 300 yrs. Afterwards, oscillating OC concentrations in the topsoils were found between P 700 yrs and P 2000 yrs (Table 1). In the subsoils, OC concentrations were generally lower compared to the topsoil OC values. OC concentrations in the deepest subsoil horizons tended to decrease with increasing soil age and ranged from 5.4 mg g^{-1} (P 50) to 1.4 mg g^{-1} in P 2000 (Table 1). IC concentrations of bulk soil varied in the topsoil between 0.2 mg g^{-1} (P 100) and 2.1 mg g^{-1} (P 50) and in the subsoil from 0.6 mg g^{-1} (P 300) to 3.8 mg g^{-1} (P 50). The topsoil of P 300 was free of carbonates but there were abruptly higher values below the plow pan. Decalcification of the entire soil profile was observed in P 700, P 1000, and P 2000 (Table 1). OC stocks of topsoils (sum of puddled horizon and plow pan) increased from 3.3 kg m^{-2} in paddy 50 yrs up to 5.5 kg m^{-2} in paddy 2000 yrs. However, a continuous increase (with paddy soil evolution) of the topsoil OC stocks was only observed within the first 300 yrs. P 300 showed the highest topsoil OC stock overall, at about 6.1 kg m^{-2} (Table 1, Fig. 2). After the first 300 yrs of soil evolution, the topsoil OC stocks oscillate between P 700 and P 2000 (Table 1, Fig. 2). Compared to the stocks in the topsoils, the subsoil OC stocks of P 50, P 100, P 700 and P 1000 were considerably higher but without a chronological trend.

3.2. Mass distribution and OC concentrations of particle size fractions

We obtained almost the same mass distribution among the particle size fractions in the plow pan as in the puddled horizon

Table 1

Paddy soil chronosequence: Depths, horizon denominations, texture classes, bulk densities (BD), organic carbon (OC), inorganic carbon (IC) concentrations and OC stocks of bulk soils. All numbers give the arithmetic mean (bold) of three replicates with standard errors.

Site	Depth (mean) (cm)	Horizon (FAO) ^a	Texture class	BD (g cm ⁻³)	OC (mg g ⁻¹)	IC (mg g ⁻¹)	OC stocks (kg m ⁻²)	Σ OC stocks (kg m ⁻²)				
P 50	0–13	Alrp	SiCL	1.16 ± 0.05	<i>ab</i>	16.44 ± 0.20	<i>c</i>	1.90 ± 0.06	<i>a</i>	2.50 ± 0.26	<i>a</i>	3.3
	13–22	Ardp	SiCL	1.56 ± 0.02	<i>a</i>	5.72 ± 0.12	<i>c</i>	2.13 ± 0.75	<i>a</i>	0.80 ± 0.02	<i>a</i>	
	22–37	Bwg1	SiCL	1.47 ± 0.01	<i>b</i>	5.11 ± 0.24	<i>a</i>	2.36 ± 0.61	<i>a</i>	1.10 ± 0.06	<i>a</i>	
	*37–50	Bwg2	SiL	1.47 ± 0.02	<i>b</i>	5.18 ± 0.20	<i>a</i>	2.42 ± 0.49	<i>a</i>	0.90 ± 0.04	<i>a</i>	
	50–70	Bwg3	SiCL	1.45 ± 0.02	<i>a</i>	5.07 ± 0.04	<i>a</i>	3.42 ± 0.11	<i>a</i>	1.50 ± 0.01	<i>a</i>	
P 100	*70–100	Blg	SiCL	1.41 ± 0.01		5.44 ± 0.20		3.78 ± 0.06	<i>a</i>	2.30 ± 0.07		5.8
	0–15	Alp	SiCL	1.13 ± 0.04	<i>ab</i>	16.67 ± 0.88	<i>c</i>	b.d.l.	<i>b</i>	2.90 ± 0.19	<i>a</i>	3.6
	15–22	Ardp	SiCL	1.56 ± 0.02	<i>a</i>	6.61 ± 1.27	<i>c</i>	0.20 ± 0.20	<i>b</i>	0.70 ± 0.14	<i>a</i>	
	22–30	Bwg1	SiCL	1.55 ± 0.00	<i>ab</i>	5.80 ± 0.12	<i>a</i>	1.88 ± 0.56	<i>ab</i>	0.70 ± 0.15	<i>a</i>	
	*30–50	Bwg2	SiCL	1.53 ± 0.03	<i>ab</i>	4.72 ± 0.20	<i>a</i>	2.88 ± 0.28	<i>a</i>	1.42 ± 0.06	<i>a</i>	
50–75	Bwlg1	SiCL	1.49 ± 0.02	<i>a</i>	4.72 ± 0.08	<i>a</i>	2.80 ± 0.04	<i>b</i>	1.76 ± 0.04	<i>a</i>		
P 300	*75–100	Bwlg2	SiCL	1.39 ± 0.06		5.21 ± 0.12		2.56 ± 0.37	<i>ab</i>	1.81 ± 0.10		5.7
	0–18	Alp	SiL	1.17 ± 0.05	<i>ab</i>	22.60 ± 2.00	<i>b</i>	b.d.l.	<i>b</i>	4.73 ± 0.42	<i>b</i>	6.1
	18–24	Ardp	SiCL	1.50 ± 0.04	<i>a</i>	14.87 ± 2.37	<i>ab</i>	b.d.l.	<i>b</i>	1.32 ± 0.27	<i>a</i>	
	24–30	Bwdl	SiL	1.61 ± 0.04	<i>a</i>	7.12 ± 1.27	<i>a</i>	0.57 ± 0.41	<i>bc</i>	0.68 ± 0.11	<i>a</i>	
	*30–48	Bwl	SiCL	1.63 ± 0.02	<i>a</i>	5.30 ± 0.04	<i>a</i>	0.48 ± 0.27	<i>b</i>	1.60 ± 0.10	<i>a</i>	
48–70	Bwlg1	SiCL	1.48 ± 0.03	<i>a</i>	4.89 ± 0.00	<i>a</i>	1.13 ± 0.26	<i>c</i>	1.32 ± 0.13	<i>a</i>		
P 700	*70–100	Bwlg2	SiCL	1.46 ± 0.03		4.65 ± 0.08		1.82 ± 0.97	<i>bc</i>	2.03 ± 0.04		5.6
	0–15	Alp	SiCL	1.09 ± 0.02	<i>ab</i>	20.90 ± 0.17	<i>b</i>	b.d.l.	<i>b</i>	3.50 ± 0.19	<i>ab</i>	4.3
	15–22	Ardp	SiCL	1.46 ± 0.03	<i>a</i>	8.58 ± 0.73	<i>bc</i>	b.d.l.	<i>b</i>	0.79 ± 0.03	<i>a</i>	
	22–45	Bg	SiCL	1.49 ± 0.01	<i>b</i>	4.12 ± 1.00	<i>a</i>	b.d.l.	<i>c</i>	1.44 ± 0.29	<i>a</i>	
	*45–57	2Ahgb	SiC	1.53 ± 0.04	<i>ab</i>	5.28 ± 0.69	<i>a</i>	b.d.l.	<i>b</i>	1.10 ± 0.57	<i>a</i>	
57–95	2Blg	SiC	1.45 ± 0.01	<i>a</i>	3.29 ± 0.53	<i>bc</i>	b.d.l.	<i>d</i>	1.80 ± 0.18	<i>a</i>		
P1000	*95–105	3Ahlg	SiCL	1.50 ± 0.05		5.95 ± 1.05		b.d.l.	<i>c</i>	1.10 ± n.d.		5.9
	*105–119	3Blg	SiL	1.47 ± n.d.		2.08 ± n.d.		b.d.l.		0.43 ± n.d.		
	0–17	Alp	SiCL	1.21 ± 0.02	<i>a</i>	12.90 ± 0.55	<i>c</i>	b.d.l.	<i>b</i>	2.60 ± 0.23	<i>a</i>	
	17–23	Aldp	SiCL	1.50 ± 0.04	<i>a</i>	6.07 ± 0.45	<i>c</i>	b.d.l.	<i>b</i>	0.58 ± 0.09	<i>a</i>	
	23–38	2Ahgb	SiC	1.52 ± 0.02	<i>b</i>	4.63 ± 0.53	<i>a</i>	b.d.l.	<i>c</i>	1.06 ± 0.26	<i>a</i>	
P2000	*38–55	2Bg	SiC	1.43 ± 0.02	<i>b</i>	2.81 ± 0.20	<i>b</i>	b.d.l.	<i>b</i>	0.69 ± 0.06	<i>a</i>	6.8
	55–83	2Bl1	SiC	1.29 ± 0.01	<i>b</i>	3.92 ± 0.20	<i>ab</i>	b.d.l.	<i>d</i>	1.40 ± 0.05	<i>a</i>	
	*83–101	3Ahlb	SiC	1.41 ± n.d.		15.42 ± n.d.		b.d.l.	<i>c</i>	2.84 ± n.d.		
	*101–108	3Bl	SiC	1.41 ± n.d.		3.52 ± n.d.		b.d.l.		0.80 ± n.d.		
	0–16	Alp	SiL	1.02 ± 0.04	<i>b</i>	29.99 ± 0.90	<i>a</i>	b.d.l.	<i>b</i>	4.40 ± 0.27	<i>b</i>	
P2000	16–20	Ar(d)p	SiL	1.20 ± 0.06	<i>b</i>	20.60 ± n.d.	<i>a</i>	b.d.l.	<i>b</i>	1.13 ± 0.39	<i>a</i>	5.5
	20–28	Bdg	SiL	1.55 ± 0.02	<i>ab</i>	5.49 ± 0.04	<i>a</i>	b.d.l.	<i>c</i>	0.70 ± 0.09	<i>a</i>	
	*28–45	2AhgB	SiCL	1.57 ± 0.04	<i>a</i>	3.49 ± 0.04	<i>b</i>	b.d.l.	<i>b</i>	0.50 ± n.d.	<i>a</i>	
	45–62	2Bg1	SiC	1.49 ± 0.05	<i>a</i>	2.62 ± 0.61	<i>c</i>	b.d.l.	<i>d</i>	0.70 ± 0.10	<i>b</i>	
	*62–82	2Bg2	SiCL	1.48 ± 0.03		1.70 ± n.d.		b.d.l.	<i>c</i>	0.40 ± 0.08		
*82–108	2Blg	SiCL	1.45 ± 0.01		1.41 ± 0.04		b.d.l.		0.55 ± 0.09		2.8	

Texture classes could only be determined in one soil profile only. SiL = Silt loam; SiC = Silty clay; SiCL = Silty clay loam.

b.d.l. = Below the detection limit.

n.d. = Not detected (this horizon could be detected in one soil profile only).

Σ = Added up OC stocks of top- and subsoils.

* = Due to less than three cases, no statistical analyses were possible.

Italic letters indicate significant differences (≤ 0.05) between same horizons of different paddy age groups.

^a Guidelines for soil profile description, FAO (2006).

(Fig. 3a, b). The mass proportion of S + POM and cSi was only 20% but in contrast, the mass proportion of the fraction <20 μm was about 80% of the total bulk soil, with the highest total mass in medium silt (average of 46%). The mass values of medium silt ranged from 347 g kg⁻¹ in the plow pan of P 50 to 516 g kg⁻¹ in the puddled horizon of P 1000 (Fig. 3a, b). The mass proportion of fine clay showed relatively low values between 46 g kg⁻¹ (P 2000 puddled horizon) to 92 g kg⁻¹ (P 1000 plow pan) (Fig. 3a,b).

The largest OC variability, but also the highest concentrations of OC were shown by the S + POM fraction (Table 2). Medium silt showed the lowest OC concentrations of all silt-sized fractions, with values between 0.6 mg g⁻¹ in the plow pan of P 50 and 10 mg g⁻¹ in the puddled horizon of P 2000 (Table 2). Fine and coarse clay exhibited the highest OC concentrations of the mineral fine fraction (<20 μm) within the chronosequence, with highest values of 55 mg g⁻¹ and 56 mg g⁻¹ in the puddled horizon of P 2000 (Table 2).

3.3. OC contribution of particle size fractions to the bulk soil

The OC contribution of the particle size fractions to the bulk soil was distributed differently within the paddy age groups (Fig. 3c, d)

and ranged from 0.2 mg g⁻¹ in coarse and medium silt (plow pan of P 50 and P 100) to approximately 8 mg g⁻¹ in coarse clay (puddled horizon of P 700 and P 2000).

Excluding P 1000, the fraction <20 μm of the puddled horizons indicated a continuous increase within the chronosequence, but the soil fractions were characterized by different OC accretions (Fig. 3c). The OC contribution of coarse and medium silt to the bulk soil increased the most by six times (Figs. 3c and 4a). Fine silt and coarse clay stored the largest amount of OC in the puddled horizons of all fractions <20 μm, with considerably increasing OC values with time of soil evolution. For example, the OC contribution of coarse clay increased from 4.4 mg g⁻¹ (P 50) to 8.2 mg g⁻¹ (P 2000). However, the OC contribution of the fine clay fractions remained relatively constant and ranged in the puddled horizon from 1.5 mg g⁻¹ (P 50) to 2.5 mg g⁻¹ (P 300 and P 2000) (Fig. 3c). The accretion of the OC contributions in the plow pan of the fraction <20 μm increased more compared to the accretion of the OC contribution in the puddled horizon (Fig. 3d). Fig. 4b indicates lower OC contributions in the young soils but also an enormous accrual of the OC contribution in the particle size fractions within the chronosequence. For example, the accretion of the OC contributions of medium silt increased seventeen times and ranged

from 0.2 mg g^{-1} (P 50) to 3.4 mg g^{-1} (P 2000) (Fig. 3d). In fine silt the contribution of OC to the bulk soil increased fourteen times, varying between 0.3 mg g^{-1} (P 50) and 4.3 mg g^{-1} (P 2000) (Fig. 3d). In comparison with the puddled horizon, the accretion of the OC contributions in the plow pan of the coarse clay and fine clay fraction increased continuously more, whereas the carbon content was much lower in the plow pan of these fractions (Fig. 3d). Within the chronosequence, P 700 and P 1000 showed a considerably lower OC contribution in the fractions $<20 \mu\text{m}$ in the plow pan (Fig. 4b).

3.4. OC saturations in the fraction $<20 \mu\text{m}$ of paddy soils

We calculated the actual OC saturations of the puddled horizon as well as of the plow pan and observed different developments of the OC saturation within the chronosequence (Fig. 4a, b and small graphs therein). The puddled horizons showed a continuously increasing actual OC saturation from 9 g kg^{-1} (P 50) to 20 g kg^{-1} (P 2000). A more pronounced accretion of the actual OC saturation was observed in the following plow pans as well, ranging from 2 g kg^{-1} (P 50) to 17 g kg^{-1} (P 2000). However, the plow pan showed lower actual OC saturations within each age group compared to the puddled topsoil horizon (Fig. 4a, b). The 1000-yr-old paddy site is an exception, with a calculated actual OC saturation being similar to the OC saturation of the youngest paddy site.

Finally, we calculated the potential OC storage capacity of the fractions $<20 \mu\text{m}$ according to the empirical equation of Hassink (1997). Independently of soil age and soil depth, we found no change in the potential OC storage capacity; it was apparently identical throughout the paddy soil chronosequence, ranging from 30 g kg^{-1} (P 300) to 36 g kg^{-1} (P 700) (small graphs in Fig. 4a, b).

4. Discussion

The soil types of the chronosequence range from Gleyic Cambisols (P50, P100, P300) to Endogleyic Stagnosols (P700, P1000, P2000), indicating that soil development processes affect mainly hydroxymorphic pattern which is most likely due to waterlogged conditions during frequent flooding of the soils over long-term periods. However, soil texture classes range between Silt loam and Silty clay without chronological trend or trend in soil depth, highlighting that the parent material was relatively homogeneous and processes of soil development did not affect soil texture distribution so far.

4.1. Development of bulk density during a few decades of paddy soil evolution

All investigated soils had low bulk densities in the puddled topsoil horizons, higher values in the plow pans and slightly decreasing bulk densities with increasing soil depth. Statistical analysis revealed no differences for topsoil bulk densities except for P 1000 yrs and P 2000 yrs, which showed only slight variations in the puddled topsoil horizon. However, all paddy topsoils are characterized by similar texture classes (Table 1). In addition the physical fractionation showed a homogeneous mass distribution of the soil fractions during paddy soil evolution (Fig. 3a, b). Therefore we assume that the slight variations in bulk densities resulted most likely from slightly different tillage practices and not from differences in soil texture.

Generally, the puddling practice led to a less dense and large-pored topsoil layer which is able to store a high amount of irrigation water (Mousavi et al., 2009; Yoshida and Adachi, 2002). However, higher bulk density values in the plow pan are also the result of repeated puddling with water buffaloes or machines over a long period of rice cultivation, leading to the desired compaction and reduced permeability. According to Eickhorst and Tippkötter (2009), our bulk density values are typical for paddy soils and were caused by the specific paddy management. Development and depth distribution of bulk densities were finalized

within the first 50 yrs of paddy soil evolution and showed no further differentiation between the soil ages. These results are supported by Janssen and Lennartz (2006), who found a percolation rate reduced by twenty times due to plow pan formation after just 20 years and by seventeen times after about 100 yrs of paddy management.

To conclude, the short-term development of a dense plow pan is a typical feature of paddy soils, with possible consequences for the processes involved in SOM accumulation as discussed in the following sections.

4.2. Decalcification of paddy soils within a few centuries of soil evolution

Our results show a statistically significant carbonate loss in the upper-most puddled topsoil horizon within the first 100 yrs and a complete decalcification of all topsoil horizons within the first 300 yrs, while the entire soil profile was decalcified after 700 yrs (Table 1). Comparable data are only available for non-paddy wetlands, but not for marine-derived paddy soils. Mueller (1994) described a loss of carbonates only in the upper 50 cm of the soil profile after 700 yrs of soil development in a dyked, silty-clayey marshland soil in Northern Germany. In contrast, Iost et al. (2007) already observed an incipient loss of carbonates in 20-year-old reclaimed marsh topsoil from Zhejiang Province PR China. Intensive decalcification is generally observed in hydric soils subject to periodic changes between oxidation and reduction (van den Berg and Loch, 2000). We assume the specific paddy management to be responsible for the accelerated loss of carbonates in the topsoils. Carbonates were leached by periodical flooding and drainage of the paddy fields during rice cultivation. The dense plow pan disconnected top- and subsoils, leading to retarded decalcification of the subsoils and consequently of the entire soil profile. In conclusion, decalcification of marine-derived paddy soils is a two-phase process: fast decalcification of topsoils during the first 300 yrs and slow decalcification of subsoils over 700 yrs, due to the plow pan cutting of soil formation in topsoil from the subsoil.

4.3. OC concentrations and stocks in top- and subsoil develop differently over several centuries of paddy soil evolution

Topsoil OC concentrations and stocks showed generally a strong increase from 50 to 300 yrs of paddy management and were considerably higher compared to the respective subsoils. This is in contrast to the relatively low SOM contents which are often observed in arable soils (Hassink, 1997; Jenkinson, 1990). Since paddy soils are at least several months under waterlogged conditions, we assume decelerated OC decomposition to be responsible for this observation. Our results are in accordance with Wu (2011), whose data also indicated higher OC stocks in paddy soils compared to other arable ecosystems. Varying topsoil (puddled horizon and plow pan) OC concentrations after the first 300 yrs of soil evolution are most likely induced by the paddy management. Slight differences in organic fertilizer application or management of crop residues could be responsible for oscillating OC concentrations and stocks.

Marine sediments in the investigated region had OC concentrations of approximately 5 mg g^{-1} (Iost et al., 2007). The subsoil horizons of the younger paddy soils (P 50, P 100, P 300 yrs) of the investigated chronosequence show similar OC concentrations between 4.7 and 5.8 mg g^{-1} (Table 1). After 700 yrs of paddy soil evolution, a significant loss of the marine-derived OC is observed in all subsoil horizons, resulting in lower OC concentrations and stocks in the subsoils, when buried topsoil horizons are not considered. In conclusions, our results support the understanding that paddy management favors SOC accumulation in the topsoils, but interrupts the OC accumulation in the subsoils due to the low permeability of the plow pan.

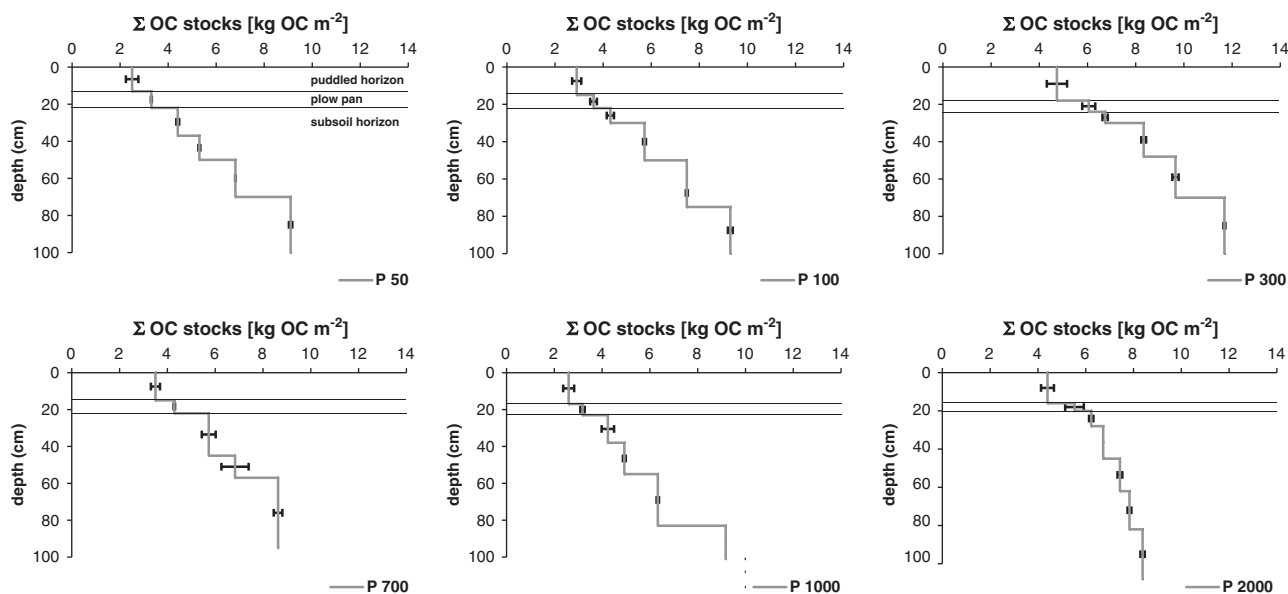


Fig. 2. Cumulative OC stocks of the paddy soil chronosequence (P 50, P 100, P 300, P 700, P 1000, P 2000 yrs). Error bars show the standard error of the OC stocks of 3 replicates. The black lines represent the division of the soil profiles in puddled horizon, plow pan and subsoil horizon.

4.4. OC accumulation in particle size fractions – comparison between puddled horizon and plow pan

Both topsoil horizons are characterized by increasing OC contributions of silt- and clay-sized fractions within the paddy chronosequence (Fig. 3c, d). Especially in the plow pan, all three silt-sized fractions are important OC accumulators. Starting with low initial OC contributions in the “young” paddy soils (P 50 and P 100 yrs), both silt fractions are characterized by a strong accretion of OC during 2000 yrs of soil development. For example, the accretion of the OC contribution in mSi increased in the plow pan eighteen times from 0.2 up to 3.4 mg g⁻¹ (Fig. 3d).

Compared to the puddled horizon, the plow pan was characterized by a stronger accretion of OC in all silt- and clay-sized fractions (Fig. 3d). As a consequence, the increase of OC values during paddy soil evolution is retarded in the plow pan compared to the puddled horizon. This underlines our assumption that the low permeability of the plow pan – acting as a transport barrier between the puddled topsoil and the subsoil horizons – leads to the decelerated accumulation of OC. We suspect that the lower and discontinuous SOC entry in the plow pan and the subsoil compared to the puddled horizon is directly induced by management. The delayed OC transport is caused by the relatively slow transport processes through paddy plow layers and the plow pan maturing process over several decades (Janssen and Lennartz, 2006). This lower and discontinuous SOC entry in the plow pan results in a less strong relationship ($R^2 = 0.75$) between the OC content and the duration of soil evolution compared to the puddled horizon, where we identified a close relationship ($R^2 = 0.98$) between the years of paddy management and the actual OC saturation (small graphs in Fig. 4a, b).

In conclusions, both topsoil horizons showed a continuous OC accumulation in particle size fractions. However, the relatively dense plow pan was characterized by a retarded and discontinuous increase of OC in all soil fractions.

4.5. OC accumulation in specific particle size fractions with increasing soil age

Coarse clay presented the highest OC contribution to the bulk soil in both topsoil horizons and was therefore the most important fraction for OC accumulation during soil evolution (Fig. 3c, d). In a study on long-term impacts of reduced tillage on SOC stabilization, Chivenge et al. (2007)

described the clay-sized fraction as the most stable soil fraction for OC accumulation. In addition to that, we observed a strong accretion of OC in cSi and mSi, starting with low initial OC contributions in the “young” paddy soils which increased up to a high OC contribution in the 2000 yrs old paddy site (Fig. 3c, d). Therefore, cSi and mSi was identified as an important long-term OC sink over time. This could probably be explained by the formation of silt-sized microaggregates, which are known to have more OC per unit material because additional OC binds the primary organo-mineral complexes into silt-sized aggregates (Tisdall and Oades, 1982; Six et al., 2002). Beside this, we assume the retarded decomposition of OC under waterlogged conditions during several months of the year to be responsible for OC accumulation (Kögel-Knabner et al., 2010), also in coarser particle size fractions. In addition, the intensive and homogeneous incorporation of crop residues due to the frequent plowing and puddling (Gaunt et al., 1995) of paddy topsoils is most likely responsible for the preferred accumulation in these mineral associated fractions (Huang et al., 2010).

In contrast to the silt fractions, the fC fraction seems to be already saturated because the OC contributions are very low and have changed only slightly during 2000 yrs of paddy soil evolution. Von Lützw et al. (2007) already observed that fC does not always follow the usual distribution of higher OC contributions with declining particle sizes. Von Lützw et al. (2007) explained that the dispersion procedures during physical fractionation could lead to an incomplete disaggregation of the particle sizes. Therefore, coarser clay fractions could consist of aggregated fine clay particles which protected SOM. A complete dispersion of the particle size fractions is absolutely necessary to isolate silt- and clay-sized particles (Christensen, 2001). A second possible explanation relates to the different OC storage in clay sub-fractions due to a shift in the mineral composition and a resulting selective sorption of SOM with different functional groups on specific clay minerals (Laird et al., 2001).

Hassink et al. (1997) described the fraction <20 μm as an indicator for long-term processes of soil development and Theng (1979) explained that one of the principal factors responsible for physical protection of organic matter in soils is its ability to associate with clay and silt particles. In this context, Hassink (1997) investigated a number of soils and identified the fraction <20 μm as an important determinant of the stability of OM in soils.

The cSi fraction was excluded by Hassink (1997) from the fine mineral fraction because cultivation decreased the amount of OC in

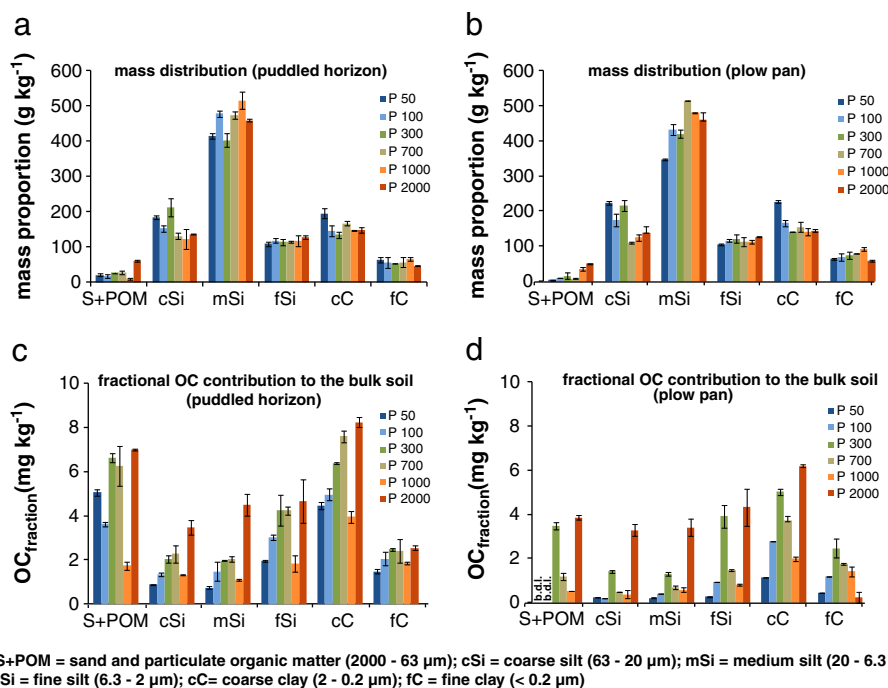


Fig. 3. Mass distributions a; b) and OC contributions c; d) of soil fractions after particle size fractionation. Data of mass proportion are given as means of three replicates and of OC concentration as means of 2 replications. Error bars show the standard deviation.

the fraction >20 μm. Additionally Hassink (1997) characterized the fractions >20 μm to be less protected and therefore more susceptible to decomposition. However, in paddy soils we identified obviously also an enhanced accretion of OC in the cSi fraction (Fig. 3c, d). Since paddy soils are at least several months under waterlogged conditions, we assume decelerated OC decomposition to be responsible for similar OC contributions in cSi and mSi fraction.

To summarize, the chronosequence approach clearly showed different OC accumulation rates for silt- and clay-sized fractions. The particle size fractionation of paddy topsoils showed a detailed separation between a largely saturated fine clay fraction after 50 yrs of soil evolution and a strong accretion of OC in silt-sized fractions. In conclusion, cSi and mSi (strong accretion of OC) and cC (high capacity

for OC accumulation, Chivenge et al., 2007) are largely involved in the SOC accumulation in paddy topsoils.

4.6. Paddy soils do not reach their potential OC saturation during 2000 yrs of soil evolution

The potential OC saturation of the fraction <20 μm remained constant over the years of paddy soil evolution when calculated with the empirical equation of Hassink (1997) (small graphs in Fig. 4a, b). The particle size fractionation showed homogeneous mass proportions of all fractions throughout the chronosequence in the puddled horizon and in the plow pan (Fig. 3a, b), leading to similar OC storage capacities. The higher actual OC saturation in the puddled

Table 2
Organic carbon (OC) concentrations of the soil fractions after particle size fractionation. Data of OC concentrations give the arithmetic mean (bold) of two replications with standard deviations.

Soil fraction			S + POM ^a	cSi ^b	mSi ^c	fSi ^d	cC ^e	fC ^f
	Depth (cm)	Horizon (FAO) ^g	OC (mg g ⁻¹)	OC (mg g ⁻¹)	OC (mg g ⁻¹)	OC (mg g ⁻¹)	OC (mg g ⁻¹)	OC (mg g ⁻¹)
P50	0–13	Alrp	250.4 ± 8.7	4.8 ± 0.2	1.8 ± 0.1	18.0 ± 0.3	22.8 ± 0.3	23.2 ± 0.2
	13–22	Ardp	b.d.l ± b.d.l	1.0 ± 0.0	0.6 ± 0.0	2.4 ± 0.1	5.0 ± 0.1	6.7 ± 0.3
P100	0–15	Alp	211.8 ± 7.2	8.8 ± 0.3	3.1 ± 0.9	25.5 ± 0.8	34.0 ± 1.1	37.1 ± 1.4
	15–22	Ardp	b.d.l ± b.d.l	1.1 ± 0.0	0.9 ± 0.0	8.0 ± 0.0	16.6 ± 0.0	17.2 ± 0.0
P300	0–18	Alp	235.6 ± 18.0	9.5 ± 0.4	4.9 ± 0.2	37.5 ± 3.4	47.5 ± 3.3	46.0 ± 1.2
	18–24	Ardp	224.2 ± 14.5	6.5 ± 0.2	3.1 ± 0.3	32.2 ± 1.0	35.7 ± 1.0	32.9 ± 1.1
P700	0–15	Alp	229.3 ± 17.1	17.3 ± 1.3	4.3 ± 0.3	36.9 ± 1.9	45.4 ± 1.8	42.5 ± 3.7
	15–22	Arpd	160.7 ± 8.5	4.4 ± 0.1	1.3 ± 0.2	13.0 ± 1.1	24.0 ± 3.6	22.0 ± 0.6
P1000	0–17	Alp	186.0 ± 4.5	10.7 ± 1.8	2.1 ± 0.1	15.6 ± 1.0	26.8 ± 1.4	28.5 ± 0.3
	17–23	Aldp	14.3 ± 0.2	3.0 ± 1.3	1.2 ± 0.2	7.2 ± 0.1	14.1 ± 0.2	15.3 ± 3.2
P2000	0–15	Alp	114.9 ± 3.7	25.6 ± 0.3	9.8 ± 1.0	36.3 ± 8.9	55.5 ± 1.3	55.0 ± 3.4
	15–20	Ar(d)p	76.9 ± 2.0	23.6 ± 1.1	7.4 ± 5.0	34.2 ± 6.3	43.6 ± 1.4	45.1 ± 1.6

^a Sand particulate organic matter; 200–63 μm.

^b Coarse silt; 63–20 μm.

^c Medium silt; 20–6.3 μm.

^d Fine silt; 6.3–2 μm.

^e Coarse clay; 2–0.2 μm.

^f Fine clay; <0.2 μm.

^g Guidelines for soil description, FAO (2006). b.d.l. = below the detection limit.

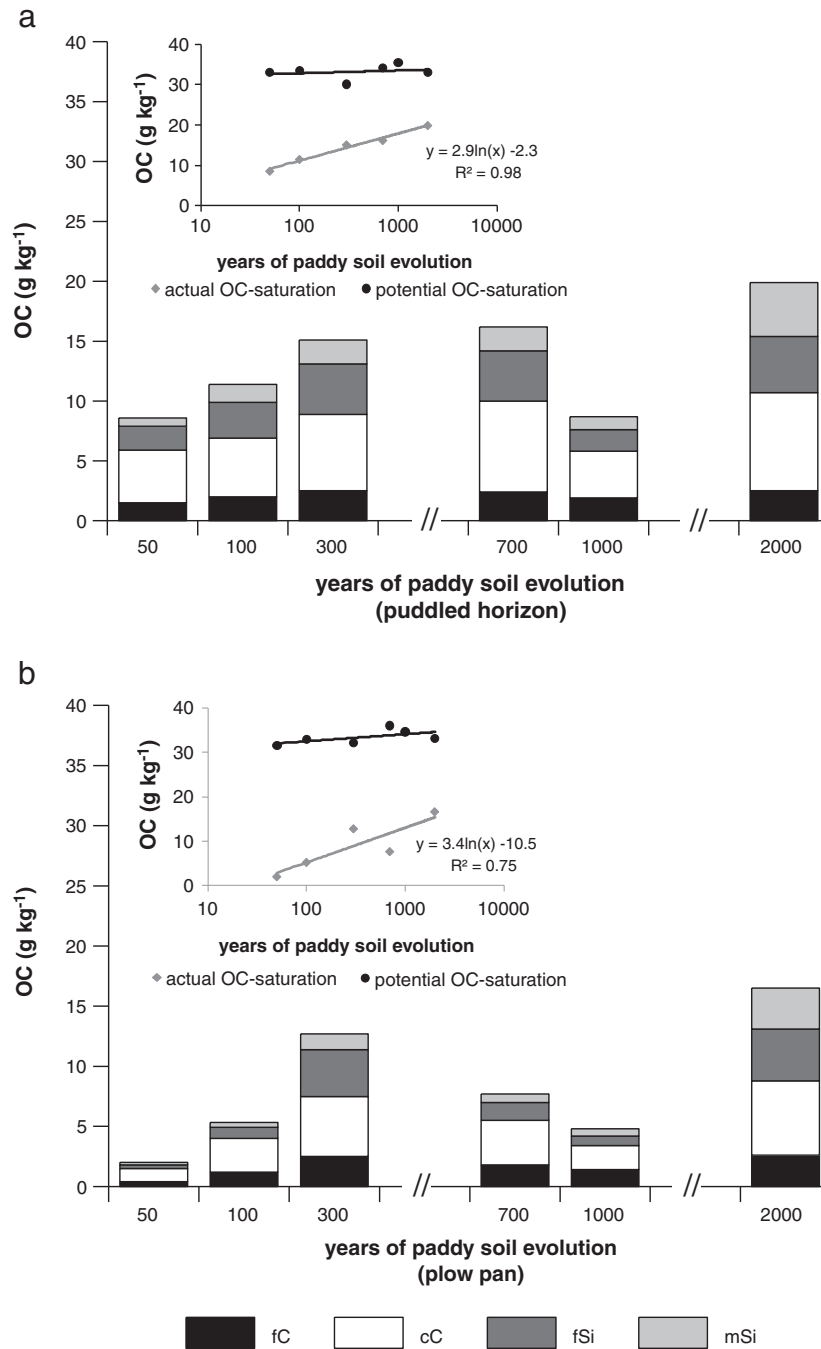


Fig. 4. Relationship between actual and potential OC saturation (small graphs therein) and the OC contribution (big graphs) of the fraction <20 μm to the bulk soil in a) the puddled horizon and b) the plow pan and the years of paddy soil evolution.

horizons was related to the higher OC content in fractions <20 μm, which in turn increased the OC stocks. However, all calculated actual OC saturation values are much lower than the potential OC saturation. The correlation between the years of paddy soil evolution and actual OC saturation did not reach the calculated maxima (potential OC saturation) and indicated a deceleration of OC accumulation over time (Fig. 4a, b). Nevertheless, silt and clay fractions are important OC accumulators, and Hassink (1997) explained the more effective OC association of the fraction <20 μm by the greater physical protection of SOM against decomposition. Hassink (1997) determined the potential OC saturation using grassland soils but many studies do not reach the calculated maxima (Steffens et al., 2009); therefore a re-

evaluation and an adjustment of the potential OC saturation is necessary for paddy soils.

4.7. 1000-year-old paddy site – an exception?

The mass distribution (Fig. 3a, b) showed no differences between the 1000-year-old site and the other paddy sites. The subsoil of P 1000 yrs represents a typical horizon sequence and a characteristic soil development for such an old paddy soil (Table 1). However, comparably low OC values were found for the topsoil, but not for the subsoil of P 1000 yrs (Fig. 2). In particular, P 1000 yrs showed OC concentrations in the clay-sized fraction on the level of a 50-year-old

paddy soil (puddled horizon). In addition, the concentration of OC (puddled horizon) was in the fine silt fraction even lower than the OC values of the youngest paddy soil (Table 2). Other studies on the same paddy soil chronosequence (Li et al., 2007) showed a higher OC content in the topsoil of adjacent P 1000 yrs sites. In our study, we investigated a 1000 yr-old-paddy site which was closer to the dike. Topsoil material of this site was regularly removed in order to construct and rebuild dikes (personal communication of Prof. Cao with local residents). The removal of OC-rich topsoil material and the subsequent incorporation of OC-depleted subsoil material by plowing and puddling is most likely responsible for the low OC content in the topsoil and in the soil fractions.

In addition, also an unadjusted management of this site might have led to the exceptionally low OC values (Hassink, 1997; Hassink et al., 1997; Jenkinson, 1988; Song et al., 2005). For example, Lugo and Brown (1993) showed that management methods such as the removal of plant litter and omission of organic fertilization could lead to a loss of SOC in tropical soils. Differences concerning the method of plowing (mechanical or traditional by animals) as well as the type of fertilizer are also reflected by the OC concentrations and stocks.

In conclusion, we assume the removal of OC-rich topsoil material in combination with an unadjusted agricultural management of the topsoils to be responsible for the exceptionally low OC concentrations in P 1000 yrs topsoils.

5. Conclusions

The formation of the plow pan as indicated by the bulk density profile is a short-term process developing over a short period of puddling and is already finalized within the first 50 yrs of paddy soil evolution. This leads to a decoupling between topsoil and subsoil of the subsequent processes of soil IC loss and OC accumulation. Our results showed a loss of carbonates in the upper-most topsoil horizon within the first 100 yrs by irrigation and drainage. In the subsoil, decalcification was significantly retarded, pointing towards reduced percolation and leaching due to the formation of the plow pan. The complete carbonate removal from the entire soil profile needed 700 yrs of paddy management. Topsoil OC stocks of the differently aged paddy soils increased with slight variations within the 2000 yrs of rice cultivation, whereas the subsoil is dominated by an overall loss of OC inherited from the marine sediment. The accumulation of OC in different fractions of the topsoils developed over a long-term period and needed several centuries of paddy soil evolution. The OC accumulation during 2000 yrs of paddy soil formation is due to strong accretion of OC in the silt-sized and coarse clay fraction, whereas the amount of OC in the S + POM fraction remains constant. The coarse clay and fine silt fraction showed the largest storage capacity of OC, which is replenished in a continuous process. Coarse and medium silt was identified to be an important long-term OC sink during paddy soil evolution, which is accelerated in later stages of paddy soil formation. On the one hand, this may be attributed to soil microaggregation, which seems to evolve only after more than 1000 yrs of paddy soil formation. On the other hand, the retarded decomposition of OC under waterlogged conditions during several months of the year might be responsible for an OC accretion also in coarser particle size fraction medium silt. The calculated actual OC saturation levels of the fractions <20 μm strongly increase with increasing soil age, except for the fine clay fraction, which already seems to be OC saturated. Our findings underline the importance of fine fractions for increasing OC storage, although the process of OC accumulation in the fractions <20 μm seems not to be complete even after 2000 yrs of paddy soil evolution.

Acknowledgements

The authors would like to thank Rui Yin and the Institute of Soil Science, Chinese Academy of Sciences in Nanjing for support during

sampling at the chronosequence site around Cixi and for logistic handling. Peter Schad and Elisabeth Eder are gratefully acknowledged for soil description and soil sampling and Reinhold Jahn for helpful comments. We thank Monika Heilmeyer for technical assistance and Martina Bauer, Carolin Botond, Robert U. Hagemann, Tahereh Javaheri, Juliane Teichmann, Maria Vonach for student research assistance. We are grateful to the Deutsche Forschungsgemeinschaft (DFG) for their generous funding of the Research Unit FOR 995 "Biogeochemistry of paddy soil evolution".

References

- Cheng, Y., Yang, L.-Z., Cao, Z.-H., Ci, E., Yin, S., 2009. Chronosequential changes of selected pedogenic properties in paddy soils as compared with non-paddy soils. *Geoderma* 151, 31–41.
- Chivenge, P.P., Muwira, H.K., Giller, K.E., Mapfumo, P., Six, J., 2007. Long-term impact of reduced tillage and residue management on soil carbon stabilization: implications for conservation agriculture on contrasting soils. *Soil and Tillage Research* 94, 328–337.
- Christensen, B.T., 2001. Physical fractionation of soil and structural and functional complexity in organic matter turnover. *European Journal of Soil Science* 52, 345–353.
- Ci, E., Yang, L., Cheng, Y., Shi, L., Yin, S., 2008. Effect of cultivation history on distribution of organic carbon and structure of humus in paddy soils. *Acta Pedologica Sinica* 45 (5), 950–956 (in Chinese with English abstract).
- Eickhorst, T., Tippkötter, R., 2009. Management-induced structural dynamics in paddy soils of south east China simulated in microcosms. *Soil and Tillage Research* 102, 168–178.
- FAO, 2006. Guidelines for Soil Description. FAO, Rome. 97 pp.
- Gaunt, J.L., Neue, H.-U., Cassman, K.G., Oik, D.C., Arah, J.R.M., Witt, C., Ottow, J.C.G., Grant, J.F., 1995. Microbial biomass and organic matter turnover in wetland rice soils. *Biology and Fertility of Soils* 19, 333–342.
- Gong, Z., Xu, Q., 1990. Paddy soils. *Soils of China*. Science Press, Beijing, pp. 233–260.
- Hassink, J., 1997. The capacity of soil to preserve organic C and N by their association with clay and silt particles. *Plant and Soil* 191, 77–87.
- Hassink, J., Whitmore, A.P., Kubàt, J., 1997. Size and density fractionation of soil organic matter and the physical capacity of soils to protect organic matter. *European Journal of Agronomy* 7, 189–199.
- Huang, S., Rui, W., Peng, X., Huang, Q., Zhang, W., 2010. Organic carbon fractions affected by long-term fertilization in a subtropical paddy soil. *Nutrient Cycling in Agroecosystems* 86, 153–160.
- Iost, S., Landgraf, D., Makeschin, F., 2007. Chemical soil properties of reclaimed marsh soil from Zhejiang Province, PR China. *Geoderma* 142, 245–250.
- IUSS Working Group WRB, 2007, 2007. World reference base for soil resources 2007. : World Soil Resources Reports, 103. FAO, Rome.
- Janssen, M., Lennartz, B., 2006. Horizontal and vertical water fluxes in paddy rice fields of subtropical China. *Advances Geology Ecology* 38, 344–354.
- Jenkinson, D.S., 1988. Soil organic matter and its dynamics, A Wild (Editor), *Russel's Soil Conditions and Plant Growth*, 11th edition. Longman, New York, pp. 564–607.
- Jenkinson, D.S., 1990. The turnover of organic carbon and nitrogen in the soil. *Philosophical Transactions of the Royal Society Series B* 329, 361–368.
- Kögel-Knabner, I., Amelung, W., Cao, Z.-H., Fiedler, S., Frenzel, P., Jahn, R., Kalbitz, K., Kölbl, A., Schloter, M., 2010. Biogeochemistry of paddy soils. *Geoderma* 157, 1–14.
- Laird, D.A., Martens, D.A., Kingery, W.L., 2001. Nature of clay-humic complexes in an agricultural soil. I. Chemical, biochemical, and spectroscopic analyses. *Soil Society of America Journal* 65, 1413–1418.
- Lal, R., 2002. Soil carbon sequestration in China through agricultural intensification, and restoration of degraded and desertified ecosystems. *Land Degradation and Development* 13, 469–478.
- Li, J., Dong, Y., Cao, Z., Wang, H., 2007. Distribution of polycyclic aromatic hydrocarbons (PAHs) in the surface and subsurface soils in Cixi County. *Acta Scientiae Circumstantiae* 27 (11), 1909–1914 (in Chinese with English abstract).
- Lugo, A.E., Brown, S., 1993. Management of tropical soils as sinks or sources of atmospheric carbon. *Plant and Soil* 149, 27–41.
- Mousavi, S.F., Yousefi-Moghadam, Mostafazadeh-Fard, B., Hemmat, A., Yazdani, M.R., 2009. Effect of puddling intensity on physical properties of a silt clay soil under laboratory and field conditions. *Paddy Water Environ* 7, 45–54.
- Mueller, W., 1994. On the genesis of tidal marsh soils. II. Carbonate sedimentation, decalcification. *Zeitschrift fuer Pflanzenernaehrung und Bodenkunde* 157, 333–343.
- Neue, H.U., Gaunt, J.L., Wang, Z.P., Becker-Heidmann, P., Quijano, C., 1997. Carbon in tropical wetlands. *Geoderma* 79, 163–185.
- Pan, G., Li, L., Wu, L., Zhang, X., 2003. Storage and sequestration potential of topsoil organic carbon in China's paddy soils. *Global Change Biology* 10, 79–92.
- Scharpenseel, H.W., Pfeiffer, E.-M., Becker-Heidmann, P., 1996. Organic carbon storage in tropical hydromorphic soils. In: Carter, M.R., Stewart, B.A. (Eds.), *Structure and organic matter storage in agricultural soils*. : *Advances in Soil Science*. Lewis Publishers, Boca Raton, pp. 361–392.
- Six, J., Conant, R.T., Paul, E.A., Paustian, K., 2002. Stabilization mechanisms of soil organic matter: implications for C-saturation of soils. *Plant and Soil* 241, 155–176.
- Song, G., Li, L., Pan, G., Zhang, Q., 2005. Topsoil organic carbon storage of China and its loss by cultivation. *Biogeochemistry* 74, 47–62.
- Steffens, M., Kölbl, A., Kögel-Knabner, I., 2009. Alternation of soil organic matter pools and aggregation in semi-arid steppe topsoils as driven by organic matter input. *European Journal of Soil Science* 60, 198–212.

- Tanji, K.K., Gao, S., Scardaci, S.C., Chow, A.T., 2003. Characterization redox status of paddy soils with incorporated rice straw. *Geoderma* 114, 333–353.
- Theng, B.K.G., 1979. *Formation and Properties of Clay-Polymer Complexes*. Elsevier, Amsterdam.
- Tisdall, J.M., Oades, J.M., 1982. Organic matter and water-stable aggregates in soils. *Journal of Soil Science* 33, 141–163.
- van den Berg, G.A., Loch, J.P.G., 2000. Decalcification of soils subject to periodic waterlogging. *European Journal of Soil Science* 51, 27–33.
- von Lützow, M., Kögel-Knabner, I., Ekschmitt, K., Flessa, H., Guggenberger, G., Matzner, E., Marschner, B., 2007. SOM fractionation methods: relevance to functional pools and to stabilization mechanisms. *Soil Biology and Biochemistry* 39, 2183–2207.
- Walker, L.R., Wardle, D.A., Bardgett, R.D., Clarkson, B.D., 2010. The use of chronosequences in studies of ecological succession and soil development. *Journal of Ecology* 98, 725–736.
- Wu, J., 2011. Carbon accumulation in paddy ecosystems in subtropical China: evidence from landscape studies. *European Journal of Soil Science* 62, 29–34.
- Yoshida, S., Adachi, K., 2002. Influences of puddling intensity on the water retention characteristics of clayey paddy soil. In: IUSS (Ed.), *Proceedings of the 17th World Congress of Soil Science: 14–21 August 2002, Vol. 5, Symposium no. 53, Bangkok, Thailand*, pp. 235 1–235 9.
- Zhang, G.L., Gong, Z.T., 2003. Pedogenic evolution of paddy soils in different soil landscapes. *Geoderma* 115, 15–29.
- Zhang, M., He, Z., 2004. Long-term changes in organic carbon and nutrients of an Ultisol under rice cropping in southeast China. *Geoderma* 118, 167–179.
- Zhang, M., Lu, H., Zhao, X.J., Li, R.A., 2004. A comparative study of soil fertility change of upland soil in Cixi Country. *Chinese Journal Soil Science* 35, 91–93.
- Zhao, Q., Zhong, L., Yingfei, X., 1997. Organic carbon storage in soils of southeast China. *Nutrient Cycling in Agroecosystems* 49, 229–234.
- Zou, P., Fu, J., Cao, Z., 2011. Chronosequence of paddy soils and phosphorus sorption-desorption properties. *Journal of Soil and Sediments* 11, 249–259.

ELSEVIER LICENSE
TERMS AND CONDITIONS
Oct 29, 2012

This is a License Agreement between Livia Wissing ("You") and Elsevier ("Elsevier") provided by Copyright Clearance Center ("CCC"). The license consists of your order details, the terms and conditions provided by Elsevier, and the payment terms and conditions.

All payments must be made in full to CCC. For payment instructions, please see information listed at the bottom of this form.

Supplier	Elsevier Limited The Boulevard, Langford Lane Kidlington, Oxford, OX5 1GB, UK
Registered Company Number	1982084
Customer name	Livia Wissing
Customer address	Chair of Soil Science Freising, Bavaria 85354
License number	3018270312378
License date	Oct 29, 2012
Licensed content publisher	Elsevier
Licensed content publication	Soil and Tillage Research
Licensed content title	Management-induced organic carbon accumulation in paddy soils: The role of organo-mineral associations
Licensed content author	Livia Wissing, Angelika Kölbl, Werner Häusler, Peter Schad, Zhi-Hong Cao, Ingrid Kögel-Knabner
Licensed content date	January 2013
Licensed content volume number	126
Licensed content issue number	
Number of pages	12
Start Page	60
End Page	71
Type of Use	reuse in a thesis/dissertation
Portion	full article
Format	both print and electronic
Are you the author of this Elsevier article?	Yes
Will you be translating?	No
Order reference number	
Title of your thesis/dissertation	Evolution of mineral-associated organic matter in paddy soils - a chronosequence study
Expected completion date	Nov 2012
Estimated size (number of pages)	100
Elsevier VAT number	GB 494 6272 12
Permissions price	0.00 EUR
VAT/Local Sales Tax	0.0 USD / 0.0 GBP
Total	0.00 EUR
Terms and Conditions	

INTRODUCTION

1. The publisher for this copyrighted material is Elsevier. By clicking "accept" in connection with completing this licensing transaction, you agree that the following terms and conditions apply to this transaction (along with the Billing and Payment terms and conditions established by Copyright Clearance Center, Inc. ("CCC"), at the time that you opened your Rightslink account and that are available at any time at <http://myaccount.copyright.com>).

GENERAL TERMS

2. Elsevier hereby grants you permission to reproduce the aforementioned material subject to the terms and conditions indicated.

3. Acknowledgement: If any part of the material to be used (for example, figures) has appeared in our publication with credit or acknowledgement to another source, permission must also be sought from that source. If such permission is not obtained then that material may not be included in your publication/copies. Suitable acknowledgement to the source must be made, either as a footnote or in a reference list at the end of your publication, as follows:

“Reprinted from Publication title, Vol /edition number, Author(s), Title of article / title of chapter, Pages No., Copyright (Year), with permission from Elsevier [OR APPLICABLE SOCIETY COPYRIGHT OWNER].” Also Lancet special credit - “Reprinted from The Lancet, Vol. number, Author(s), Title of article, Pages No., Copyright (Year), with permission from Elsevier.”

4. Reproduction of this material is confined to the purpose and/or media for which permission is hereby given.

5. Altering/Modifying Material: Not Permitted. However figures and illustrations may be altered/adapted minimally to serve your work. Any other abbreviations, additions, deletions and/or any other alterations shall be made only with prior written authorization of Elsevier Ltd. (Please contact Elsevier at permissions@elsevier.com)

6. If the permission fee for the requested use of our material is waived in this instance, please be advised that your future requests for Elsevier materials may attract a fee.

7. Reservation of Rights: Publisher reserves all rights not specifically granted in the combination of (i) the license details provided by you and accepted in the course of this licensing transaction, (ii) these terms and conditions and (iii) CCC's Billing and Payment terms and conditions.

8. License Contingent Upon Payment: While you may exercise the rights licensed immediately upon issuance of the license at the end of the licensing process for the transaction, provided that you have disclosed complete and accurate details of your proposed use, no license is finally effective unless and until full payment is received from you (either by publisher or by CCC) as provided in CCC's Billing and Payment terms and conditions. If full payment is not received on a timely basis, then any license preliminarily granted shall be deemed automatically revoked and shall be void as if never granted. Further, in the event that you breach any of these terms and conditions or any of CCC's Billing and Payment terms and conditions, the license is automatically revoked and shall be void as if never granted. Use of materials as described in a revoked license, as well as any use of the materials beyond the scope of an unrevoked license, may constitute copyright infringement and publisher reserves the right to take any and all action to protect its copyright in the materials.

9. Warranties: Publisher makes no representations or warranties with respect to the licensed material.

10. Indemnity: You hereby indemnify and agree to hold harmless publisher and CCC, and their respective officers, directors, employees and agents, from and against any and all claims arising out of your use of the licensed material other than as specifically authorized pursuant to this license.

11. No Transfer of License: This license is personal to you and may not be sublicensed, assigned, or transferred by you to any other person without publisher's written permission.

12. No Amendment Except in Writing: This license may not be amended except in a writing signed by both parties (or, in the case of publisher, by CCC on publisher's behalf).

13. Objection to Contrary Terms: Publisher hereby objects to any terms contained in any purchase order, acknowledgment, check endorsement or other writing prepared by you, which terms are inconsistent with these terms and conditions or CCC's Billing and Payment terms and conditions.

These terms and conditions, together with CCC's Billing and Payment terms and conditions (which are incorporated herein), comprise the entire agreement between you and publisher (and CCC) concerning this licensing transaction. In the event of any conflict between your obligations established by these terms and conditions and those established by CCC's Billing and Payment terms and conditions, these terms and conditions shall control.

14. **Revocation:** Elsevier or Copyright Clearance Center may deny the permissions described in this License at their sole discretion, for any reason or no reason, with a full refund payable to you. Notice of such denial will be made using the contact information provided by you. Failure to receive such notice will not alter or invalidate the denial. In no event will Elsevier or Copyright Clearance Center be responsible or liable for any costs, expenses or damage incurred by you as a result of a denial of your permission request, other than a refund of the amount(s) paid by you to Elsevier and/or Copyright Clearance Center for denied permissions.

LIMITED LICENSE

The following terms and conditions apply only to specific license types:

15. **Translation:** This permission is granted for non-exclusive world **English** rights only unless your license was granted for translation rights. If you licensed translation rights you may only translate this content into the languages you requested. A professional translator must perform all translations and reproduce the content word for word preserving the integrity of the article. If this license is to re-use 1 or 2 figures then permission is granted for non-exclusive world rights in all languages.

16. **Website:** The following terms and conditions apply to electronic reserve and author websites:
Electronic reserve: If licensed material is to be posted to website, the web site is to be password-protected and made available only to bona fide students registered on a relevant course if: This license was made in connection with a course, This permission is granted for 1 year only. You may obtain a license for future website posting, All content posted to the web site must maintain the copyright information line on the bottom of each image,

A hyper-text must be included to the Homepage of the journal from which you are licensing at <http://www.sciencedirect.com/science/journal/xxxxx> or the Elsevier homepage for books at <http://www.elsevier.com> , and

Central Storage: This license does not include permission for a scanned version of the material to be stored in a central repository such as that provided by Heron/XanEdu.

17. **Author website** for journals with the following additional clauses:

All content posted to the web site must maintain the copyright information line on the bottom of each image, and the permission granted is limited to the personal version of your paper. You are not allowed to download and post the published electronic version of your article (whether PDF or HTML, proof or final version), nor may you scan the printed edition to create an electronic version. A hyper-text must be included to the Homepage of the journal from which you are licensing at <http://www.sciencedirect.com/science/journal/xxxxx> . As part of our normal production process, you will receive an e-mail notice when your article appears on Elsevier's online service ScienceDirect (www.sciencedirect.com). That e-mail will include the article's Digital Object Identifier (DOI). This number provides the electronic link to the published article and should be included in the posting of your personal version. We ask that you wait until you receive this e-mail and have the DOI to do any posting.

Central Storage: This license does not include permission for a scanned version of the material to be stored in a central repository such as that provided by Heron/XanEdu.

18. **Author website** for books with the following additional clauses: Authors are permitted to place a brief summary of their work online only. A hyper-text must be included to the Elsevier homepage at <http://www.elsevier.com> . All content posted to the web site must maintain the copyright information line on the bottom of each image. You are not allowed to download and post the published electronic version of your chapter, nor may you scan the printed edition to create an electronic version.

Central Storage: This license does not include permission for a scanned version of the material to be stored in a central repository such as that provided by Heron/XanEdu.

19. **Website** (regular and for author): A hyper-text must be included to the Homepage of the journal from which you are licensing at <http://www.sciencedirect.com/science/journal/xxxxx>. or for books to the Elsevier homepage at <http://www.elsevier.com>

20. **Thesis/Dissertation**: If your license is for use in a thesis/dissertation your thesis may be submitted to your institution in either print or electronic form. Should your thesis be published commercially, please reapply for permission. These requirements include permission for the Library and Archives of Canada to supply single copies, on demand, of the complete thesis and include permission for UMI to supply single copies, on demand, of the complete thesis. Should your thesis be published commercially, please reapply for permission.

21. **Other Conditions**:

v1.6

If you would like to pay for this license now, please remit this license along with your payment made payable to "COPYRIGHT CLEARANCE CENTER" otherwise you will be invoiced within 48 hours of the license date. Payment should be in the form of a check or money order referencing your account number and this invoice number RLNK500886253. Once you receive your invoice for this order, you may pay your invoice by credit card. Please follow instructions provided at that time.

Make Payment To:

Copyright Clearance Center

Dept 001

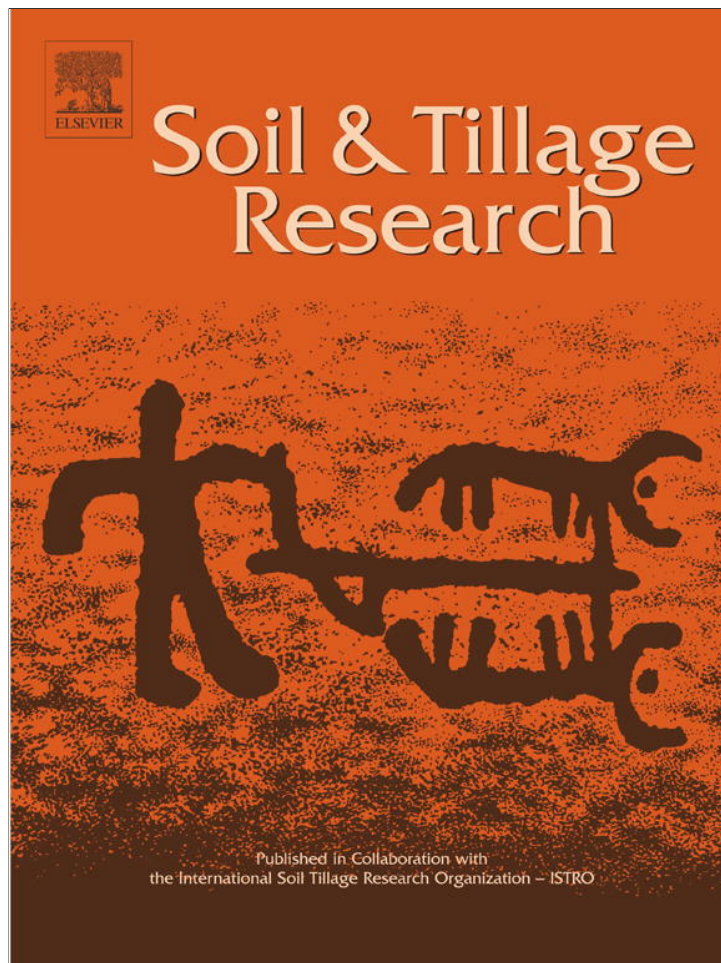
P.O. Box 843006

Boston, MA 02284-3006

For suggestions or comments regarding this order, contact RightsLink Customer Support: customercare@copyright.com or +1-877-622-5543 (toll free in the US) or +1-978-646-2777.

Gratis licenses (referencing \$0 in the Total field) are free. Please retain this printable license for your reference. No payment is required.

Provided for non-commercial research and education use.
Not for reproduction, distribution or commercial use.



(This is a sample cover image for this issue. The actual cover is not yet available at this time.)

This article appeared in a journal published by Elsevier. The attached copy is furnished to the author for internal non-commercial research and education use, including for instruction at the authors institution and sharing with colleagues.

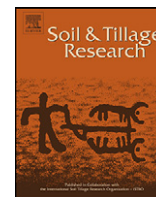
Other uses, including reproduction and distribution, or selling or licensing copies, or posting to personal, institutional or third party websites are prohibited.

In most cases authors are permitted to post their version of the article (e.g. in Word or Tex form) to their personal website or institutional repository. Authors requiring further information regarding Elsevier's archiving and manuscript policies are encouraged to visit:

<http://www.elsevier.com/copyright>

Contents lists available at [SciVerse ScienceDirect](http://www.sciencedirect.com)

Soil & Tillage Research

journal homepage: www.elsevier.com/locate/still

Management-induced organic carbon accumulation in paddy soils: The role of organo-mineral associations

Livia Wissing^{a,*}, Angelika Kölbl^a, Werner Häusler^a, Peter Schad^a, Zhi-Hong Cao^b, Ingrid Kögel-Knabner^{a,c}

^a Lehrstuhl für Bodenkunde, Department of Ecology and Ecosystem Management, Center of Life and Food Sciences Weihenstephan, Technische Universität München, D-85350 Freising-Weihenstephan, Germany

^b Institute of Soil Science, Chinese Academy of Sciences, Nanjing 210008, PR China

^c Institute for Advanced Study, Technische Universität München, Lichtenbergstrasse 2a, D-85748 Garching, Germany

ARTICLE INFO

Article history:

Received 13 June 2012

Received in revised form 3 August 2012

Accepted 5 August 2012

Keywords:

Soil management

Rice cultivation

Chronosequence

Soil mineralogy

Soil organic carbon composition

Fine mineral fraction

ABSTRACT

Iron (Fe) oxides strongly interact with organic matter in soil and play an important role in the stabilization of organic matter. These processes are often influenced by soil cultivation, including tillage, crop rotation and irrigation. We assessed the effect of Fe oxides on organic carbon (OC) accumulation during the development of soils used for paddy rice production in comparison to non-irrigated cropping systems. Soil samples were taken from two chronosequences derived from uniform parent material in the Zhejiang Province (PR China). Bulk soils and soil fractions were analyzed for OC concentrations, soil mineralogy and soil organic matter (SOM) composition was determined by solid-state ¹³C NMR spectroscopy. Paddy soils were characterized by increasing OC concentrations, from 18 mg g⁻¹ to 30 mg g⁻¹, during 2000 years of rice cultivation, but OC concentrations of non-paddy soils were low in all age classes (11 mg g⁻¹). SOM composition revealed from Solid-state ¹³C NMR spectroscopy did not change during pedogenesis in either chronosequence. Selective enrichment of lignin-derived compounds, caused by long-term paddy rice management, could not be confirmed by the present study. The management of paddy soils creates an environment of Fe oxide formation which was different to those in non-paddy soils. Paddy soils are dominated by poorly crystalline Fe oxides (Fe_o) and significantly lower content of crystalline Fe oxides (Fe_d – Fe_o). This was in contrast to non-paddy soils, which are characterized by high proportions of crystalline Fe oxides. The paddy-specific Fe oxide composition was effective after only 50 years of soil development and the proportion Fe oxides did not alter during further pedogenesis. This chronosequence study revealed that the potential for OC accumulation was higher in paddy versus non-paddy soils and was already reached at earliest stages of paddy soil development. Changes in paddy soil management associated with redox cycle changes will not only affect Fe oxide composition of paddy soils but most probably also OC storage potential.

© 2012 Elsevier B.V. All rights reserved.

1. Introduction

Paddy soils are hydromorphic soils formed under intense anthropogenic influence (Gong, 1983), as rice cultivation requires special management practices (flooding, puddling, and drainage). The redox conditions of paddy soils vary during cultivation, with anoxic conditions prevailing during the rice growing season. Between rice crops, artificial drainage leads to oxic conditions, and the soils are cultivated with upland crops or kept dry and fallow

(Gaunt et al., 1995). The properties of paddy soils are influenced by the cycles of the water regime; it changes between submerged, puddled condition and drainage (Eickhorst and Tippkötter, 2009; Kögel-Knabner et al., 2010). The periodic redox cycles induced by specific paddy soil management strategies have strong effects on long-term biogeochemical processes (Kögel-Knabner et al., 2010) and can result in permanent and temporary changes in soil properties (Bahmanyar, 2007). Thus, the physical, chemical and biological properties are different from those of upland soils (Li et al., 2005) used for cultivation of non-irrigated crops. Recent problems related to water quality and water scarcity due to the intensification of agriculture, as well as increasing water consumption ask for water saving management techniques (Janssen and Lennartz, 2006) and alternate wetting and drying (AWD) is suggested to replace continuous flooding (Dong et al., 2012).

* Corresponding author. Tel.: +49 08161 71 3734; fax: +49 08161 71 4466.

E-mail addresses: lwissing@wzw.tum.de (L. Wissing), koelbl@wzw.tum.de (A. Kölbl), haeusler@wzw.tum.de (W. Häusler), schad@wzw.tum.de (P. Schad), zhihongcaoli@126.com (Z.-H. Cao), koegel@wzw.tum.de (I. Kögel-Knabner).

Paddy management with rice cropping under irrigated, anaerobic conditions is considered to favor the accumulation of soil organic matter (SOM) (Zhang and He, 2004; Sahrawat, 2004). Furthermore, it is supposed that the rates of SOM decomposition are slower under anoxic conditions than under oxic conditions (Sahrawat, 2004). Thus, the paddy soil management favors the SOM accumulation in the topsoils (Cheng et al., 2009), and its OM content are significantly higher compared to corresponding non-paddy soils (Pan et al., 2003a; Sahrawat, 2004; Zhang and He, 2004). Results from Wissing et al. (2011) showed a preferred SOM accumulation in the fractions 63–20 μm and 20–6.3 μm as an organic carbon (OC) sink, and in the fraction 2–0.2 μm as the most important fraction for OC accumulation during paddy soil evolution.

The mechanisms of OC accumulation under paddy management are not well understood. Changes in SOM composition under rice cropping have been studied mainly in humic acid extracts (Olk et al., 1996, 1998, 2002; Mahieu et al., 2002). Wetland rice cropping results in increasing proportions of less humified organic material in SOM, as revealed by the abundance of diester P, amide N and phenolic C (Olk et al., 1996; Mahieu et al., 2000a, 2002) in humic acid extracts. Olk et al. (1996) and Smernik et al. (2004) showed an accumulation of lignin residues in paddy soil humic acids using solid-state ^{13}C NMR spectroscopic analysis. Lignin accumulation is considered to be caused by the resistance of the aromatic lignin structures to degradation under anaerobic conditions (Colberg, 1988; Olk et al., 2002). As a consequence of oxygen deficiency phenolic functional groups are incorporated into young SOM fractions (Olk et al., 1996). Bierke et al. (2008) explained that adding crop residue under intensified rice cropping increases lignin-derived phenols, which may accumulate because of anaerobic conditions and incomplete decomposition.

Several studies have investigated alternating redox potentials in submerged soils (Howeler and Bouldin, 1971; Ponnampereuma, 1972) associated with the reduction and oxidation of iron (Fe) in a waterlogged state (Islam and Choudhury, 1959; Ratering and Schnell, 2000). Zhang et al. (2003) showed in a laboratory experiment that soil flooding increases the poorly crystalline proportions of Fe oxides (determined as oxalate soluble Fe_o), mainly at the expense of total pedogenetic Fe oxides (dithionite-citrate-bicarbonate soluble Fe_d). The authors explained their results as partial transformation of crystalline Fe oxides ($\text{Fe}_\text{d} - \text{Fe}_\text{o}$) to less crystalline forms under anoxic conditions. Other studies have also found that repeated soil flooding and drainage for rice cultivation leads to an accumulation of Fe_o oxides (Kuo and Mikkelsen, 1979; Willet and Higgins, 1980; Sah and Mikkelsen, 1986) and thus may lead to a decline of crystalline Fe oxides (Darke et al., 1997). In contrast, the laboratory study of Thompson et al. (2006) demonstrated increasing crystallinity of Fe oxides with repeated redox cycles. Zhang and Lin (2002) suggested that long-term rice cultivation in combination with high OM content might be responsible for a lower crystallinity of Fe oxides in some paddy soils. The higher amount of organic compounds may have a preventive effect on the crystallization of ferrihydrite (Schwertmann, 1966). Li et al. (2005) investigated topsoils (0–20 cm) of a paddy chronosequence (0–80 years) and found declining Fe_d contents with years of paddy soil cultivation. This could be explained by downwards movement of ferrous Fe from the paddy topsoil during flooded conditions (Zhang and Gong, 2003), leading to Fe-enriched illuvial subsoil horizons (Zhang and Gong, 2003; Chen et al., 2011).

Fe oxides influence the soil's physical and chemical properties, such as phosphate sorption (Sah et al., 1989; de Mello et al., 1998), soil microstructure (Takahashi and Toriyama, 2004) and OM stabilization (Skjemstad et al., 1989; Wagai and Mayer, 2007). It is established in the literature that there is a strong interaction

between Fe oxides and OM (Shang and Tiessen, 1998; Kaiser and Guggenberger, 2000; Kiem and Kögel-Knabner, 2002). Studies on the mechanisms of OM stabilization report the protection of OM via soil aggregation induced by Fe oxides (Shang and Tiessen, 1998; Wagai and Mayer, 2007), or by direct interactions with Fe oxide surfaces (Kaiser and Guggenberger, 2003; Kleber et al., 2004; Eusterhues et al., 2005; Mikutta et al., 2006). Fe_o oxides are known to have a highly reactive mineral surface (Parfitt, 1989; Torn et al., 1997; Eusterhues et al., 2005), with the surface area of Fe oxides increasing as their crystallinity decreases (Borggaard, 1982). It has been shown that OM bound to ferrihydrite (an oxalate extractable Fe oxide) is stabilized, and this seems to be a major mechanism of carbon sequestration (Kalbitz et al., 2005). The literature provides little information about the crystallinity of Fe oxides in different soil fractions during pedogenesis. Only a few authors have investigated the distribution of Fe oxides between particle size fractions and found mainly increasing Fe_d and Fe_o contents with decreasing size of soil fractions in oxic soils (Eusterhues et al., 2005; Pronk et al., 2011). The effect of long-term paddy rice management on Fe oxide formation and the accumulation of OC has not yet been investigated.

The aim of this study was to investigate the OM accumulation in the mineral fraction in paddy soils. A paddy (P) and non-paddy (NP) soil chronosequence derived from uniform parent material provide the opportunity to study the accumulation of OM in association with the formation of Fe_d and Fe_o oxides developed under specific conditions of the paddy soil regime. Samples were taken from two chronosequences in Zhejiang Province, PR China, consisting of differently aged paddy (50–2000 years) and non-paddy soils (50–700 years). Particle size fractionation was applied to isolate soil fractions with different OC content, SOM composition and Fe oxide content. Dithionite and oxalate extractions were done on bulk soil and soil fractions $<20 \mu\text{m}$. To evaluate the effect of the presence of Fe oxides on the OM accumulation, we investigated the relationship between the content of Fe_o oxides and the concentration of OC. To characterize the SOM composition, we complemented analyses with solid-state ^{13}C NMR spectroscopy. We hypothesize the following: (i) SOM decomposition is different in P and NP soils: lignin-derived phenols will accumulate during paddy soil development because of the long-term paddy management, which prevent the degradation of phenolic compounds (Olk et al., 2002). (ii) The proportion of Fe_o oxides is influenced by soil development: the proportion of Fe_o oxides will increase with soil age because of the long-term paddy rice cultivation under submerged conditions. (iii) The presumably increasing proportion of Fe_o oxides within the paddy soil chronosequence will lead to higher proportions of accumulated SOM in paddy soils.

2. Materials and methods

2.1. Study area and soil description

The study area is located in the eastern part of the PR China, near the city Cixi (30°10'N, 121°14'E), Zhejiang Province. During the past 2000 years, several dikes were built for land reclamation, which has resulted in a chronosequence of soils under agricultural use. The parent material of the soils consists of calcareous marine sediments. Parts of the land were used more than 5 months per year (Zou et al., 2011) for irrigated paddy rice cultivation, followed by an upland crop (paddy soils). Other parts were used year-round for a variety of non-irrigated upland crops e.g. cotton, wheat, barley, oil rape, broad bean and vegetables (non-paddy soils). From June until October, paddy soils are flooded, and thus the soils are under anoxic conditions. After drainage, soils are oxic and can be planted with non-irrigated crops like oilseed rape, wheat and

watermelons (Cheng et al., 2009). The paddy (50–1000 years) and non-paddy (50–700 years) soil sequence was determined according to the record in the county annals of the Zhejiang Province. The county annals contain detailed information about the exact position and construction of dikes (Cheng et al., 2009). Information in Chinese is obtainable at <http://www.cixi.gov.cn/> (Cheng et al., 2009). The description of the 2000-year-old paddy site can be found in Zou et al. (2011). The paddy chronosequence consists of 6 different stages: 50, 100, 300, 700, 1000 and 2000 years, which were named P 50, P 100, etc. A detailed description of the paddy soils and the paddy chronosequence is given by Wissing et al. (2011). The non-paddy soil sequence consists of 4 different age stages of soil development: 50, 100, 300 and 700 years, which are abbreviated NP 50, NP 100, etc. Paddy and non-paddy soils were sampled in triplicate from adjacent independent fields, described by the FAO guidelines for soil description (2006) and classified according to the IUSS Working Group WRB (2007). The following soil types were identified (from Wissing et al. (2011), revised): Endogleyic Anthraquic Cambisols (P 50, 100, 300) and Endogleyic Hydragric Anthrosols (P 700, 1000, 2000). Non-paddy soils are classified as Endogleyic Cambisols (NP 50, 100) and Haplic Cambisols (NP 300, 700). The soils were described according to the morphological characteristics of the profile.

This study discusses the uppermost A horizon: in non-paddy soil the ploughed horizon (or the upper part of it) and in paddy soil the puddled horizon (or the upper part of an A horizon that is divided into two subhorizons). They were described by the following subordinate characteristics: l = mottling as capillary fringes; p = altered by plowing. Soils have been sampled under similar weather conditions and paddy soils were sampled under similar soil moisture conditions. Whereas the upper part of the Ap horizon had more pronounced redox features, a differentiation was made in Ap1 and Ap2. Soils without a differentiation in redox features in the Ap horizon have only one Ap. The redox potential of paddy soils was measured by the laboratory of the Institute for Agricultural and Nutritional Sciences at the Martin-Luther University of Halle-Wittenberg. The Eh values in the uppermost 10 cm of the paddy soils ranged between 570 mV and –12 mV during the upland crop phase and –170 mV to –200 mV during the paddy soil phase invariably in young (P 100), medium (P 700) and old paddy soils (P 2000) (personal communication Vanessa Vogelsang, Sabine Fiedler). OC input data for the chronosequences with up to 2000 years of agricultural use are not available. However, sampling sites with similar cropping history during the last decades were chosen for the respective paddy and non-paddy chronosequences. The OC content of the Ap1 and Ap2 horizon was similar because of the periodical puddling and plowing which led to an intermixed soil with uniform OC contents in the puddled horizons. Bulk soil samples were air-dried and sieved to a size of <2 mm for further analyses. The OC concentrations in the soils were highest in the topsoils. Therefore, all soil analyses were done on the uppermost A horizon.

2.2. Soil texture and carbon concentrations

Soil texture was determined after dissolution of carbonates with HCl and removal of OM with H₂O₂. The sand content was obtained via wet sieving at >63 μm; silt and clay were determined by X-ray detection (Sedigraph 5100, Micromeritics GmbH, Aachen).

Total carbon concentrations (C_{tot}) were determined in duplicate by dry combustion at 950 °C on a Vario EL elemental analyzer (Elementar Analysensysteme, Hanau, Germany). The inorganic carbon (IC) concentration was determined in duplicate by the laboratory of the Institute for Agricultural and Nutritional Sciences at the Martin-Luther University in Halle-Wittenberg

after dissolution of carbonates with 42% phosphoric acid and subsequent infrared detection of the evolving CO₂ (C-MAT 550, Ströhlein GmbH, Viernsen, Germany). The organic carbon concentration was calculated by subtracting the concentration of IC from C_{tot}:

$$\text{OC} (\text{mg g}^{-1}) = C_{\text{tot}} (\text{mg g}^{-1}) - \text{IC} (\text{mg g}^{-1}) \quad (1)$$

2.3. Particle size fractionation of the topsoil

Before fractionation, all soils were pre-treated with 0.1 M HCl (final pH value = 4.8) to remove carbonates. HCl and the dissolved Ca²⁺ ions were removed by centrifugation (20 min, at 3423 × g). The particle size fractionation was done according to Wissing et al. (2011), using first an ultrasonic treatment with an energy input of 60 J mL⁻¹ to destroy macroaggregates (>200 μm). The complete dispersion of microaggregates (<200 μm) was achieved with an additional ultrasonic treatment (440 J mL⁻¹). The fraction <20 μm was further separated by sedimentation in Atterberg cylinders (silt-sized fractions) and by centrifugation (clay-sized fractions). We isolated the following 6 particle-size fractions: sand and particulate organic matter (S + POM, 2000–63 μm), coarse silt (cSi, 63–20 μm), medium silt (mSi, 20–6.3 μm), fine silt (fSi, 6.3–2 μm), coarse clay (cC, 2–0.2 μm) and fine clay (fC, <0.2 μm). All fractions were freeze-dried and weighed to obtain the mass proportion of each fraction to the bulk soil.

The C_{tot} concentrations of the particle-size fractions were measured in duplicate by dry combustion (EuroEA Elemental Analyzer 3000, HEKAtech, Wegberg, Germany). Because of the HCl treatment prior to the physical fractionation procedure, all mineral fractions were free of carbonates, and the C_{tot} content was equal to the OC concentration.

2.4. Soil organic carbon composition

Bulk soil materials were treated with HF (Eusterhues et al., 2007) prior to measurement to concentrate the OC content and to reduce interfering paramagnetic effects of iron-containing silica minerals. Ten grams of sample material was shaken with 50 mL of 10% (w-to-w) HF for 12 h in polyethylene bottles. After centrifugation, the supernatants were siphoned off and discarded. The procedure was repeated 5 times at room temperature. The remaining sediment was washed 5 times with 40 mL deionized water and freeze-dried. Afterwards the HF treated bulk soils were analyzed for their OC contents and further the OC recoveries were determined. The soil fractions were not treated by HF in order to keep the fractions intact for further analyses. We analyzed paddy and non-paddy bulk soils and all soil fractions <6.3 μm by solid-state ¹³C NMR spectroscopy (Bruker Biospin DSX 200 NMR spectrometer, Rheinstetten, Germany). The cross-polarization magic angle spinning (CPMAS) technique (Schaefer and Stejskal, 1976), with a spinning speed of 5.0 kHz or 6.8 kHz and a contact time of 1 ms was applied. The chemical shifts of ¹³C were calibrated to tetramethylsilane (0 ppm), and the pulse delay was 400 ms. Depending on the signal-to-noise ratio, line broadening between 75 and 150 Hz was applied, and a minimum of 120 000 scans were accumulated for each sample. All spectra were integrated using the following 4 major chemical shift regions: –10 to 45 ppm (alkyl-C), 45–110 ppm (O/N-alkyl-C), 110–160 ppm (aryl-C), and 160–220 ppm (carboxyl-C) (Knicker and Lüdemann, 1995).

Paramagnetic iron-containing silica minerals can lead to signal loss of O/N-alkyl C (Schöning et al., 2005) and broadening are too severe to obtain useful solid state ¹³C NMR spectra (Smernik and Oades, 1999). As described by Arshad et al. (1988) and Schöning

et al. (2005) this is only relevant for soils or fractions with an OC:Fe ratio <1. Therefore, we calculated the OC:Fe ratios according to Arshad et al. (1988) for bulk soils and the soil fractions <6.3 μm.

2.5. Soil mineralogy

Total pedogenetic Fe oxides (Fe_d) of the selective fractions mSi, fSi, cC and fC were analyzed by using the dithionite–citrate–bicarbonate (DCB) method according to Mehra and Jackson (1960). The poorly crystalline fraction of Fe oxides (Fe_o) was extracted using the oxalate method (Schwertmann, 1964). The Fe concentration was measured by inductively coupled plasma optical emission spectroscopy (ICP-OES) (Vista-Pro, CCD simultaneous, Varian, Darmstadt, Germany). The following equation was used to calculate the crystalline fraction of Fe oxides (Fe_d – Fe_o):

$$Fe_d - Fe_o \text{ (mg g}^{-1}\text{)} = Fe_d \text{ (mg g}^{-1}\text{)} - Fe_o \text{ (mg g}^{-1}\text{)} \quad (2)$$

The ratio of Fe_d fraction to Fe_o fraction is

$$\frac{Fe_o}{Fe_d} = \frac{Fe_o \text{ (mg g}^{-1}\text{)}}{Fe_d \text{ (mg g}^{-1}\text{)}} \quad (3)$$

Data for S + POM and cSi fractions are not presented here because of their low concentration of Fe oxides. All subsequent analyses were done on fractions <20 μm. Aliquots of both clay fractions (<0.2 μm and 2–0.2 μm) were pre-treated with H₂O₂ (30%) to remove OM. The X-ray diffraction (XRD) patterns were recorded with a Co radiation source using a Philips PW 1070 diffractometer. Random powder samples were measured from 5° to 60° in steps of 0.02° with a counting time of 5 s for each step. To evaluate expandable clay minerals, the samples were treated with glycol as well as KCl and stepwise heated to 100°, 200° and 550°. Clay minerals were identified according to Moore and Reynolds (1989) and the different mineral phases were determined by semievaluation. The Fe_d concentrations of the soil fractions varied between <0.1% and 3.3% therefore Fe oxides could not be detected by XRD analyses.

2.6. Statistical analyses

We tested the effect of soil management and soil age with SPSS Statistics 19 (IBM SPSS Company). The effect of the soil

management was analyzed by the nonparametric Mann–Whitney U test. The mean values of all soils (mean of 50–700 years and mean of 50–2000 years of pedogenesis) were compared and * represents statistical significant differences ($p \leq 0.05$) between paddy and non-paddy soils. The investigated paddy chronosequence consist of six different age stages, namely 50, 100, 300, 700, 1000 and 2000 years of paddy soil development. In contrast, the non-paddy chronosequence consist only of 50, 100, 300 and 700 years of soil development. To compare the development of soil parameters like the OC content, soil texture and mass distribution, we separated the paddy soil evolution in two phases. This allows the comparison of a total of 700 years of paddy versus non-paddy soils and in addition a total of 2000 years of paddy soil evolution.

The analysis of variance (ANOVA) with the Post Hoc tests Tukey-B and Bonferroni was used to test the effect of the soil age on the bulk soil parameters pH values, OC, Fe_d and Fe_o concentrations and NMR data of the paddy and non-paddy. All data were analyzed for homogeneity of variances by Levene test and the analysis of normality was performed with Shapiro–Wilk test. Significant differences ($p \leq 0.05$) within the paddy and non-paddy chronosequence are indicated by italic letters.

The Pearson correlation coefficients were calculated to test the effect of the soil age on the soil fraction parameters mass distribution, texture, OC, Fe_d and Fe_o concentrations. Wissing et al. (2011) explained already exceptionally low OC concentrations for P 1000 topsoils due to partial removal of topsoil material. Therefore, this site was excluded for correlation analyses.

3. Results

3.1. Properties of bulk soil

The pH values of paddy bulk soils (Table 1) were neutral to slightly acidic and decreased significantly ($p \leq 0.05$) with soil age from 7.4 (P 50) to 5.1 (P 2000). Non-paddy soils had pH values from 7.3 (NP 50, 100) to 5.9 (NP 700) which decreased significantly ($p \leq 0.05$) with soil development. The pH values of paddy soils were not significant different as compared to those of non-paddy soil. The OC concentrations of non-paddy soils (Table 1) remained constant during pedogenesis and ranged from 10.5 mg g⁻¹ (NP 300) to 11 mg g⁻¹ in NP 700. The OC values of non-paddy soils followed no significant trend with aging of the soils. Paddy soils

Table 1

Characteristics of uppermost A horizon of the paddy (P) and non-paddy (NP) soils: depths, horizon denominations, pH values, organic carbon (OC) concentrations, dithionite (Fe_d) and oxalate (Fe_o) extractable iron (Fe) oxides and texture of bulk soil. pH and OC values, Fe_d and Fe_o concentrations give the arithmetic mean ($n = 3$) with standard errors. The soil texture analysis was determined as a single measurement. Significant differences ($p \leq 0.05$) within the paddy and non-paddy chronosequence are indicated by italic letters and * represents significant differences ($p \leq 0.05$) between paddy and non-paddy soils.

Site	Depth (cm)	Horizon (FAO) ^a	pH (KCl) ^b	OC (mg g ⁻¹)	Fe _d (mg g ⁻¹)	Fe _o (mg g ⁻¹)	Texture ^d (g kg ⁻¹)			
							63–20 μm	20–6.3 μm	6.3–2 μm	<2 μm
P 50	0–7	Alp	7.4 <i>a</i>	17.8 ± 0.5 <i>b</i>	7.0 ± 0.1 <i>a</i>	2.6 ± 0.6 <i>a</i>	151	384	137	290
P 100	0–9	Alp1	5.0 <i>bc</i>	17.6 ± 1.0 <i>bc</i>	6.8 ± 0.4 <i>a</i>	3.0 ± 0.3 <i>a</i>	129	365	153	279
P 300	0–18	Alp	5.8 <i>b</i>	^c 22.6 ± 2.0 <i>bc</i>	6.6 ± 0.1 <i>a</i>	2.2 ± 0.3 <i>a</i>	164	405	131	245
P 700	0–10	Alp1	6.7 <i>a</i>	22.3 ± 2.2 <i>b</i>	6.8 ± 0.2 <i>a</i>	3.3 ± 0.7 <i>a</i>	132	394	156	286
P 1000	0–10	Alp	5.2 <i>bc</i>	14.0 ± 0.8 <i>c</i>	7.3 ± 0.2 <i>a</i>	3.0 ± 0.4 <i>a</i>	119	431	163	277
P 2000	0–15	Alp	5.1 <i>c</i>	^c 30.0 ± 0.9 <i>a</i>	4.4 ± 0.1 <i>b</i>	2.8 ± 0.2 <i>a</i>	107	404	171	242
Mean (50–700 years)			6.2	*20.1	6.8	*2.8	144	387	144	275
Mean (50–2000 years)			5.9	*20.7	6.5	*2.8	134	397	*152	*270
NP 50	0–9	Ap	7.3 <i>a</i>	10.6 ± 0.0 <i>a</i>	6.3 ± 0.2 <i>a</i>	1.5 ± 0.3 <i>a</i>	185	464	108	208
NP 100	0–14	Ap1	7.3 <i>a</i>	10.8 ± 0.0 <i>a</i>	7.0 ± 0.3 <i>a</i>	1.3 ± 0.2 <i>a</i>	140	413	134	272
NP 300	0–11	Ap	7.0 <i>a</i>	10.5 ± 0.0 <i>a</i>	6.3 ± 0.1 <i>a</i>	0.7 ± 0.2 <i>a</i>	163	443	129	237
NP 700	0–11	Ap1	5.9 <i>b</i>	11.0 ± 0.3 <i>a</i>	5.0 ± 0.9 <i>a</i>	1.5 ± 0.6 <i>a</i>	223	450	90	190
Mean (50–700 years)			6.9	10.7	6.2	1.3	178	*443	115	227

^a Guidelines for soil profile description, FAO (2006).

^b pH values were determined by the laboratory of the Institute for Agricultural and Nutritional Sciences at the Martin-Luther University in Halle-Wittenberg.

^c Organic carbon data was already published in Wissing et al. (2011).

^d Coarse silt (63–20 μm); medium silt (20–6.3 μm); fine silt (6.3–2 μm); total clay (<2 μm).

had higher OC concentrations (Table 1), ranging from 14 mg g⁻¹ in P 1000 and 30 mg g⁻¹ in P 2000. The OC values showed a significantly ($p \leq 0.05$) doubling from 17.8 mg g⁻¹ (P 50) to 30 (P 2000) mg g⁻¹. The oscillating OC concentrations between P 300 years and P 2000 years were already described by Wissing et al. (2011). Furthermore, statistical analysis confirmed significant higher ($p \leq 0.05$) OC values for paddy soils as compared to non-paddy soils (Table 1). Paddy soils had Fe_d concentrations (Table 1) of 7 mg g⁻¹ within the first 1000 years of paddy soil development and decreased significantly ($p \leq 0.05$) with soil age to 4.4 mg g⁻¹ (P 2000). The Fe_d concentrations of non-paddy soils ranged from 5 mg g⁻¹ (NP 700) to 7 mg g⁻¹ (NP 100) but showed no significant differences during soil development and also compared to paddy soils (Table 1). The Fe_o concentrations (Table 1) of non-paddy soils were 1.5 mg g⁻¹ in NP 50 and NP 700 and 0.7 mg g⁻¹ in NP 300. Paddy soils are characterized by significant higher ($p \leq 0.05$) Fe_o concentrations, ranging from 2.2 mg g⁻¹ in P 300 to 3.3 mg g⁻¹ in P 700. Statistical analyses showed no significant trend for the Fe_o values during paddy and non-paddy soil development (Table 1). Results from soil texture analysis (Table 1) showed high proportions of medium silt in all soils (P 365–431 g kg⁻¹ and NP 413–464 g kg⁻¹) which was significantly higher ($p \leq 0.05$) in non-paddy soils. The total clay content was 4% higher in paddy soils compared to non-paddy soils, but we tested no significant differences between the mean values of the clay content within 700 years of soil development. The total clay proportion was significantly higher ($p \leq 0.05$; mean over 2000 years of soil development) in paddy as compared to non-paddy soil and ranged from 190 g kg⁻¹ to 272 g kg⁻¹ (NP) and from

242 g kg⁻¹ to 290 g kg⁻¹ (P). Statistical analyses by Pearson correlation showed no significant trend of soil texture during pedogenesis of paddy and non-paddy soils.

3.2. Mass distribution and OC concentrations of particle-size fractions

We obtained the highest mass proportion (Table 2) in medium silt (mean: P 444/459 g kg⁻¹ and NP 485 g kg⁻¹), and the lowest was presented by the fine clay fractions (mean: P 54 g kg⁻¹ and NP 50 g kg⁻¹). Paddy soils had slightly higher OC values in the clay-sized fractions but we tested no statistically significant differences in clay contents between paddy and non-paddy soils (Table 2). Non-paddy soils were characterized by significant lower ($p \leq 0.05$) proportions of fine silt (mean: 82 g kg⁻¹) compared to paddy soils (mean: 116/113 g kg⁻¹) (Table 2). No significant chronological trend was calculated for the mass proportion of all soils by Pearson correlation. Compared to texture analyses, soil fractionation led to lower mass values in the fractions fine silt (difference: P 18–47 g kg⁻¹; NP 27–40 g kg⁻¹) and total clay (difference: P 48–90 g kg⁻¹; NP 43–62 g kg⁻¹). Soil texture led in almost all cases to higher mass values of medium silt (33–114 g kg⁻¹) but without trend during pedogenesis (see Tables 1 and 2).

The OC values of the non-paddy soil fractions followed no significant chronological trend but were highest in NP 700 (Table 2). Paddy soils presented significant higher ($p \leq 0.05$; mean over 2000 years of soil development) OC concentrations in both clay fractions as compared to non-paddy soils (Table 2). Medium silt showed the lowest OC concentrations in both chronosequences (Table 2) and without significant differences between paddy and

Table 2

Properties of the uppermost A horizon of the paddy (P) and non-paddy (NP) soils: depths, mass distribution and organic carbon (OC) concentrations of the soil fractions (<20 μm). Data of OC concentrations ($n=2$) and mass proportion ($n=3$ paddy; $n=2$ non-paddy) are given as the arithmetic mean with standard deviations. Significant differences between paddy and non-paddy soils are indicated by * ($p \leq 0.05$).

Site	Depth (cm)	Soil fraction ^a			
		20–6.3 μm	6.3–2 μm	2–0.2 μm	<0.2 μm
Mass (g kg⁻¹)					
^b P 50	0–7	422 ± 3.5	113 ± 2.1	185 ± 5.8	55 ± 5.5
^b P 100	0–9	479 ± 5.7	112 ± 1.4	138 ± 3.5	51 ± 2.1
^b P 300	0–18	402 ± 22.7	113 ± 13.6	134 ± 7.6	54 ± 0.6
^b P 700	0–10	474 ± 5.9	114 ± 4.6	170 ± 2.6	57 ± 4.5
^b P 1000	0–10	521 ± 31.8	116 ± 26.9	148 ± 2.1	62 ± 2.1
^b P 2000	0–15	459 ± 8.7	128 ± 5.1	148 ± 6.0	46 ± 1.5
Mean (50–700 years)		444	*113	157	54
Mean (50–2000 years)		459	*116	154	54
NP 50	0–9	430 ± 15.8	74 ± 3.8	114 ± 8.5	36 ± 6.7
NP 100	0–14	446 ± 48.8	94 ± 4.2	153 ± 9.9	59 ± 3.5
NP 300	0–11	530 ± 9.2	97 ± 0.7	129 ± 1.4	65 ± 2.1
NP 700	0–11	536 ± 0.7	63 ± 1.4	86 ± 6.4	42 ± 0.7
Mean (50–700 years)		485	82	120	50
OC (%)					
P 50	0–7	0.2 ± 0.0	2.2 ± 0.3	2.6 ± 0.0	2.6 ± 0.2
P 100	0–9	0.4 ± 0.0	2.5 ± 0.3	3.6 ± 0.0	4.0 ± 0.2
P 300	0–18	0.5 ± 0.0	3.8 ± 0.3	4.5 ± 0.1	4.5 ± 0.2
P 700	0–10	0.5 ± 0.1	4.0 ± 0.2	4.8 ± 0.2	4.4 ± 0.4
P 1000	0–10	0.2 ± 0.0	1.6 ± 0.1	2.8 ± 0.1	2.9 ± 0.1
P 2000	0–15	1.0 ± 0.1	3.5 ± 0.7	5.6 ± 0.2	5.5 ± 0.3
Mean (50–700 years)		0.4	3.1	3.9	3.9
Mean (50–2000 years)		0.5	2.9	*4.0	*4.0
NP 50	0–9	0.4 ± 0.0	1.8 ± 0.1	2.2 ± 0.0	2.6 ± 0.6
NP 100	0–14	0.3 ± 0.0	1.0 ± 0.0	1.3 ± 0.0	1.6 ± 0.2
NP 300	0–11	0.2 ± 0.0	1.8 ± 0.0	2.5 ± 0.1	2.3 ± 0.0
NP 700	0–11	0.2 ± 0.0	2.9 ± 0.1	2.9 ± 0.0	2.8 ± 0.2
Mean (50–700 years)		0.3	1.9	2.2	2.3

^a m Si: medium silt (20–6.3 μm); fSi: fine silt (6.3–2 μm); cC: coarse clay (2–0.2 μm); fine clay (<0.2 μm).

^b Mass distribution of paddy soils was already published by Wissing et al. (2011).

non-paddy soils. The highest OC concentrations were measured in coarse clay (paddy: 2.6–5.6%; non-paddy: 1.3–2.9%) and in fine clay fractions (paddy: 2.6–5.5%; non-paddy: 1.6–2.8%). The OC concentration increased with decreasing particle size and during pedogenesis when P 1000 was excluded. Additionally, OC concentrations increased significantly with increasing soil age for each particle size fraction, with Pearson correlation coefficients ranging from 0.5 (fSi) and 0.8 (cC and fC) to 1 (mSi). Wissing et al. (2011) described already increasing OC contents with increasing soil age for the clay-sized fraction, which were attributed to a long-term accumulation of stabilized and old OM specifically in these fractions. Furthermore, the fine clay fraction was characterized by higher percents of modern carbon (1–10 pMC) and is therefore older as compared to the bulk soil (Kalbitz et al., submitted for publication).

3.3. Chemical composition of SOM

Results from solid-state ^{13}C NMR spectroscopy showed similar SOM compositions in the bulk soils (Fig. 1) and we tested no significant differences of the bulk soil SOM composition between paddy and non-paddy soils. Pearson correlation showed no significant chronological trend during paddy and non-paddy soil development. All soils are characterized by a high average proportion of O/N-Alkyl-C (paddy 44% and non-paddy 42%; Fig. 1 and Appendix). Carboxyl-C showed the lowest relative proportion of all bulk soil functional C groups, with an average of 12% in paddy and 13% in non-paddy soils. Spectra of bulk soils showed no chronological increase of lignin-derived phenols during paddy soil development (Fig. 1). The HF treated bulk soils of paddy soils had OC recoveries of 75% and 98%. The OC recoveries of non-paddy bulk soils were lower and ranged from 59% to 77%. We calculated only for the bulk soil of NP 700 OC recoveries of more than 100% after HF treatment.

Furthermore, both soils had statistically the same SOM composition in the soil fractions $<6.3\ \mu\text{m}$ (Fig. 2 and Appendix). All analyzed soil fractions were characterized by similar O/N-alkyl-C proportions as compared to those of the bulk soils and was the

most abundant functional C group, followed by aryl-C, alkyl-C and carboxyl-C (Fig. 2 and Appendix). The average O/N-alkyl-C (Appendix) was in paddy 42% (fSi), 40% (cC) and 37% (fC) and in non-paddy 37% (fSi), 38% (cC) and 37% (fC). All soil fractions are characterized by a high proportion of aryl-C compounds: P 8–33%, and NP 24–33%. As particle size decreased, a relative enrichment of carboxyl-C, from 12% to 17%, and a decline of O/N-alkyl-C, from 42% to 37%, was observed in paddy soils. Spectra of coarse and fine clay (Fig. 2) showed no accumulation of lignin-derived phenols during paddy and non-paddy soils development. Bulk soils and all soil fractions $<6.3\ \mu\text{m}$ had an OC:Fe ratio >1 , indicating that paramagnetic iron-containing silica minerals did not affect solid state ^{13}C NMR spectra.

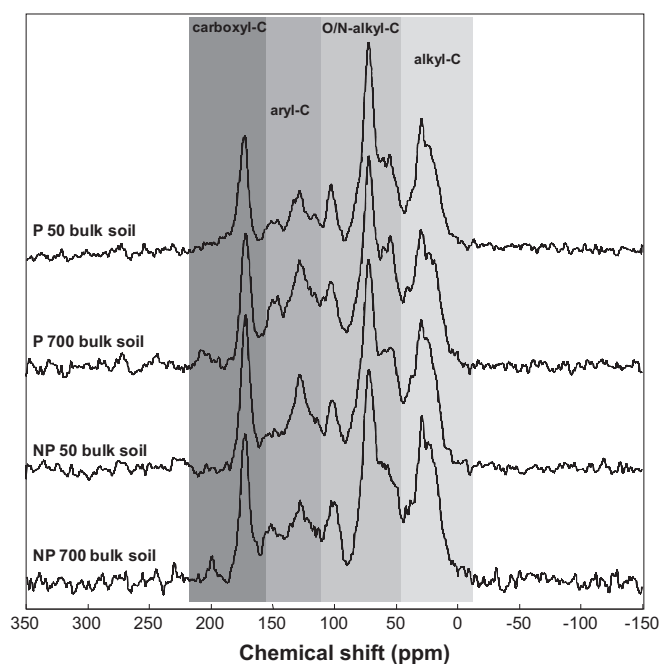
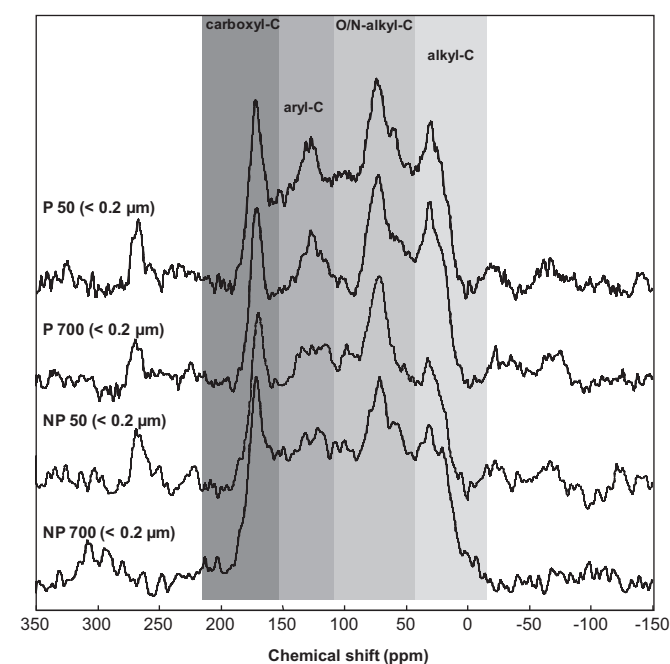
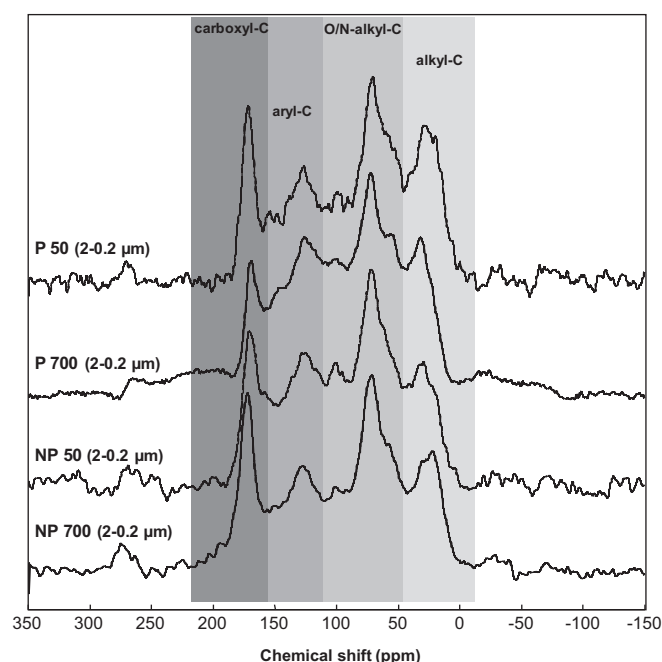


Fig. 1. Solid state ^{13}C nuclear magnetic resonance spectra of bulk soil of paddy (P) and non-paddy (NP) soils (uppermost A horizon).

Fig. 2. Solid state ^{13}C nuclear magnetic resonance spectra of the fractions coarse clay (2–0.2 μm) and fine clay (<0.2 μm) of paddy (P) and non-paddy (NP) soils (uppermost A horizon).

In the previous study of Wissing et al. (2011), paddy topsoils showed continuously increasing OC contents with increasing soil age, which are indicative for long-term OC accumulation processes throughout the chronosequence. Therefore, we are convinced that similar ^{13}C NMR spectra can be explained by long-term stabilization of OM under similar conditions rather than by recent OM accumulation.

3.4. Soil mineralogy

We observed increasing Fe_d and Fe_o oxide concentrations with decreasing particle size in both chronosequences with highest Fe_d and Fe_o values in the fine clay fraction (Table 3 and Fig. 3a, b). We could not identify a significant chronological trend for the Fe_d and Fe_o oxide concentrations by Pearson correlation. The Fe_d oxide concentration was lowest in medium silt, ranging in paddy soils from 1.4 mg g^{-1} to 3 mg g^{-1} and in non-paddy soils from 0.1 mg g^{-1} to 0.2 mg g^{-1} . We tested for paddy soils significantly higher ($p \leq 0.05$) Fe_d oxide concentrations in medium silt as compared to non-paddy (Table 3). The Fe_d values in fine silt and both clay fractions were higher in non-paddy soils but no significant differences were tested between paddy and non-paddy. The Fe_d oxide concentration in fine clay varied in paddy soils from 13 mg g^{-1} (P 2000) to 27.2 mg g^{-1} (P 700) and in non-paddy soils from 22.8 (NP 100) to 32.7 (NP 300). Paddy soils are characterized by higher concentrations of Fe_o oxides and the higher Fe_o values were in all paddy soil fractions significant at $p \leq 0.05$ as compared with non-paddy soils (Table 3). The average Fe_o oxides concentration was in paddy soils 0.9 mg g^{-1} (medium silt); $5.5/5.2 \text{ mg g}^{-1}$ (fine silt); $10.8/10.7 \text{ mg g}^{-1}$ (coarse clay) and $14.5/14.0 \text{ mg g}^{-1}$

(fine clay). Non-paddy soils had lower concentrations of Fe_o oxides: $<0.1 \text{ mg g}^{-1}$ in medium silt; 2.3 mg g^{-1} in fine silt; 5.3 mg g^{-1} in coarse clay and 8.8 mg g^{-1} in fine clay (Table 3). Thus, we tested lower ratios of Fe_o/Fe_d (Fig. 3a, b) in non-paddy soils, indicating significantly higher ($p \leq 0.05$; data not shown) crystallinity compared to corresponding paddy soils. The crystalline Fe oxides ($\text{Fe}_d - \text{Fe}_o$) increased with decreasing size of particles in both chronosequences, but the proportion of crystalline Fe oxides was significantly higher ($p \leq 0.05$; data not shown) in all non-paddy soil fractions (Fig. 3a, b). A semievaluation of Fe oxides could not be conducted by XRD analyses because of the low concentrations of Fe_d oxides (0.1% and 3.3%) in paddy and non-paddy soils.

Clay minerals were detected by XRD analyses and results showed that kaolinite, illite, chlorite and secondary chlorite are clay minerals in both soil sequences (Fig. 4a, b). Illite was the major clay mineral in both soils and varied in the coarse clay; fine clay fraction was characterized by less illite. Given the similar soil mineralogy of both chronosequences (Fig. 4a, b), management obviously does not induce changes in mineralogy during soil development. Based on these results, the long-term paddy management seems to have less influence on the clay mineralogy of the uniform parent material of marine-derived paddy and non-paddy soils. The relationship between the concentration of Fe_o oxides and the OC values of the soil fractions $<20 \mu\text{m}$ (mean values of the total soils) is summarized in Fig. 5 and statistically significant correlations were observed for the paddy ($p \leq 0.019$) and non-paddy ($p \leq 0.002$) soil fractions $<20 \mu\text{m}$. Compared to non-paddy soils, all fractions of paddy soils are characterized by higher amounts of OC at higher Fe_o concentrations (Fig. 5). The fine

Table 3
Dithionite (Fe_d) and oxalate (Fe_o) extractable iron (Fe) of paddy (P) and non-paddy (NP) soil fractions (uppermost A horizon) with standard error. Fe_d and Fe_o extractable Fe oxides were determined as a single measurement. Significant differences between paddy and non-paddy soils are indicated by * ($p \leq 0.05$).

Fe concentration		Soil fraction ^a			
Site	Depth (cm)	20–6.3 μm	6.3–2 μm	<2 μm	<0.2 μm
		Fe_d (mg g^{-1})			
P 50	0–7	2.4	9.1	20.7	24.3
P 100	0–9	3.0	11.6	18.6	22.6
P 300	0–18	2.6	12.5	17.9	19.7
P 700	0–10	2.6	13.4	20.7	27.2
P 1000	0–10	2.1	9.2	22.3	26.8
P 2000	0–15	1.4	6.2	11.8	13.0
Mean (50–700)		*2.6 ± 0.2	11.7 ± 1.8	19.5 ± 1.5	23.4 ± 3.1
Mean (50–2000)		*2.3 ± 0.5	10.3 ± 2.7	18.7 ± 3.7	22.3 ± 5.3
NP 50	0–9	0.1	12.1	25.6	24.6
NP 100	0–14	0.2	10.4	21.8	22.8
NP 300	0–11	0.1	10.2	21.9	32.7
NP 700	0–11	0.1	9.1	20.5	31.4
Mean (50–700)		0.1 ± 0.0	10.5 ± 1.2	22.4 ± 2.2	27.9 ± 4.9
		Fe_o (mg g^{-1})			
P 50	0–7	0.8	4.8	11.0	15.8
P 100	0–9	0.8	5.0	10.6	14.6
P 300	0–18	0.5	4.8	8.9	10.7
P 700	0–10	1.4	7.2	12.7	16.8
P 1000	0–10	0.8	4.5	11.7	14.9
P 2000	0–15	0.8	4.5	9.4	11.1
Mean (50–700)		*0.9 ± 0.4	*5.5 ± 1.2	*10.8 ± 1.5	*14.5 ± 2.7
Mean (50–2000)		*0.9 ± 0.3	*5.2 ± 1.0	*10.7 ± 1.4	*14.0 ± 2.5
NP 50	0–9	0.0	3.2	7.7	12.2
NP 100	0–14	0.0	2.0	5.1	8.2
NP 300	0–11	0.0	1.6	2.0	6.0
NP 700	0–11	0.0	2.4	6.3	8.6
Mean (50–700)		0.0 ± 0.0	2.3 ± 0.7	5.3 ± 2.4	8.8 ± 2.6

^a m Si: medium silt (20–6.3 μm); fSi: fine silt (6.3–2 μm); cC: coarse clay (2–0.2 μm); fC: fine clay (<0.2 μm).

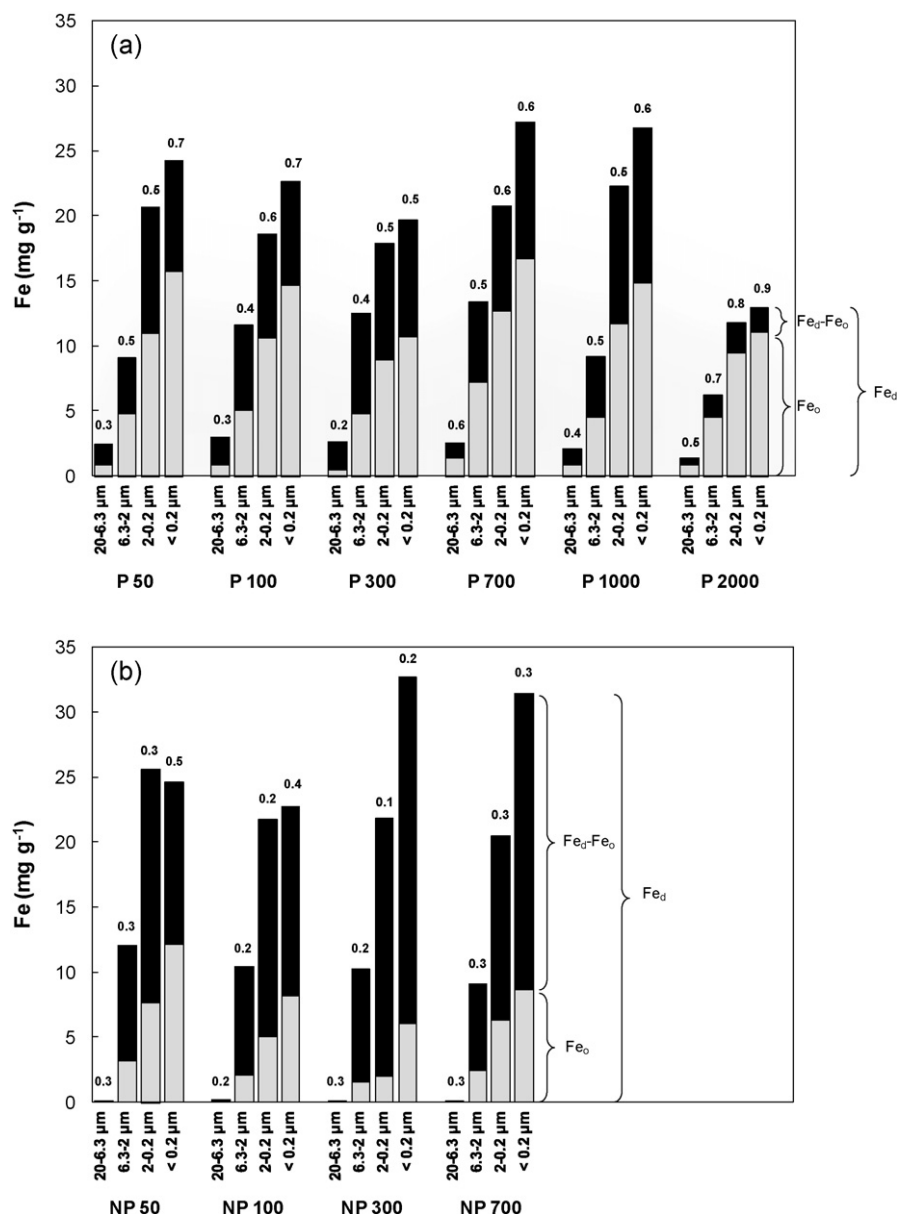


Fig. 3. Dithionite (Fe_d) and oxalate (Fe_o) extractable iron (Fe) oxides and the ratio of Fe_o/Fe_d of (a) paddy (P) and (b) non-paddy (NP) soil fractions (20–6.3 μm = medium silt; 6.3–2 μm = fine silt; 2–0.2 μm = coarse clay; <0.2 μm = fine clay) of the uppermost A horizon.

clay fraction of both soils presented higher concentration of Fe_o oxides but OC concentrations similar to coarse clay. There was no correlation between the bulk soil OC content and the concentration of Fe_o oxides, because for the bulk soil there are other OC fractions e.g., particulate organic matter presented relevant contributions to total OC content.

4. Discussion

4.1. SOM composition does not show accumulation of lignin-derived phenols under long-term paddy soil management conditions

Paddy and non-paddy bulk soils are characterized by statistically the same SOM composition. Furthermore the soil fractions (which were not treated by HF) show similar SOM compositions compared to those of the bulk soil (Figs. 1 and 2). The composition of SOM does not significantly differ either between paddy and non-paddy soils or does not change during soil development (Fig. 2). The long-term rice cropping management results in more OC

content but does not affect the composition of SOM with ongoing pedogenesis. Higher OM contents in paddy soils are supposed to be due to greater input from plant residues or charred material, or to accumulation of lignin-derived compounds (Neue et al., 1997; Cao et al., 2006; Kögel-Knabner et al., 2010). Therefore, we hypothesized that paddy and non-paddy soils are characterized by different SOM compositions because of the accumulation of lignin-derived phenols during paddy soil development, which is due to the long-term rice cropping management. All paddy and non-paddy soils are characterized by mean aryl-C contents between 21% and 28%. The major signal intensity centered at 130 ppm points to the accumulation of condensed aromatic structures, whereas no distinct phenol signal around 150 ppm could be identified. Results from Bierke et al. (2008) demonstrated that multiple annual rice cropping systems shorten the fallow period, which reduces the time for aerobic degradation of lignin-derived phenols and crop residues. Also, Olk et al. (1998, 2006) described an accumulation of phenolic compounds due to anaerobic conditions under intensified irrigated rice cropping. In

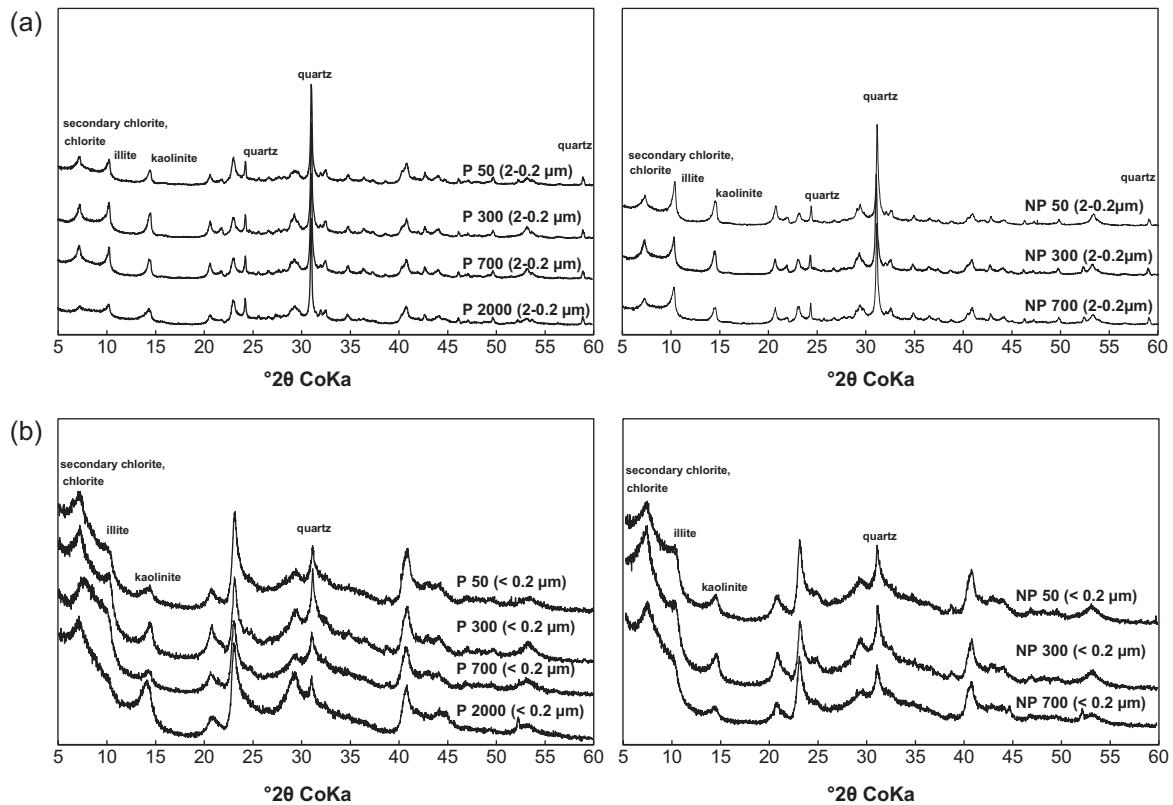


Fig. 4. X-ray diffraction curves of (a) coarse clay (2–0.2 μm) and (b) fine clay (<0.2 μm) fractions of paddy (P) and non-paddy (NP) soils (uppermost A horizon).

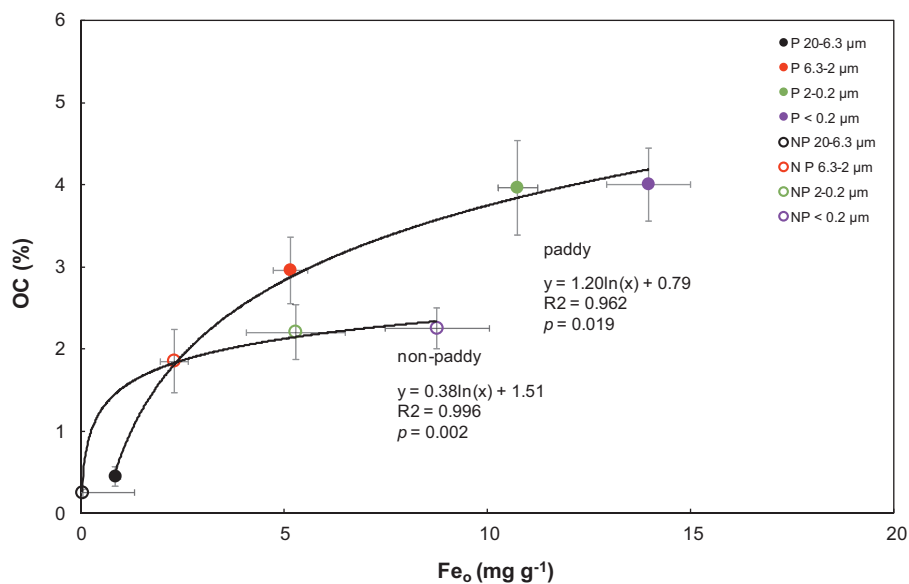


Fig. 5. Relation between oxalate (Fe_o) extractable iron (Fe) oxides and the organic carbon (OC) concentrations of the paddy (P) and non-paddy (NP) soil fractions (20–6.3 μm = medium silt; 6.3–2 μm = fine silt; 2–0.2 μm = coarse clay; <0.2 μm = fine clay) with standard errors.

contrast to these studies, selective enrichment of lignin-derived phenols in the paddy soil fractions was not found, even for long-term paddy soil management. The aryl-C chemical-shift region is remarkably similar for paddy and non-paddy mineral fractions <2 μm and does not show a specific accumulation of condensed aromatic structures in the paddy soils, such as charred OM residues. Overall, paddy management obviously induces higher OM quantity in all soil fractions, but it does not affect SOM composition during paddy soil development.

4.2. Paddy soil management induces specific environment of Fe oxide formation

The present chronosequence, derived from calcareous marine sediments, presents a low degree of soil development, shown by unchanged soil mineralogy, soil texture, and only slightly acidic pH values seem to be not sufficient to alter minerals and Fe oxides. The pedogenesis of paddy soils does not induce any chronological trend of the pedogenetic Fe oxides (Fe_d) during the first 1000 years of

pedogenesis, as already described by Cheng et al. (2009). We found slightly declining proportions of Fe_d oxides only after 2000 years of rice cultivation in paddy topsoil. It seems that a long-term duration of pedogenesis with paddy rice cultivation is necessary to induce loss of Fe_d oxides from the topsoils. Zhang and Gong (2003) reported a decrease of Fe_d oxides with increasing age of paddy soils for chronosequences of strongly developed soils. The authors attributed this finding to gradual, long-term losses with runoff and drainage and explained that reduction and mobilization lead to a decline of Fe_d oxides in paddy soils.

We expected to find increasing proportions of Fe_o oxides in the paddy soils with increasing duration of soil development, induced by submergence due to long-term paddy management, leading to reduced crystallization of Fe oxides (Zhang et al., 2003). Increasing proportions of Fe_o oxides were not confirmed and Fe_o oxides remained unchanged during pedogenesis. The paddy soil chronosequence is dominated by poorly crystalline forms of Fe oxides and significant lower content of crystalline Fe oxides ($Fe_d - Fe_o$) compared to the associated non-paddy soils. The management of the paddy soils creates an environment of Fe oxide formation which is different to those in non-paddy soils. The paddy-specific soil condition of Fe oxide formation is already reached after 50 years of soil development and does not alter Fe oxide proportions since this earliest stage of pedogenesis. Also Wang et al. (1992) ascribed in a study on Fe mineralogy the low content of crystalline Fe oxides to the paddy management which retard the formation of crystalline Fe oxides. Zhang and Lin (2002) reported that the paddy management led to a decreased crystallinity of soil Fe oxides, because crystalline Fe oxides can be transformed to poorly crystalline forms when artificially submerged (Zhang et al., 2003). In contrast to that, the lower content of Fe_o oxides in oxic soils are explained by the dehydration of Fe_o oxides and subsequent shift to a system of greater crystallinity (Sherman et al., 1964). Fe_o oxides in non-flooded soils are formed by dissolution and precipitation reactions involving soil minerals (Wang et al., 1991) and become more crystalline over time (Schwertmann and Taylor, 1989). Our data do not confirm the concept that repeated alternating redox cycles lead to the formation of more strongly crystalline forms of Fe oxides (Thompson et al., 2006).

Greenland and Mott (1978) and Borggaard (1982) pointed out that pedogenetic Fe oxides can occur as coatings on clay mineral particles. Habibullah et al. (1971) showed that only Fe_o oxides are able to form coatings on clay particles, but only in flooded soils. Thus, the paddy management leads to relatively high proportions of Fe_o oxides in clay-sized fractions, where they might form coatings on clay particles. This is in contrast to non-paddy soils, which have a different regime of Fe oxide formation, characterized by higher proportions of crystalline Fe oxides in the fine mineral fractions.

4.3. Paddy soil management favors high OC accumulation due to high ratio of Fe_o/Fe_d

The literature provides two options why paddy management favors the accumulation of OC: (i) paddy soils obtain high inputs of OC (Gong and Xu, 1990; Tanji et al., 2003) and (ii) the management of the soils seems to retard the OC decomposition (Neue et al., 1997; Sahrawat, 2004), both leading to a relatively great tendency to accumulate OC. OC accumulates preferentially in the fine mineral fraction, with highest capacities for OC accumulation in clay-sized fractions (Wissing et al., 2011). The present study shows that these fine mineral fractions are characterized by a paddy-specific mineral composition emerging already within 50 years of paddy management. The management of paddy soils results in high proportions of Fe_o oxides which are associated with high OC

concentrations within the fine silt fraction and both clay fractions (Fig. 5). In contrast, the non-paddy soil fractions have lower Fe_o oxides and lower OC concentrations. Thus, paddy management induces in early stages of soil development a self-sustaining system, connecting high inputs and retarded decomposition of OM with the preferred formation of poorly crystalline Fe oxides (Wang et al., 1992). This leads to Fe_o -OM associations which are stable during the entire paddy soil evolution period investigated here. Fe_o oxides (e.g., ferrihydrite) are known to have a large mineral surface compared to crystalline Fe oxides (Borggaard, 1982; Adams and Kassim, 1984; Kiem and Kögel-Knabner, 2002; Wagai and Mayer, 2007), and because of the higher Fe_o oxide content, the potential to accumulate OC is more pronounced in paddy clay fractions compared to non-paddy soils. The stabilization of OC by association with Fe_o oxides has already been identified as a relevant process in paddy soils by Pan et al. (2003a, 2003b). Zhang and Lin (2002) also found a higher ratio of Fe_o/Fe_d with ongoing paddy soil management and higher OC contents with longer paddy rice cultivation. Soils with high OC content contain greater organic acid content, which may have an inhibitory effect on crystallization and lead to retardation of Fe oxides crystallization (Schwertmann, 1966; Schwertmann et al., 1982). To summarize, the higher proportion of poorly crystalline Fe oxides present already after 50 years of paddy soil development provides a higher potential for SOM accumulation in the fine fraction of these soils compared to soils from the same parent material but under non-paddy management.

5. Conclusions

A paddy and a non-paddy (upland) chronosequence with similar soil texture and mineralogy, derived from the same parent marine sediments, showed specific management induced differences in the topsoil horizons. The paddy management resulted in higher OM quantities but did not affect the SOM composition during soil development. Selective enrichment of lignin-derived phenols, because of the long-term paddy rice management, could not be confirmed in the present study. The paddy soil chronosequence is dominated by poorly crystalline forms of Fe oxides and significant lower contents of crystalline Fe oxides ($Fe_d - Fe_o$) in topsoils. This is in contrast to non-paddy soils, which have a different regime of Fe oxide formation, characterized by higher proportions of crystalline Fe oxides. Pedogenetic Fe oxides stayed constant during the first 1000 years of rice cultivation. Clay mineralogy remained unchanged during paddy soil development, indicating that the management may have little influence on clay mineralogy. The paddy-specific soil conditions of Fe oxide formation are already effective in the earliest stage of soil development after 50 years and do not induce any changes during later stages of paddy soil formation. These management-induced higher proportions of Fe_o are associated with a higher OC accumulation in the paddy soils from the earliest stage of soil evolution. Our results demonstrate for the first time that paddy soils have higher potentials for SOC accumulation compared to respective non-paddy soils, due to the different environments for Fe oxide formation. Thus, OC in the paddy soil fine fractions accumulates during the first 1000 years of paddy soil development, whereas it stays constant in non-paddy soils. The OC accrual in the paddy topsoil due to association with poorly crystalline Fe oxides might be terminated when Fe oxide leaching is initiated in later stages of paddy soil evolution, but this was not found in the present chronosequence even after 2000 years of paddy management. Our results have major implications for the assessment of new management techniques for paddy soils such as alternating wetting and drying, as these will affect redox conditions and thus most probably also Fe oxide composition and OC storage potential.

Acknowledgements

The authors thank Rui Yin and the Institute of Soil Science, Chinese Academy of Sciences, in Nanjing. We thank Jian-Rong Fu for support during sampling at the chronosequence site around Cixi and for logistic handling. Reinhold Jahn, Sabine Fiedler and Vanessa Vogelsang from the Institute for Agricultural and Nutritional Sciences at the Martin-Luther University in Halle-Wittenberg are gratefully acknowledged for providing us with inorganic carbon data, pH and Eh values. We thank Monika Heilmeyer for technical assistance and Martina Bauer, Carolin Botond, Robert U. Hagemann, Tahereh Javaheri, Juliane Teichmann, and Maria Vonach for student research assistance. We are grateful to the Deutsche Forschungsgemeinschaft (DFG) for their generous funding of Research Unit FOR 995 "Biogeochemistry of paddy soil evolution."

Appendix A. Supplementary data

Supplementary data associated with this article can be found, in the online version, at <http://dx.doi.org/10.1016/j.still.2012.08.004>.

References

- Adams, W.A., Kassim, J.K., 1984. Iron oxyhydroxides in soils developed from Lower Palaeozoic sedimentary rocks in mid-Wales and implications for some pedogenic processes. *Journal of Soil Science* 35, 117–126.
- Arshad, M.A., Ripmeester, J.A., Schnitzer, M., 1988. Attempts to improve solid state ¹³C NMR spectra of whole mineral soils. *Canadian Journal of Soil Science* 68, 593–602.
- Bahmanyar, M.A., 2007. The influence of continuous rice cultivation and different water logging periods on morphology, clay mineralogy, Eh, pH and K in paddy soils. *Pakistan Journal of Biological Sciences* 10 (17), 2844–2849.
- Bierke, A., Kaiser, K., Guggenberger, G., 2008. Crop residue management effects on organic matter in paddy soils – the lignin component. *Geoderma* 146, 48–57.
- Borggaard, O.K., 1982. The influence of iron oxides on the surface area of soil. *Journal of Soil Science* 33, 443–449.
- Cao, Z.H., Ding, J.L., Hu, Z.Y., Knicker, H., Kögel-Knabner, I., Yang, L.Z., Yin, R., Lin, X.G., Dong, Y.H., 2006. Ancient paddy soils from the Neolithic age in China's Yangtze River Delta. *Naturwissenschaften* 93, 232–236.
- Chen, L.-M., Zhang, G.-L., Efland, W.R., 2011. Soil characteristic response times and pedogenic thresholds during the 1000-year evolution of a paddy soil chronosequence. *Soil Science Society of America Journal* 75 (5), 1–14.
- Cheng, Y., Yang, L.-Z., Cao, Z.-H., Ci, E., Yin, S., 2009. Chronosequential changes of selected pedogenic properties in paddy soils as compared with non-paddy soils. *Geoderma* 151, 31–41.
- Colberg, P.J., 1988. Anaerobic microbial degradation of cellulose, lignin, oligolignols, and monoaromatic lignin derivatives. In: Zehnder, A.J.B. (Ed.), *Biology of Anaerobic Microorganisms*. Wiley, New York, (cited from Olk et al., 1996), pp. 333–372.
- Darke, A.K., Walbridge, M.R., Lockaby, B.G., 1997. Changes in Al and Fe crystallinity and P sorption capacity in a floodplain forest soil subjected to artificially manipulated flooding regimes in field mesocosms. *Wetlands Ecology and Management* 4, 235–244.
- de Mello, J.W.V., Barrón, V., Torrent, J., 1998. Phosphorus and iron mobilization in flooded soils from Brazil. *Soil Sciences* 163 (2), 122–132.
- Dong, N.M., Brandt, K.K., Sørensen, J., Hung, N.N., Hach, C.V., Tan, P.S., Dalsgaard, T., 2012. Effects of alternating wetting and drying versus continuous flooding on fertilizer nitrogen fate in rice fields in the Mekong Delta, Vietnam. *Soil Biology and Biochemistry* 47, 166–174.
- Eickhorst, T., Tippkötter, R., 2009. Management-induced structural dynamics in paddy soils of south east China simulated in microcosms. *Soil and Tillage Research* 102, 168–178.
- Eusterhues, K., Rumpel, C., Kögel-Knabner, I., 2005. Organo-mineral associations in sandy acid forest soils: importance of specific surface area, iron oxides and micropores. *European Journal of Soil Science* 56, 753–763.
- Eusterhues, K., Rumpel, C., Kögel-Knabner, I., 2007. Composition and radiocarbon age of HF-resistant soil organic matter in a Podzol and a Cambisol. *Organic Geochemistry* 38 (8), 1356–1372.
- FAO, 2006. Guidelines for Soil Description. FAO, Rome, 97 pp.
- Gaunt, J.L., Neue, H.-U., Cassman, K.G., Olk, D.C., Arah, J.R.M., Witt, C., Ottow, J.C.G., Grant, I.F., 1995. Microbial biomass and organic matter turnover in wetland rice soils. *Biology and Fertility of Soils* 19, 333–342.
- Gong, Z.-T., 1983. Pedogenesis of paddy soils and its significance in soil classification. *Soil Sciences* 135 (1), 5–10.
- Gong, Z.-T., Xu, Q., 1990. Paddy Soils. Soils of China. Science Press, Beijing, pp. 233–260.
- Greenland, D.J., Mott, C.J.B., 1978. Surface of soil particles. In: Greenland, D.J., Hayes, M.H.B. (Eds.), *The Chemistry of Soil Constituents*. John Wiley and Sons, Chichester, pp. 321–353.
- Habibullah, A.K.M., Greenland, D.J., Brammer, H., 1971. Clay mineralogy of some seasonally flooded soils of East Pakistan. *Journal of Soil Science* 22 (2), 179–190.
- Howeler, R.H., Bouldin, D.R., 1971. The diffusion and consumption of oxygen in submerged soils. *Soil Science Society of America Journal* 35, 202–208.
- Islam, M.A., Choudhury, A.A., 1959. Distribution of iron, manganese and phosphorus in the paddy soil profile. *Journal of Agricultural Science* 54, 318–320.
- IUSS Working Group WRB, 2007. World Reference Base for Soil Resources 2007. World Soil Resources Reports, vol. 103. FAO, Rome.
- Janssen, M., Lennartz, B., 2006. Horizontal and vertical water fluxes in paddy rice fields of subtropical China. *Advances in Geoecology* 38, 344–354.
- Kaiser, K., Guggenberger, G., 2000. The role of DOM sorption to mineral surfaces in the preservation of organic matter in soils. *Organic Geochemistry* 31, 711–725.
- Kaiser, K., Guggenberger, G., 2003. Mineral surfaces and soil organic matter. *European Journal of Soil Science* 54 (2), 219–236.
- Kalbitz, K., Kaiser, K., Fiedler, S., Kölbl, A., Amelung, W., Bräuer, T., Cao, Z.H., Don, A., Grootes, P., Jahn, R., Schwark, L., Vogelsang, V., Wissing, L., Kögel-Knabner, I. The carbon count of 2000 years of rice cultivation, submitted for publication.
- Kalbitz, K., Schwesig, D., Rethemeyer, J., Matzner, E., 2005. Stabilization of dissolved organic matter by sorption to the mineral soil. *Soil Biology and Biochemistry* 37, 1319–1331.
- Kiem, R., Kögel-Knabner, I., 2002. Refractory organic carbon in particle-size fractions of arable soils. II: Organic carbon in relation to mineral surface area and iron oxides in fractions <6 μm. *Organic Geochemistry* 33, 1699–1713.
- Kleber, M., Mertz, C., Zikeli, S., Knicker, H., Jahn, R., 2004. Changes in surface reactivity and organic matter composition of clay subfractions with duration of fertilizer deprivation. *European Journal of Soil Science* 55, 381–391.
- Knicker, H., Lüdemann, H.-D., 1995. N-15 and C-13 CPDMS and solution NMR studies of N-15 enriched plant material during 600 days of microbial degradation. *Organic Geochemistry* 23, 329–341.
- Kögel-Knabner, I., Amelung, W., Cao, Z.-H., Fiedler, S., Frenzel, P., Jahn, R., Kalbitz, K., Kölbl, A., Schloter, M., 2010. Biogeochemistry of paddy soils. *Geoderma* 157, 1–14.
- Kuo, S., Mikkelsen, D.S., 1979. Distribution of iron and phosphorus in flooded and unflooded soil profiles and their relation to P adsorption. *Soil Sciences* 127, 18–25.
- Li, Z.-P., Zhang, T.-L., Li, D.-C., Velde, B., Han, F.-X., 2005. Changes in soil properties of paddy fields across a cultivation chronosequence in subtropical China. *Pedosphere* 15 (1), 110–119.
- Mahieu, N., Olk, D.C., Randall, E.W., 2000a. Accumulation of heterocyclic nitrogen in humified organic matter: a ¹⁵N NMR study of lowland rice soils. *European Journal of Soil Science* 51, 379–389.
- Mahieu, N., Olk, D.C., Randall, E.W., 2002. Multinuclear magnetic resonance analysis of two humic acid fractions from lowland rice soils. *Journal of Environment Quality* 31, 421–430.
- Mehra, O.P., Jackson, M.L., 1960. Iron oxide removal from soils and clays by a dithionite-citrate system buffered with sodium bicarbonate. In: *Clays and Clay Minerals, Proceedings of the 7th National Conference*. pp. 317–327.
- Mikutta, R., Kleber, M., Torn, M.S., Jahn, R., 2006. Stabilization of soil organic matter: association with minerals or chemical recalcitrance? *Biogeochemistry* 77, 25–56.
- Moore, D.M., Reynolds, R.C., 1989. X-ray Diffraction and the Identification and Analysis of Clay Minerals. Oxford University Press, London.
- Neue, H.U., Gaunt, J.L., Wang, Z.P., Becker-Heidmann, P., Quijano, C., 1997. Carbon in tropical wetlands. *Geoderma* 79, 163–185.
- Olk, D.C., Cassman, K.G., Randall, E.W., Kinches, P., Sanger, L.J., Anderson, J.M., 1996. Changes in chemical properties of organic matter with intensified rice cropping in tropical lowland soil. *European Journal of Soil Science* 47, 293–303.
- Olk, D.C., Cassman, K.G., Mahieu, N., Randall, E.W., 1998. Conserved chemical properties of young humic acid fractions in tropical lowland soil under intensive irrigated rice cropping. *European Journal of Soil Science* 49, 337–349.
- Olk, D.C., Dancel, M.C., Moscoso, E., Jimenez, R.R., Dayrit, F.M., 2002. Accumulation of lignin residues in organic matter fractions of lowland rice soils: a pyrolysis-GC-MS study. *Soil Sciences* 167, 590–606.
- Olk, D.C., Cassman, K.G., Schmidt-Rohr, K., Andersd, M.M., Mao, J.-D., Deenikf, J.L., 2006. Chemical stabilization of soil organic nitrogen by phenolic lignin residues in anaerobic agroecosystems. *Soil Biology and Biochemistry* 38, 3303–3312.
- Pan, G., Li, L., Wu, L., Zhang, X., 2003a. Storage and sequestration potential of topsoil organic carbon in China's paddy soils. *Global Change Biology* 10, 79–92.
- Pan, G.X., Li, L.Q., Zhang, X.H., Dai, J.Y., Zhou, Y.C., Zhang, P.J., 2003b. Soil organic carbon storage of China and the sequestration dynamics in agricultural lands. *Advanced Earth Sciences* 18, 609–618 (in Chinese).
- Parfitt, R.L., 1989. Phosphate reactions with natural allophane, ferrihydrite and goethite. *Journal of Soil Science* 40, 359–369.
- Pronk, G.J., Heister, K., Kögel-Knabner, I., 2011. Iron oxides as major available interfaces component in loamy arable topsoils. *Soil Science Society of America Journal* 75, 1729–1732.
- Ponnamperuma, F.N., 1972. The chemistry of submerged soils. *Advances in Agronomy* 24, 29–96.
- Ratering, S., Schnell, S., 2000. Localization of iron-reducing activity in paddy soil by profile studies. *Biogeochemistry* 48, 341–365.
- Sah, R.N., Mikkelsen, D.S., 1986. Sorption and bioavailability of phosphorus during the drainage period of flooded-drained soil. *Plant and Soil* 92, 265–278.

- Sah, R.N., Mikkelsen, D.S., Hafez, A.A., 1989. Phosphorus behaviour in flooded-drained soils. III. Phosphorus desorption and availability. *Soil Science Society of America Journal* 53, 1729–1732.
- Sahrawat, K.L., 2004. Organic matter accumulation in submerged soils. *Advances in Agronomy* 81, 169–201.
- Schaefer, J., Stejskal, E.O., 1976. Carbon-13 nuclear magnetic resonance of polymers spinning at magic angle. *Journal of the American Chemical Society* 98, 1031–1032.
- Schöning, I., Knicker, H., Kögel-Knabner, I., 2005. Intimate association between O/N-alkyl carbon and iron oxides in clay fractions of forest soils. *Organic Geochemistry* 36, 1378–1390.
- Schwertmann, U., 1964. Differenzierung der Eisenoxide des Bodens durch Extraktion mit Ammoniumoxalat-Lösung. *Zeitschrift für Pflanzenernährung, Düngung, Bodenkunde* 105, 194–202.
- Schwertmann, U., 1966. Inhibitory effect of soil organic matter on crystallization of amorphous ferric hydroxide. *Nature* 212, 645–646.
- Schwertmann, U., Schulze, D.G., Murad, E., 1982. Identification of ferrihydrite in soils by dissolution kinetics, differential X-ray diffraction, and Mössbauer Spectroscopy. *Soil Science Society of America Journal* 46, 869–875.
- Schwertmann, U., Taylor, R.M., 1989. Iron oxides. In: Dixon, J.B., Weed, S.B. (Eds.), *Minerals in Soil Environments*. Soil Science Society of America Journal, Madison, WI, (cited from Drake et al., 1997), pp. 380–438.
- Shang, C., Tiessen, H., 1998. Organic matter stabilization in two semiarid tropical soils: size, density, and magnetic separations. *Soil Science Society of America Journal* 62, 1247–1257.
- Sherman, G.D., Matsusaka, Y., Ikawa, H., Uehara, G., 1964. The role of amorphous fraction in the properties of tropical soils. *Agrochimica* 7, 146–163.
- Skjemstad, J.O., Bushby, H.V.A., Hansen, R.W., 1989. Extractable Fe in the surface horizons of a range of soils from Queensland. *Australian Journal of Soil Research* 28, 259–266.
- Smernik, R.J., Oades, J.M., 1999. Effects of added paramagnetic ions on the ¹³C CP/MAS NMR spectrum of a de-ashed soil. *Geoderma* 89, 219–248.
- Smernik, R.J., Olk, D.C., Mahieu, N., 2004. Quantitative solid-state ¹³C NMR spectroscopy of organic matter fractions in lowland rice soils. *European Journal of Soil Science* 55, 367–379.
- Takahashi, T., Toriyama, K., 2004. Review: method to evaluate uplandization in converted field from a paddy based on crystallinity of free iron oxides. *Japan Agricultural Research Quarterly* 38 (3), 155–159.
- Tanji, K.K., Gao, S., Scardaci, S.C., Chow, A.T., 2003. Characterization redox status of paddy soils with incorporated rice straw. *Geoderma* 114, 333–353.
- Thompson, A., Chadwick, O.A., Rancourt, D.G., Chorover, J., 2006. Iron-oxide crystallinity increases during redox oscillations. *Geochimica et Cosmochimica Acta* 70, 1710–1727.
- Torn, M.S., Trumbore, S.E., Chadwick, O.A., Vitousek, P.M., Hendricks, D.M., 1997. Mineral control of soil organic carbon storage and turnover. *Nature* 389, 170–173.
- Wagai, R., Mayer, L.M., 2007. Sorptive stabilisation of organic matter in soils by hydrous iron oxides. *Geochimica et Cosmochimica Acta* 71, 25–35.
- Wang, H.D., Harris, W.G., Yuan, T.L., 1991. Noncrystalline phosphates in Florida phosphatic soils. Division S-2-soil chemistry. *Soil Science Society of America Journal* 55, 665–669.
- Wang, Y., Zhou, X., Wu, J., 1992. Mössbauer study on the iron oxide minerals of paddy soils derived from red soil in Fujian, China. *Hyperfine Interactions* 70, 1037–1040.
- Willet, I.R., Higgins, M.L., 1980. Phosphate sorption and extractable iron in soils during irrigated rice-upland crop rotations. *Australian Journal of Experimental Agriculture* 20, 346–353.
- Wissing, L., Kölbl, A., Vogelsang, V., Fu, J., Cao, Z.H., Kögel-Knabner, I., 2011. Organic carbon accumulation in a 2000-year chronosequence of paddy soil evolution. *Catena* 87, 376–385.
- Zhang, G.L., Gong, Z.T., 2003. Pedogenic evolution of paddy soils in different soil landscapes. *Geoderma* 115, 15–29.
- Zhang, M., He, Z., 2004. Long-term changes in organic carbon and nutrients of an Ultisol under rice cropping in southeast China. *Geoderma* 118, 167–179.
- Zhang, Y., Lin, X., 2002. Relation between Fe-oxides transformation and phosphorus adsorption in the oxic and anoxic layers of two paddy soils as affected by flooding. *Journal of Zhejiang University* 28 (5), 485–491.
- Zhang, Y., Lin, X., Werner, W., 2003. The effect of soil flooding on the transformation of Fe oxides and the adsorption/desorption behaviour of phosphate. *Journal of Plant Nutrition and Soil Science* 166, 68–75.
- Zou, P., Fu, J., Cao, Z., 2011. Chronosequence of paddy soils and phosphorus sorption-desorption properties. *Journal of Soils and Sediments* 11, 249–259.

Decalcification increases the accessibility of soil mineral surfaces for organic carbon accumulation in paddy soils

On the basis of the manuscript

Livia Wissing ^a, Angelika Kölbl ^a, Peter Schad ^a, Tino Bräuer ^b, Zhi-Hong Cao ^c, Ingrid Kögel-Knabner ^{a,d}

manuscript submitted

^aLehrstuhl für Bodenkunde, Department Ecology and Ecosystem Management, Center of Life and Food Sciences Weihenstephan, Technische Universität München, D-85350 Freising-Weihenstephan, Germany

^bLeibniz-Labor für Altersbestimmung und Isotopenforschung, Christian-Albrechts Universität zu Kiel, Max-Eyth Str. 11, D-24118 Kiel, Germany

^cInstitute of Soil Science, Chinese Academy of Sciences, Nanjing 210008, PR China

^dInstitute for Advanced Study, Technische Universität München, Lichtenbergstrasse 2a, D-85748 Garching, Germany

1 **Decalcification increases the accessibility of soil mineral surfaces for organic carbon**
2 **accumulation in paddy soils**

3

4 Livia Wissing ^{a,*}, Angelika Kölbl ^a, Peter Schad ^a, Tino Bräuer ^b, Zhi-Hong Cao ^c, Ingrid
5 Kögel-Knabner ^{a,d}

6

7 ^aLehrstuhl für Bodenkunde, Department Ecology and Ecosystem Management, Center of Life
8 and Food Sciences Weihenstephan, Technische Universität München, D-85350 Freising-
9 Weihenstephan, Germany

10 E-mail addresses: koegel@wzw.tum.de; koelbl@wzw.tum.de; schad@wzw.tum.de

11

12 ^bLeibniz-Labor für Altersbestimmung und Isotopenforschung, Christian-Albrechts Universität
13 zu Kiel, Max-Eyth Str. 11, D-24118 Kiel, Germany

14 E-mail address: tbraeuer@leibniz.uni-kiel.de

15

16 ^cInstitute of Soil Science, Chinese Academy of Sciences, Nanjing 210008, PR China

17 E-mail address: zhihongcaoli@126.com

18

19 ^dInstitute for Advanced Study, Technische Universität München, Lichtenbergstrasse 2a, D-
20 85748 Garching, Germany

21

22

23 ^{*}Corresponding author:

24 Livia Wissing, Tel. +49 (0)8161-71 -3734, Fax: +49 (0)8161 71 -4466, E-mail address:

25 l.wissing@wzw.tum.de

26

27 **Abstract**

28 We studied organic carbon (OC) accumulation due to organo-mineral associations during soil
29 development on calcareous parent material. Two chronosequences in Zhejiang Province, PR
30 China, were investigated; one under paddy cultivation with a maximum soil age of 2000
31 years, and the other under upland crops where the oldest soil was 700 years old. Bulk soils
32 and soil fractions of the uppermost A horizons were analyzed for OC concentrations, ¹⁴C
33 contents, total pedogenic iron concentration and oxalate extractable proportions of iron. The
34 specific surface area of soil minerals was measured with the Brunauer-Emmett-Teller (BET-
35 N₂) method under four conditions: untreated, after organic matter removal, after iron removal
36 and after removal of both. Initial soil formation on calcareous marine sediments includes soil
37 decalcification and OC accumulation. Paddy soils are characterized by an advanced
38 decalcification, higher OC contents and a pronounced accumulation of recent OC.
39 Unexpectedly, there was no evidence of formation of secondary minerals during soil
40 development, which could provide new surfaces for OC accumulation. However, the study
41 revealed higher OC coverings of mineral surfaces after decalcification in paddy soils. In
42 contrast, the surface area of minerals in non-paddy soils, in which decalcification was much
43 lower, seemed to be partly inaccessible for OC covering due to strong microaggregation by
44 cementation with carbonate and Ca²⁺-bridging. The accelerated decalcification of paddy soils
45 led to enhanced accessibility of mineral surfaces for OC covering, which intensified OC
46 accumulation from the early stages of soil formation onward.

47

48 **Key Words**

49 pedogenesis, chronosequence, paddy rice cultivation, iron oxides, specific surface area

50

51 **1. Introduction**

52 One of the first soil-forming processes with calcareous parent material is decalcification,
53 which has to be completed before secondary minerals start to form (Talibudeen and
54 Arambarri, 1964). Decalcification provides additional mineral surfaces for SOM accumulation
55 and includes carbonate dissolution and leaching of dissolved ions, with the possibility of the
56 formation of secondary carbonates (Lelong and Souchier, 1982; van Breemen and Protz,
57 1988). If the calcareous material is of marine origin dewatering, subsidence, oxidation of
58 sulfides (if present), desalination and decalcification are the first processes of soil formation
59 (Müller-Althen, 1994b; Portnoy, 1999; Giani and Landt, 2000). The carbonate loss in many
60 soils which derived from marine sediments is accelerated by sulfide oxidation by which
61 sulfuric acid is formed and calcium carbonate is dissolved (Brümmer et al., 1971). Sulfuric
62 acid is neutralized by the dissolution of carbonates (Brümmer et al., 1971). The loss of
63 carbonate leads to a decrease in pH in many soils (van den Berg and Loch, 2000).

64 The accumulation of SOM is another important soil-forming process. Calcareous soils may be
65 associated with higher SOM contents than non-calcareous soils (Oades, 1988). SOM is also
66 stabilized and physically protected from decomposition by coatings of calcium carbonate on
67 OM (le Tacon, 1978) or by cementation of soil aggregates with calcium carbonate (Oyonarte
68 et al., 1994). Persistent carbonate-OM coatings may form on coarse fragments and stabilize a
69 substantial portion of SOM (Schaeztl, 1991). Organo-mineral associations are considered to
70 be the major mechanism of SOM stabilization (Balabane and Plante, 2004; Eusterhues et al.,
71 2005). A positive correlation of the SOM content with the clay content is described by several
72 studies (Jenkinson and Rayner, 1977; Jenkinson et al., 1987; Bosatta and Agren, 1997). This
73 is attributed to a slow turnover time of the clay-bound OM (Balesdent et al., 1987) because
74 organo-mineral associations are more resistant to biodegradation (Chenu and Plante, 2006).

75 Mineral surfaces are known to be responsible for the OM stabilization in soils because clay
76 minerals, such as smectites and vermiculites, provide a high surface area up to $800 \text{ m}^2 \text{ g}^{-1}$

77 (Carter et al., 1986; Robert and Chenu, 1992) and in general stabilize more SOM than sand-
78 sized minerals, which can be attributed to higher adsorption to mineral surfaces (Balabane and
79 Plante, 2004). Mayer (1994) showed in a study on the relationship between mineral surfaces
80 and organic carbon (OC) concentrations that the availability of the surface area controls the
81 OC concentration. Thus, the adsorption on mineral surfaces seems to be an important process
82 in SOM stabilization (Kaiser and Guggenberger, 2003). A positive correlation between OM
83 and iron oxides in oxic soils is known from the literature (e.g., Kaiser and Guggenberger,
84 2000; Kiem and Kögel-Knabner, 2002). This is explained by the large mineral surface area of
85 iron oxides and the possibility of OM adsorption on their surface (Tipping, 1981; Wagai and
86 Mayer, 2007) or by their ability to interconnect particles to aggregates (Eusterhues et al.,
87 2005). Eusterhues et al. (2005) investigated the importance of iron oxide surfaces for the
88 formation of organo-mineral associations in different subsoils and found that nearly all
89 mineral-associated OM was stabilized by interactions with iron oxide minerals. Most of the
90 previously mentioned studies were done on relatively acid forest and agricultural soils or
91 sandy subsoils. Investigations on the importance of silicate (clay) minerals and iron oxides for
92 OC accumulation are not available for soil development starting from calcareous parent
93 material with successive decalcification.

94 At Hangzhou Bay, PR China, new agricultural land has been created by consecutive land
95 reclamation with protective dikes over the past 2000 years, and it has been used for cultivation
96 of flooded paddy rice or non-inundated upland crops. The parent material is a calcareous
97 marine sediment, which is influenced by suspended Yangtze River load. The management of the
98 paddy soils (e.g., flooding and drainage) produces special soil properties. Flooding and
99 discharge lead to a gradual carbonate loss and subsequent pH decrease during rice cultivation
100 (Wissing et al., 2011). Thus, the pedogenesis of paddy soils differs remarkably from that of
101 corresponding non-inundated croplands (Li et al., 2005) where decalcification is much slower.
102 Faster decalcification caused by the paddy management accelerates other pedogenetic

103 processes. Paddy soil development favors OC accumulation due to high inputs of OC (Gong
104 and Xu, 1990; Tanji et al., 2003) and/or retards the OC decomposition because of the
105 periodical anoxic conditions that lead to enhanced SOM accumulation (Neue et al., 1997; Lal,
106 2002; Zhang and He, 2004; Sahrawat, 2004; Wu, 2011; Wissing et al., 2011), confirmed by a
107 higher ¹⁴C-documented replacement of “old” carbon by “modern” carbon over time than in
108 non-inundated non-paddy soils due to plow pan development (Bräuer et al., 2012). The
109 accumulation of SOM by association with oxalate-extractable iron (Fe_{ox}) has already been
110 identified as a relevant feature in paddy soils (Pan et al., 2003a, 2003b). Wissing et al. (2012)
111 found higher Fe_{ox} contents in paddy soils than in non-inundated upland soils. The authors
112 pointed out that the higher proportion of Fe_{ox} seems to be responsible for a large proportion of
113 mineral-associated SOM in paddy soils. Thus, the ability to stabilize OC is more pronounced
114 in paddy soils compared to corresponding upland soils (Wissing et al., 2012).

115 The present study investigated soil development from calcareous parent material to assess the
116 OM accumulation due to organo-mineral associations. The major research question is: How
117 do the soil-forming processes decalcification and OC accumulation interact in soils that were
118 managed differently? We used two different chronosequences in Zhejiang Province, PR
119 China, to compare soil development based on the degree of carbonate loss, starting from
120 calcareous parent material with successive decalcification. Therefore, we addressed the
121 following three research questions:

- 122 (i) How does the decalcification control other soil-forming processes; e.g., OM
123 accumulation, and is the formation of clay minerals and iron oxides in rapidly
124 decalcified soils accelerated?
- 125 (ii) Is the OC covering of the clay mineral and iron oxide surfaces higher in
126 decalcified (paddy) soils, and does the OC covering increase with soil
127 development?

128 (iii) Do clay minerals and iron (hydr) oxides contribute in equal amounts to the OC
129 accumulation?

130 For this approach, samples were taken from differently aged paddy (50–2000 years) and non-
131 paddy soils (50–700 years). A particle size fractionation of the Ap horizon was applied to the
132 soils in order to isolate the clay-sized fractions, and their iron oxides were extracted by using
133 the dithionite-citrate-bicarbonate (DCB) method. The specific surface area (SSA) of the <20
134 μm fraction were measured by the Brunauer-Emmett-Teller (BET- N_2) method (Brunauer et al.,
135 1938). To investigate the accessibility of those mineral surfaces for OC covering during
136 pedogenesis, we used selective removal of OM and iron by combining hydrogen peroxide
137 (H_2O_2) and DCB treatments.

138

139 **2. Materials and methods**

140 *2.1. Study area and soil description*

141 The study area was located in the eastern part of the PR China, near the city of Cixi (30°10'N,
142 121°14'E), Zhejiang Province. The investigation region is affected by river runoff and tide and the
143 parent material consists of estuarine sediment, which originated from the Yangtze (Changjiang) River.
144 During the past 2000 years several dikes had been built for land reclamation, which resulted
145 in a chronosequence of soils under agricultural use. Parts of the land were used for paddy rice
146 cultivation under flooded conditions, followed by a winter crop (paddy soils). Other parts
147 were used for a variety of non-inundated upland crops (non-paddy soils). The paddy (50–1000
148 years) and non-paddy (50–700 years) soil sequences were determined according to the records
149 in the county annals of the Zhejiang Province. The description of the 2000-year-old paddy site
150 can be found in Zou et al. (2011). Information in Chinese is obtainable at
151 <http://www.cixi.gov.cn/> (Cheng et al., 2009). The paddy chronosequence contained a
152 succession of 50, 100, 300, 700, 1000 and 2000 years of soil development. The non-paddy
153 chronosequence consisted of four different age stages: 50, 100, 300 and 700 years. Soils are
154 abbreviated as P 50, P 100, etc. and NP 50, NP 100, etc., respectively. Additionally, one
155 profile was situated at the mudflat (estuarine sediment; tidal wetland), representing the parent
156 material (day 0 of terrestrial soil development); another was in a nearby 30-year-old marsh
157 land, which had not been under agricultural use (Kölbl et al., submitted). It was mentioned by
158 Kölbl et al. (submitted) that the similarity in soil texture across a whole chronosequence is a
159 strong indicator that all soils developed from similar parent materials. Furthermore, the
160 authors used lipid biomarkers to show the homogeneity of the original coastal sediments and
161 to enable the reconstruction of a consistent land use history for both chronosequences. Paddy
162 and non-paddy soils were sampled in triplicate from adjacent independent fields, described by
163 the FAO Guidelines for Soil Description (FAO, 2006) and classified according to
164 International Union of Soil Sciences Working Group (2007). The following soil types were

165 identified (revised from Wissing et al., 2011): Endogleyic Anthraquic Cambisols (P 50, 100,
166 300) and Endogleyic Hydragric Anthrosols (P 700, 1000, 2000). Non-paddy soils were
167 classified as Endogleyic Hyposalic Endofluvic Cambisol (NP 50), Endogleyic Cambisol (NP
168 100) and Haplic Cambisols (NP 300, 700). This study discusses the uppermost A horizon: in
169 non-paddy soils, the plowed horizon and in paddy soils, the puddled horizon (Alp). The
170 meaning of the lowercase letters is l = mottling as in capillary fringes, and p = altered by
171 plowing (FAO, 2006). If the upper part of the Alp horizon had more pronounced redox
172 features, the horizon was subdivided into Alp1 and Alp2, and only Alp1 was analyzed in the
173 present study. Similarly, thick Ap horizons in non-paddy soils were subdivided into Ap1 and
174 Ap2, with only Ap1 analyzed here. Paddy soils were sampled under similar soil moisture
175 conditions. OC input data for the chronosequences with up to 700 or 2000 years of
176 agricultural use are not available. However, sampling sites with similar cropping history
177 during the last decades were chosen for the respective paddy and non-paddy chronosequences.
178 The OC content of the A(l)p1 and A(l)p2 horizons was similar because of the periodical
179 puddling and plowing. Bulk soil samples were air-dried and sieved to a size of <2 mm for
180 further analyses.

181

182 2.2. Carbon content

183 Total carbon concentrations (C_{tot}) of bulk soils were determined in duplicate by dry
184 combustion at 950°C on a Vario EL elemental analyzer (Elementar Analysensysteme, Hanau,
185 Germany). The inorganic carbon (IC) concentration was determined in duplicate by the
186 Institute for Agricultural and Nutritional Sciences of the Martin Luther University in Halle-
187 Wittenberg by dissolving carbonates with 42% phosphoric acid and measuring the evolving
188 CO₂ by infrared detection (C-MAT 550, Ströhlein GmbH, Viersen, Germany). The OC
189 concentration was calculated by subtracting the concentration of IC from C_{tot} concentration:

$$190 \text{ OC (mg g}^{-1}\text{)} = C_{\text{tot}} \text{ (mg g}^{-1}\text{)} - \text{IC (mg g}^{-1}\text{)} \quad (1)$$

191 The C_{tot} concentrations of particle size fractions were measured in duplicate by dry
192 combustion (EuroEA Elemental Analyzer 3000, HEKAtech, Wegberg, Germany). Due to the
193 hydrochloric acid (HCl) treatment prior to the physical fractionation procedure (see section
194 2.3), all mineral soil fractions were free of carbonates and the C_{tot} concentration was equal the
195 OC concentration.

196

197 *2.3. Particle size fractionation*

198 Before fractionation, all soils were pre-treated with 0.1 M HCl (final pH value = 4.8) to
199 remove carbonates. HCl and the dissolved Ca^{2+} ions were removed by centrifugation (20
200 minutes, at 3423 g). The particle size fractionation was done according to Wissing et al.
201 (2011). Briefly, to disrupt sand-sized macroaggregates, ultrasonic treatment with an energy
202 input of 60 J mL^{-1} was used, followed by wet sieving to separate sand and particulate OM
203 (2000–63 μm) from the residue. The complete dispersion of microaggregates (<200 μm) was
204 achieved by an additional ultrasonic treatment (440 J mL^{-1}). The <20 μm fraction was further
205 separated by sedimentation in Atterberg cylinders (silt-sized fractions) and centrifugation
206 (clay-sized fractions). The following six particle size fractions were isolated: sand and
207 particulate OM (S+POM, 2000–63 μm), coarse silt (cSi, 63–20 μm), medium silt (mSi, 20–
208 6.3 μm), fine silt (fSi, 6.3–2.0 μm), coarse clay (cC, 2.0–0.2 μm) and fine clay (fC, <0.2 μm).
209 All fractions were freeze-dried and weighed to obtain the mass proportion of each fraction to
210 the bulk soil.

211

212 *2.4. Soil mineralogy*

213 Total pedogenic iron (dithionite-extractable iron [Fe_d]) of the bulk soil and the soil fractions
214 <20 μm were determined according to Mehra and Jackson (1960) by using the DCB method.
215 The proportion of Fe_{ox} was extracted using the oxalate method of Schwertmann (1964). The Fe

216 concentration was measured by inductively coupled plasma optical emission spectroscopy
217 (ICP-OES) (Vista-Pro, CCD simultaneous, Varian, Darmstadt, Germany).
218 Aliquots of both clay fractions (2.0–0.2 μm and $<0.2 \mu\text{m}$) were pre-treated with H_2O_2 (30%)
219 to remove OM (see section 2.5). The X-ray diffraction (XRD) patterns were recorded with a
220 Co radiation source using a Philips PW 1070 diffractometer. Random powder samples were
221 measured from 5°C–60°C in steps of 0.02°C with a counting time of 5 seconds for each step.
222 To evaluate expandable clay minerals, the samples were treated with glycol as well as with
223 KCl and stepwise heated to 100°C, 200°C and 550°C. Clay minerals were identified
224 according to Moore and Reynolds (1989) and the different mineral phases were determined by
225 semi-evaluation. Fe_d concentrations of the paddy and non-paddy soil fractions vary between
226 0.1% and 3.3% (Wissing et al., 2012), therefore iron oxides could not be detected by XRD
227 analyses.

228

229 *2.5. Organic matter oxidation*

230 A H_2O_2 treatment was applied to the $<20 \mu\text{m}$ soil fractions in order to oxidize OM. Aliquots
231 of the 20–6.3 μm (2 g), 6.3–2.0 μm (500 mg), 2.0–0.2 μm (300 mg) and $<0.2 \mu\text{m}$ (300 mg)
232 soil fractions were weighed into beakers to which 100 mL (bulk soil) and 20 mL (soil
233 fractions) of 30% H_2O_2 was added. To accelerate the oxidation reaction, soil samples were
234 heated to 60°C on a sand bath. Samples were placed in an oven at 60°C for 24 hours to
235 remove the remaining H_2O_2 . Silt-sized fractions were centrifuged for 20 minutes at 4470 g,
236 and the clay fraction for 1 hour at 4470 g. Afterwards, samples were freeze-dried and retained
237 for XRD and BET- N_2 analyses and OC measurement.

238

239 *2.6. Determination of the SSA*

240 The SSA of $<20 \mu\text{m}$ soil fractions was determined by the BET- N_2 method (Brunauer et al.,
241 1938). Gas adsorption of 11 points was measured in the relative pressure range of 0.05 to 0.3

242 with an Autosorb-1 analyzer (Quantachrome, Syosset, NY, USA). To avoid adsorbed water
243 and volatile substances, samples were outgassed for at least 24 hours in vacuum under helium
244 flow at 40°C before measurement. Also before measurement, all soil samples were weighed to
245 calculate the mass proportion of each sample. Analyses of SSA were carried out on untreated
246 soil samples ($SSA_{\text{untreated}}$), after H_2O_2 treatment ($SSA_{H_2O_2}$), after DCB extraction (SSA_{DCB})
247 and after H_2O_2 treatment followed by DCB extraction ($SSA_{H_2O_2+DCB}$). The mass loss after
248 H_2O_2 treatment due to OM extraction was 0%–3% in the 20–6.3 μm fraction; 5%–11% in the
249 2.0–0.2 μm fraction; 2%–22% in the 2.0–0.2 μm fraction and 0%–9% in the <0.2 μm fraction.
250 The percentage proportion of the SSA ($\text{m}^2 \text{g}^{-1}$) covered by OC was calculated:

$$251 \quad \% \text{ SSA covered by OC} = (SSA_{H_2O_2} - SSA_{\text{untreated}}) / SSA_{H_2O_2} \times 100 \quad (2)$$

252

253 *2.7. Radiocarbon content*

254 The radiocarbon (^{14}C) concentration was determined in single measurement at the Leibniz-
255 Laboratory at the Christian-Albrechts University in Kiel with a 3×10^6 V HVE Tandemtron
256 AMS (accelerator mass spectrometry) system (Bräuer et al., 2012), with a 1- σ precision of
257 about 0.25% modern carbon (pMC) (Nadeau et al., 1997).

258

259 *2.8. Statistical Analyses*

260 We tested the effect of soil management and soil age with SPSS Statistics 19 (IBM SPSS
261 Company). The effect of soil management was analyzed by the nonparametric Mann-Whitney
262 *U*-test. The mean values of all soils (mean of 50–700 years and mean of 50–2000 years of
263 pedogenesis) were compared, with $p \leq 0.05$ representing statistically significant differences
264 between paddy and non-paddy soils.

265 Analysis of variance (ANOVA) with the post hoc tests Tukey-B and Bonferroni was used to
266 test the effect of soil age on the bulk soil parameters pH values, IC, OC, Fe_d and Fe_{ox}
267 concentrations. All data were analyzed for homogeneity of variances by Levene test, and the

268 analysis of normality was performed with the Shapiro-Wilk test. Significant differences (p
269 ≤ 0.05) within the paddy and non-paddy chronosequence are indicated with italic letters.
270

271 **3. Results**

272 *3.1. Bulk soil parameters*

273 The uppermost A horizon of the mudflat and the marshland had slightly alkaline pH values of
274 8.2 and 7.8, respectively (Table 1). The bulk soil pH values (Table 1) of the uppermost topsoil
275 horizon were neutral to slightly acidic in paddy soils and decreased significantly ($p \leq 0.05$)
276 from 7.4 (P 50) to 5.1 (P 2000). The pH values of the non-paddy soils also decreased
277 significantly ($p \leq 0.05$) with increasing soil age, from 7.3 (NP 50, 100) to 5.9 (NP 700). The
278 pH values did not differ significantly between paddy and non-paddy soils, but the loss of
279 carbonates was markedly faster in paddy soils than in corresponding non-paddy soils (Table
280 1). The upper-most topsoil horizon of paddy soils was free of carbonates; only the youngest
281 soil (P 50) still contained carbonates (1.5 mg g^{-1}). The IC concentrations of non-paddy soils
282 decreased significantly ($p \leq 0.05$) with soil age from 1.6 mg g^{-1} to 0.1 mg g^{-1} (Table 1).
283 Mudflat and the marshland were characterized by the largest IC concentrations of 5.0 mg g^{-1}
284 and 4.2 mg g^{-1} , respectively (Table 1). The OC concentration was 5.1 mg g^{-1} in the mudflat
285 and increased to 10.9 mg g^{-1} in the marshland (Table 1). The OC concentration in paddy soils
286 (Table 1) was 17.8 mg g^{-1} (P 50) and increased significantly with age ($p \leq 0.05$) to 30 mg g^{-1}
287 (P 2000). The OC values particularly increased during the first 300 years of soil development.
288 Afterwards the paddy soil chronosequence was characterized by oscillating OC
289 concentrations, reaching their maximum at up to 2000 years (Wissing et al., 2011). Non-
290 paddy soils had lower OC concentrations ($10.5\text{--}11 \text{ mg g}^{-1}$) which remained constant with
291 increasing soil age (Table 1). The statistical analysis confirmed significantly higher ($p \leq 0.05$)
292 OC values in paddy soils than in non-paddy soils (Table 1). The Fe_d concentration (Table 1)
293 remained constant, around 7.0 mg g^{-1} , during 1000 years of paddy soil development. The Fe_d
294 concentration of non-paddy soils ranged from 7.0 mg g^{-1} to 5.0 mg g^{-1} but without a
295 significant trend. Nevertheless, P 2000 had the lowest Fe_d values. The Fe_d concentration
296 decreased significantly ($p \leq 0.05$) in paddy soils with time. The statistical analysis did not

297 show any significant differences of the Fe_d concentration between paddy and non-paddy soils
298 (Table 1). The Fe_{ox} concentration was highest in the mudflat (4.1 mg g^{-1}) but decreased
299 afterwards in the marshland to 2.4 mg g^{-1} (Table 1). In paddy soils, the Fe_{ox} concentration
300 ranged from 3.3 mg g^{-1} (P 700) to 2.2 mg g^{-1} (P 300) but did not show any significant trend
301 with soil age. Non-paddy soils were characterized by significantly ($p \leq 0.05$) lower Fe_{ox}
302 values, ranging from 1.5 to 0.7 mg g^{-1} but without any significant trend with time (Table 1).
303 The cation exchange capacity (CEC_{pot}) stayed constant over time in the uppermost A horizon
304 (see Kölbl et al., submitted). CEC_{pot} at pH 7 in the paddy soils ranged between 171 and 215
305 mmolc kg^{-1} soil and in non-paddy soils between 159 and 185 mmolc kg^{-1} soil (data from
306 Kölbl et al., submitted). Base saturation (BS) was only meaningful for carbonate-free horizons
307 (Kölbl et al., submitted). In the uppermost horizons of the paddy soils, the BS ranged between
308 69% and 82% for P 100 to P 1000 but only reached 58% in P 2000. The BS in non-paddy
309 soils tended to be higher (Table 1). The total clay content (Table 1) was 4% higher in paddy
310 soils than in non-paddy soils, but we found no significant differences between the mean
311 values of the clay content within 700 years of soil development. The total clay proportion was
312 significantly higher ($p \leq 0.05$; mean over 2000 years of soil development) in the paddy soil
313 chronosequence and ranged from 242 to 290 g kg^{-1} and in non-paddy soils from 190 to 272 g
314 kg^{-1} .

315

316 3.2. ^{14}C content of bulk soils and the $<0.2 \mu\text{m}$ soil fraction

317 The ^{14}C content of bulk soils (Table 2) ranged from 99 pMC (P 700) to 112 pMC (P 2000) in
318 paddy soils and from 98 pMC (NP 100) to 103 pMC (NP 700) in non-paddy soils. The P 700
319 site was characterized by a lower ^{14}C content, which was attributed (Müller-Niggemann et al.,
320 2012) to a markedly high proportion of *n*-alkenes due to contamination with fossil fuels. The
321 lowest ^{14}C content of 61 pMC was determined for the mudflat, followed by 90 pMC in the
322 marshland (Table 2). The $<0.2 \mu\text{m}$ fraction had lower ^{14}C values compared to those of the

323 bulk soil (Table 2). The ^{14}C content ranged from 85 pMC (NP 100) to 98 pMC (NP 50) in
324 non-paddy soils and the conventional age was older in non-paddy than in corresponding
325 paddy soils (Table 2). Paddy soils had ^{14}C values between 92 pMC (P 50) and 108 pMC (P
326 2000) and the carbon was more modern than in non-paddy soils. The highest proportion of
327 “old” inherited carbon was found in the mudflat and the marshland soils (Table 2).

328

329 *3.3. Soil mineralogy of the soil fractions*

330 Fe concentration of the uppermost A horizons stayed constant for the first 1000 years of
331 pedogenesis. The paddy soil chronosequence was characterized by higher proportions of Fe_{ox}
332 than the non-paddy soils, which in turn had higher $\text{Fe}_{\text{d}}\text{-Fe}_{\text{ox}}$ values (Wissing et al., 2012). The
333 Fe_{d} concentrations (see Wissing et al., 2012) ranged between 11.8 mg g^{-1} (P 2000) and 22.3
334 mg g^{-1} (P 1000) in paddy coarse clay fraction and between 13.0 mg g^{-1} (P 2000) and 27.2
335 mg g^{-1} (P 700) in fine clay. Non-paddy soils had Fe_{d} concentrations of 25.6 mg g^{-1} (NP 50)
336 and 20.5 mg g^{-1} (NP 700) in coarse clay and 32.7 mg g^{-1} (NP 300) and 22.8 mg g^{-1} (NP 100)
337 in fine clay (data from Wissing et al., 2012). Paddy coarse clay fraction had Fe_{ox}
338 concentrations between 8.9 mg g^{-1} (P 300) and 12.7 mg g^{-1} (P 700) and between 11.1 mg g^{-1}
339 (P 2000) and 16.8 mg g^{-1} (P 700) in fine clay. The Fe_{ox} concentrations ranged from 2.0 mg g^{-1}
340 (NP 300) and 7.7 mg g^{-1} (NP 50) in non-paddy soils coarse clay and from 6.0 mg g^{-1} (NP
341 300) and 12.2 mg g^{-1} (NP 50) in fine clay (data from Wissing et al., 2012). Results from XRD
342 analyses (Table 3) showed that kaolinite, illite, chlorite and secondary chlorite are clay
343 minerals in both soil sequences. Illite was the major clay mineral and varied between 40%–
344 67% (P) and 55%–63% (NP) in the $2.0\text{--}0.2 \mu\text{m}$ fraction. The $<0.2 \mu\text{m}$ fraction was
345 characterized by less illite, 32%–48% (P) and 46%–54% (NP) (Table 3).

346

347 *3.4. Properties of the SSA of different $<20 \mu\text{m}$ soil fractions*

348 The $SSA_{\text{untreated}}$ of the soil fractions (Fig. 1a, 1b in gray) increased with decreasing particle
349 size in both chronosequences. Chronologically decreasing $SSA_{\text{untreated}}$ values were observed
350 only in the 6.3–2.0 μm fraction, ranging from 13 $\text{m}^2 \text{g}^{-1}$ (P 50) to 7 $\text{m}^2 \text{g}^{-1}$ (P 2000) in paddy
351 soils and from 16 $\text{m}^2 \text{g}^{-1}$ (NP 50) to 11 $\text{m}^2 \text{g}^{-1}$ (NP 700) in non-paddy soils. All other fractions
352 also showed decreasing $SSA_{\text{untreated}}$ values but without any chronological trend. The
353 $SSA_{\text{untreated}}$ values ranged from 44 $\text{m}^2 \text{g}^{-1}$ (P 50) to 25 $\text{m}^2 \text{g}^{-1}$ (P 2000) in the 2.0–0.2 μm
354 fraction and from 45 $\text{m}^2 \text{g}^{-1}$ (NP 50) to 39 $\text{m}^2 \text{g}^{-1}$ (NP 700) in non-paddy soils. The values
355 decreased also in the $>0.2 \mu\text{m}$ fraction (P: 80–25 $\text{m}^2 \text{g}^{-1}$ and NP: 79–72 $\text{m}^2 \text{g}^{-1}$) (Fig. 1a, 1b).
356 Compared to $SSA_{\text{untreated}}$, the OM removal led to an increase of the $SSA_{\text{H}_2\text{O}_2}$ in paddy soils
357 (11%–75%) and in non-paddy soils (18%–41 %) (Fig. 1a, 1b in black). In particular, the
358 paddy soil clay fractions showed markedly larger $SSA_{\text{H}_2\text{O}_2}$ values (Fig. 1a), which increased
359 during soil development (in the 2.0–0.2 μm fraction from 28% to 50% and from 31% to 75%
360 in the $>0.2 \mu\text{m}$ fraction). When compared to the $SSA_{\text{untreated}}$ values, the silt and coarse clay
361 fractions from non-paddy soils were characterized by almost no increase of the mineral
362 surface after OM removal. The removal of pedogenic iron by DCB treatment (SSA_{DCB})
363 resulted in the smallest SSA in paddy and non-paddy soils (Table 4). Clay-sized fractions of
364 paddy soils showed decreasing SSA_{DCB} values with soil age. The SSA_{DCB} of the 2.0–0.2 μm
365 fraction declined from 28 $\text{m}^2 \text{g}^{-1}$ (P 50) to 23 $\text{m}^2 \text{g}^{-1}$ (P 2000) and that of the $>0.2 \mu\text{m}$ fraction
366 declined from 69 $\text{m}^2 \text{g}^{-1}$ (P 50) to 39 $\text{m}^2 \text{g}^{-1}$ (P 2000). With increasing non-paddy soil age, the
367 $>0.2 \mu\text{m}$ fraction $>0.2 \mu\text{m}$ also showed decreasing SSA_{DCB} values from 85 $\text{m}^2 \text{g}^{-1}$ (NP 50) to
368 69 $\text{m}^2 \text{g}^{-1}$ (NP 700), whereas no consistent trend was detected for the silt and coarse clay
369 fractions (Table 4). The combined treatment of OM oxidation and removal of Fe_d led to the
370 largest SSA values overall (Table 4), and the values were the highest in the fine clay fractions
371 of both soils, ranging from 77 $\text{m}^2 \text{g}^{-1}$ (P 300) up to 319 $\text{m}^2 \text{g}^{-1}$ (P 1000) in paddy soils and
372 from 68 $\text{m}^2 \text{g}^{-1}$ (NP 100) to 118 $\text{m}^2 \text{g}^{-1}$ (NP 300) in non-paddy soils without a chronological
373 trend. The H_2O_2 treatment released up to 98% of SOC in the clay-sized fractions (Table 5).

374 The amount of H₂O₂-resistant OC ranged from 8% (P 100) to 2% (P 100, P 2000) in paddy
375 clay fraction and from 15% (NP 100) to 3% (NP 300) in non-paddy soils. The amount of
376 H₂O₂-resistant OC was highest in the 20–6.3 μm fraction, ranging from 6% up to 36% in
377 paddy soils and from 31% to 54% in non-paddy soils (Table 5).

378 The relation between the Fe_d content and the SSA before and after Fe_d removal is shown in
379 Fig. 2a and 2b. The proportion of Fe_d was highest in both clay fractions. Therefore, increasing
380 SSA values were related to the decrease of the particle size fraction (Fig. 2a), but we could not
381 confirm the formation of additional mineral surfaces from iron oxides during soil
382 development (Fig. 2b). The relation between the OC content and the SSA before and after
383 OM removal is summarized in Fig. 3a and 3b. The OC content of fine silt and both clay
384 fractions strongly increased with decreasing particle size as well as with increasing soil age
385 (except for P 1000). This was strongly related to the decline of the SSA (R² increased with
386 decreasing particle size from 0.28 to 0.96; see Fig. 3a). After removal of OC with H₂O₂, the
387 correlation between SSA and the original OC content of the respective soil fraction was much
388 smaller (Fig. 3b) compared to the untreated SSA (Fig. 3a). However, both paddy and non-
389 paddy soil fractions can be fitted by the same regression line because the relation between the
390 SSA and the OC content is irrespective of the soil management (Fig. 3a, 3b).

391

392 **4. Discussion**

393 *4.1. Paddy management accelerates soil decalcification and OC accumulation*

394 In the Cixi coastal region of Zhejiang Province, where land reclamation has been in effect for
395 at least 2000 years, the substrate for all paddy and non-inundated non-paddy soils is
396 predominantly marine tidal flat sediment (Kölbl et al., submitted). These calcareous marine
397 sediments are derived from the Yangtze River (Changjiang), which is the major route of
398 terrestrial material to the East China Sea (Kölbl et al., submitted). The coastal sediments were
399 diked and drained and gradually became oxic. Portnoy (1999) described an acceleration of the
400 initial soil forming processes due to soil diking and drainage, especially sulfide oxidation
401 causes changes in redox condition, lowers soil pH and alters mobility of iron (Zottoli, 1973;
402 Lord, 1980), and it may also accelerate initial soil-forming processes (Portnoy, 1999). In
403 addition, management of those marshland soils may further influence their soil properties. In
404 the present study, paddy soils were characterized by an accelerated decalcification (Table 1)
405 induced by specific soil management. Carbonate was leached by periodical flooding and
406 drainage of the paddy soils during rice cultivation (Wissing et al., 2011). However, how much
407 the intense and accelerated decalcification of periodically flooded paddy soils affects
408 pedogenesis, including OC accumulation and mineral formation, is still unclear. In particular,
409 the formation of mineral surface areas and their accessibility may provide additional
410 information on OM accumulation processes.

411

412 *4.2. Providers of mineral surfaces*

413 *4.2.1. OM associations with different mineral surfaces*

414 The higher OM content in paddy soils results in smaller untreated SSAs than in corresponding
415 non-paddy soils (Fig. 1). The removal of OM with H₂O₂ leads to large OC losses (P: 92%–
416 98% and NP: 85%–97%) for the clay-sized fractions (Table 5) and to a distinct increase of the
417 BET-N₂ surface area. Such results have been reported by numerous authors (Burford et al.,

418 1964; Theng et al., 1999; Kahle et al., 2002a; Kiem and Kögel-Knabner, 2002; Wagai et al.,
419 2009; Dümig et al., 2012). The higher SSA values due to the H₂O₂ treatment were particularly
420 large for the fine mineral fractions (see also Burford et al., 1964), especially for clay-sized
421 fractions of paddy soils (Fig. 1). To illustrate our understanding of SSAs, their coverage with
422 OM and the effect of different treatments, we designed a schematic overview, showing the
423 effect of OM oxidation by H₂O₂, removal of iron by DCB treatment (Fig. 4) and H₂O₂
424 treatment combined with the subsequent removal of iron (Fig. 5). Mineral surfaces that were
425 covered by OM (Fig. 4b, 4d), did not contribute significantly to the N₂ area, but the surface
426 areas were accessible to N₂ after OM removal (Chiou, 1990; Theng et al., 1999). Some
427 nitrogen may have been adsorbed by coarse OM, but the loss of surface due to OM removal
428 was in all instances less than the increase due to areas rendered accessible (Burford et al.,
429 1964). However, the H₂O₂ treatment most likely had no effect on pure iron oxides and pure
430 clay minerals without OM (Fig. 4a, 4c) and also no effect on OM, which was protected by soil
431 minerals (Fig. 4f). Clay-sized fractions of paddy and non-paddy soils had low Fe_d
432 concentrations of 1%–3% (Wissing et al., 2012), and the removal of Fe_d (SSA_{DCB}) by DCB
433 treatment led to lower SSA values (Table 4) than those of untreated clay fractions (Fig. 1).
434 Losses of surface area were induced if iron oxides occurred without being protected by OM
435 (Fig. 4a versus 4b) or if the surface area of clay minerals covered by iron oxides was smaller
436 than the entire outer surface area of the iron oxides (Fig. 4e). The subsequent removal of Fe_d
437 after H₂O₂ treatment (SSA_{H₂O₂+DCB}: silicate surface area without OM and iron oxide minerals)
438 caused an increase in SSA and presented the largest mineral surface for almost all silt-sized
439 fractions of both soil groups and for paddy fine clay and non-paddy coarse clay (Fig. 4; Table
440 4 especially the <0.2 μm fraction of P 1000 and P 2000). Hodson et al. (1998) explained that
441 removal of oxyhydroxides may break up the aggregation with the clay-sized particles and
442 cause a marked increase in SSA. In the SOM-rich paddy soils of the present study, the
443 described break-up of soil aggregates was only achieved after the removal of protective SOM

444 (Fig. 5). Therefore, the combined treatment (H_2O_2 + DCB) showed a higher effect on SSA
445 than each treatment alone.

446

447 *4.2.2. Evolution of mineral surface area during soil decalcification*

448 Sorption of organic molecules to the surface area of the mineral phase is mainly due to
449 expandable phyllosilicates (Theng et al., 1999; Kennedy et al., 2002) and poorly crystalline
450 iron oxides (Borggaard, 1982; Kennedy et al., 2002). In general, increasing soil evolution is
451 characterized by advanced mineral weathering. Silicate weathering reduces sizes of primary
452 particles combined with the formation of clay-sized secondary minerals (Hodson et al., 1998).
453 Such trends are commonly observed in chronosequences (Muhs, 1982; Merritts et al., 1991)
454 and cause increases of the mineral surface area with time. In the investigated
455 chronosequences, the SSA after OM removal did not increase with soil age (Fig. 1a, 1b) and
456 therefore gave no indication for mineral weathering. Smaller particle sizes went along with
457 larger Fe_d contents (Fig. 2a), but we observed no increase of the Fe_d proportion with
458 development of both soil groups (Fig. 2b). The mineral surface after H_2O_2 and DCB treatment
459 (Table 4) likewise showed no consistent trend with time and gave no indication for further
460 clay mineral formation. Therefore, we could not confirm that the formation of soil silicate
461 minerals and oxides is more pronounced in decalcified soils. Our results provide no evidence
462 that the decalcification of (paddy) soils resulted in the formation of additional mineral
463 surfaces during the time span of our chronosequences. Both chronosequences do not indicate
464 a further formation of clay minerals after deposition of the estuarine sediment from the Yantze
465 River. This is supported by unchanged soil mineralogy (Wissing et al., 2012), and the slightly
466 acidic pH values may not have been sufficient for mineral weathering. This is in line with
467 Dümig et al. (2012) who investigated a relatively young chronosequence (15–120 years) that
468 developed after glacier retreat, and they could likewise not confirm a chronological trend of
469 SSA values over time. The authors explained the OC accumulation may be faster than the

470 supply of mineral surfaces by weathering during initial soil development, which appears to be
471 opposite at later stages of pedogenesis. White et al. (1996) and Hodson et al. (1998) found
472 increasing SSA values with ongoing soil development in much older soil chronosequences
473 (0.2–3000 ky; 80–13,000 years), indicating decreasing particle sizes due to progressive
474 weathering (Hodson et al., 1998).

475

476 *4.2.3. Contribution of silicate (clay) and iron oxide surfaces for OC accumulation*

477 The OC contents of the <2.0 μm fractions increased with soil age, resulting in decreasing
478 surface areas of the mineral phase. The OC accumulation was strongest in the <0.2 μm
479 fraction (having the highest mineral surface area). In the <0.2 μm fraction of paddy soils, the
480 proportion of SSA that was covered by OC rose from 31% in P 50 to 75% in P 2000 (Table
481 5). In contrast, the increase in non-paddy soils was much less, from about 30% (NP 50) to
482 41% in NP 700 Table 5). This was reflected by a strong linear relationship of the $\text{SSA}_{\text{untreated}}$
483 values and the OC contents of paddy (and to a lesser extent: non-paddy clay-sized fractions;
484 Fig. 5a). The correlation increased with decreasing particle size and was highest in the <0.2
485 μm fraction. The results supported higher coverings of the mineral surfaces by OM in
486 decalcified paddy soils. Lower OC coverings in non-paddy soils may have been caused by a
487 reduced accessibility of the mineral surfaces. Compared to the respective soil age of the paddy
488 soils, non-paddy soils showed higher pH and higher BS values, suggesting a relatively high
489 concentration of (bivalent) cations, which promoted aggregation of the clay minerals.
490 Therefore, we attribute the lower OM coverings and the smaller OM accumulation in non-
491 paddy soils to a reduced accessibility of SSA due to strong microaggregation by Ca^{2+} ion
492 bridging. Especially in the calcareous non-paddy soils (NP 50, NP 100, NP 300), cementation
493 by calcium carbonate might have additionally contributed to the aggregation of clay minerals
494 (Fig. 5). To summarize, the assumed increase in OC covering during soil development could
495 not be confirmed for non-decalcified soils.

496 Fe oxides determined by oxalate extraction, e.g. ferrihydrite, are known to stabilize OC
497 because of their large and highly reactive external surface area, with values between 200 and
498 $1200 \text{ m}^2 \text{ g}^{-1}$ (Bracewell et al., 1970; Borggaard, 1982; Parfitt, 1989). Recent studies with
499 Mössbauer spectroscopy revealed, that chemical extraction methods are not mineral selective. For
500 example, acid-ammonium oxalate dissolves not only ferrihydrite but also for the most part, if not
501 completely, goethite with very small particle size, i.e., nano-goethite (see Cornell and Schwertmann
502 2003; Thompson et al. 2006b; 2011). Van der Zee et al. (2003) found a nano-goethite with a particle
503 size of only 5 nm and mentioned that these sizes are comparable to the values 1–3 nm for natural and
504 synthetic two line ferrihydrites. Mansfeldt et al. (2011) had repeatedly pointed out that the extraction
505 with oxalate is not specifically selective for ferrihydrite. Iron associated with OM will also be
506 extracted by oxalate. This might be of major importance in the uppermost OM-rich soil horizons in
507 paddy soils of the present study. Overall, oxalate extractable Fe in paddy soils may consist of
508 ferrihydrite as well as nano-goethite. Wissing et al. (2012) showed that the higher contents of
509 Fe_{ox} in paddy soils seem to be associated with higher proportions of mineral-associated SOM
510 than in non-paddy soils. The authors mentioned that the ability to stabilize OM is therefore
511 more pronounced in paddy soils than in non-paddy soils. However, for the paddy
512 chronosequence, the Fe_{ox} concentrations in the uppermost soil horizons showed no trend with
513 age from the mudflat to P 2000. Comparing the mudflat with the non-paddy soils, we found a
514 marked decrease in Fe_{ox} concentrations within the first 50 years and then again no trend till
515 700 years. The Fe_{d} concentration showed no trends at all. We assumed that the oxic
516 conditions and the smaller OC concentrations in the non-paddy soils allowed a certain
517 crystallization of iron oxides in the first 50 years of soil development. This was not the case in
518 the paddy soils with periodically reducing conditions and higher OC accumulations.
519 Obviously, there was no correlation between the constant values of Fe_{ox} and the increasing
520 OC concentrations in the $<2.0\text{--}0.2 \mu\text{m}$ fraction (data not shown).

521 Therefore, we assumed silicate minerals play the dominant role in OC stabilization during
522 early paddy soil formation on calcareous parent material. This is further supported by the fact
523 that the treatment with H₂O₂ and the subsequent removal of Fe_d revealed the largest surface
524 area, especially for the <0.2 μm fractions in P 1000 and P 2000. As pointed out earlier, we
525 attributed this to the continuous disaggregation of clay minerals due to the loss of carbonate
526 cementation and Ca²⁺ ions bridging.

527 The paddy-specific soil-forming processes (Fig. 6) were markedly different from those of
528 non-paddy soils:

529 (1) A marked proportion of modern carbon (confirmed by higher OC accumulation) was
530 added to the inherited carbon during 100 years of paddy soil development, whereas
531 non-paddy soils generally preserved their carbon signature (Table 2), indicating a
532 slower accumulation of modern OC.

533 (2) The decalcification of the topsoil horizons was already finished within 100 years of
534 paddy soil development, whereas the decalcification of non-paddy soils required
535 almost 700 years (Fig. 6). We suggest that potentially strong aggregation by carbonate
536 Ca²⁺ ion bridges most likely reduces the OM accumulation in non-paddy soils.

537 (3) The periodical changes in redox conditions and the higher amounts of OM in paddy
538 soils (Fig. 6) allowed the persistence of Fe_{ox} (Wissing et al., 2012).

539 Crystallization of iron oxides may be retarded and inhibited in soils with water-soluble
540 constituents such as organic compounds, which have a high affinity towards iron oxide
541 surfaces (Schwertmann, 1966, 1982; Eusterhues et al., 2008). In contrast, non-paddy soils
542 provide less mineral surface in the form of Fe_{ox} due to missing redox cycles and as a
543 consequence of low OC concentrations.

544

545 **5. Conclusions**

546 We investigated the soil development on calcareous marine sediments using two
547 chronosequences with similar parent material; one used for paddy rice cultivation, the other
548 for upland crops. Within 2000 years of pedogenesis, no change in clay mineral composition
549 and mineral surface area was observed. But the soils differed in the degree of decalcification
550 and OC accumulation and in the formation of iron. Paddy soil management led to an enhanced
551 decalcification and larger OC accumulation. Management-induced redox cycles led to a larger
552 proportion of Fe_{ox}. Their large SSA added to the surface area of clay minerals and provided
553 additional options for OC covering. As carbonates and Ca²⁺ ions seemed to interconnect clay
554 minerals, making their surface accessible to OC, the faster dissolution of carbonate and
555 leaching of Ca²⁺ ions in paddy soils made additional clay mineral surfaces available to OC.
556 The smaller accumulation of mineral-associated SOM in non-paddy soils was additionally
557 confirmed by the retarded replacement of the inherited carbon. The enhanced accessibility of
558 mineral surfaces for OC covering was obviously due to the accelerated decalcification of the
559 paddy soils.

560

561 **Acknowledgments**

562 The authors thank Rui Yin and the Institute of Soil Science, Chinese Academy of Sciences, in
563 Nanjing for support during sampling at the chronosequence site around Cixi and for logistic
564 handling. We thank especially Reinhold Jahn and Vanessa Vogelsang for providing us with
565 inorganic carbon data and Pieter Grootes and Tino Bräuer for determination of the
566 radiocarbon content. Markus Steffens is acknowledged for assisting with statistical analysis
567 and Werner Häusler for the support concerning the soil mineralogy measurements. We thank
568 Monika Heilmeyer for technical assistance and Martina Bauer, Carolin Botond, Robert U.
569 Hagemann, Tahereh Javaheri, Juliane Teichmann and Maria Vonach for student research

570 assistance. We are grateful to the Deutsche Forschungsgemeinschaft (DFG) for their generous
571 funding of Research Unit FOR 995 “Biogeochemistry of paddy soil evolution.”

572

573

574 **References**

- 575 Balabane, M., Plante, A.F., 2004. Aggregation and carbon storage in silty soil using physical
576 fractionation techniques. *Eur. J. Soil Sci.* 55, 415–427.
- 577 Balesdent, J., Mariotti, A., Guillet, B., 1987. Natural ^{13}C abundance as a tracer for studies of
578 soil organic matter dynamics. *Soil Biol. Biochem.* 19, 25–30.
- 579 Borggaard, O.K., 1982. The influence of iron oxides on the surface area of soil. *J. Soil Sci.* 33,
580 443–449.
- 581 Bosatta, E., Agren, G.I., 1997. Theoretical analyses of soil texture effects on organic matter
582 dynamics. *Soil Biol. Biochem.* 29, 1633–1638.
- 583 Bracewell, J.M., Campbell, A.S., Mitchell B.D., 1970. An assessment of some thermal and
584 chemical techniques used in the study of the poorly-ordered aluminosilicates in soil
585 clays. *Clay Mineral.* 8, 325–335.
- 586 Bräuer, T., Grootes, P.M., Nadeau, M.-J., Andersen, N., 2012. Downward carbon transport in
587 a 2000-year rice paddy soil chronosequence traced by radiocarbon measurements.
588 *Nucl. Instr. Meth. B*, <http://dx.doi.org/10.1016/j.nimb.2012.07.012>.
- 589 Brümmer, G., Grünwaldt, H.S., Schroeder, D., 1971. Beiträge zur Genese und Klassifizierung
590 der Marschen. II. Zur Schwefelmetabolik in Schlickten und Salzmarschen. *Zs.*
591 *Pflanzenernähr. Bodenkd.* 128, 208–220.
- 592 Brunauer, S., Emmett, P.H., Teller, E., (1938). Adsorption of gases in multimolecular layers.
593 *J. Am. Chem. Soc.* 60 (2), 309–319.
- 594 Burford, J.R., Deshpande, T.L., Greenland, D.J., Quirk, J.P., 1964. Influence of organic
595 materials on the determination of the specific surface area of soils. *J. Soil Sci* 15 (2),
596 192–201.
- 597 Carter, D.L., Mortland, M.M., Kemper, W.D., 1986. In *Methods of soil analysis, Part 1.*
598 *Physical and mineralogical methods.* American Society of Agronomy— Soil Sci. Soc.
599 Am., Madison, USA. Agronomy Monograph no. 9, second ed.

600 Cheng, Y., Yang, L.-Z., Cao, Z.-H., Ci, E., Yin, S., 2009. Chronosequential changes of
601 selected pedogenic properties in paddy soils as compared with non-paddy soils.
602 *Geoderma* 151, 31–41.

603 Chenu, C., Plante, A.F., 2006. Clay-sized organo-mineral complexes in a cultivation
604 chronosequence: revisiting the concept of the 'primary organo-mineral complex'. *Eur.*
605 *J. Soil Sci.* 57 (4), 596–607.

606 Chiou, C.T., 1990. The surface area of soil organic matter. *Environ. Sci. Technol.* 24, 1164–
607 1166.

608 Cornell, R.M., Schwertmann, U., 2003. The iron oxides. Structure, properties, reactions,
609 occurrences and uses, 2nd edn. Wiley-VHC, Weinheim

610 Dümig, A., Häusler, W., Steffens, M., Kögel-Knabner, I., 2012. Clay fractions from a soil
611 chronosequence after glacier retreat reveal the initial evolution of organo-mineral
612 associations. *Geochim. Cosmochim. Acta* 85, 1–18.

613 Eusterhues, K., Rumpel, C., Kögel-Knabner, I., 2005. Organo-mineral associations in sandy
614 acid forest soils: importance of specific surface area, iron oxides and micropores. *Eur.*
615 *J. Soil Sci.* 56, 753–763.

616 Eusterhues, K., Wagner, F.E., Häusler, W., Hanzlik, M., Knicker, H., Totsche, K. U., Kögel-
617 Knabner, I., Schwertmann, U., 2008. Characterization of ferrihydrite-soils organic
618 matter coprecipitates by X-ray diffraction and Mössbauer spectroscopy. *Environ. Sci.*
619 *Technol.* 42, 7891–7897.

620 FAO, 2006. Guidelines for soil description. FAO, Rome, 97 pp.

621 Giani, L., Landt, A., 2000. Initiale Marschbodenentwicklung aus brackigen Sedimenten des
622 Dollarts an der südwestlichen Nordseeküste. [Initial marsh soil development from
623 brackish sediments of the Dollart on the southwestern North Sea coast]. *J. Plant Nutr.*
624 *Soil Sci.* 163, 549–553.

625 Gong, Z.T., Xu, Q., 1990. Paddy soils. *Soils of China*. Science Press, Beijing, pp. 233–260.

626 Hodson, M.E., Langan, S.J., Kennedy, F.M., Bain, D.C., 1998. Variation in soil surface area
627 in a chronosequence of soils from Glen Feshie, Scotland and its implications for
628 mineral weathering rate calculations. *Geoderma* 85, 1–18.

629 International Union of Soil Sciences Working Group, 2007. World reference base for soil
630 resources 2007. World Soil Resources Reports, vol. 103. FAO, Rome.

631 Jenkinson, D.S., Hart, P.B.S., Rayner, J.H., Parry, L.C., 1987. Modelling the turnover of
632 organic matter in long-term experiments at Rothamsted. *INTECOL Bulletin* 15, 1–8
633 (cited from Eusterhues et al., 2005).

634 Jenkinson, D.S., Rayner, J.H., 1977. The turnover of soil organic matter in some of the
635 Rothamsted classical experiments. *Soil Sci.* 123, 298–305 (cited from Balabane and
636 Plante, 2004).

637 Kahle, M., Kleber, M., Jahn, R., 2002a. Predicting carbon content in illitic clay fractions from
638 surface area, cation exchange capacity and dithionite-extractable iron. *Eur. J. Soil Sci.*
639 53, 639–644.

640 Kaiser, K., Guggenberger, G., 2000. The role of DOM sorption to mineral surfaces in the
641 preservation of organic matter in soils 31, 711–725.

642 Kaiser, K., Guggenberger, G., 2003. Mineral surfaces and soil organic matter. *Eur. J. Soil Sci.*
643 54 (2), 219–236.

644 Kennedy, M.J., Pevear, D.R., Hill, R.J., 2002. Mineral surface control of organic carbon in
645 black shale. *Science* 295, 657–660.

646 Kiem, R., Kögel-Knabner, I., 2002. Refractory organic carbon in particle-size fractions of
647 arable soils II: organic carbon in relation to mineral surface area and iron oxides in
648 fractions < 6 µm. *Org. Geochem.* 33, 1699–1713.

649 Kishchuk, B.E., 2000. Calcareous soils, their properties and potential limitations to conifer
650 growth in Southeastern British Columbia and western Alberta: A literature review.
651 *Nat. Resour. Can., Can. For. Serv., North. For. Cent., Edmonton Alberta and*

652 Invermere Forest District Enhanced Forest Management Pilot Project, BC Min.. For.,
653 Invermere, British Columbia. Inf. Rep. NOR-X-370.

654 Kölbl, A., Schad, P., Jahn, R., Amelung, W., Bannert, A., Cao, Z.H., Fiedler, S., Kalbitz, K.,
655 Lehndorff, E., Müller-Niggemann, C., Schloter, M., Schwark, L., Vogelsang, V.,
656 Wissing, L., Kögel-Knabner, I., (submitted). Accelerated soil formation due to paddy
657 management on marshlands (Zhejiang Province, China).

658 Lal, R., 2002. Soil carbon sequestration in China through agricultural intensification, and
659 restoration of degraded and desertified ecosystems. *Land Degrad. Dev.* 13, 469–478.

660 le Tacon, F., 1978. La presence de calcaire dans le sol. Influence sur le comportement de
661 l'Épicea commun (*Picea excels* Link.) et du Pin noir d'Autriche (*Pinus nigra*
662 *nigricans* Host.). [The presence of calcium carbonate in soil. Influence on the
663 behaviour of Norway spruce (*Picea excels* Link.) and Austrian pine (*Pinus nigra*
664 *nigricans* Host.)]. *Ann. Sci. For.* 35, 165–174 (cited from Kishchuk, 2000).

665 Lelong, F., Souchier, B. 1982. Identification and quantitative evaluation of the mineral
666 constituents. Pages 3–20 in M. Bonneau and B. Souchier, eds. *Constituents and*
667 *properties of soils.* Academic Press, Toronto, Ontario (cited from Kishchuk, 2000).

668 Li, Z.-P., Zhang, T.-L., Li, D.-C., Velde, B., Han, F.-X., 2005. Changes in soil properties of
669 paddy fields across a cultivation chronosequence in subtropical China. *Pedosphere* 15
670 (1), 110–119.

671 Lord, C.J., III, 1980. The chemistry and cycling of iron, manganese, and sulfur in salt marsh
672 sediments. PhD dissertation, Univ. Delaware, Newark, USA (cited from Portnoy and
673 Giblin, 1997).

674 Mansfeldt, T., Schuth, S., Häusler, W., Wagner, F.E., Kaufhold, S., Overesch, M., 2011. Iron
675 oxide mineralogy and stable iron isotope composition in a Gleysol with petroglycic
676 properties. *J Soils Sediments* 12 (1), 97–114.

677 Mayer, L., 1994. Relationship between mineral surfaces and organic carbon concentrations in
678 soils and sediments. *Chem. Geol.* 114, 347–363.

679 Mehra, O.P., Jackson, M.L., 1960. Iron oxide removal from soils and clays by a dithionite-
680 citrate system buffered with sodium bicarbonate. *Clays and Clay Minerals, Proceedings*
681 *of the 7th National Conference: 317–327.*

682 Merritts, D.J., Chadwick, O.A., Hendricks, D.M., 1991. Rates and processes of soil evolution
683 on uplifted marine terraces, northern California. *Geoderma* 51, 241–275.

684 Moore, D.M., Reynolds, R.C., 1989. X-ray diffraction and the identification and analysis of
685 clay minerals. Oxford University Press, London.

686 Muhs, D.R., 1982. A soil chronosequence on Quaternary marine terraces San Clemente
687 Island, California. *Geoderma* 28, 257–283.

688 Müller-Althen, W., 1994b. On the genesis of tidal marsh soils. II. Kalksedimentation,
689 Entkalkung. *J. Plant Nutr. Soil Sci.* 157, 333–343.

690 Müller-Niggemann, C., Bannert, A., Schloter, M., Lehndorff, E., Schwark, L., 2012. Intra-
691 versus inter-site macroscale variation in biogeochemical properties along a paddy soil
692 chronosequence. *Biogeosciences* 9 (3), 1237–1251.

693 Nadeau, M.-J., Schleicher, M., Grootes, P.M., Erlenkeuser, H., Gottdang, A., Mom, D.J.W.,
694 Samthein, J.M., Willkomm, H., 1997. *Nucl. Instrum. Meth. Phys. Res. B* 123 (1997)
695 22.

696 Neue, H.U., Gaunt, J.L., Wang, Z.P., Becker-Heidmann, P., Quijano, C., 1997. Carbon in
697 tropical wetlands. *Geoderma* 79, 163–185.

698 Oades, J.M., 1988. The retention of organic matter in soils. *Biogeochemistry* 5, 35–70.

699 Oyonarte, C., Pérez-Pujalte, A., Delgado, G., Delgado, R., Almendros, G., 1994. Factors
700 affecting soil organic matter turnover in a Mediterranean ecosystem from Sierra de
701 Gador (Spain): an analytical approach. *Commun. Soil Sci. Plant Anal.* 25, 1929–1945
702 (cited from Kishchuk, 2000).

703 Pan, G., Li, L., Wu, L., Zhang, X., 2003a. Storage and sequestration potential of topsoil
704 organic carbon in China's paddy soils. *Glob. Chang. Biol.* 10, 79–92

705 Pan, G.X., Li, L.Q., Zhang, X.H., Dai, J.Y., Zhou, Y.C., Zhang, P.J., 2003b. Soil organic
706 carbon storage of China and the sequestration dynamics in agricultural lands. *Adv.*
707 *Earth Sci.* 18, 609–618 (in Chinese).

708 Parfitt, R.L., 1989. Phosphate reactions with natural allophane, ferrihydrite and goethite. *J.*
709 *Soil Sci.* 40, 359–369.

710 Portnoy, J.W., 1999. Salt marsh diking and restoration: biochemical implications of altered
711 wetland hydrology. *Environ. Manag.* 24, 111–120.

712 Portnoy, J.W., Giblin, A.E., 1997. Effects of historic tidal restrictions on salt marsh sediment
713 chemistry. *Biogeochemistry* 36, 275–303.

714 Robert, M., Chenu, C., 1992. Interactions between soil minerals and microorganisms, in:
715 Stotzky, G., Bollag, J.M. (Eds.), *Soil Biochemistry*, Vol. 7. Marcel Dekker, New York,
716 pp. 307–404.

717 Sahrawat, K.L., 2004. Organic matter accumulation in submerged soils. *Adv. Agron.* 81, 169–
718 201.

719 Schaetzl, R.J., 1991. Factors affecting the formation of dark, thick epipedons beneath forest
720 vegetation, Michigan, USA, *J. Soil Sci.* 42, 501–512 (cited from Kishchuk, 2000).

721 Schwertmann, U., 1964. Differenzierung der Eisenoxide des Bodens durch Extraktion mit
722 Ammoniumoxalat-Lösung. *Zeitschrift für Pflanzenernährung, Düngung, Bodenkunde*
723 105 (3), 194–202.

724 Schwertmann, U., 1966. Inhibitory effect of soil organic matter on crystallization of
725 amorphous ferric hydroxide. *Nature* 212, 645–646.

726 Schwertmann, U., Schulze, D.G., Murad, E., 1982. Identification of ferrihydrite in soils by
727 dissolution kinetics, differential X-ray diffraction, and Mössbauer spectroscopy. *Soil*
728 *Sci. Soc. Am. J.* 46, 869–875.

729 Talibudeen, O., Arambarri, P., 1964. The influence of the amount and the origin of calcium
730 carbonates on the isotopically exchangeable phosphate in calcareous soils. *J. Agric.*
731 *Sci. Camb.* 62, 93–97.

732 Tanji, K.K., Gao, S., Scardaci, S.C., Chow, A.T., 2003. Characterization redox status of
733 paddy soils with incorporated rice straw. *Geoderma* 114, 333–353.

734 Theng, B.K.G., Ristori, G.G., Santi, C.A., Percival, H.J., 1999. An improved method for
735 determining the specific surface areas of topsoils with varied organic matter content,
736 texture and clay mineral composition. *Eur. J. Soil Sci.* 50, 309–316.

737 Thompson, A., Rancourt, D.G., Chadwick, O.A., Chorover, J., 2011. Iron solid-phase
738 differentiation along a redox gradient in basaltic soils. *Geochim. Cosmochim. Acta* 75,
739 119–133

740 Thompson, A., Chadwick, O.A., Rancourt, D.G., Chorover, J., 2006b. Iron-oxide crystallinity
741 increases during redox oscillations. *Geochim. Cosmochim. Acta* 70, 1710–1727.

742 Tipping, E., 1981. The adsorption of aquatic humic substances by iron oxides. *Geochim.*
743 *Cosmochim. Acta* 45 (2), 191–199.

744 van Breemen, N., Protz, R., 1988. Rates of calcium carbonate removal from soils. *Can. J. Soil*
745 *Sci.* 68, 449–454.

746 van der Zee, C., Roberts, D.R., Rancourt, D.G., Slomp, C.P., 2003. Nanogoethite is the
747 dominant reactive oxyhydroxide phase in lake and marine sediments. *Geology* 31,
748 993–996.

749 van den Berg, G.A., Loch, J.P.G., 2000. Decalcification of soils subject to periodic
750 waterlogging. *Eur. J. Soil Sci.* 51, 27–33.

751 Wagai, R. and L.M. Mayer, 2007. Sorptive stabilization of organic matter in soils by hydrous
752 iron oxides. *Geochim. Cosmochim. Acta* 71, 25–35.

753 Wagai, R., Mayer, L.M., Kitayama, K., 2009. Extent and nature of organic coverage of soil
754 mineral surfaces assessed by a gas sorption approach. *Geoderma* 149 (1–2), 152–160.

755 White, A.F., Blum, A.E., Schulz, M.S., Bullen, T.D., Harden, J.W., Peterson, M.L., 1996.
756 Chemical weathering rates of a soil chronosequence on granitic alluvium: I.
757 Quantification of mineralogical and surface area changes and calculation of primary
758 silicate reaction rates. *Geochim. Cosmochim. Acta* 60 (14), 2533–2550.

759 Wissing, L., Kölbl, A., Vogelsang, V., Fu, J., Cao, Z., Kögel-Knabner, I., 2011. Organic
760 carbon accumulation in a 2000-year chronosequence of paddy soil evolution. *Catena*
761 87, 376–385.

762 Wissing, L., Kölbl, A., Häusler, W., Schad, P., Cao, Z., Kögel-Knabner, I., 2012.
763 Management-induced organic carbon accumulation in paddy soils: The role of organo-
764 mineral associations. *Soil Tillage Res.* <http://dx.doi.org/10.1016/j.still.2012.08.004>

765 Wu, J., 2011. Carbon accumulation in paddy ecosystems in subtropical China: evidence from
766 landscape studies. *Eur. J. Soil Sci.* 62, 29–34.

767 Zhang, M., He, Z., 2004. Long-term changes in organic carbon and nutrients of an Ultisol
768 under rice cropping in southeast China. *Geoderma* 118, 167–179.

769 Zottoli, R., 1973. *Introduction to marine environments*. CV Mosby Company, Saint Louis,
770 Mosby, USA (cited from Portnoy and Giblin, 1997).

771 Zou, P., Fu, J., Cao, Z., 2011. Chronosequence of paddy soils and phosphorus sorption–
772 desorption properties. *J. Soil Sediments* 11, 249–259.

773
774

775 **Table 1**

776 Properties of mudflat (0 years), 30-year-old marshland, and paddy (P) and non-paddy (NP) bulk soils (uppermost A horizons): Depths, horizon denominations,
 777 pH values, concentrations of inorganic carbon (IC) and organic carbon (OC), dithionite- and oxalate-extractable iron oxides (Fe_d and Fe_{ox}, respectively) and base
 778 saturation (BS) and the clay content from soil texture analysis. All numbers give the arithmetic mean ($n = 3$) with standard errors. Significant differences ($p \leq$
 779 0.05) within the paddy and non-paddy chronosequence are indicated by italic letters and * represents significant differences ($p \leq 0.05$) between paddy and non-
 780 paddy soils.

Site	Depth (cm)	Horizon (FAO) ^b	^c pH (KCl)	^d IC (mg g ⁻¹)	^d OC (mg g ⁻¹)	^d Fe _d (mg g ⁻¹)	^d Fe _{ox} (mg g ⁻¹)	^e BS (% of CEC _{pot})	^f Clay content <2.0 μm (g kg ⁻¹)
^a Mudflat (0 years)	0 - 30	-	8.2 ± -	5.0 ± -	5.1 ± -	5.3 ± -	4.1 ± -	>100	-
^a Marsh (30 years)	0 - 13	-	7.8 ± -	4.2 ± -	10.9 ± -	6.2 ± -	2.4 ± -	>100	-
P 50	0 - 7	Alp	7.4 ± 0.0 <i>a</i>	1.5 ± 0.3 <i>a</i>	17.8 ± 0.5 <i>b</i>	7.0 ± 0.1 <i>a</i>	2.6 ± 0.6 <i>a</i>	>100	290
P 100	0 - 9	Alp1	5.0 ± 0.2 <i>bc</i>	b.d.l ± - <i>b</i>	17.6 ± 1.0 <i>bc</i>	6.8 ± 0.4 <i>a</i>	3.0 ± 0.3 <i>a</i>	72	279
P 300	0 - 18	Alp	5.8 ± 0.3 <i>b</i>	b.d.l ± - <i>b</i>	^c 22.6 ± 2.0 <i>bc</i>	6.6 ± 0.1 <i>a</i>	2.2 ± 0.3 <i>a</i>	71	245
P 700	0 - 10	Alp1	6.7 ± 0.1 <i>a</i>	b.d.l ± - <i>b</i>	22.3 ± 2.2 <i>b</i>	6.8 ± 0.2 <i>a</i>	3.3 ± 0.7 <i>a</i>	82	286
P 1000	0 - 10	Alp	5.2 ± 0.3 <i>bc</i>	b.d.l ± - <i>b</i>	14.0 ± 0.8 <i>c</i>	7.3 ± 0.2 <i>a</i>	3.0 ± 0.4 <i>a</i>	69	277
P 2000	0 - 15	Alp	5.1 ± 0.1 <i>c</i>	b.d.l ± - <i>b</i>	^c 30.0 ± 0.9 <i>a</i>	4.4 ± 0.1 <i>b</i>	2.8 ± 0.2 <i>a</i>	58	242
mean (50 - 700 yrs)			6.2		*20.1	6.8	*2.8		275
mean (50 - 2000 yrs)			5.9		*20.7	6.5	*2.8		*270
NP 50	0 - 9	Ap	7.3 ± 0.1 <i>a</i>	1.6 ± 0.1 <i>a</i>	10.6 ± 0.0 <i>a</i>	6.3 ± 0.2 <i>a</i>	1.5 ± 0.3 <i>a</i>	>100	208
NP 100	0 - 14	Ap1	7.3 ± 0.1 <i>a</i>	0.7 ± 0.1 <i>ab</i>	10.8 ± 0.0 <i>a</i>	7.0 ± 0.3 <i>a</i>	1.3 ± 0.2 <i>a</i>	>100	272
NP 300	0 - 11	Ap	7.0 ± 0.2 <i>a</i>	0.1 ± 0.2 <i>b</i>	10.5 ± 0.0 <i>a</i>	6.3 ± 0.1 <i>a</i>	0.7 ± 0.2 <i>a</i>	95	237
NP 700	0 - 11	Ap1	5.9 ± 0.3 <i>b</i>	b.d.l ± -	11.0 ± 0.3 <i>a</i>	5.0 ± 0.9 <i>a</i>	1.5 ± 0.6 <i>a</i>	74	190
mean (50 - 700 yrs)			6.9		10.7	6.2	1.3		227

^apH values, carbon data and base saturation (BS) of the mudflat and the marshland were already shown in Kölbl et al., (submitted).

^bGuidelines for soil profile description, FAO (2006).

^cpH values were determined by the laboratory of the Institute for Agricultural and Nutritional Sciences at the Martin-Luther University in Halle-Wittenberg. pH values were already published in Wissing et al. (2012).

^dCarbon data, dithionite (Fe_d) and oxalate extractable (Fe_{ox}) iron oxides of paddy and non-paddy soils were already published in Wissing et al. (2011; 2012).

^eBS of the paddy and non-paddy soils was already published in Kölbl et al. (submitted).

^fClay content from soil texture analysis was already published in Wissing et al. (2012)

b.d.l. = below the detection limit

Statistics of pH values, OC, Fe_d and Fe_{ox} concentrations were already published in Wissing et al. (2012).

781 **Table 2**

782 Radiocarbon (^{14}C) content in percent modern carbon (pMC) and the conventional carbon age of
 783 mudflat, marshland, paddy (P) and non-paddy (NP) bulk soil and the $<0.2\ \mu\text{m}$ fraction (uppermost A
 784 horizons).

785

Site	Depth (cm)	^{14}C (corrected pMC)		Conventional Age	
		bulk soil	$<0.2\ \mu\text{m}$	bulk soil	$<0.2\ \mu\text{m}$
^a Mudflat	0 - 2	62 ± 0.2	-	3900 ± 30 BP	-
	18 - 20	61 ± 0.2	-	4000 ± 30 BP	-
^b Marsh	2 - 3	90 ± 0.3	-	840 ± 30 BP	-
P 50	0 - 7	102 ± 0.4	92 ± 0.3	modern	640 ± 20 BP
P 100	0 - 9	106 ± 0.3	104 ± 0.3	modern	modern
P 300	0 - 18	101 ± 0.3	106 ± 0.4	modern	modern
P 700	0 - 10	99 ± 0.3	97 ± 0.3	110 ± 20 BP	270 ± 20 BP
P 1000	0 - 10	103 ± 0.3	102 ± 0.3	modern	modern
P 2000	0 - 15	112 ± 0.3	108 ± 0.3	modern	modern
NP 50	0 - 9	101 ± 0.4	98 ± 0.3	modern	170 ± 20 BP
NP 100	0 - 14	98 ± 0.3	85 ± 0.3	150 ± 30 BP	1300 ± 30 BP
NP 300	0 - 11	101 ± 0.3	96 ± 0.3	modern	300 ± 20 BP
NP 700	0 - 11	103 ± 0.3	97 ± 0.3	modern	280 ± 20 BP

¹⁴C data of paddy and non-paddy soils were determined by the Leibnitz-Laboratory at the Christian-Albrechts-University in Kiel.

^aData from Bräuer et al. (2012)

^bPersonal communication with Tino Bräuer (unpublished data).

786 **Table 3**

787 The proportion of clay minerals in the <2.0 μm soil fraction of paddy (P) and non-paddy (NP) soils
 788 (uppermost A horizons). Data were determined in a single measurement.

789

Soil fraction ^a	Site	Depth (cm)	14 Å	10-14 Å	Illite (%)	Kaolinite (%)
			Chlorite (%)	Mixed layer minerals (%)		
2.0-0.2 μm	P 50	0 - 7	19	12	63	6
	P 300	0 - 18	15	12	67	6
	P 700	0 - 10	19	11	64	6
	P 2000	0 - 15	10	46	40	4
2.0-0.2 μm	NP 50	0 - 9	17	20	58	5
	NP 300	0 - 11	20	21	55	4
	NP 700	0 - 11	15	20	63	3
<0.2 μm	P 50	0 - 7	13	34	48	5
	P 300	0 - 18	22	38	32	8
	P 700	0 - 10	14	45	37	4
	P 2000	0 - 15	12	37	32	19
<0.2 μm	NP 50	0 - 9	19	23	54	3
	NP 300	0 - 11	21	29	46	4
	NP 700	0 - 11	22	24	52	2

^acoarse clay (2.0 - 0.2 μm); fine clay (<0.2 μm)

790 **Table 4**

791 BET-N₂ specific surface area (SSA) of paddy (P) and non-paddy (NP) <20 μm soil fractions
 792 (uppermost A horizons): SSA after dithionite-citrate-bicarbonate (DCB) extraction, hydrogen peroxide
 793 (H₂O₂) treatment and DCB extraction and the SSA covered by organic carbon (OC). SSA data were
 794 determined in a single measurement. * represents significant differences (*p* ≤ 0.05) between paddy and
 795 non-paddy soils.

796

^a Soil fraction	Site	Depth (cm)	SSA		SSA covered by OC (%)
			DCB (m ² g ⁻¹)	H ₂ O ₂ +DCB (m ² g ⁻¹)	
	P 50	0 - 7	2	5	-
	P 100	0 - 9	2	12	21
	P 300	0 - 18	2	7	11
	P 700	0 - 10	2	38	-
	P 1000	0 - 10	3	10	-
	P 2000	0 - 15	3	21	33
20-6.3 μm	mean		2	16	
	NP 50	0 - 9	2	5	34
	NP 100	0 - 14	2	5	-
	NP 300	0 - 11	2	7	-
	NP 700	0 - 11	2	23	-
	mean		2	10	

	Site	Depth (cm)	SSA		SSA covered by OC (%)
			DCB (m ² g ⁻¹)	H ₂ O ₂ +DCB (m ² g ⁻¹)	
	P 50	0 - 7	8	11	13
	P 100	0 - 9	10	24	27
	P 300	0 - 18	14	20	18
	P 700	0 - 10	9	9	38
	P 1000	0 - 10	9	15	-
	P 2000	0 - 15	8	12	37
6.3-2 μm	mean		9	15	
	NP 50	0 - 9	10	20	-
	NP 100	0 - 14	7	15	-
	NP 300	0 - 11	7	30	-
	NP 700	0 - 11	10	13	-
	mean		8	20	

^a Soil fraction	Site	Depth (cm)	SSA		SSA covered by OC (%)	
			DCB	H ₂ O ₂ +DCB		
			(m ² g ⁻¹)	(m ² g ⁻¹)		
2-0.2 μm	P 50	0 - 7	28	40	28	
	P 100	0 - 9	27	27	50	
	P 300	0 - 18	26	48	35	
	P 700	0 - 10	23	62	28	
	P 1000	0 - 10	22	34	13	
	P 2000	0 - 15	23	35	50	
	mean		25	41		
	NP 50	0 - 9	23	47	-	
	NP 100	0 - 14	23	52	-	
	NP 300	0 - 11	26	36	-	
	NP 700	0 - 11	26	53	18	
	mean		24	47		
	<0.2 μm	P 50	0 - 7	69	123	31
		P 100	0 - 9	65	146	49
P 300		0 - 18	56	77	56	
P 700		0 - 10	60	84	68	
P 1000		0 - 10	33	319	40	
P 2000		0 - 15	39	308	75	
mean			53	176		
NP 50		0 - 9	85	105	30	
NP 100		0 - 14	79	68	18	
NP 300		0 - 11	81	118	24	
NP 700		0 - 11	69	104	41	
mean			*78	99		

^a20 - 6.3 μm = medium silt; 6.3 - 2 μm = fine silt; 2 - 0.2 μm = coarse clay; <2 μm = fine clay

799 **Table 5**

800 Hydrogen peroxide (H₂O₂) resistant organic carbon (OC) of the paddy (P) and non-paddy (NP) soil
 801 <20 µm fractions (uppermost A horizons). Data were determined in a single measurement.

802

Site	Depth (cm)	H₂O₂ resistant OC (%)			
		^a Soil fraction			
		20-6.3 µm	6.3-2.0 µm	2.0-0.2 µm	<0.2 µm
P 50	0 - 7	n.d.	7	7	4
P 100	0 - 9	17	6	8	2
P 300	0 - 18	12	6	5	3
P 700	0 - 10	17	6	4	3
P 1000	0 - 10	36	9	7	4
P 2000	0 - 15	6	3	4	2
NP 50	0 - 9	54	11	9	4
NP 100	0 - 14	31	11	15	5
NP 300	0 - 11	25	8	9	3
NP 700	0 - 11	31	8	8	4

810 ^a20 -6.3 µm = medium silt; 6.3 - 2.0 µm = fine silt; 2.0 - 0.2 µm = coarse clay; <2 = fine clay
 811 n.d. = not detected

811

812

813

Figure captions

814 **Figure 1** BET-N₂ Specific surface area (SSA) of a) paddy (P) and b) non-paddy (NP) soil fractions
815 (20–6.3 μm = medium silt; 6.3–2.0 μm = fine silt; 2.0–0.2 μm = coarse clay; <0.2 μm = fine clay)
816 before (gray) and after oxidation of organic matter by hydrogen peroxide (H₂O₂) (black) of the
817 uppermost A horizons.

818

819 **Figure 2** Relation between dithionite-extractable iron oxides (Fe_d) and BET-N₂ specific surface area
820 (SSA) (a) untreated and b) H₂O₂-treated paddy (P) and non-paddy (NP) soil fractions of the uppermost
821 A horizons (20–6.3 μm = medium silt; 6.3–2.0 μm = fine silt; 2.0–0.2 μm = coarse clay; <0.2 μm =
822 fine clay).

823

824 **Figure 3** Relation between organic carbon (OC) content and BET-N₂ specific surface area (SSA) (a)
825 untreated and b) H₂O₂-treated paddy (P) and non-paddy (NP) soil fractions of the uppermost A
826 horizons (20–6.3 μm = medium silt; 6.3–2.0 μm = fine silt; 2.0–0.2 μm = coarse clay; <0.2 μm = fine
827 clay).

828

829 **Figure 4** The effect of organic matter (OM) oxidation by H₂O₂, removal of Fe_d oxides by dithionite-
830 citrate-bicarbonate (DCB) treatment and H₂O₂ oxidation combined with the subsequent removal Fe_d
831 oxides on clay-sized particles and Fe_d oxides and their specific surface area (SSA). The SSA increases
832 are indicated by +, decrease by – and no change by ±. The different letters indicates the untreated a)
833 Fe_d oxides, b) Fe_d oxides with OM, c) clay minerals (in non-paddy soils with carbonates and Ca²⁺
834 bridges), (d) clay mineral with OM, e) clay mineral with Fe_d oxides, f) clay mineral with Fe_d oxides
835 and OM of paddy (P) and non-paddy soils (NP), respectively.

836

837 **Figure 5** The effect of organic matter (OM) oxidation by H₂O₂, removal of Fe_d oxides by dithionite-
838 citrate-bicarbonate (DCB) treatment and H₂O₂ oxidation combined with the subsequent removal Fe_d
839 oxides on clay-sized particles and Fe_d oxides and their specific surface area in comparison to untreated
840 paddy and non-paddy soils. The different letters indicates a) the untreated soil cluster consisting of

841 clay minerals (in non-paddy soils with calcium carbonate cementation and Ca^{2+} bridges, Fe_d oxides),
842 Fe_d oxides and OM and b) the soil cluster treated by H_2O_2 and the subsequent removal of Fe_d oxides of
843 paddy (P) and non-paddy soils (NP), respectively.

844

845 **Figure 6** Chronological changes of dominant soil forming processes in paddy versus non-paddy soils.

846

847

848

849

850

851

852

853

854

855

856

857

858

859

860

861

862

863

864

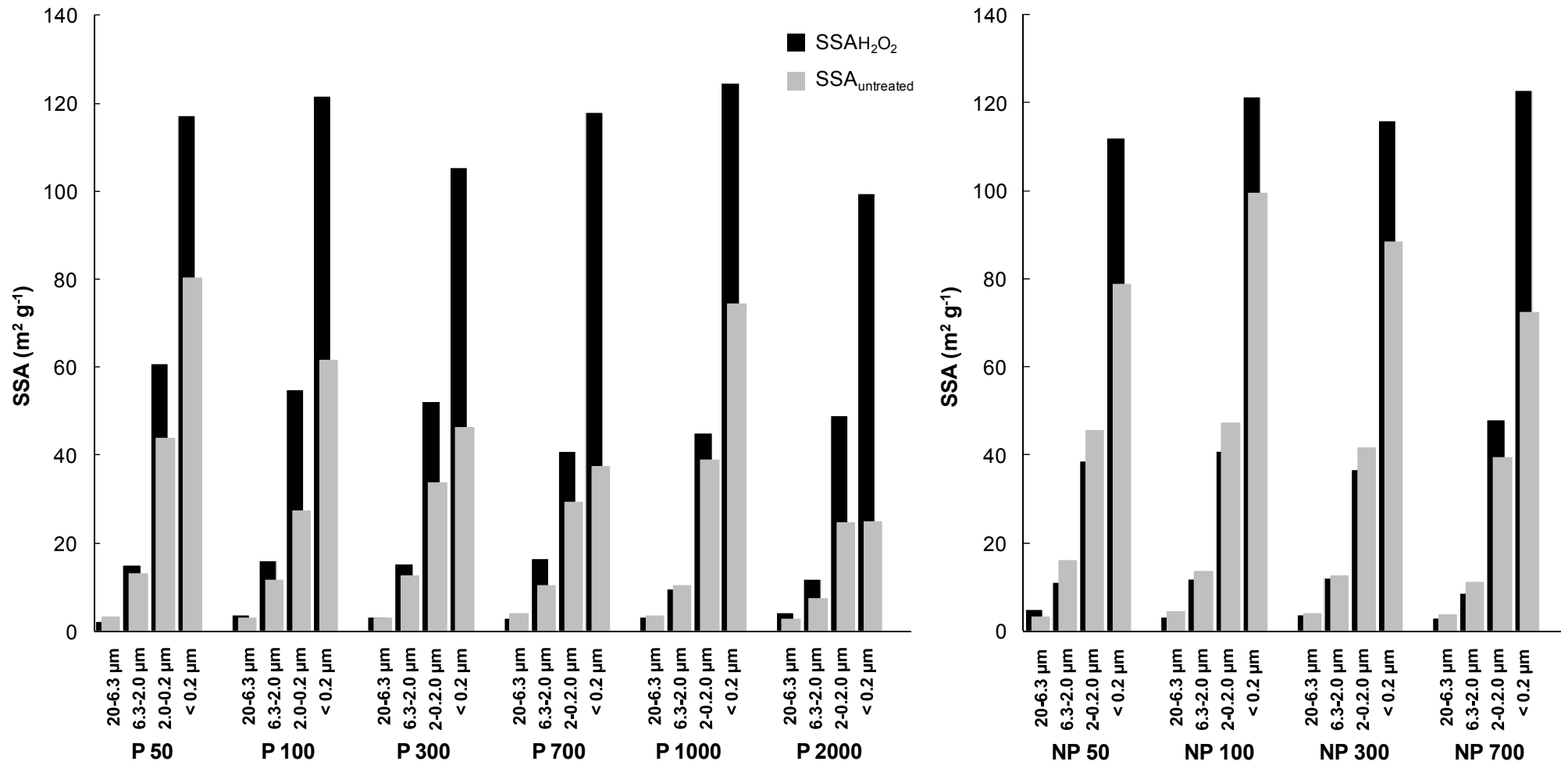
865

866

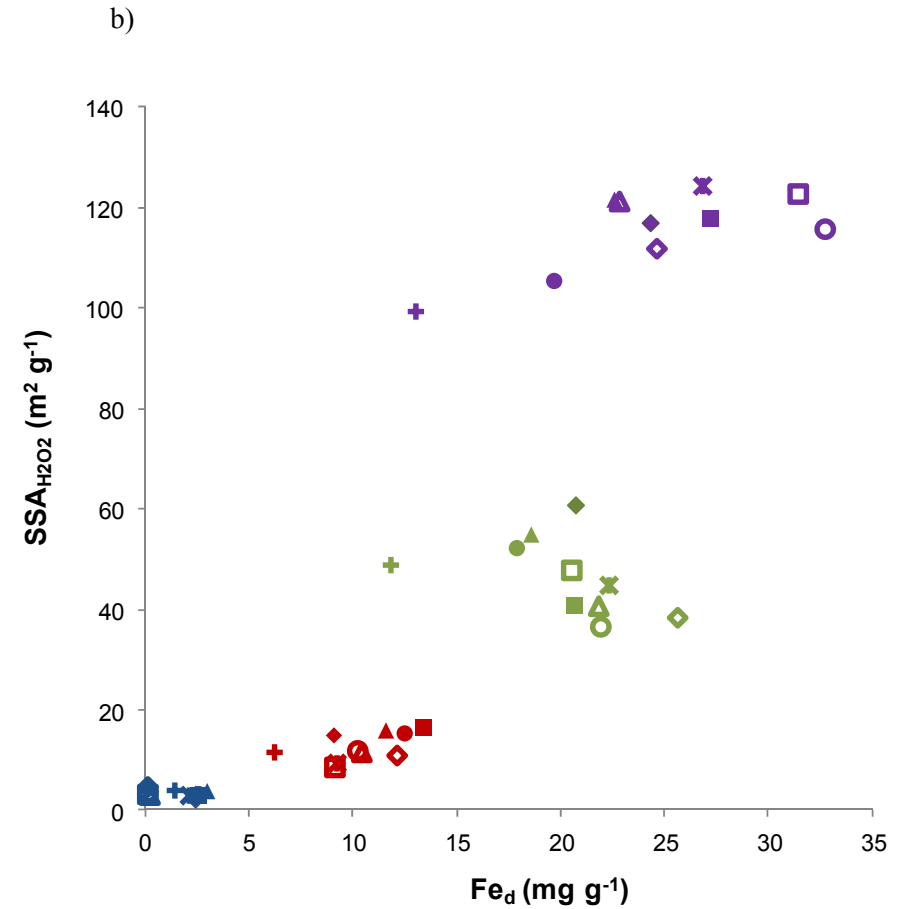
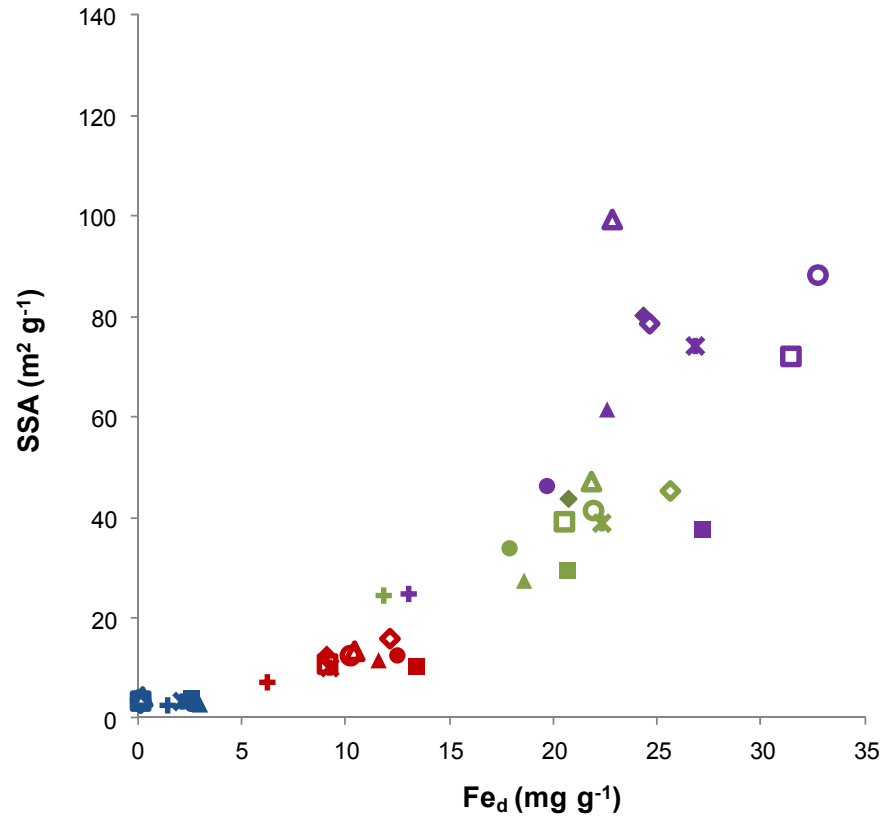
867

868

869 **Figure 1** BET-N₂ Specific surface area (SSA) of a) paddy (P) and b) non-paddy (NP) soil fractions (20–6.3 μm = medium silt; 6.3–2.0 μm = fine silt; 2.0–0.2
 870 μm = coarse clay; <0.2 μm = fine clay) before (gray) and after oxidation of organic matter by hydrogen peroxide (H₂O₂) (black) of the uppermost A horizons.
 871 a) b)

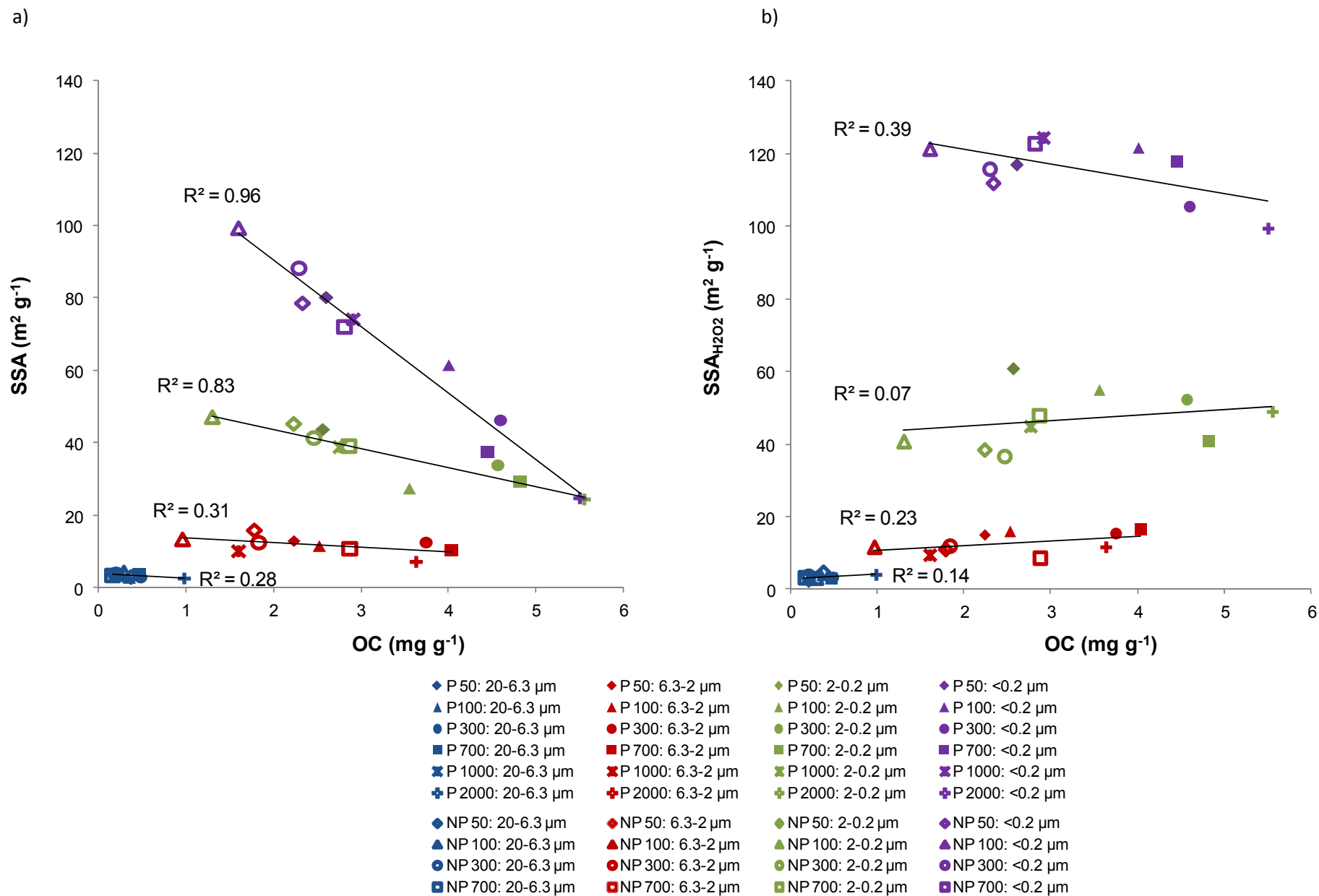


872 **Figure 2** Relation between dithionite-extractable iron oxides (Fe_d) and BET- N_2 specific surface area (SSA) (a) untreated and b) H_2O_2 -treated paddy (P) and non-
 873 paddy (NP) soil fractions of the uppermost A horizons (20–6.3 μm = medium silt; 6.3–2.0 μm = fine silt; 2.0–0.2 μm = coarse clay; <0.2 μm = fine clay).
 874 a)



- | | | | |
|--------------------------|-------------------------|-------------------------|------------------------|
| ◆ P 50: 20-6.3 μm | ◆ P 50: 6.3-2 μm | ◆ P 50: 2-0.2 μm | ◆ P 50: <0.2 μm |
| ▲ P 100: 20-6.3 μm | ▲ P 100: 6.3-2 μm | ▲ P 100: 2-0.2 μm | ▲ P 100: <0.2 μm |
| ● P 300: 20-6.3 μm | ● P 300: 6.3-2 μm | ● P 300: 2-0.2 μm | ● P 300: <0.2 μm |
| ■ P 700: 20-6.3 μm | ■ P 700: 6.3-2 μm | ■ P 700: 2-0.2 μm | ■ P 700: <0.2 μm |
| ✕ P 1000: 20-6.3 μm | ✕ P 1000: 6.3-2 μm | ✕ P 1000: 2-0.2 μm | ✕ P 1000: <0.2 μm |
| ⊕ P 2000: 20-6.3 μm | ⊕ P 2000: 6.3-2 μm | ⊕ P 2000: 2-0.2 μm | ⊕ P 2000: <0.2 μm |
| ◆ NP 50: 20-6.3 μm | ◆ NP 50: 6.3-2 μm | ◆ NP 50: 2-0.2 μm | ◆ NP 50: <0.2 μm |
| ▲ NP 100: 20-6.3 μm | ▲ NP 100: 6.3-2 μm | ▲ NP 100: 2-0.2 μm | ▲ NP 100: <0.2 μm |
| ● NP 300: 20-6.3 μm | ● NP 300: 6.3-2 μm | ● NP 300: 2-0.2 μm | ● NP 300: <0.2 μm |
| ■ NP 700: 20-6.3 μm | ■ NP 700: 6.3-2 μm | ■ NP 700: 2-0.2 μm | ■ NP 700: <0.2 μm |






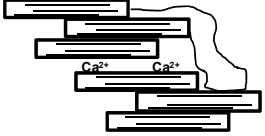






875 **Figure 3** Relation between organic carbon (OC) content and BET-N₂ specific surface area (SSA) (a) untreated and b) H₂O₂-treated paddy (P) and non-paddy
 876 (NP) soil fractions of the uppermost A horizons (20–6.3 μm = medium silt; 6.3–2.0 μm = fine silt; 2.0–0.2 μm = coarse clay; <0.2 μm = fine clay).
 877 a)





878 **Figure 4** Schematic overview of the effect of organic matter (OM) oxidation by H₂O₂, removal of Fe_d
 879 oxides by dithionite-citrate-bicarbonate (DCB) treatment and H₂O₂ oxidation combined with the
 880 subsequent removal Fe_d oxides on clay-sized particles and Fe_d oxides and their specific surface area
 881 (SSA). The SSA increases are indicated by +, decrease by – and no change by ±. The different letters
 882 indicates the untreated a) Fe_d oxides, b) Fe_d oxides with OM, c) clay minerals (in non-paddy soils with
 883 carbonates and Ca²⁺ bridges), (d) clay mineral with OM, e) clay mineral with Fe_d oxides, f) clay
 884 mineral with Fe_d oxides and OM of paddy (P) and non-paddy soils (NP), respectively.


885

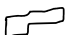
Specific surface area change


	untreated	H ₂ O ₂	DCB	H ₂ O ₂ + DCB	untreated
	paddy soils	P / NP	P / NP	P / NP	non-paddy soils
a		± / ±	- / -	- / -	
b		+ / +	± / -	- / -	
c		± / ±	± / ±	± / ±	
d		+ / +	± / ±	+ / +	
e		± / ±	(±) / (±)	(+) / (+)	
f		± / ±	- / -	(+) / (+)	


Clay mineral

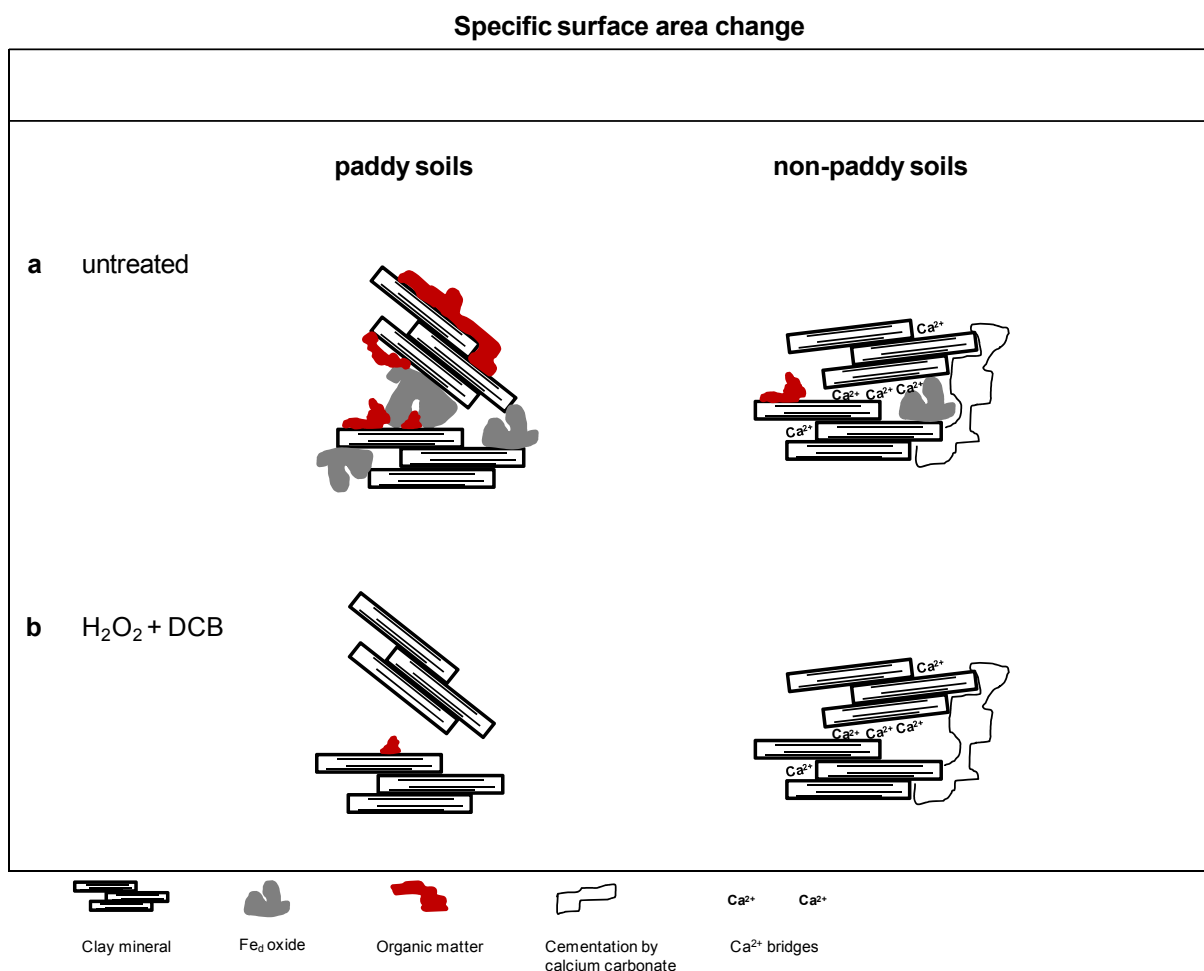

Fe_d oxide


Organic matter


Cementation by calcium carbonate


Ca²⁺ bridges

886 **Figure 5** Schematic overview of the effect of organic matter (OM) oxidation by H_2O_2 , removal of Fe_d
 887 oxides by dithionite-citrate-bicarbonate (DCB) treatment and H_2O_2 oxidation combined with the
 888 subsequent removal Fe_d oxides on clay-sized particles and Fe_d oxides and their specific surface area in
 889 comparison to untreated paddy and non-paddy soils. The different letters indicates a) the untreated soil
 890 cluster consisting of clay minerals (in non-paddy soils with calcium carbonate cementation and Ca^{2+}
 891 bridges, Fe_d oxides and OM and b) the soil cluster treated by H_2O_2 and the subsequent
 892 removal of Fe_d oxides of paddy (P) and non-paddy soils (NP), respectively.
 893



894 **Figure 6** Chronological changes of dominant soil forming processes in paddy versus non-paddy soils.

895

